



UNIL | Université de Lausanne

Unicentre

CH-1015 Lausanne

<http://serval.unil.ch>

Year : 2019

Characterisation of immune-modulating lymphocyte populations in melanoma patients

De Jonge Kaat

De Jonge Kaat, 2019, Characterisation of immune-modulating lymphocyte populations in melanoma patients

Originally published at : Thesis, University of Lausanne

Posted at the University of Lausanne Open Archive <http://serval.unil.ch>

Document URN : urn:nbn:ch:serval-BIB_07D8F3E7B9169

Droits d'auteur

L'Université de Lausanne attire expressément l'attention des utilisateurs sur le fait que tous les documents publiés dans l'Archive SERVAL sont protégés par le droit d'auteur, conformément à la loi fédérale sur le droit d'auteur et les droits voisins (LDA). A ce titre, il est indispensable d'obtenir le consentement préalable de l'auteur et/ou de l'éditeur avant toute utilisation d'une oeuvre ou d'une partie d'une oeuvre ne relevant pas d'une utilisation à des fins personnelles au sens de la LDA (art. 19, al. 1 lettre a). A défaut, tout contrevenant s'expose aux sanctions prévues par cette loi. Nous déclinons toute responsabilité en la matière.

Copyright

The University of Lausanne expressly draws the attention of users to the fact that all documents published in the SERVAL Archive are protected by copyright in accordance with federal law on copyright and similar rights (LDA). Accordingly it is indispensable to obtain prior consent from the author and/or publisher before any use of a work or part of a work for purposes other than personal use within the meaning of LDA (art. 19, para. 1 letter a). Failure to do so will expose offenders to the sanctions laid down by this law. We accept no liability in this respect.



UNIL | Université de Lausanne

Faculté de biologie
et de médecine

Département

**Characterisation of immune-modulating lymphocyte populations in
melanoma patients**

Thèse de doctorat ès sciences de la vie (PhD)

présentée à la

Faculté de biologie et de médecine
de l'Université de Lausanne

par

Kaat DE JONGE

Master of Science in the bio-engineering sciences: Cell-and gene biotechnology at the
Free University of Brussels (VUB)

Jury

Prof. Mureille Bochud, Président
Prof. Daniel Speiser, Directeur de thèse
Dr. Petra Baumgärtner, Co-directrice
Prof. Olaia Naveiras, experte
Prof. Martin Bachmann, expert
Prof. Werner Held, expert

Lausanne 2019

Imprimatur

Vu le rapport présenté par le jury d'examen, composé de

Président-e	Madame	Prof.	Murielle	Bochud
Directeur-trice de thèse	Monsieur	Prof.	Daniel	Speiser
Co-directeur-trice	Madame	Dre	Petra	Baumgärtner
Expert-e-s	Monsieur	Prof.	Werner	Held
	Madame	Prof.	Olaia	Naveiras
	Monsieur	Prof.	Martin	Bachmann

le Conseil de Faculté autorise l'impression de la thèse de

Madame Kaat De Jonge

Master in bioengineering, Vrije Universiteit, Bruxelles, Belgique

intitulée

**Characterisation of immune-modulating lymphocyte
populations in melanoma patients**

Lausanne, le 21 juin 2019

pour le Doyen
de la Faculté de biologie et de médecine


Prof. Murielle Bochud



UNIL | Université de Lausanne

Faculté de biologie
et de médecine

Département

**Caractérisation des populations lymphocytaires modulant la réponse
immunitaire dans les patients atteints du mélanome**

Thèse de doctorat ès sciences de la vie (PhD)

présentée à la

Faculté de biologie et de médecine
de l'Université de Lausanne

par

Kaat DE JONGE

Master of Science in the bio-engineering sciences: Cell-and gene biotechnology at the
Free University of Brussels (VUB)

Jury

Prof. Mureille Bochud, Président
Prof. Daniel Speiser, Directeur de thèse
Dr. Petra Baumgärtner, Co-directrice
Prof. Olaia Naveiras, experte
Prof. Martin Bachmann, expert
Prof. Werner Held, expert

Imprimatur

Vu le rapport présenté par le jury d'examen, composé de

Président-e	Madame	Prof.	Murielle	Bochud
Directeur-trice de thèse	Monsieur	Prof.	Daniel	Speiser
Co-directeur-trice	Madame	Dre	Petra	Baumgärtner
Expert-e-s	Monsieur	Prof.	Werner	Held
	Madame	Prof.	Olaiia	Naveiras
	Monsieur	Prof.	Martin	Bachmann

le Conseil de Faculté autorise l'impression de la thèse de

Madame Kaat De Jonge

Master in bioengineering, Vrije Universiteit, Bruxelles, Belgique

intitulée

**Characterisation of immune-modulating lymphocyte
populations in melanoma patients**

Lausanne, le 21 juin 2019

pour le Doyen
de la Faculté de biologie et de médecine


Prof. Murielle Bochud

Table of Contents

Table of Contents	3
1. Résumé	5
2. Summary	7
3. Résumé large public	8
4. Acknowledgments	9
5. Abbreviations	9
6. General introduction	13
6.1. The Immune system	13
6.2. Cells of the immune system	13
6.2.1. Innate immunity	13
6.2.2. Adaptive immunity or acquired immunity	16
6.3. Melanoma	19
6.3.1. Epidemiology	19
6.3.2. Risk factors	19
6.3.3. Diagnosis	20
6.3.4. Treatment	20
6.4. Tumour micro-environment	20
7. My PhD projects	24
8. Circulating CD56 ^{bright} NK cells inversely correlate with survival of melanoma patients	26
8.1. Introduction	26
8.2. Aim	32
8.3. Co-author contributions	33
8.4. Manuscript	34
8.4.1. Supplementary data of the manuscript	44
8.5. Discussion and perspectives	53
9. Characterisation of immune-modulating B cells in late stage melanoma patients	54
9.1. Introduction	54
9.2. Aim	59
9.3. Material and Methods	60
9.3.1. Melanoma patients	60
9.3.2. Human cell preparation and flow cytometry	60

9.3.3.	Cell sorting and RNA sequencing.....	61
9.3.4.	Statistics and analysis.....	62
9.4.	Results	63
9.4.1.	Patient B cells are potent cytokine producers	63
9.4.2.	Previous immunotherapy and stage of the patients correlate with B cell functionality	63
9.4.3.	Pro-inflammatory B cells correlate inversely with overall survival in Ipilimumab treated patients	67
9.4.4.	B cells from the TME are significantly different from peripheral B cells from patients and healthy donor controls.....	67
9.5.	Discussion and perspectives.....	72
10.	Characterization of a new lymphocytic population, termed Orphan lymphoid cells (OLC), in the blood of healthy humans	75
10.1.	Introduction.....	75
10.2.	Aim	77
10.3.	Material and Methods.....	78
10.3.1.	Human cell preparation and flow cytometry	78
10.3.2.	Cell sorting and RNA sequencing.....	78
10.4.	Results	80
10.4.1.	Discovery of Orphan Lymphoid Cells (OLCs)	80
10.4.2.	OLCs express the common γ – chain receptor	80
10.4.3.	OLCs are a morphologically homogeneous population	81
10.4.4.	RNA signatures represent a mixed T-NK cell signature.....	81
10.5.	Discussion and Perspectives.....	86
11.	General discussion.....	88
12.	References.....	89
13.	Annexes	110
14.	Curriculum Vitae.....	148

1. Résumé

Le but de ma thèse a été d'approfondir nos connaissances immunologiques dans des patients atteints de mélanomes en étendant nos recherches à trois types cellulaires moins étudiés dans ce cadre : les cellules NK, les lymphocytes B et une population que nous avons baptisé cellules lymphoïdes orphelines.

Pendant mon premier projet, on a étudié les différents rôles des cellules tueuses naturelles (NK) dans des patients atteint d'un mélanome avancé (stade III/IV). Une analyse de régression multivariée Cox montre que l'abondance des cellules NK CD56^{bright} corrèle négativement avec la survie globale, ainsi qu'avec la présence de métastases distantes. Les cellules NK CD56^{bright} des patients expriment plus de CD11a, CD38 et CD95 en comparaison avec les cellules dérivées de donneurs sains. Ceci démontre que les cellules ont un phénotype activé qui jouer un rôle dans la régulation immunitaire des patients atteint d'un mélanome. Après stimulation *in vitro* des cellules NK CD56^{bright} des patients, nous mesurons une production moindre de TNF α et de GM-CSF en comparaison avec ces mêmes cellules provenant de contrôles sains. En outre, la production d'IFN γ par les cellules NK CD56^{bright} corrèle inversement avec la survie globale. Nos résultats soulignent que l'abondance et la fonction des cellules NK CD56^{bright} sont associées avec la survie des patients atteint d'un mélanome, ce qui accentue le potentiel des sous-classes des cellules NK pour la découverte des marqueurs biologiques et pour le ciblage thérapeutique.

Comme deuxième projet, j'ai caractérisé les cellules B de patients atteints d'un mélanome. Nos résultats montrent que la réponse fonctionnelle des cellules B périphériques des patients traités par immunothérapie est moins capable de produire du TNF α , de la LT α et de l'IL-10 en comparaison avec les patients qui n'ont pas reçu d'immunothérapie. Les cellules B trouvées dans les patients qui ne répondent pas à l'immunothérapie (Ipilimumab) produisent plus d'IL-6, de TNF α et d'IL-10 mais moins de GM-CSF. De plus, le niveau d'IL-6, de TNF α et d'IL-10 corréler inversement avec la survie globale. Ceci montre que les cellules B ont en même temps un potentiel pro-inflammatoire et régulateur qui impacte négativement la survie. Le séquençage de l'ARN des cellules B pures dérivées de l'environnement tumoral montre un enrichissement des gènes inflammatoires comme l'IL-6, l'IL-10 et la LT α . Un des gènes le plus significativement surexprimé est IDO. Globalement, notre recherche indique que les cellules B contribuent à l'établissement et à la soutenance d'une réponse immunitaire pro-tumorale par la production de cytokines en même temps pro-inflammatoires et régulatrices. Les cellules B peuvent servir comme nouvelles cibles et/ou marqueurs biologiques pour la thérapie.

Pour mon troisième projet, nous avons caractérisé une population de cellules, qui est jusqu'à maintenant inconnue, nommé cellules lymphoïdes orphelines (CLOs). Elles constituent environ 0.2% des lymphocytes périphériques. Les CLOs n'expriment aucun des marqueurs de lignées standards mais elles expriment CD44, CD45, CD132 et pour une fraction de cellules, CD62L. La morphologie, analysée par l'Amnis Image Stream, et l'analyse des composants principaux obtenus par séquençage d'ARN montre une population homogène. En plus, le profil obtenu par séquençage d'ARN montre un phénotype proche, mais suffisamment différents des cellules T et NK. Plus de recherches sont nécessaires pour établir la fonction de ces cellules, leur distribution dans les tissus et le lien avec les autres cellules immunitaires.

2. Summary

According to the World Health Organisation, cancer is the second leading cause of death in the world, causing an estimated 9.6 million deaths in 2018. In the last decades, huge strides have been made into new therapy avenues producing long lasting effects. Most of these immune-therapies focus on activating cytotoxic T cells within the tumour-microenvironment. Within the tumour-microenvironment the tumour cells as well as other types of immune cells like regulatory T cells and myeloid-derived suppressor cells can suppress the function of the anti-tumour immune response.

We hypothesized that some of the still infrequently studied lymphocytes may also hamper anti-tumour T cell responses. The aim of my thesis work was to determine whether NK cells, B cells and/or further non-T lymphocyte populations may have immunosuppressive roles, and thus could be harmful for melanoma patients.

During my first project, we studied the roles of peripheral NK cells in human late stage (III/IV) melanoma patients. We found that the abundance of CD56^{bright} NK cells negatively correlate with overall patient survival, together with distant metastases, in a multivariate cox regression analysis. The patients' CD56^{bright} NK cells showed upregulation of CD11a, CD38 and CD95 as compared to healthy controls, pointing to an activated phenotype as well as a possible immune regulatory role. After stimulation *in vitro*, CD56^{bright} NK cells produced less TNF α and GM-CSF in patients than controls. Our results emphasizing the potential of NK cell subsets for biomarker discovery and future therapeutic targeting.

The characterisation of B cells in melanoma patients became the topic of my second project. Peripheral B cells from patients not responding to immunotherapy (Ipilimumab) produced higher levels of IL-6, TNF α and IL-10 but less GM-CSF. Moreover, IL-6, TNF α and IL-10 levels also inversely correlate with overall survival. RNA sequencing from sorted B cells from within the tumour micro-environment show an enrichment in inflammatory genes, including expression of IL-6, IL-10 and LT α . One of the highest overexpressed genes is IDO. Overall, our research suggests that B cells contribute to the pro-tumoural immune response by producing both inflammatory and regulatory cytokines. B cells could thus be new targets, and/or exploited as biomarkers for therapy.

During my third project we identified a so far unknown cell population which we termed Orphan Lymphoid Cells (OLCs). They make up around 0.2% of human circulating lymphocytes. OLCs are negative for all major lineage markers but express CD44, CD45, common γ -chain (CD132) and partially CD62L. Morphological analysis and principal component analysis by RNA sequencing shows a homogeneous population. Moreover, RNA sequencing profiling shows a phenotype between T and NK cells while being distinctly different. While these data establish the existence of a new lymphocyte population in humans, more work is needed to clarify their functionality, tissue distribution and link to other immune cells.

3. Résumé grande public

Il est estimé qu'en Europe 27 personnes sur 100 000 sont mortes d'un mélanome en 2018. De nouvelles thérapies efficaces sont basées sur l'amplification de la réaction immunitaire contre le cancer. Pendant ma thèse le but était d'approfondir notre connaissance dans le domaine de l'immunologie lors de cette pathologie.

Pendant mon premier projet, nous avons étudié les différents rôles des cellules tueuses naturelles (NK) dans des patients atteints d'un mélanome avancé. Nous avons trouvé que l'abondance d'un sous type de cellules NK corrèle négativement avec la survie globale. Ce sous type de cellules NK des patients ont un phénotype de cellules plus activées que les cellules des donneurs sains. Après stimulation, les cellules NK dérivées de patients sont moins capables de produire des agents pro-inflammatoires. Nos résultats soulignent que l'abondance et la fonction des cellules NK sont associées avec la survie des patients atteints d'un mélanome, ce qui accentue le potentiel des sous-classes des cellules NK pour la découverte des marqueurs biologiques et pour le ciblage thérapeutique.

La caractérisation des cellules B, un deuxième type de cellules immunitaire plus connu pour leur capacité à produire des anticorps, dans les patients atteints d'un mélanome est devenue le sujet mon deuxième projet. Nous avons montré que la réponse fonctionnelle des cellules B périphériques des patients ayant reçu un traitement par immunothérapie, sont moins capable de produire des agents pro-inflammatoires et régulateurs en comparaison avec des patients qui n'ont pas reçu l'immunothérapie. De plus, des patients qui n'ont pas répondu à la thérapie immunitaire ont des cellules B qui sont plus actives. Le taux de fonctionnalité corrèle négativement avec la survie globale de ces patients. L'analyse des cellules B dérivées de l'environnement tumoral montre un enrichissement des gènes inflammatoires et régulateurs. Nos recherches suggèrent que les cellules B contribuent à l'établissement et à la soutenance d'une réponse immunitaire pro-tumorale. Les cellules B peuvent servir comme nouvelles cibles et/ou marqueurs biologiques pour la thérapie.

Lors de mon troisième projet, nous avons caractérisé une population de cellules, qui est jusqu'à maintenant inconnue, nommé cellules lymphoïdes orphelines (CLOs). Elles représentent environ 0.2% des lymphocytes périphériques. Les CLOs n'expriment aucun des marqueurs de lignées standards mais elles expriment CD44, CD45, CD132 et pour une fraction, CD62L. Nous avons pu établir que ces cellules ont un profil proche des lymphocytes T et NK, mais avec des distinctions majeures. Plus de recherches sont nécessaires pour établir la fonction de ces cellules, leur distribution dans les tissus et le lien avec les autres cellules immunitaires.

4. Acknowledgments

First of all, I would like to thank Prof. Daniel Speiser for giving me the opportunity to perform my PhD work in his lab. Moreover, for giving me the freedom to determine the direction of my projects according to my personal interest, for his availability for discussions as well as all the advice he provided for presentations and written documents and for giving me the possibility to present my work at different conferences. Secondly, I would like to thank my co-director Petra Baumgärtner for teaching me the majority of the techniques used during my PhD, especially flow cytometry and cell culture. Furthermore, for her believe in the project during difficult times and her very practical view on how to move forward.

I would also like to thank my previous master student Anna Ebering for the high quality work she performed and contributions she made. I would also like to show my appreciation for the clinical research team, H el ene Maby-El Hajjami, Hajer Ouertatani-Sakouhi and Paula Marcos Mond ejar for their consistent patient follow-up and swift replies for any need for information. I also would like to thank all the colleagues with whom I have collaborated over the years and who have given me multiple opportunities to learn new techniques. I would like to thank Natacha Bordry, for the confidence she had in me and teaching me immunofluorescent data analysis as well as all the discussion and advice. I would also like to express my gratitude to Julien Racle and David Gfeller for giving me the opportunity to work together with them as well as giving me an insight into the world of bio-informatics.

I was lucky to find a group of friends in the lab when moving here, so I would like to thank Amandine Bovay, Am elie Cachot, Claire Imbratta and B ereng ere Salom e for the evenings and moments we spent together. Also, all the past and present members of the lab Christophe Martignier, Damien Saugy, Nicole Montandon, Natalie Neubert, Timothy Murray, Silvia Fuertes-Marraco, Karin Sch auble, No emie Wald, Nicolas Gestermann, Laure Till e, Marine Leblond, Gregory Verdeil, Connie Gilfillan, Sina Nassiri and S ebastien Lofek for the good atmosphere and their openness for discussion. As well the groups of Pedro Romero, Camilla Jandus and Nathalie Rufer for creating a comfortable work environment and the possibilities for discussion in between groups.

Overall, I would like to thank everyone who made me feel welcome in Switzerland and who accompanied me on this journey. Including my parents and sister for their continued support and belief in me, for their multiple visits and kilograms of smuggled Belgian chocolate. My university friends Laura Gygax, Katrien Van Gucht, Laurine Dupont, Fien Demeyer en Sari Van Den Herrewegen for their friendship and support. Last but not least my partner, Alexander, for all the moments we spent together, during the stressful and the less stressful times the last years and especially for his unwavering belief in me.

5. Abbreviations

ADCC	Antibody-dependent cell cytotoxicity
ALR	AIM2-like receptor
APC	Antigen presenting cell
BCR	B cell receptor
B _{reg}	Regulatory B cell
C	Complement
CHILP	common helper ILC progenitor
CLR	C-type lectin receptor
CMP	Clonogenic common myeloid progenitor
DAMP	Danger associated molecular patterns
DC	Dendritic cell
EILP	the early innate lymphoid progenitor
GMP	Granulocytes and macrophages progenitor cells
HSC	Hematopoietic stem cells
IDO	Indole amine 2,3 dioxygenase
IFN	Interferon
IL	Interleukin
ILC	Innate lymphoid cell
ITAM	Intracellular tyrosine-based activating motive
ITIM	Intracellular tyrosine-based inhibitory motive
LMPP	Lymphoid-primed multipotent progenitor
LT HSC	Long lived hematopoietic stem cells
LTi	Lymphoid tissue inducer cell
MDSC	Myeloid-derived suppressor cell

MEP	Megakaryocytes and erythrocytes
MHC	Major histocompatibility complex
MPP	Multipotent progenitor cells
NCR	Natural cytotoxicity receptor
NK cell	Natural killer cell
NLR	NOD-like receptor
OLC	Orphan lymphoid cell
PAMP	Pathogen associated molecular patterns
PRR	Pattern recognition receptors
RLR	RIG-I-like receptor
SEREX	serological analysis of tumour antigens by recombinant cDNA expression cloning
ST HSC	Short lived hematopoietic stem cells
TAM	Tumour-associated macrophages
TCR	T cell receptor
TGF	Transforming growth factor
Th	T helper cell
TIL	Tumour-infiltrating lymphocytes
TILN	Tumour-infiltrated lymph nodes
TLR	Toll-like receptor
TLS	Tertiary lymphoid structures
TME	Tumour micro-environment
TNF	Tumour necrosis factor
T _{reg}	Regulatory T cell
VEGF	Vaso-endothelial growth factors

α LP

α lymphoid precursor

6. General introduction

6.1. The Immune system

Every day our body encounters numerous pathogens and foreign agents. A human being is protected by a first line of defence, barriers that physically protect us from the outside world. These first barriers between the outside world and the inner body are amongst others the skin, the mucosa in the gastrointestinal tract and the respiratory tract. Epithelial surfaces not only act as a physical barrier but also combat pathogens with chemical and biological compounds ¹. When a pathogen has succeeded to overcome these barriers, the immune system of our body comes in action. It consists of a fast-acting component, the innate immune system, and a slower acting component, the adaptive immune system. Both are tightly interrelated ².

6.2. Cells of the immune system

Immune cells are derived from long-term hematopoietic stem cells (HSC) which reside in the bone marrow. Cells in the bloodstream have a defined half-life and thus need to be regularly replaced to ensure homeostasis in the body. HSC consists of long lived (LT) and short lived (ST) HSC. LT HSC possess a broad range of self-renewability capabilities. These capacities diminish with increasing lineage differentiation. ST HSC give rise to a multipotent progenitor cells (MPP). They split into several lineages, the common myeloid progenitor (CMP) giving rise to megakaryocyte and erythrocyte progenitor (MEP), as well as the granulocyte and macrophage progenitor cells (GMP) and the lymphoid-primed multipotent progenitor (LMPP) ³. The LMPP is able to give rise to the common lymphoid progenitor (CLP), the GMP and granulocyte/macrophage T cell progenitor. A lot of the steps for full commitment to a lineage are still unproven and up to debate ⁴. The LMPP also gives rise to the dendritic cell (DC) progenitor ⁵. DCs can be found all over the body and many subtypes exist. Differentiation can differ for different subtypes and take place in different organs ⁶. The CLP gives rise to T and B cell progenitors as well as the common innate lymphoid cell (ILC) progenitor. This common ILC progenitor in turn gives rise to natural killer (NK) and ILC progenitor cells ⁷.

6.2.1. Innate immunity

The innate immune system is the first line of defence once the physical barriers of the body have been breached. This system responds rapidly and in a non-pathogen-specific way. Cells like NK cells, ILCs,

neutrophils, basophils and macrophages are part of the innate immune system as well as soluble molecules such as the complement system and anti-microbial peptides^{8,9}.

Cells of the innate immune system do not recognize pathogen specific antigens, but danger signals¹⁰. These danger signals can be certain structures or molecules derived from the pathogen (pathogen associated molecular patterns (PAMP)) or signals derived from stressed or dying cells (danger associated molecular patterns (DAMP))^{11,12}. PAMPs are conserved structures expressed constitutively by pathogens including lipopolysaccharide, lipoproteins, peptidoglycan and lipoteichoic acids, but also nucleic acids from viral origin or viral coat proteins^{13,14}. These conserved structures are recognized by specialized receptors, termed pattern recognition receptors (PRR) on immune cells. PRRs are found extra- and intracellularly¹⁵. PRRs can be divided into five different classes: Toll-like receptors (TLRs), NOD-like receptors (NLRs), RIG-I-like receptors (RLRs), C-type lectin receptors (CLRs) and two AIM2-like receptors (ALRs), which are absent in melanoma¹⁶. TLRs are expressed on members of both the innate and adaptive immunity as well as some non-immune cells like fibroblasts. They are the most described PRRs family member. Ten receptors have been identified in humans¹⁷. The leucine rich repeats of the outer membrane are responsible for binding and recognizing PAMPs. Upon ligation, a dimerization (hetero/homo) occurs, leading to the recruitment of adaptor molecules to the intracellular signalling domain¹⁸. Downstream signalling can be dependent or independent of adaptor molecule MyD88. The downstream targets of this pathway are the transcription factors NF- κ B, AP-1 and IRFs resulting in inflammation and an anti-pathogen response¹⁹. TLR3/4 can also interact directly or indirectly with the adaptor protein TRIF independent of MyD88, leading to type I interferon production and a delayed activation of NF- κ B²⁰.

The complement (C) system plays a central role in the innate immune response, involving multiple different molecules and cells. Its function consists of opsonisation, inflammation and lysis²¹. In humans, complement molecules are mostly produced in the liver, however certain molecules can also be produced by other cell types like monocytes, fibroblasts and epithelial cells. The complement system is organized in a proteolytic cascade²². Activation can occur in three different ways: via the classical, the alternative and the lectin pathway. All pathways lead to the formation of a membrane attack complex, resulting in the release of inflammatory proteins in the bloodstream. Consequentially, dilatation of blood vessels, promotion of leukocyte adhesion and infiltration of these leukocytes in the tissues is promoted^{10,21,22}.

Cells of the innate immune system comprise neutrophils, eosinophils, basophils, ILCs, NK, mast cells, DCs and macrophages. Neutrophils, eosinophils, mast cells and basophils are also referred to more generally as granulocytes and are important in inflammatory reactions. They develop completely in the bone

marrow before migrating into the periphery^{23,24}. Granulocytes are known for their capability to release granules upon activation. These granules can hold proteolytic enzymes, antimicrobial peptides or cytotoxins^{25,26}. An added functionality of neutrophils and eosinophils is the formation of extracellular traps. The cells explode when they die and thus release their DNA into the extracellular space, hence trapping pathogens and exposing them to proteases^{27,28}.

DCs are the bridge between innate and adaptive immunity. They possess the capability to present antigens to members of the adaptive immune system, in turn activating them. DCs are professional antigen presenting cells (APC). They are found in tissues as well as lymphoid organs. DCs capture antigens within the tissues where they reside or within the periphery and travel to the lymphoid organs to present them. They can then promote either inflammation or central tolerance²⁹. Many different subsets exist. Conventional DCs (cDC) 1 in mice or CD141⁺ DCs in human can be found in lymphoid as in non-lymphoid tissues. They are strong interferon (IFN) III producers³⁰. In both humans and mice cDC1s are proficient cross-presenting cells, which means that they can present antigens taken up from the cytosol on major histocompatibility complex (MHC) class I molecules in order to prime CD8 T cells. They are mostly efficient in presenting antigens derived from dead cells³¹. cDC2 in mice or CD1c⁺ DCs in humans are present in lymphoid tissues as well as the periphery. They are potent producers of interleukin (IL)-12 upon activation, moreover they are also potent cross-presenting cells^{5,31}. Plasmacytoid DCs (pDCs) are specialized in producing type I interferons and inducing anti-viral immune responses³².

Macrophages are granular cells that can be tissue-resident or derived from monocytes upon inflammation. Dependent upon external stimuli they will respond in a different way. Macrophages mostly activated by TLR ligation, leading to IFN γ signalling, are mainly associated with viral and bacterial inflammation. These macrophages are most commonly called M1 macrophages. However, macrophages responding to allergies, helminths and asthma are mostly associated with the production of type two cytokines like IL-4 and IL-13. They are important in the wound healing process. They are called M2 macrophages^{33,34}. Rather than being mutually exclusive, these states often (partly) co-exist³⁵.

The group of innate lymphoid cells consists of ILCs and NK cells. They mirror the different subsets of T cells but lack antigen-specific receptors. Beside NK cells, three groups of ILCs exist: ILC1, ILC2 and ILC3. These subsets mirror the functions of CD4⁺ T cells and NK cells mirror cytotoxic T cells³⁶. ILC1s express the transcription factor T-bet and produce IFN γ and tumour necrosis factor (TNF) α after stimulation with IL-12 and IL-18. ILC2s produce IL-4 (in humans), IL-5, IL-13 and AREG after stimulation with IL-25, IL-33 and TSLP and express GATA3 as transcription factor. Group 3 ILCs can be further subdivided into lymphoid

tissue inducer (LTi) cells, natural cytotoxicity receptor (NCR)⁻ and NCR⁺ ILC3. They all express ROR γ T and produce IL-17A/F (except NCR⁺ ILC) and IL-22. The inducing cytokines are IL-23 and IL-1 β ³⁷. ILCs are activated very early on in the immune response as a reaction to signals or cytokines expressed by tissue-resident cells resulting in a strong amplification of the signal⁷. NK cells are cytotoxic cells able to kill altered self-cells like tumour and virally infected cells. The fate of a cell is based on the balance of ligation of activation and inhibitory receptors. Inhibitory receptors recognize amongst others MHC I molecules. Activating receptors recognize for example stress and viral inducible ligands (Figure 1)³⁸. Moreover, they are able to release large amounts of pro-inflammatory cytokines, like IFN γ and TNF α when activated³⁹. Two different subsets of human NK cells exists, based on the expression level of CD56 (neural adhesion molecule NCAM) and CD16 (low affinity Fc receptor). CD56^{bright} cells express high amounts of CD56 and do not express CD16. In the periphery they are a minor subset, around 5% of NK cells, but most prominent in lymph nodes and tissues. They have a lower cytolytic capacity but are very potent cytokine producers. CD56^{dim} cells on the other hand are also CD16 positive, they represent around 95% of NK cells in the periphery. They are considered as the most mature and are potent killers⁴⁰.

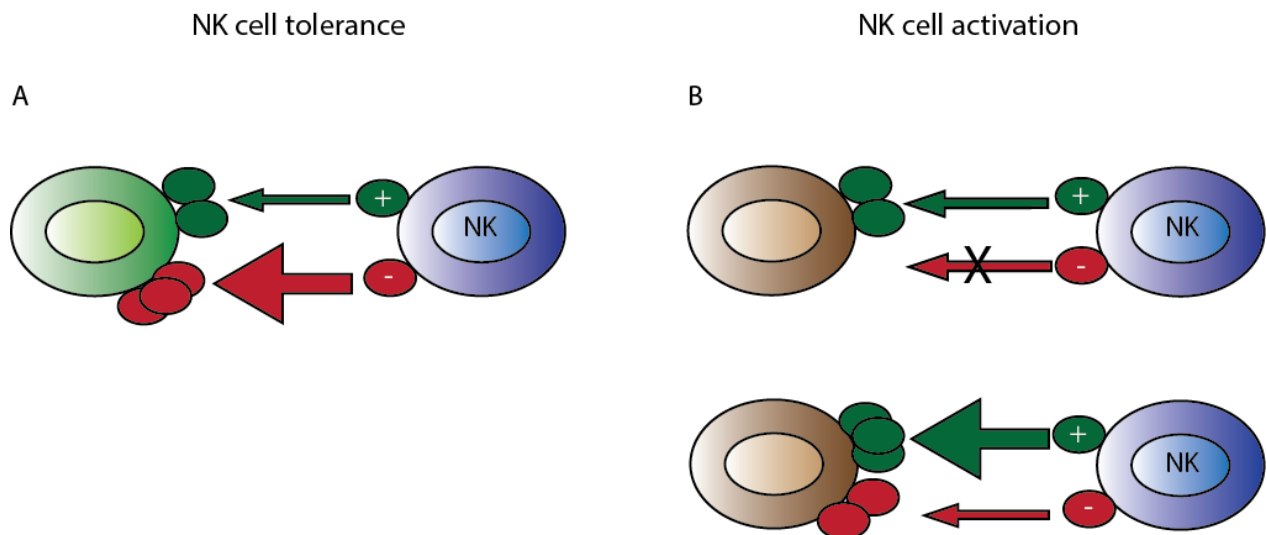


Figure 1 | NK cell activation or tolerance depends on the balance of inhibitory and activating signals received. A. NK cell tolerance occurs when more self-antigens (ligand) are present on the cell surface than activating ligands. Leading to the NK cell ignoring/tolerating this cell. B. NK cells become activated if no inhibitory ligands are present or if the number of activating ligands is higher than the number of inhibitory, leading to a net activating signal in the NK cells⁴¹.

6.2.2. Adaptive immunity or acquired immunity

The innate immunity works fast but it is pathogen non-specific, the adaptive or acquired immunity needs more time to generate a response. However, cells involved in this part of the immune system recognize

antigens in a specific way and are capable of memory formation, meaning that upon a second encounter of the same antigen, the response is faster and more vigorous ⁴². This specificity is made possible due to the occurrence of gene rearrangements within the B and T cell receptors (BCR and TCR) during development, leading to an enormous number of possibilities. A diversity of 10^{18} B cell receptors and 10^{15} $\alpha:\beta$ TCRs is estimated ^{43,44}.

T cells develop in the bone marrow but maturation takes place in the thymus. Due to the nature of the TCR generation by gene rearrangement many TCRs have unwanted specificities, either recognizing a self-antigen either being unable to interact with self-MHC. The thymus eliminates the former (negative selection) and the latter (positive selection), thus assuring that the $\alpha:\beta$ TCRs of mature T cells are restricted to self-MHC and are inefficient in recognizing self-peptides ⁴⁵.

T cells can be divided into two major subsets, based on the expression of CD4 or CD8. Both cell types recognize antigens loaded on MHC molecules on APCs or target cells. The provenance of the antigens can be self or non-self ⁴⁶. MHC class I molecules present peptides of 8-10 amino acids, MHC class II present peptides with a length of 13-25 amino acids ^{47,48}. Peptides loaded on MHC class I molecules are from endogenous origin. They are degraded in the proteasome and represent the endoplasmic reticulum (ER) of the cell. This allows the immune system to identify viral infected or tumour cells. CD8 or cytotoxic T cells bind to MHC I ⁴⁹. Since MHC I allows for the cell to convey its inner state, they are present on all cells. MHC class II molecules on the other hand are only expressed on APCs (macrophages, DCs and B cells) ⁴⁸. MHC II-peptide complexes interact with CD4 T cells. Antigens are taken up by APCs from the extracellular space, processed and presented. However, cross-presentation can occur in some DCs, during this process antigens from exogenous descent are presented to CD8 T cells on MHC I molecules. In this case the DCs themselves do not need to be infected ⁵⁰. T cell priming does not only involve TCR-peptide-MHC interaction but also ligation of co-stimulatory molecules ⁵¹. IL-12 or type I interferons are important as a third ⁵². Without these two additional signals T cells become anergic ⁵¹.

Cytotoxic T cells (CTL), characterized by the expression of CD8, kill their target by releasing lytic granules. These granules contain among others perforins, a pore forming peptide and granzymes, a serine esterase. Once granzymes reach the cytosol of the target cells, they trigger apoptotic cell death by activating caspases ⁵³.

CD4 or helper T cells can be further subdivided into a number of helper subsets and contain as well a subset of regulatory cells. Dependent on the immunological situation, different effector cytokines are

produced. These polarization states are defined by a master transcription factor and the cytokines produced⁵⁴. Th1 cells provide protection from intracellular pathogens and differentiation is mainly induced by IL-12 and IFN γ , produced by NK cells and other T cells⁵⁵. This leads to the activation of the transcription factor T-bet and the production of IFN γ ⁵⁶. T helper type 2 cells are important in helminth, allergy and asthma responses. They are induced from naïve cells by IL-4. This induces GATA-3 expression and in turn production of IL-4 is established^{57,58}. A third polarization state of CD4 T cells is Th17. They are induced by TGF β and IL-6, which induces the transcription factor ROR γ T. In turn Th17 cells produce IL-17, they are potent inducers of tissue inflammation and have also been associated with auto-immune diseases^{59,60}. Newer subsets include Th9 and Th22, both based on the cytokines they produce, IL-9 and IL-22⁶¹. IL-9 is induced by IL-4 and TGF β and the activation of transcription factor PU.1. IL-9 seems to play a role in helminth and allergic responses^{61,62}. Th22 cells produce IL-22 and TNF α , they can mostly be found in the skin. They are induced by IL-23 and IL-1 β in combination or not with IL-6⁶³. Follicular helper T cells are a separate subset of CD4 T cells that reside in the secondary lymphoid organs, they are necessary for B cell activation and memory formation. T_{FH} express the master regulator Bcl-6⁶⁴. A separate subset of helper T cells exists that counteracts inflammation, they are termed regulatory T cells (T_{reg}). The regulatory cytokines produced are IL-10 and TGF β , under the master transcription factor FoxP3⁶⁵.

B lymphocytes recognize antigens via their BCR, a membrane-bound antibody, and mainly characterized by the expression of CD19, CD20, CD21, CD81 and BAFF-family receptors. They develop totally within the bone marrow. Just as for T cells gene rearrangement takes place to ensure maximal diversity of receptors. However, the possibility exists that some of these receptors recognise self-antigens. Negative selection thus takes place to limit this option⁶⁶. Naïve B cells can be activated in a T cell dependent or independent manner. They express both IgM and IgD on the cell surface. T-cell independent activation leads to IgM secretion, however, without T cell support no affinity maturation or class switching takes place. This response is mostly polyspecific and acts like a barrier between innate and adaptive immunity⁶⁷. Activation of B cells with the help of T helper cells prompts a germinal centre reaction leading to not only highly effective antibody secreting cells (plasma cells) but also memory formation. In order for memory cells to be formed, activated B cells undergo somatic hypermutation leading to enhanced affinity BCRs and induces class switching of the antibodies. The class of isotype depends on the type of immune response needed⁶⁸. These switched memory cells express the marker CD27 but do no longer express IgD⁶⁹. An unswitched type of memory B cells also exists, they have left the germinal centre after the hypermutation but before the class switching, they thus still express IgD or IgM⁷⁰. A subset that expresses neither IgD nor CD27 exists within the periphery of humans, they also seem to belong to the memory compartment but

are poorly characterized. Within this population a mixture of IgA, IgM or IgG expressing B cells that have undergone hypermutation^{71,72}. The isotype of the antibody defines a lot its functionality. IgM is secreted as a pentamer increasing the avidity of multi-epitope binding. IgD has a long hinge region allowing for the ability to bind to low density antigens^{73,74}. This makes these isotypes very useful in early infections⁷⁵. IgG can be further subdivided into four classes IgG1-4. IgG3 having the greatest effector function, before IgG1, IgG2 and IgG4⁷⁶. The distribution and the affinity for the Fc-receptors determines for the most part their effector function⁷⁷. IgA is a mucosal antibody that can be excreted within the lumen⁷⁸. IgE is involved in helminth immunity and allergy and are potent activators of mast cells^{79,80}.

Recently, a population of regulatory B cells (B_{regs}) has been described, in mice called B10 cells. Up to date no markers have been described to characterize these cells specifically except for their function⁸¹. Even sequencing of IL-10 producing B cells did not lead to the identification of a specific transcription factor, giving rise to the theory that these cells are primarily induced by the environment and do not represent a separate lineage⁸². Regulatory B cells have been described to be able to inhibit numerous cell types like CTL, CD4 T cells, effector B cells, DCs and myeloid cells⁸³⁻⁹¹. Inhibition is induced via multiple mechanisms including IL-10, IL-35 or TGFβ⁸¹.

6.3. Melanoma

Melanoma is a type of skin cancer that develops in melanocytes⁹².

6.3.1. Epidemiology

An estimated 144 new cases with 27 deaths per 100 000 inhabitants for both sexes was assessed in 2018 in Europe⁹³. In Switzerland 6.7% of all new cancer cases are malignant melanoma, it's the fourth most prevalent cancer type in men and women. 2% of all cancer deaths are attributed to melanoma (period 2011-2015)⁹⁴.

6.3.2. Risk factors

Melanoma risk factors can be divided into environmental and genetic factors. They are multifactorial. Almost 8-10% of patients have a family history of melanoma. People with a light complexion (light skin, hair and eye colour) have a considerable higher risk of developing melanoma⁹⁵. The number of naevi (common and atypical) was found to be a very important risk factor⁹⁶. The most important environmental risk factor is sun exposure, but also artificial UV exposure in tanning beds contributes^{97,98}. UV radiation is able to induce DNA damage, when this damage is inadequately repaired, activation of oncogenes or silencing of tumour suppressor genes can induce oncogenesis^{99,100}.

6.3.3. Diagnosis

Early detection is very important in lowering the chances of disease severity. This is made possible by localization of melanoma on the skin. A number of criteria were developed to be used by the public and physicians, called ABCDE, which stands for Asymmetry, Border irregularity, Colour variegation, Diameter > 6mm and Evolving ¹⁰¹. A histology report gives more clarification and should indicate the maximum thickness (mm) (Breslow), mitotic rate, presence of ulceration, presence and extent of regression and clearance of the surgical margins, as well as information on the anatomical site and the type of melanoma (superficial spreading melanoma, lentigo maligna melanoma, acrolentiginous melanoma, nodular melanoma, others). Mutational genotyping is recommended in case of metastatic disease ¹⁰². Melanomas are staged, from I to IV with IV being the most advanced disease stage, based on the characteristics of tumour, the nodes and the presence and location of metastases ¹⁰³.

6.3.4. Treatment

Localized disease is treated by surgical removal of the tumour while respecting sufficient safety margins. Radiotherapy can be considered in the case of inadequate resection margins. In the case of non-resectable in-transit metastases other treatment options can be considered like infusion with Melphalan, a chemotherapeutical agent. In the case of systemic metastatic disease, immunotherapy strategies like α -CTLA-4 or α -PD-1 have shown good results as well as kinase inhibitors. A second line of treatment is chemotherapy ¹⁰⁴.

6.4. Tumour micro-environment

A cancer is not only made up of tumour cells but the environment also contains immune and stromal cells, which we call the tumour micro-environment (TME) ¹⁰⁵. Cells of the immune system, adaptive and innate, are able to recognize tumour cells. Tumour-specific antibodies have been found in patients, indicating a successful B cell response ^{106,107}. Tumour-specific CD8 T cells can be found within the tumour as well as in the periphery ^{108,109}. Tumour-specific CTLs are able to lyse autologous tumour cells *in vitro* ¹¹⁰. The antigens recognized can be from mutated proteins, which are patient specific (neo-antigens), as well as specific to the tissue of origin of the tumour, genes overexpressed in the tumour, of viral descent or cancer-germline genes ^{111,112}. In melanoma the presence of tumour-infiltrating lymphocytes (TILs) is a prognostic factor for survival ^{113,114}. Especially the presence of T cells, both CD8 and CD4 T (mostly Th1) cells was found to correlate with survival in multiple cancer types ¹¹⁵⁻¹¹⁷. Additionally NK cells are able to kill tumour cells *in vitro* as well as *in vivo* ¹¹⁸⁻¹²⁰. For a successful anti-tumour response a lot of different steps need to take place in an efficient way. First of all, antigens (neo- or germline encoded) released by the tumour need to be taken up for processing by DCs ^{121,122}. Uptake of antigens needs to be accompanied by additional pro-

inflammatory signals like cytokines, TLR ligands from dying tumour cells, but also chemotherapeutical agents are able to induce immunogenic cell death in order to avoid peripheral tolerance and the induction of T_{regs} by APCs^{123–125}. For potent stimulation of T cells, presentation on the cell surface by class I or II MHC molecules needs to be accompanied by co-stimulatory molecules and cytokines, this last step takes traditionally place in the lymph nodes¹²⁶. It can, however, also take place in so called tertiary lymphoid structures (TLS), these structures form spontaneously within the tissue and have lymphoid properties, like a distinct T and B cell zone¹²⁷. Once the priming is complete the T cell needs to traffic back to the TME to carry out their effector function¹²⁸. Killing the cancer cells will complete the circle since it leads to a consecutive release of antigen (Figure 2). However, in cancer patients this circle does not work optimally, at each of these steps things can go wrong.

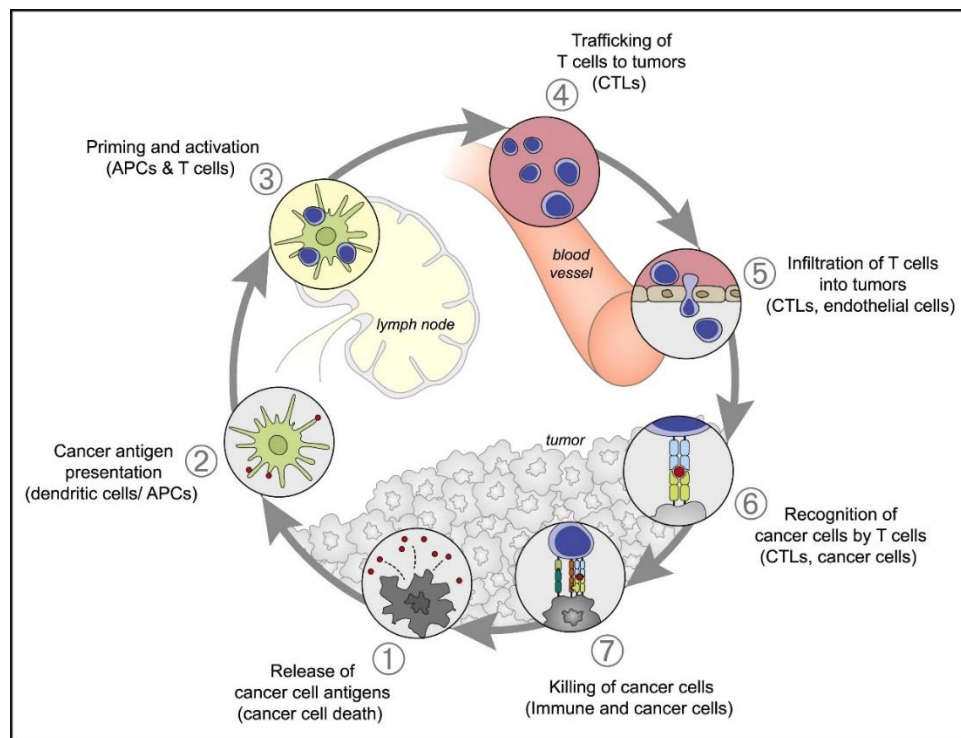


Figure 2 | The cancer immunity cycle consists of seven distinct steps, including the release of cancer antigen at the tumour site, uptake of these antigens by APCs and trafficking to the lymph nodes, priming of T cells, homing of activated T cells to the tumour site, infiltration in the tumour and killing of the recognized tumour cells, which restarts the cycle with the release of antigens¹²⁹.

Dysfunctional T cells can disrupt the cancer-immunity cycle. After the induction of a strong inflammatory response, multiple mechanisms are in place to limit unnecessary inflammation that could damage the body¹³⁰. Since tumours express self-antigens, a regulatory response is put in place, often strengthened by molecules produced or ligands expressed on the surface of the tumour cells¹³¹. T_{regs} can be found, sometimes in high numbers within the TME, their presence is associated with bad prognosis. They are able

to suppress T cell response by producing regulatory cytokines IL-10, transforming growth factor (TGF)- β and express the inhibitory receptor CTLA-4¹³²⁻¹³⁴. T_{reg} depletion was shown to retard tumour growth *in vivo*¹³⁵. Moreover, immune checkpoint blockade antibodies against CTLA-4 could lead via antibody-dependent cell cytotoxicity (ADCC) to the depletion of CTLA-4 expressing T_{regs}.¹³⁶ DCs found in the TME are often immature and tolerogenic¹³⁷. They can induce anergy in T cells or induce T_{regs}.¹³⁸ Myeloid-derived suppressor cells (MDSC) are cells from myeloid descent that did not differentiate further into DCs, macrophages or granulocytes. They have potent immunosuppressive capacities, their mechanisms include: production of nitric oxide, reactive oxygen species, indole amine 2,3 dioxygenase (IDO), IL-10 and TGF β ¹³⁹. The functionality of tumour associated macrophages (TAM) depends on the polarization. M1 type macrophages are able to suppress tumour growth¹⁴⁰. M2-like macrophages reside in hypoxic regions of the tumour and suppress type I inflammatory responses by producing arginase-1, suppressive cytokines like IL-10 and stimulate directly tumour progression by producing angiogenic factors like vaso-endothelial growth factors (VEGF), metalloprotease (MMP)-9, due to the production of tissue remodelling factors metastasis is favoured by M2-like TAMs¹⁴¹⁻¹⁴⁴. New therapies are focusing on reprogramming TAMs to support complementary therapies and improve efficacy¹⁴⁵⁻¹⁴⁸. A big part of the TME is made up of fibroblasts, they exhibit great plasticity and are able to suppress immune responses and facilitate tumour growth and metastasis¹⁴⁹⁻¹⁵¹. Also tumour cells themselves produce immunosuppressive factors via a conserved mechanism to limit tissue inflammation, like the expression of PD-L1 or IDO¹⁵². They are also able to downregulate MHC expression to avoid T but not NK cell recognition¹⁵³. All these factors interplay, leading to the creation of an immunosuppressive TME (Figure 3).

Dysfunctional T cells are characterized by the expression of one or more inhibitory receptors like, PD-1, CTLA-4, TIM-3, LAG-3, etc.¹⁵⁴. This state is defined by a effector-function impaired state, a condition first described in chronic viral infections¹⁵⁵⁻¹⁵⁷. Immunotherapy has taken advantage of the expression of these inhibitory receptors by developing blocking antibodies¹⁵⁸. This strategy has led to durable response in a number of cancer types and patients, especially antibodies targeting CTLA-4 and PD-1 are a big success^{159,160}.

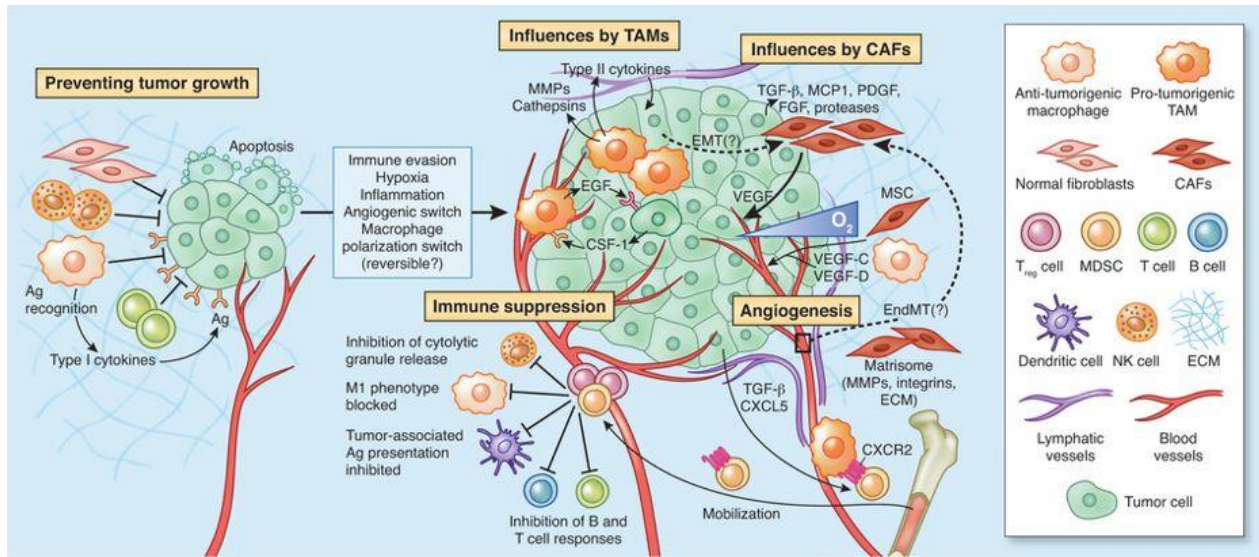


Figure 3 | Several immunosuppressive mechanisms have been discovered within the tumour microenvironment. Ranging from direct T cell expression by the tumour cells to the recruitment of immune suppressive cells like CAFs, T_{regs} and myeloid cells¹⁶¹.

7. My PhD projects

According to the World Health Organisation, cancer is the second leading cause of death in the world, causing an estimated 9.6 million deaths in 2018. Strategies to reduce this number are: diminishing risk factors like smoking, alcohol use and unhealthy diet as well as early detection. There is a good chance for a cure if cancer is detected early and treated adequately. In the last decades, huge strides have been made into new therapy avenues producing long lasting effects. Especially the development of immune checkpoint blocking antibodies have been a big breakthrough, leading Science magazine to call cancer immunotherapy the breakthrough of the year 2013. However, not all patients respond to immunotherapy and it is more successful in some cancers than others. New avenues need thus to be explored. Immunotherapy as we mostly know it today, is highly focussed on the role of cytotoxic T cells, however they are not the only cells taking part in immune responses in the tumour microenvironment and systemically.

In my thesis, I asked the question whether other types of lymphocytes impact on tumour growth and clinical outcome of melanoma patients. My work was focused on three lymphocytic populations: NK cells, B cells, and a novel not yet described type of human lymphocytes.

NK cells are innate cells that have an innate ability to kill tumour cells *in vitro*. They have been shown to be important in immune surveillance. However, most information we have on the functionality of NK cells comes from mouse models. Moreover, conflicting studies have reported that NK cells are both, tumour-promoting and tumour-inhibiting. Therefore, my first project is focussed on the possible role of NK cells and its subsets in the immune response to melanoma.

During my second project, we delved into the characterisation of B cells in melanoma patients, their implications in tumour still being unclear. B cells have been described to have a dual role within the tumour immune response, both pro-and anti-tumorigenic. We characterized B cells in the periphery and the tumour microenvironment of patients before receiving treatment.

The object of these two first projects was to better understand the complexity of the immune response in patients against melanoma in the hopes of advancing the knowledge leading to new therapeutic avenues as well as biomarker discovery.

The third project was born out of the NK cell project. During the course of my PhD we stumbled upon an undescribed immune population that comprises around 0.2% of lymphocytes within the PBMCs of healthy

donors. We have termed these cells Orphan Lymphoid Cells (OLCs). During this project, the objective was to characterize this novel cell population and to identify their molecular features.

Overall our goal was to further our knowledge about the immune system in health and disease, particularly in cancer.

8. Circulating CD56^{bright} NK cells inversely correlate with survival of melanoma patients

8.1. Introduction

NK cells are important players in anti-intracellular pathogen immunity. Different subsets exist in different tissues¹⁶². NK cells have been shown to be particularly important in controlling infections of the herpes virus family in patients with NK cell deficiencies¹⁶³. The expression of both inhibitory and activating receptors results in tolerance towards healthy cells and activation upon the encounter of unhealthy cells. Moreover, NK cells adapt highly to the environment in which they find themselves⁴¹. NK cells do not only contribute to immunity by killing target cells but also modulate responses. They are major producers of the cytokines IFN γ and TNF α , but also IL-10, GM-CSF, G-CSF and IL-3. Moreover, they have also been reported to produce multiple chemokines like MCP-1 (CCL2), MIP1 α (CCL3), MIP1 β (CCL4), RANTES (CCL5), lymphotactin (CCL5) and IL-8 (CXCL8)¹⁶⁴. During T cell priming, NK cells are an early source of IFN γ , able to induce a Th1 response¹⁶⁵. Early in infection cross-talks take place between DCs and NK cells. Mature DCs promote NK cell activation by producing type I IFNs, IL-12 or TNF α . As a consequence, NK cells produce TNF α and IFN γ leading to a further maturation of DCs¹⁶⁶. NK cells can also enhance cross-presentation. Namely, during killing of target cells, antigens are released that can be presented to CTLs¹⁶⁷. Moreover, NK cells participate in a process called DC-editing. During this process NK cells specifically kill immature DCs and spare the mature ones. This mechanism ensures proper activation of T cells by DCs expressing sufficient co-stimulatory molecules¹⁶⁸.

In humans, the two main subsets of NK cells are CD56^{bright} and CD56^{dim} NK cells. It is thought that CD56^{bright} cells are the precursors of the cytotoxic CD56^{dim} NK cells. The former gain a CD56^{dim} signature upon cytokine activation and possess longer telomeres than their more mature counterpart¹⁶⁹. NK cell activation or tolerance is based on a balance of interactions between activating and inhibitory receptors (Figure 4). Activating receptors could be receptors for soluble ligands like cytokines or receptors involved in cell-to-cell contact. All NK cells express the common γ chain. CD56^{bright} express additionally IL-2R α whereas CD56^{dim} express the lower affinity receptor IL-2R β . The latter is able to bind both IL-2 and IL-15¹⁷⁰. A variety of receptors induces cytotoxicity upon ligation of NCRs, including NKp46, NKp30 and NKp44. NKp46 and NKp30 are expressed at all activation stages. NKp46 has also been used as an NK cell specific marker¹⁷¹. It has been reported that NKp46 binds to hemagglutinin on virus-infected cells¹⁷². NCR receptors transduce signals intracellularly via CD3 ζ , Fc ϵ R1 γ and DAP12¹⁷³. One of the abilities of NK cells is not only to recognise virally infected cells but also stressed cells. The receptor responsible for this

recognition is NKG2D. The ligands on target cells are related to MHC I molecules, the MIC-A/B and ULBP1-6 ligands¹¹⁹. Another activating receptor that is preferentially expressed on CD56^{dim} NK cells is the FcγRIIIA (CD16) receptor that binds the Fc-portion of antibodies with low affinity and is important in inducing NK cell mediated ADCC¹⁷⁴. Many ligands for activating receptors are also expressed by normal and healthy cells. However, mechanism need to be in place to ensure the absence of auto-reactivity¹⁷⁵. The amount of inhibitory ligands engaged counterbalances the activating receptors engaged. If this balance tips over to activation due to too low inhibitory signals or overwhelming activating ligands, the NK cell will get activated⁴¹. MHC class I molecules are widely expressed and are one of the types of molecules recognised by inhibitory receptors on NK cells. The recognition of MHC is ensured by a number of receptors: leukocyte Ig-like receptor B1 (LILRB1), human killer Ig-like receptors (KIR) and NKG2A. These receptors are not expressed by all NK cells but rather in a random fashion. Other inhibitory receptors include LAIR-1 and KLRG1¹⁷⁶.

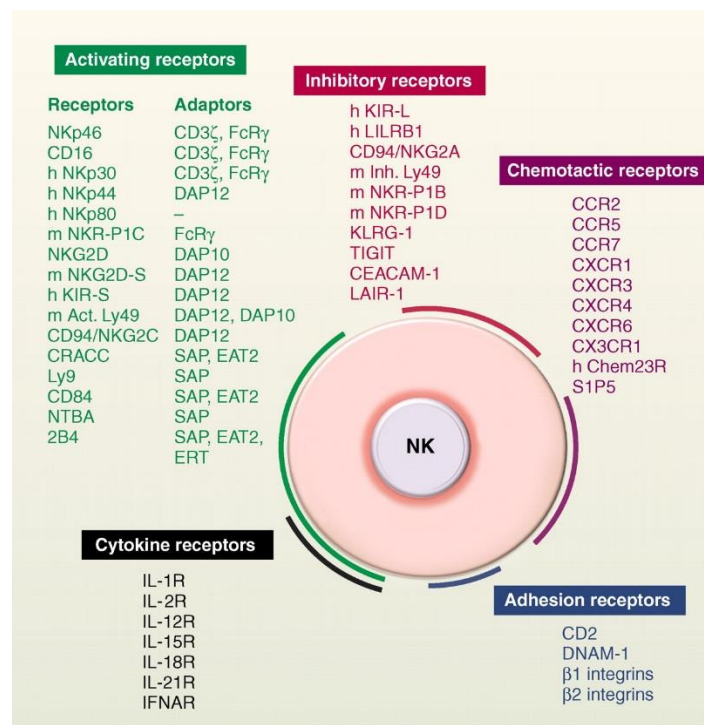


Figure 4| NK cells express a wide array of receptors, including activating receptors (green) and their corresponding adaptor molecules, inhibitory receptors (red), chemotactic receptors (purple), cytokine receptors (black and adhesion receptors (blue). h specifies only expression in humans, m in mice, no specification indicates expression in both humans and mice⁴¹.

Recent findings have demonstrated that NK are not only able to promote the immune response but are also able to impair them. It was shown in a mouse model of LCMV infection that in the absence of NK cells early in infection, CTL responses but not T helper responses were more potent and led to the clearance of an otherwise chronic infection. This increased responses seem to depend on the co-stimulatory capacity of DCs. *In vitro* DCs isolated from NK cell depleted mice were able to activate CD8 T cells better than DCs from wild-type mice. This mechanism is especially important in early infection¹⁷⁷. During MCMV infection, it was shown in mice that NK cells can directly kill infected DCs limiting T cell immunity¹⁷⁸. Moreover, during the bidirectional crosstalk between NK cells and DCs, NK cells also produce some IL-10, leading to a negative regulation¹⁷⁹. It seems that the mechanism to improve DC presentation or limit it, is dependent on the ratio of NK cells to DCs. A low ratio induces activation whereas a high ratio favours limitation of T cell priming by DCs¹⁶⁸. During early infection, T cells undergo a rapid clonal expansion. NK cells are able to kill these early activated T cells. Some of the NK cell receptors involved in this process have been described and include NKG2D, DNAM-1, NKp46, 2B4, LFA and FasL^{180,181}. Indirect regulation of T cells has also been reported, NK cells produce IL-10 during chronic viral infection in mice thus limiting the immune pathology¹⁸². T cells are protected after type I interferon sensing, this leads to a downregulation of NK cell ligands¹⁸³. This mechanism seems to ensure that only fully activated T cells, having received the three signals for activation survive as well as limiting immune pathology¹⁸¹. These mechanisms seem particularly important during early infection. However, NK cells also play a regulatory role during the later stages of chronic infection, since depletion of NK cells after the peak of the CTL response led to an improvement^{184,185}. NK cells are thus able to shape the immune response in a multitude of ways (Figure 5).

NK cells are often seen as a positive factor in the anti-tumour immune response since their involvement in immune surveillance has been shown multiple times^{118–120,186}. NK cells are a valuable alternative to CTLs for tumour killing. They do not require clonal selection and expansion, moreover they are safe to use in an allogeneic setting for adoptive transfer. Furthermore, their important interactions with DCs are also relevant in the TME. NK cells have been shown to produce CCL5 and XCL1 that attract cDC1, important for the establishment of an anti-tumour immune response¹⁸⁷. Also the trafficking of stimulatory DCs to the TME is mediated by, among others, NK cells via the production of FLT3LG¹⁸⁸. Multiple ligands for activating receptors are also expressed by tumour cells as reviewed by Vitale, *et al.*¹⁸⁹. NK cells are indispensable in the success of graft-versus-leukaemia by transfer of T cell-depleted, MHC haploid-identical, allogeneic, hematopoietic stem cells. In this instance a mismatch between the KIRs of the donor and the MHC class I expressed by the host cell can lead to NK cell activation based on the missing self-hypothesis. The success of this therapy has sparked further interest into the development of NK cell based therapies like adoptive

NK cell transfer, infusion of recombinant cytokines (IL-2/IL-15) to boost NK cell functionality and infusion of chimeric antigen receptor (CAR) NK cells¹⁹⁰. NK cell infiltration was associated with a favourable disease outcome in oesophageal carcinoma patients, head and neck squamous cell carcinoma patients, gastric cancer, HCC patients and CRC patients^{191–194}.

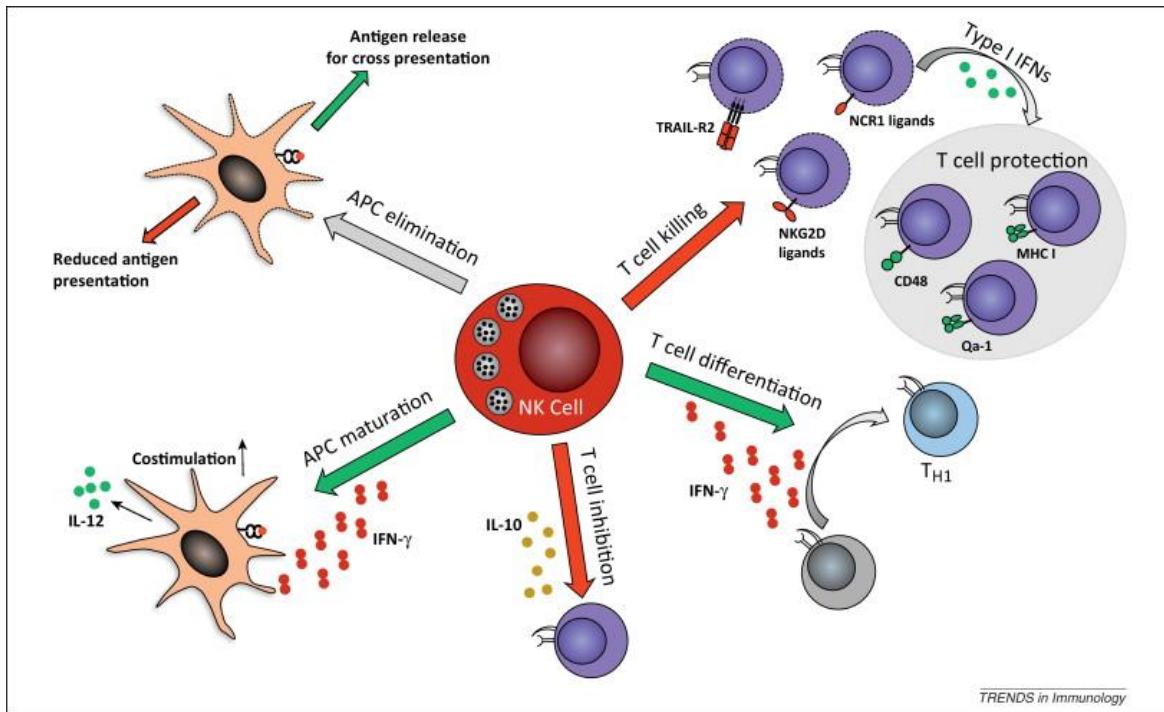


Figure 5| NK cells influence the immune response in a both stimulatory (green) and inhibitory (red) manner. They are able to induce APC maturation by producing IFN γ . APC elimination can lead to the release of antigens for cross-presentation but also limits the amount of DCs available for antigen-presentation. They are able to induce a Th1 response by producing IFN γ and limit the T cell response by producing IL-10. T cell killing occurs to ensure only persistence of fully activated T cells. Type I interferon sensing by T cells protects them from NK cell mediated killing¹⁹⁵.

However, during previous research often NK cell non-specific markers are used like CD56 and CD57. In solid cancers the efficacy of NK cell-mediated cytotoxicity remains unclear¹⁸⁹. Just as described for T cells, NK cells can become exhausted within the TME. It was shown that NK cells isolated from human tumours displayed impaired effector functions, characterized by a decrease in IFN γ , granzyme B and perforin production, lower degranulation capacity (as measured by CD107a) and an impaired killing capacity^{196–198}. This functional exhaustion can co-occur with a downregulation of activation receptors like NKG2D, NCRs and CD16¹⁹⁹. Upregulation of the immune checkpoint PD-1 has also been reported²⁰⁰. Not only activating receptors are decreased, but also the upregulation of inhibitory receptors like NKG2A has been described¹⁹⁶. NKG2A blocking antibodies are able to reverse this exhaustion and increase the effector functionality of both NK and T cells²⁰¹. Research has also discovered a role for NK cells in the direct promotion of tumour progression. NK cells are found in the peritumoural and stromal area of the tumour in NSCLC patients,

displaying a decidual NK cell phenotype (CD56^{superbright} CD16⁻) producing angiogenic factors like VEGF, PIGF and IL-8^{197,202,203}. It is thought that the presence of TGFβ and hypoxia within the TME could lead to the induction of a decidual phenotype derived from CD56^{bright} NK cells^{204,205}. The tumour employs additional methods to escape NK cell killing, for example by expressing PD-L1 and producing IL-10 and PGE₂²⁰⁶. Moreover, tumour cells can shed soluble ligands for activating receptors NKp30 and NKG2D, which can lead to their desensitization²⁰⁷. The inhibitory ligand HLA-G is expressed and secreted by tumour cells, upon interaction with NK cells via KIR2DL4, NK cells secrete pro-inflammatory and pro-angiogenic factors²⁰⁸. Soluble HLA-G also modulates chemokine receptor expression and thus an alteration of trafficking to the TME could take place²⁰⁹. The interaction between NK cells and tumour cells are very complex and can be both anti-as pro-tumoural (Figure 6).

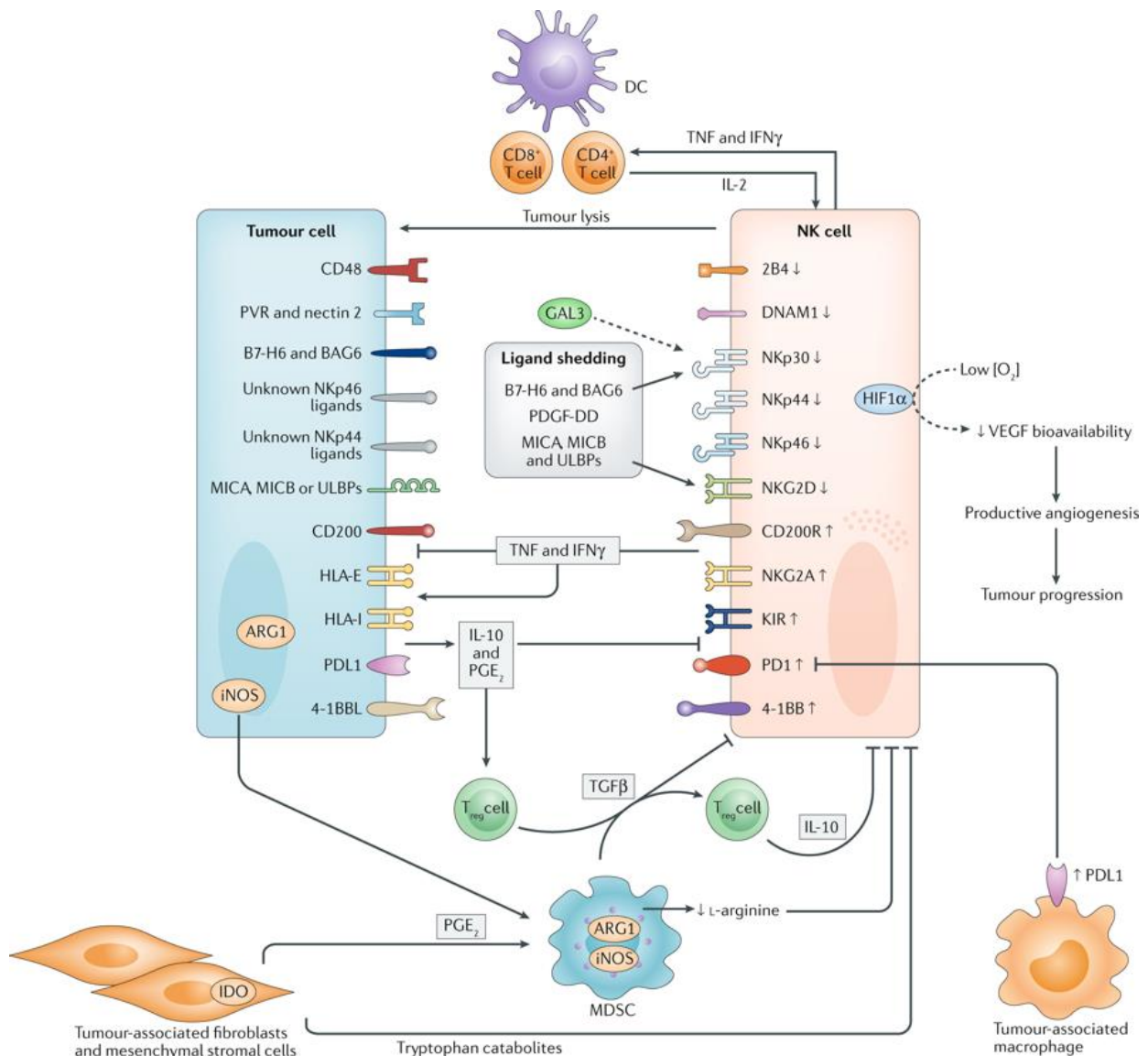


Figure 6 | The interplay between NK cells and tumour cells as well as other cells of the TME is complex. NK cells can directly kill by lysis or inhibit tumour progression by producing IFN γ or TNF α . They can via those cytokine also induce T cell activation. However, multiple mechanisms are in place to inhibit their functionality ranging from ligand shedding, inhibition by IL-10 and PGE $_2$ produced by the tumour and TGF β and IL-10 produced by regulatory T cells, IL-10 by MDSCs or tryptophan catabolites produced by fibroblasts. Ligation of PD-L1 on tumour or tumour-associated macrophages with PD-1 on NK cells can also lead to the attenuation of their functionality ²⁰⁶.

8.2. Aim

In melanoma patients NK subsets (CD56^{bright} and CD56^{dim}) frequencies have been described as either unaltered or decreased in the blood of metastatic melanoma patients ²¹⁰⁻²¹². Alterations in receptor expression was reported, including lower expression levels of activation receptor NKG2D on CD56^{dim} NK cells and increased KIR levels on CD56^{bright} cells, as well as an overall downregulation of NKp46 was reported by others ^{210,211}. Functional assessments showed either impaired IFN γ production and degranulation as measured by CD107a expression or no changes in functionality ^{210,211,213}. Thus making it unclear what the role of NK cells is. Functionality was mostly assessed on total NK cell populations, irrespective of the underlying subsets, they however differ substantially in their cytolytic and cytokine producing capacities.

Our aim is to describe phenotypically and functionally NK cells and their subsets in the blood of melanoma patients. We used a cohort of patients studied extensively in the lab included in a clinical trial (ClinicalTrials.gov; Identifier: NCT00112229) and focussed on the time point before treatment in order to have a better view on the inherent immune response. Using patient samples from this clinical trial gives us the possibility to access a vast amount of clinical data and evaluate the parameters in relationship to clinical outcome.

8.3. Co-author contributions

This work is presented in an article published in March 2019 in the journal Scientific Reports.

Figure 1	Kaat de Jonge designed and performed the experiment
Figure 2	Kaat de Jonge designed and Kaat de Jonge and Petra Baumgärtner performed the experiment
Figure 3	Kaat de Jonge designed and Anna Ebering performed the experiment
Table 1	Kaat de Jonge designed and performed the experiment
Supplementary Figure 1	Kaat de Jonge designed and performed the experiment
Supplementary Figure 2	Kaat de Jonge designed and Kaat de Jonge and Anna Ebering performed the experiment
Supplementary Figure 3	Kaat de Jonge designed and Anna Ebering performed the experiment
Supplementary Figure 4	Kaat de Jonge designed and performed the experiment
Supplementary Table 1	Hélène Maby-El Hajjami provided the clinical data

Kaat de Jonge wrote the manuscript and received feedback from all co-authors. The experiments in Figure 3, Supplementary Figure 2A and Supplementary Figure 3 were designed by Kaat de Jonge and performed by Anna Ebering, a master student under my supervision. Sina Nassiri performed bio-informatics experiments that were unfortunately, at this stage, too preliminary to include in the manuscript. He provided additional advice and support on the statistical analysis performed during this study. Hélène Maby-El Hajjami and Hajer Ouertatani-Sakouhi performed the clinical follow-up of the patients in this study and provided the necessary information. Petra Baumgärtner provided support and advice for the cell culture, stimulation protocols and flow cytometry. She also, together with Daniel Speider provided supervision and guidance during my PhD thesis.

SCIENTIFIC REPORTS

OPEN

Circulating CD56^{bright} NK cells inversely correlate with survival of melanoma patients

Kaat de Jonge¹, Anna Ebering¹, Sina Nassiri^{1,3}, H el ene Maby-El Hajjami¹,
Hajer Ouertatani-Sakouhi¹, Petra Baumgaertner¹ & Daniel E. Speiser^{1,2}

Received: 27 October 2018

Accepted: 19 February 2019

Published online: 14 March 2019

The roles of NK cells in human melanoma remain only partially understood. We characterized NK cells from peripheral blood *ex vivo* by flow cytometry obtained from late stage (III/IV) melanoma patients. Interestingly, we found that the abundance of CD56^{bright} NK cells negatively correlate with overall patient survival, together with distant metastases, in a multivariate cox regression analysis. The patients' CD56^{bright} NK cells showed upregulation of CD11a, CD38 and CD95 as compared to healthy controls, pointing to an activated phenotype as well as a possible immune regulatory role in melanoma patients. After stimulation *in vitro*, CD56^{bright} NK cells produced less TNF α and GM-CSF in patients than controls. Furthermore, IFN γ production by the CD56^{bright} NK cells correlated inversely with overall survival. Our results highlight that abundance and function of CD56^{bright} NK cells are associated with melanoma patient survival, emphasizing the potential of NK cell subsets for biomarker discovery and future therapeutic targeting.

Melanoma is, next to squamous cell carcinoma and basal cell carcinoma, one of the three major types of skin cancer¹. Due to its highly metastatic potential, with metastases developing amongst others in lymph nodes, liver, lung and brain, the mortality rate is highest for melanoma amongst the three skin cancer types, although being the least frequent. While the number of people suffering from melanoma grows worldwide, the survival rates of metastatic melanoma patients remain inadequate. Treatments with immune checkpoint blocking antibodies such as Ipilimumab (anti-CTLA-4) and Nivolumab (anti-PD1) result in progressively increased rates of clinical responses. However, many patients still do not respond to available therapies². Mechanisms of response to checkpoint blockade are not completely understood. Among other players, NK cells may potentially modulate immunotherapy effects³.

NK cells are part of the innate immunity branch of the group of innate lymphoid cells (ILC)⁴. They are potent killers of virally infected as well as cancer cells without needing prior sensitizations⁵. Moreover, they are potent cytokine producers⁶. In humans, NK cells can be divided into two main subsets, comprising the immature, poorly cytotoxic but cytokine-producing CD56^{bright}, and the mature, cytolytic, weakly cytokine-producing CD56^{dim}CD16⁺ NK cells. CD56^{bright} NK cells only make up around 10% of NK cells in the periphery; they are, however, the major subtype in tissues and second lymphoid organs⁷.

NK cells are often seen as a positive factor in the anti-tumour immune response since their involvement in immune surveillance has been shown multiple times^{8–11}. For example, in rag mice that lack an adaptive immune system, the production of IFN γ by NK cells was found indispensable in the immune editing process¹². Additionally, mice without natural killer cells are less able to reject several tumour cell lines, including B16 melanoma cells⁹. Moreover, injection of pre-activated murine NK cells persisted within the tumour and they were able, in combination with radiotherapy, to significantly reduce the growth of primary tumours and metastases¹³. In melanoma patients, NK cells have been studied in both the peripheral blood as well as in tissues, however they are yet insufficiently characterized and contradictory results have been found¹⁴. Some investigators have reported unaltered frequencies of CD56^{bright} and CD56^{dim} subsets in blood of metastatic melanoma patients^{15,16}, whereas others have found a decrease in both subsets¹⁷. Moreover, peripheral NK cells appeared to have impaired IFN γ production and degranulation^{15,18}. CD56^{dim} NK cells derived from blood expressed lower levels of the activation receptor NKG2D,

¹Department of Fundamental Oncology, University of Lausanne, Epalinges, Switzerland. ²Department of Oncology, University Hospital Center (CHUV), Lausanne, Switzerland. ³Swiss Institute of Bioinformatics (SIB), B atiment G enopode, Lausanne, Switzerland. Correspondence and requests for materials should be addressed to D.E.S. (email: doc@dspeiser.ch)

and CD56^{bright} NK cells expressed higher levels of the inhibitory KIR receptor CD158b¹⁵. Fregni *et al.* reported decreased expression of the natural cytotoxicity receptor Nkp46, in line with previous publications. However, they reported no significant differences between patient and healthy controls in the production of IFN γ and the degranulation marker CD107a¹⁶. NK cells are able to infiltrate primary tumours especially in the peritumoral area¹⁶. Trosh *et al.* characterized the tumour micro-environment (TME) in metastatic melanoma by single cell analysis and found NK cells present in small numbers within the tumor¹⁹. The presence of total NK cells in the TME was found to positively correlate with clinical outcome in patients with colorectal carcinoma, gastric carcinoma and non-squamous lung carcinoma^{20–22}. Little information is available about NK cell phenotype and functionality in primary melanoma. One study showed that NK cells within tumour-infiltrating lymphocytes (TILs) are CD56^{bright}CD16^{dim}, a phenotype that is also found in regulatory decidual NK cells¹⁴. Other studies have focused on the NK cell phenotype in tumour-infiltrated lymph nodes, reporting an enrichment of CD57⁺KIR⁺CD56^{dim} NK cells, which are very efficient at killing autologous melanoma cell lines¹⁷, suggesting a fully mature and effector phenotype. The ratio of CD56^{dim}CD57⁺ to CD56^{bright}CD57⁺ seems to be biologically important and associated with survival in stage III melanoma patients¹⁷. Messaoudene *et al.* reported the presence of activated NK cells in tumour-infiltrated lymph nodes, expressing higher levels of Nkp46, NKG2D, Nkp44, DNAM-1 and Nkp30. Moreover, they found a population of CD56^{bright} NK cells expressing CD16 as well as other activation receptors and KIRs. This population could also be found in lymph nodes adjacent to tumour-infiltrated lymph nodes but not in the blood²³.

NK cell based therapies have not been successful in solid tumors²⁴. However, NK cells are associated with durable responses after various therapies. NK cells are mediators of antibody-dependent cell cytotoxicity and have been shown to interact with α -CTLA-4 antibody, whilst at the same time inducing NK cell maturation²⁵. A new experimental therapy targeting both CD8 T cells and NK cells by blocking the NKG2A receptor has shown early promising results in squamous cell carcinoma patients²⁶. Interestingly, the frequency at baseline of CD56^{bright} NK cells in blood of melanoma patients treated with Ipilimumab was negatively correlated with overall survival²⁷.

Our goal was to characterize circulating NK cells and their subpopulations as well as their functionality in late stage (III/IV) melanoma patients. We hypothesized that apart from a reduced anti-tumour function they could also play regulatory roles. We found that CD56^{bright} NK cells are negatively correlated with overall survival of the melanoma patients. Therefore, we determined the phenotypic and functional characteristics of circulating CD56^{bright} NK cells, improving the basis for a better understanding of NK cell tumour biology and future optimization of cancer immunotherapy.

Results

The frequency of circulating CD56^{bright} NK cells correlates inversely with patient survival. We studied 29 late stage (III/IV) melanoma patients²⁸ included in a vaccine clinical trial, and focused on NK cells before treatment start. PBMCs were analysed directly *ex vivo* by flow cytometry, using the gating strategy as represented in Figure 1A. 1 patient was excluded due to technical issues. 13 healthy donors were included as controls. We found no difference in the frequency of total NK cells as well as CD56^{bright}CD16⁺ and CD56^{dim}CD16⁻ NK cells between patients and healthy donors (Fig. 1B). Interestingly, patients with high frequencies or absolute numbers of CD56^{bright} NK cells had significantly shorter overall survival than patients with low frequencies or absolute numbers (Fig. 1C,D). We did not find a significant correlation between absolute numbers of CD56^{bright} and CD56^{dim}CD16⁺ NK cells, indicating that the negative correlation between overall survival and the number of CD56^{bright} NK cells is not a result of corresponding low numbers of CD56^{dim}CD16⁺ NK cells (Fig. 1D). Frequencies and numbers of peripheral CD56^{bright} NK cells did not only inversely correlate with overall but also progression free survival (Fig. 1E). No significant correlation was observed between patient survival and total NK cells, or CD56^{dim}CD16⁺ or CD56^{dim}CD16⁻ NK cells (Fig. 1C). Frequencies of NK cells and their subsets were similar in healthy donors and melanoma patients at stage III and IV (Suppl. Fig. 1A). Numbers of CD56^{bright} NK cells does not significantly differ between stage III and IV patients (Suppl. Fig. 1B). Frequencies of CD56^{bright} NK cells are not significantly different between patients having received any previous treatment (chemo, radio or immunotherapy) (Suppl. Fig. 1C–E). Since CD56^{bright} NK cells seem to be a prognostic factor for survival, we decided to characterize them in more detail.

CD56^{bright} NK cells have an activated phenotype in patients. Patient and healthy control NK cells were analysed for the expression levels of multiple NK cells markers, inhibitory and activating receptors as well as activation markers by flow cytometry. As compared to healthy donors, circulating CD56^{bright} NK cells of melanoma patients showed elevated expression of CD11a, CD38 and CD95, as measured directly *ex vivo* (Fig. 2A,B). The observations were consistent after patients were stratified according to their disease status: stage III or IV (Fig. 2C). We did not observe any difference in the expression levels of NKG2A, Nkp46 or NKG2D (Fig. 2D), and these markers were also consistently expressed in patients at different disease stages (Fig. 2E). We did not observe expression of KLRG1, CD158b1,b2,j (a pan KIR marker) or CD57 (data not shown). Elevated expression of CD11a, CD38 and CD95 indicates an activated phenotype. Moreover, CD38 is part of the adenosine pathway²⁹; adenosine is an immunoregulatory factor that promotes regulatory T cells and inhibits conventional T cell function³⁰. We found a trend for increased CD38 expression on CD56^{bright} NK cells and the prevalence of regulatory T cells (Fig. 2F). Despite the elevated expression of CD95 (FasR) we did not see evidence for increased apoptosis of the CD56^{bright} NK cells as measured by Annexin V (Suppl. Fig. 2A). CD56^{dim}CD16⁺ NK cells also seem to have an activated phenotype as characterized by higher expression of CD11a, CD95 and NKG2D. They are less highly differentiated than their counterpart in healthy donors as characterized by a lower frequency of CD57 expressing cells (Suppl. Fig. 2B,C). Levels of Nkp46, NKG2A, KLRG1, CD38, CD95 and CD158b1,b2,j on CD56^{dim}CD16⁺ NK cells were not found to be different between patients and healthy donors (Suppl. Fig. 2B). Finally, we found no expression of PD-1 and CTLA-4 by either CD56^{bright} or CD56^{dim}CD16⁺ NK cells (data not shown).

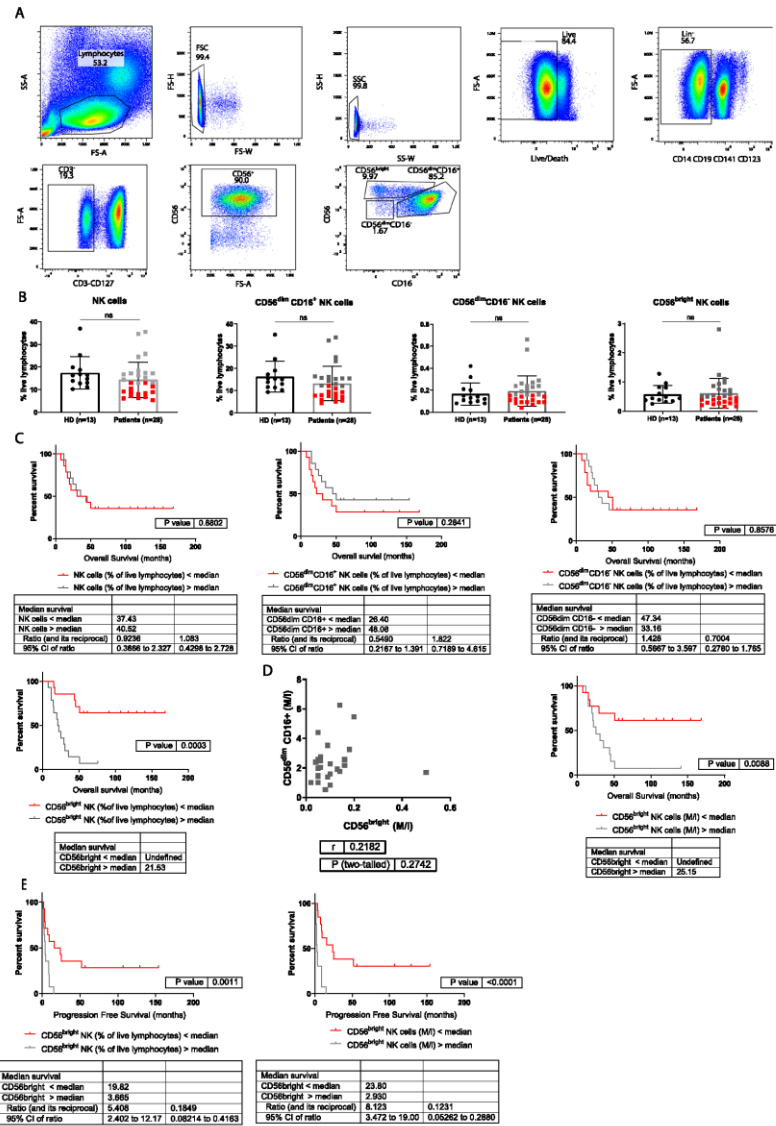


Figure 1. Frequencies of NK cells in melanoma patients and healthy controls. (A) Representative dot plots of the gating strategy used. Lymphocytes were selected using forward (FSC) and side scatter (SSC), afterwards doublets were gated out and live cells were selected. A series of negative selections was performed, first gating out DCs, monocytes and B cells using a lineage cocktail, next T cells and ILCs were gated out using CD3 and CD127. Total NK cells were positively selected using CD56 (total NK cells), this population can be further divided into CD56^{bright}, CD56^{dim}CD16⁺ and CD56^{dim}CD16⁻ NK cells. (B) Histograms of the frequencies of total NK cells, CD56^{bright}, CD56^{dim}CD16⁺ and CD56^{dim}CD16⁻ NK cells, as measured by flow cytometry in PBMC samples of 28 melanoma patients and 13 healthy donors. Frequencies of the patients with values lower than the median are indicated in red, and those higher than the median are indicated in grey. (C) Kaplan-Meier curves of overall survival, of patients with high (grey) vs. low (red) percentages of total NK cells, CD56^{dim}CD16⁺, CD56^{dim}CD16⁻ and CD56^{bright} NK cells, with the median as cut-off. (D) Absolute numbers of corresponding CD56^{dim}CD16⁺ and CD56^{bright} NK cells represented in an xy-plot. Kaplan-Meier curves of overall survival with high (grey) vs. low (red) numbers of CD56^{bright} NK cells, with the median as cut-off. E. Kaplan-Meier curves of progression free survival with high (grey) and low (red) frequencies and absolute numbers of CD56^{bright} NK cells with the median as cut-off. ns not significant, * p < 0.05, ** p < 0.01, *** p < 0.001, **** p < 0.0001.

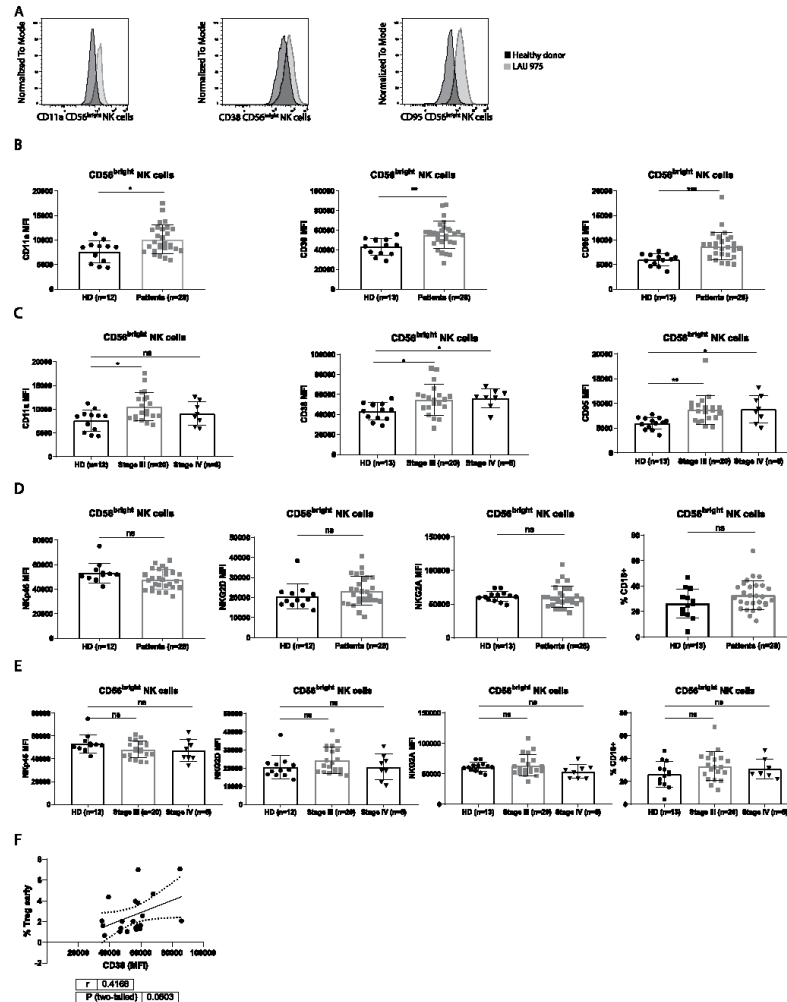


Figure 2. Phenotypic characterization of CD56^{br} NK cells by flow cytometry. (A) Representative histograms of the expression level (Median Fluorescent Intensity, MFI) of CD11a, CD38 and CD95 on CD56^{br} NK cells. The histograms show overlays; patient LAU975 (grey) and healthy donor 7 (black). (B) Summary histograms of the expression levels (MFI) of CD11a, CD38 and CD95 from patients with late stage (III/IV) melanoma and healthy donors. (C) Distribution of the expression levels (MFI) of CD11a, CD38 and CD95 from patients with late stage (III/IV) melanoma and healthy donors. (D) Summary histograms of the expression levels (MFI) of NKp46, NKG2D and NKG2A. (E) Distribution of the expression levels (MFI) of NKp46, NKG2D and NKG2A from patients with late stage (III/IV) melanoma and healthy donors. (F) Frequencies of regulatory T cells (CD25^{hi}FoxP3⁺CD127⁻) in the blood of melanoma patients before vaccination (n = 21) correlating with the expression levels of CD38 (MFI) on CD56^{br} NK cells (n = 21) from the same patients. ns not significant, *p < 0.05, **p < 0.01, ***p < 0.001, ****p < 0.0001.

Pro-inflammatory cytokine and chemokine production is partially affected in CD56^{br} NK cells. Since CD56^{br} NK cells have an activated phenotype we wondered if they are also more capable of producing cytokines and chemokines than NK cells from healthy donors. Previous publications have shown that NK cells are able to produce an array of cytokines, including Th1, Th2 as well as regulatory cytokines³¹. We used samples from 12 patients representing the whole patient population based on their frequencies of CD56^{br} NK cells (Fig. 3A), and the same previously used 13 healthy donors as controls. We stimulated NK cells for 4 hours with PMA/Ionomycin and analysed them by flow cytometry. ILCs were excluded by gating out CD127-positive cells. Previous

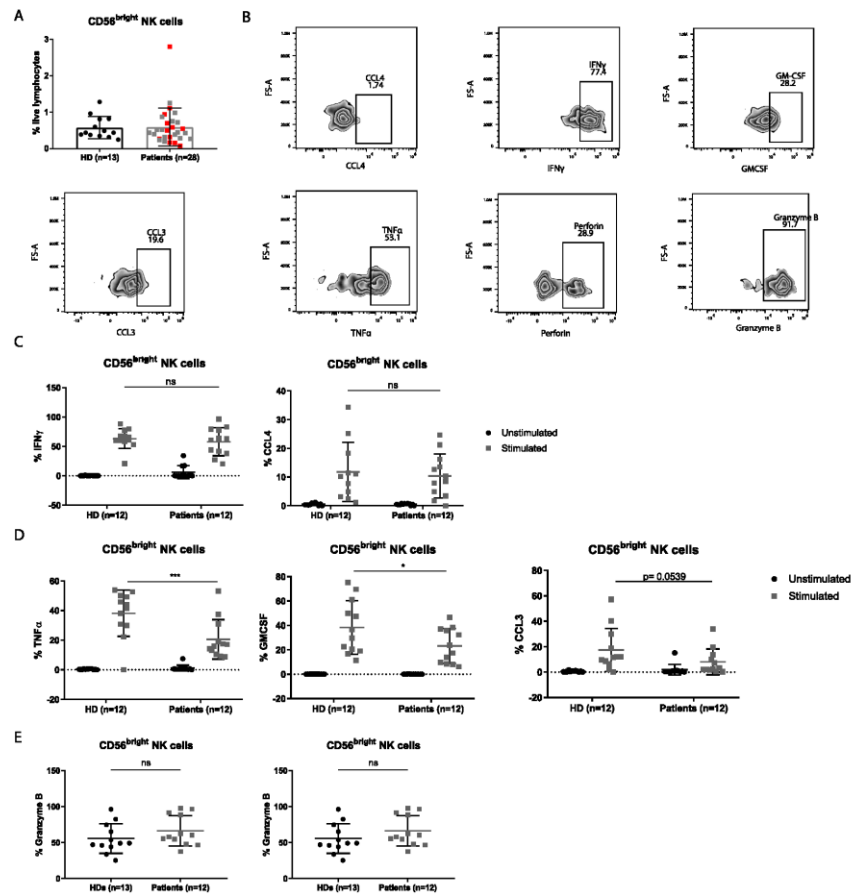


Figure 3. Functional characterization of CD56^{bright} NK cells after stimulation (4 hours) with PMA/Ionomycin. (A) Histogram of the frequencies of CD56^{bright} NK cells in patients and healthy donors. Patients included in subsequent functional experiments are indicated in red. (B) Representative dot plots of CCL4, IFN γ , GMCSF, CCL3 and TNF α after 4 hours of PMA/Ionomycin stimulation, and of perforin and granzyme B without stimulation of patient LAU627. (C) Histograms of IFN γ and CCL4 production (%) (CD56^{bright} NK cells) in healthy donors and patients before and after stimulation. (D) Histograms of TNF α , GMCSF and CCL3 production (%) (CD56^{bright} NK cells) in healthy donors and patients before and after stimulation. (E) Histograms of granzyme B and perforin (%) (CD56^{bright} NK cells) in healthy donors and patients before stimulation. ns not significant *p < 0.05, **p < 0.01, ***p < 0.001, ****p < 0.0001.

studies have reported decreased functionality of peripheral blood NK cells in melanoma patients¹⁵. We did not detect any differences between the amounts of IFN γ or CCL4 produced by CD56^{bright} NK cells from patients and healthy donors (Fig. 3B,C). In contrast, we found lower production of TNF α and GMCSF (and a trend for CCL3) in patients as compared to healthy donors (Fig. 3B,D). We did not find differences for granzyme B and perforin expression before stimulation, suggesting similar cytolytic capacity (Fig. 3B,E). IFN γ , GMCSF, perforin, granzyme B, CCL4 and NKp44 production by CD56^{dim}CD16⁺ cells did not differ between patients and healthy donors. In turn, the patients produced lower levels of TNF α and CCL3 (Suppl. Fig. 3A,B). Finally, we did not observe any production of IL-10, IL-2, LT α , IL-4, IL-13, IL-22 and IL-5 in either subset (CD56^{bright} and CD56^{dim}CD16⁺) (data not shown). Even though CD56^{bright} NK cells display an activated phenotype based on surface markers, they are not more functional than healthy controls, they are even impaired in the production of a number of cytokines.

Multivariate analysis shows significant correlation of CD56^{bright} NK cells with overall patient survival. We used the clinical as well as phenotypical and functional data from our cohort to perform a univariate Cox regression analysis for overall patient survival, with the aim to identify significant clinical and immunological

	Univariate Cox analysis				Multivariate Cox analysis			
	beta	HR	95% CI for HR	P value	beta	HR	95% CI for HR	P value
Age (years)	-0.012	0.99	0.96-1	0.42				
LDH (mgEq/l)	-0.0025	1	0.99-1	0.59				
Sex	-0.17	0.84	0.33-2.2	0.73				
Lymph node metastases	-0.23	0.8	0.28-2.3	0.67				
Satellite metastases	0.84	2.3	0.9-6	0.082				
Distant metastases	1.1	3.1	0.97-6.5	0.031*	1.077	2.937	1.028-8.393	0.044*
N stage	0.83	2.3	0.66-7.9	0.19				
DTH	-0.95	0.39	0.13-1.1	0.082				
NED or ED at study entry	0.92	2.5	0.97-6.5	0.059				
Previous radiotherapy	0.096	1.1	0.32-3.8	0.88				
Previous chemotherapy	-0.26	0.77	0.22-2.7	0.68				
Previous immunotherapy	0.076	1.1	0.42-2.8	0.88				
Any previous therapy (Radio/Chemo/Immuno)	-0.016	0.98	0.39-2.5	0.97				
MelanA+ CD8 (% CD8+ T cells)	-0.61	0.54	0.12-2.6	0.44				
CD56 ^{bright} NK cells (% live lymphocytes)	2.9	18	2.4-140	0.005**	2.963	19.364	2.293-153-524	0.007**
CD11a (MFI)	1.3	3.7	0.049-280	0.56				
NKp46 (MFI)	4.7	110	0.08-160 000	0.2				
NKG2D (MFI)	1.9	6.4	0.19-220	0.3				
NKG2A (MFI)	2.7	14	0.07-2900	0.33				
CD38 (MFI)	0.42	1.5	0.015-160	0.86				
CD95 (MFI)	0.96	2.6	0.027-260	0.68				
CD16 (% CD56 ^{dim} NK cells)	2.5	12	0.43-350	0.14				
Granzyme B (% CD56 ^{bright} NK)	4.7	110	0.54-20 000	0.083				
Perforin (% CD56 ^{bright} NK)	1.7	5.4	0.15-200	0.36				
CCL4 (% CD56 ^{dim} NK)	-2	0.13	0.012-1.5	0.098				
GMCSF (% CD56 ^{bright} NK)	-2	0.14	0.013-1.5	0.1				
IFN- γ (% CD56 ^{bright} NK)	4.3	72	1.1-4700	0.044*				
CCL3 (% CD56 ^{dim} NK)	0.71	2	0.038-11	0.41				
TNF α (% CD56 ^{dim} NK)	1.9	6.9	0.35-140	0.21				

Table 1. Univariate and multivariate analysis of overall survival by the Cox proportional hazards method. * $p < 0.05$, ** $p < 0.01$, *** $p < 0.001$, **** $p < 0.0001$.

factors. One of the immunological parameters is the frequency of Melan-A specific CD8⁺ T cells at baseline, as previously described²⁵. Interestingly, we found that presence of distant metastases, frequency of circulating CD56^{bright} NK cells, and production of IFN- γ by CD56^{bright} NK cells are inversely associated with overall patient survival (Table 1). To test if these three parameters contribute individually to survival we performed a multivariate Cox regression analysis. Since we only had 11 paired samples for our functional analyses, we decided to not analyse the impact of IFN- γ production by CD56^{bright} NK cells any further. Our multivariate analysis showed that both, the presence of distant metastases and the frequency of CD56^{bright} NK cells correlated significantly with survival (Table 1). A similar result was obtained using absolute numbers of CD56^{bright} NK cells instead of frequencies (data not shown). The frequency of CD56^{bright} NK cells was similar in patients with or without distant metastases (Suppl. Fig. 4). Together, our data suggest that the fraction of circulating CD56^{bright} NK cells may hold prognostic value in melanoma patients.

Discussion

New therapies focussing on blocking inhibitory receptors not only of CD8 T cells but also of NK cells have shown clinical success²⁶, supporting the notion that NK cells could have potentially important roles in future treatments. However, their implications in solid cancers is not entirely clear³². We analysed NK cells from a cohort of 29 late stage (III/IV) melanoma patients included in a vaccine clinical trial. All analysis was performed on samples from before vaccine treatment. In patients and healthy donors we found similar frequencies of circulating total NK cells as well as their subsets (CD56^{dim}CD16⁺ and CD56^{bright}), in line with previously published data^{15,16}. CD56^{dim}CD16⁻ NK cells were found reduced in viremic HIV patients³³. We did not find significant differences between the frequencies of CD56^{dim}CD16⁻ NK cells in healthy controls and melanoma patients. In the literature, NK cells are frequently associated with immune surveillance, often playing significant roles in tumour control³⁴. Interestingly, we found that higher frequencies and numbers of circulating CD56^{bright} NK cells were associated with reduced overall and progression free patient survival, whereas frequencies or numbers of either total NK cells as well as CD56^{dim}(CD16⁺ or CD16⁻) cells did not correlate with survival. A similar finding was previously reported by Tietze *et al.* who showed that low CD56^{bright} NK cell frequency at baseline is a good predictor of melanoma patient survival after treatment with Ipilimumab²⁷.

Since CD56^{bright} NK cells adversely correlated with overall survival, we wondered if they possessed regulatory characteristics or if they had any deficiencies in their anti-tumoural potential. Previous studies in melanoma patients have shown decreased expression of NKp46 and NKG2D as well as an increased expression of NKp44 in total NK cells^{15,16}. We did not observe differences in expression of NKp46 and NKG2D on CD56^{bright} NK cells. We found that CD56^{bright} NK cells expressed higher levels of CD38, CD11a and CD95, indicating that these cells were activated. We did not, however find evidence for increased apoptosis. CD38 is an ADP ribosyl-cyclase, which has been described to be involved in the production of adenosine, limiting CD4⁺ T cell proliferation as well as inducing regulatory T cells, mediated by CD56^{bright} cells³⁵. Indeed, we found that CD38 expression levels on CD56^{bright} NK cells correlated with the frequencies of peripheral regulatory T cells from the same patients. Furthermore, CD11a was more strongly expressed on circulating CD56^{bright} NK cells in patients than healthy donors. It is one of the receptors (together with NKp46 and NKG2D) that could induce NK cell cytotoxicity directed towards antigen specific, activated T cells; especially CD4⁺ T cells seem to be sensitive to NK cell lysis in a mouse model of LCMV infection³⁶. NK cell regulation of T cell function was shown during the priming phase⁷, and NK cell depletion during a persistent LCMV infection also led to a positive therapeutic effect³⁷. Perforin was found to be the most important mediator of T cell and NK cell mediated killing³⁸.

Apart from expression of surface markers, we also determined the functionality of healthy donor and patient-derived NK cells. We analysed the production of an array of cytokines and chemokines while making sure that ILCs did not interfere with our analysis. Previously, ILCs have not been gated out when determining cytokine production^{15,16,31}. We found no differences in the amounts of CCL4 and IFN γ produced by circulating CD56^{bright} NK cells between patients and healthy donors. Unaffected production of IFN γ has been previously reported³⁹. We found decreased production of TNF α and GM-CSF by CD56^{bright} NK cells. Even though CD56^{bright} NK cells have a more activated phenotype in patients than healthy donors, they do not produce more cytokines. They are even partially impaired. GM-CSF and TNF α are both pro-inflammatory cytokines. GM-CSF can act in a paracrine manner and recruit neutrophils, monocytes and lymphocytes as well as enhance their functions. It plays an important role in priming of T cells as well as the development of a Th1 response⁴⁰. In a phase II clinical trial, the administration of GM-CSF to late stage melanoma patients in combination with Ipilimumab proved to be more efficient than Ipilimumab alone⁴¹. TNF α is known for its direct effects on cancer cells and for shaping the immune response⁴². It is also an essential cytokine for the process of antigen cross-presentation by DCs to CD8⁺ T cells⁴³. In a mouse melanoma model, mice deficient for MIP-1 α/β had increased tumour growth as well as a higher incidence of metastases, also associated with lower local production of IFN γ , TNF α and IL-6⁴⁴.

Univariate Cox regression analysis of multiple clinical and immunological parameters identified three significant factors, namely the presence of distant metastases, the frequency of CD56^{bright} NK cells and IFN γ production by CD56^{bright} NK cells. IFN γ is usually seen as a positive mediator of the anti-tumour immune response. However, it has been shown that IFN γ produced by decidual NK cells has multiple immunoregulatory functions including inhibition of Th17 cells⁴⁵, as well as induction of angiogenesis and vessel remodeling⁴⁶. The interaction between decidual NK cells and monocytes leads to the induction of regulatory T cells as well as apoptosis of effector T cells, dependent of the IFN γ pathway⁴⁷. The fact that distant metastases correlate with poor patient survival was expected as this is well known; patients without vs. with distant metastases are in stage III vs. IV, respectively; they have significantly different survival^{48,49}. We did not observe a difference in CD56^{bright} NK cell frequencies depending on the presence of distant metastases. Both are thus independent prognostic factors for overall survival of melanoma patients.

In primary tumours, NK cells are only present in low numbers, preferentially in the peritumoral area¹⁶. In lymph node metastases, NK cells can be found at similar frequencies as in healthy donor tissue, making up less than 5% of CD45⁺ cells²⁹. Few specific markers exist to distinguish NK cell subsets in the TME¹⁶. As a result, it is challenging to detect NK cell subsets in histologic material or based on computational approaches using transcriptome data⁵⁰. Moreover, NK cells display a certain degree of plasticity⁵¹. Therefore our study was focused on circulating NK cells, specifically on CD56^{bright} and CD56^{dim} NK cells, their phenotype and functionality. Improved detection methods and studies are required to determine their roles and functions in the TME.

Our data suggest that CD56^{bright} NK cells may have a negative effect on the anti-tumour response by inhibiting T cell responses, via CD38, perforin, CD11a and IFN γ . On the other hand they produce less GM-CSF and TNF α , cytokines important in establishing an anti-tumour response. However, due to the limited amount of patients included in this study, these should be considered as preliminary findings and be confirmed in larger patient cohorts, including early disease patients. The effects on the anti-tumour immune response of CD56^{bright} NK cells warrant also further mechanistic research. Our study provides evidence that the frequencies and absolute numbers of circulating CD56^{bright} NK could be potential biomarkers in melanoma patients.

Methods

Melanoma patients. Blood was obtained from melanoma patients included in a phase I clinical trial (ClinicalTrials.gov; Identifier: NCT00112229) upon written informed consent. Eligibility criteria and study design has been previously described²⁸. The study was designed, approved and conducted according to relevant regulatory standards approved by the Ethics Commission for Clinical Research of the Faculty of Medicine and University of Lausanne (Lausanne, Switzerland), Swissmedic (Swiss Agency for Therapeutic Product) and the Protocol Review Committee of the Ludwig Institute for Cancer Research (New York). The study was performed at the Centre Hospitalier Universitaire Vaudois (CHUV) in Lausanne. All 29 stage III/IV melanoma patients were included in the present study. Clinical details of all patients are assembled in Supplementary Table 1. Only samples from before the trial treatment were used in this study. Control PBMC from healthy donors where isolated from blood donations obtained from the Blood Transfusion center. The cells were isolated by density gradient centrifugation using Lymphoprep.

Human cell preparation and flow cytometry. PBMCs were isolated from whole blood cells by Lymphoprep (Axis-Shield) centrifugation gradient and cryopreserved in liquid nitrogen. Frozen PBMCs were thawed in a water bath at 37 °C. They were stained immediately after thawing, first with antibodies directed against surface markers. The following antibodies were used for the NK cell phenotyping: anti-CD11a (BD Biosciences Cat# 347983, RRID:AB_400366), anti-PD-1 (BD Biosciences Cat# 557946, RRID:AB_647199), anti-CD56 (BioLegend Cat# 318322, RRID:AB_893389), anti-CD16 (Beckman Coulter Cat# A33098, RRID:AB_2728092), anti-NKp46 (BD Biosciences Cat#, RRID:AB_10894195), anti-NKG2D (BioLegend Cat# 320808, RRID:AB_492962), anti-CD8 (BioLegend Cat# 300920, RRID:AB_528885), anti-CD3 (Beckman Coulter Cat# A93687, RRID:AB_2728095), anti-CD127 (BioLegend Cat# 351310, RRID:AB_10960140), anti-CD14 (Beckman Coulter Cat# B01175, RRID:AB_2728099), anti-CD19 (Beckman Coulter Cat# A96418, RRID:AB_2728101), anti-CD123 (BD Biosciences Cat# 563072, RRID:AB_2728102), anti-CD141 (BD Biosciences Cat# 563298, RRID:AB_2728103), anti-KLRG1 (A488, clone 13F12F2, provided by H. Pircher), anti-CD158b (Beckman Coulter Cat# IM2278U, RRID:AB_2728104), anti-NKG2A (Miltenyi Biotec Cat# 130-105-647, RRID:AB_2655388), anti-CD57 (BD Biosciences Cat# 333169, RRID:AB_2728105), anti-CD38 (Thermo Fisher Scientific Cat# 25-0389-42, RRID:AB_1724057), anti-CD95 (BioLegend Cat# 305612, RRID:AB_314550). Secondly, a live/dead staining (LIVE/DEAD™ Fixable Near-IR Dead Cell Thermo Fisher Scientific Cat# L-34975) was performed. Cells were fixed at room temperature (RT) for 30 minutes (1% formaldehyde buffer). Cells were washed and stained with anti-CTLA-4 (BD Biosciences Cat# 555855, RRID:AB_398615), in FACS buffer with 0.1% saponin for 30 minutes at RT. The following antibodies were used for the NK cell functionality panel: anti-CD56 (BioLegend Cat# 318328, RRID:AB_11218798), anti-CD16 (BioLegend Cat# 302026, RRID:AB_2278418), anti-CD3 (Thermo Fisher Scientific Cat# 47-0036-42, RRID:AB_10717514), anti-CD137 (BioLegend Cat# 309826, RRID:AB_2566260), anti-CD69 (BioLegend Cat# 310926, RRID:AB_2074956), anti-NKp44 (BioLegend Cat# 325114, RRID:AB_2616752), anti-CD127 (BD Biosciences Cat# 563086, RRID:AB_2728655), anti-CD14 (Beckman Coulter Cat# B01175, RRID:AB_2728099), anti-CD19 (Beckman Coulter Cat# A96418, RRID:AB_2728101). Then a live/dead staining (LIVE/DEAD™ Fixable Aqua Dead Cell Stain Thermo Fisher Scientific Cat# L34965) was performed. Depending on the sample/panel, PBMCs were washed with Annexin V binding buffer (BD Biosciences) and stained for Annexin V (BD Biosciences Cat# 556419, RRID:AB_2665412). Cells were fixed at RT during 30 minutes (FoxP3 intracellular staining kit, eBioscience). Cells were washed and stained with; anti-TNFβ (Thermo Fisher Scientific Cat# BMS105FL, RRID:AB_10598519), anti-IFNγ (BioLegend Cat# 506804, RRID:AB_315454), anti-GMCSF (BioLegend Cat# 502310, RRID:AB_11150231), anti-IL-22 (R and D Systems Cat# IC7821P, RRID:AB_495011), anti-CCL4 (Thermo Fisher Scientific Cat# 46-7540-42, RRID:AB_2573845), anti-IL-13 (BD Biosciences Cat# 561162, RRID:AB_10642586), anti-perforin (BioLegend Cat# 308104, RRID:AB_314702), anti-IL-4 (BioLegend Cat# 500810, RRID:AB_315129), anti-granzyme B (Thermo Fisher Scientific Cat# GRB17, RRID:AB_2536540), anti-TNFα (BioLegend Cat# 502926, RRID:AB_2204081), anti-CCL3 (Miltenyi Biotec Cat# 130-103-631, RRID:AB_2651378) and anti-IL-5 (BD Biosciences Cat# 554396, RRID:AB_398548) in FoxP3 intracellular staining kit permeabilisation buffer (eBioscience) for 30 minutes at RT. CD4 regulatory T cells in patients PBMCs were identified *ex vivo* by staining with the following antibodies at the surface: anti-CD3 PerCP (BD Biosciences Cat# 345766, RRID:AB_2783791), anti-CD4 PE-Cy7 (Biosciences Cat# 348809, RRID:AB_2783789), anti-CD25 PE (BD Biosciences Cat# 341011, RRID:AB_2783790), anti-CD127 Pacific Blue (eBioscience Cat# 57-1278-73, AB_657602). Then a live/dead staining (LIVE/DEAD™ Fixable Aqua Dead Cell Stain Thermo Fisher Scientific Cat# L34965) was performed. The FoxP3 staining were performed after Fixation and Permeabilization using the FoxP3 intracellular staining kit permeabilisation buffer (eBioscience) using anti-FoxP3-FITC (eBioscience Cat# 11-5773-82, RRID:AB_11076963). Melan-A specific T cells were identified using tetramers as previously described²⁸. In short: enriched CD8⁺ T cells were incubated with phycoerythrin-labeled HLA-A*0201/Melan-A/MART-1 A27L peptide26-35 (ELAGIGILTV) tetramers (1 µg ml⁻¹, 60 min, 4 °C) and then with antibodies (30 min, 4 °C).

Data were acquired on a Gallios (Beckman Coulter) and LSR-II™ Flow Cytometer (BD Bioscience) and analysed using FlowJo 10.4.2 (TreeStar).

In vitro stimulation. PBMCs were isolated from whole blood and cryopreserved in liquid nitrogen. Frozen PBMCs were thawed in a water bath at 37 °C. Cells were kept at 37 °C overnight in 20U/ml human recombinant IL-2 (Proleukin) and RPMI (Gibco) with 10% FCS (Gibco). Cells were stimulated for 4 hours with 1 µg/ml Phorbol 12-Myristate 13-Acetate (PMA) (Sigma Aldrich) and 0.25 µg/ml Ionomycin. (Sigma Aldrich). 10 µg/ml of Brefeldin A (Sigma Aldrich) and 2 nM Monensin (Sigma Aldrich) were added to all conditions, as well as to the control conditions at the start of the stimulation.

Statistics and analysis. Significance of single comparisons was assessed using the Mann–Whitney test, multiple comparisons were analysed using a two-way ANOVA or with a Kruskal–Wallis test, using the GraphPad Prism 8 software. Overall survival (OS) was defined as the time between enrolment in the phase I clinical trial and latest follow-up or death. Progression-free survival (PFS) was defined as the time between clinical trial enrolment and relapse or progression of disease, based on whether the patient had no evidence of disease or evidence of disease at study entry, respectively. Apart from the clinical parameters, our data did not follow a normal distribution but a log distribution and was therefore log-transformed before statistical testing. The significance of Kaplan–Meier survival analysis was assessed by the Log-rank test (Prism 8). Cox proportional hazards model was used to test association with survival. Predictors were selected for multivariate regression based on results from univariate analyses, inclusion was based on statistical significance. Survival analysis was performed using the survival R package⁵².

Data Availability

All data generated or analysed during this study are included in this published article (and its Supplementary Information Files).

References

- Chan, X. Y., Singh, A., Osman, N. & Piva, T. J. Role played by signalling pathways in overcoming BRAF inhibitor resistance in melanoma. *Int. J. Mol. Sci.* **18**, 1–13 (2017).
- Wolchok, J. D. *et al.* Overall Survival with Combined Nivolumab and Ipilimumab in Advanced Melanoma. *N. Engl. J. Med.* NEJMoA1709684, <https://doi.org/10.1056/NEJMoA1709684> (2017).
- Hsu, J. *et al.* Contribution of NK cells to immunotherapy mediated by PD-1/PD-L1 blockade. *J. Clin. Invest.* **128**, 4654–4668 (2018).
- Vivier, E. *et al.* Innate Lymphoid Cells: 10 Years On. *Cell* **174**, 1054–1066 (2018).
- Ames, E. & Murphy, W. J. Advantages and clinical applications of natural killer cells in cancer immunotherapy. *Cancer Immunol. Immunother.* **63**, 21–28 (2014).
- Vivier, E. *et al.* Innate or Adaptive Immunity? The Example of Natural Killer Cells. *Science* **331**, 44–49 (2011).
- Crome, S. Q., Lang, P. A., Lang, K. S. & Ohashi, P. S. Natural killer cells regulate diverse T cell responses. *Trends Immunol.* **34**, 342–349 (2013).
- Kim, S., Iizuka, K., Aguilu, H. L., Weissman, I. L. & Yokoyama, W. M. *In vivo* natural killer cell activities revealed by natural killer cell-deficient mice. *Proc. Natl. Acad. Sci.* **97**, 2731–2736 (2000).
- Iannello, A. & Raulet, D. H. Immune Surveillance of Unhealthy Cells by Natural Killer cells. *Cold Spring Harb Symp Quant Biol.* **78**, 249–257 (2013).
- Whiteside, T. L. & Herberman, R. B. The role of natural killer cells in immune surveillance of cancer. *Curr. Opin. Immunol.* **7**, 704–710 (1995).
- Imai, K., Matsuyama, S., Miyake, S., Suga, K. & Nakachi, K. Natural cytotoxic activity of peripheral-blood lymphocytes and cancer incidence: an 11-year follow-up study of a general population. *Lancet* **356**, 1795–1799 (2000).
- O'Sullivan, T. *et al.* Cancer immunoeediting by the innate immune system in the absence of adaptive immunity. *J. Exp. Med.* **209**, 1869–1882 (2012).
- Ni, J., Miller, M., Stojanovic, A., Garbi, N. & Cerwenka, A. Sustained effector function of IL-12/15/18-primed NK cells against established tumors. *J. Exp. Med.* **209**, 2351–2365 (2012).
- Levi, I. *et al.* Characterization of tumor infiltrating natural killer cell subset. *Oncotarget* **6** (2015).
- Mirjadic Martinovic, K. M. *et al.* Decreased expression of NKG2D, NKp46, DNAM-1 receptors, and intracellular perforin and STAT-1 effector molecules in NK cells and their dim and bright subsets in metastatic melanoma patients. *Melanoma Res.* **24**, 258–304 (2014).
- Fregni, G. *et al.* Phenotypic and Functional Characteristics of Blood Natural Killer Cells from Melanoma Patients at Different Clinical Stages. *PLoS One* **8**, 1–9 (2013).
- Ali, T. H. *et al.* Enrichment of CD56dimKIR+CD57+ highly cytotoxic NK cells in tumour-infiltrated lymph nodes of melanoma patients. *Nat. Commun.* **5**, 1–9 (2014).
- Konjević, G., Mirjadic Martinović, K., Jurišić, V., Babović, N. & Spužić, I. Biomarkers of suppressed natural killer (NK) cell function in metastatic melanoma: Decreased NKG2D and increased CD158a receptors on CD3-CD16+ NK cells. *Biomarkers* **14**, 258–270 (2009).
- Tirosh, I. *et al.* Dissecting the multicellular ecosystem of metastatic melanoma by single-cell RNA-seq. *Science* **352**, 189–196 (2016).
- Coca, S. *et al.* The prognostic significance of intratumoral natural killer cells in patients with colorectal carcinoma. *Cancer* **79**, 2320–2328 (1997).
- Villegas, F. R. *et al.* Prognostic significance of tumor infiltrating natural killer cells subset CD57 in patients with squamous cell lung cancer. *Lung Cancer* **35**, 23–28 (2002).
- Ishigami, S. *et al.* Prognostic value of intratumoral natural killer cells in gastric carcinoma. *Cancer* **88**, 577–583 (2000).
- Messaoudene, M. *et al.* Mature cytotoxic CD56bright/CD16+ natural killer cells can infiltrate lymph nodes adjacent to metastatic melanoma. *Cancer Res.* **74**, 81–92 (2014).
- Murray, S. & Lundqvist, A. Targeting the tumor microenvironment to improve natural killer cell-based immunotherapies: On being in the right place at the right time, with resilience. *Hum. Vaccin. Immunother.* **12**, 607–611 (2016).
- Tallerico, R. *et al.* IL-15, TIM-3 and NK cells subsets predict responsiveness to anti-CTLA-4 treatment in melanoma patients. *Oncimmunology* **6** (2017).
- André, P. *et al.* Anti-NKG2A mAb Is a Checkpoint Inhibitor that Promotes Anti-tumor Immunity by Unleashing Both T and NK Cells. *Cell* 1731–1743, <https://doi.org/10.1016/j.cell.2018.10.014> (2018).
- Tietze, J. K., Angelova, D., Heppt, M. V., Ruzicka, T. & Berking, C. Low baseline levels of NK cells may predict a positive response to ipilimumab in melanoma therapy. *Exp. Dermatol.* **26**, 622–629 (2017).
- Baumgaertner, P. *et al.* Vaccination-induced functional competence of circulating human tumor-specific CD8 T-cells. *Int. J. Cancer* **130**, 2607–2617 (2012).
- Malavasi, F. *et al.* CD38 and CD157 as Receptors of the Immune System: A Bridge Between Innate and Adaptive Immunity. *Mol. Med.* **13**, 30–39 (2007).
- Ohta, A. & Sitkovsky, M. Extracellular adenosine-mediated modulation of regulatory T cells. *Front. Immunol.* **5**, 1–9 (2014).
- Fauriat, C., Long, E. E. O., Ljunggren, H.-G. & Bryceson, Y. T. Regulation of human NK-cell cytokine and chemokine production by target cell recognition. *Immunobiology* **115**, 2167–2176 (2010).
- Stabile, H., Fionda, C., Gismondi, A. & Santoni, A. Role of distinct natural killer cell subsets in anticancer response. *Front. Immunol.* **8**, 1–8 (2017).
- Amand, M. *et al.* Human CD56dimCD16dim Cells As an Individualized Natural Killer Cell Subset. *Front. Immunol.* **8** (2017).
- Hanahan, D. & Weinberg, R. A. Hallmarks of cancer: the next generation. *Cell* **144**, 646–74 (2011).
- Morandi, F. *et al.* CD56brightCD16- NK Cells Produce Adenosine through a CD38-Mediated Pathway and Act as Regulatory Cells Inhibiting Autologous CD4+ T Cell Proliferation. *J. Immunol.* **195**, 965–972 (2015).
- Waggoner, S. N., Cornberg, M., Selin, L. K. & Welsh, R. M. Natural killer cells act as rheostats modulating antiviral T cells. *Nature* **481**, 394–398 (2012).
- Waggoner, S. N., Daniels, K. A. & Welsh, R. M. Therapeutic Depletion of Natural Killer Cells Controls Persistent Infection. *J. Virol.* **88**, 1953–1960 (2014).
- Crouse, J., Kalinke, U. & Oxenius, A. Regulation of antiviral T cell responses by type I interferons. *Nat. Rev. Immunol.* **15**, 231–242 (2015).
- Fregni, G., Perier, A., Avril, M.-F. & Caignard, A. NK cells sense tumors, course of disease and treatments. *Oncimmunology* **1**, 38–47 (2012).
- Shi, Y. *et al.* Granulocyte-macrophage colony-stimulating factor (GM-CSF) and T-cell responses: What we do and don't know. *Cell Res.* **16**, 126–133 (2006).
- Hodi, F. S. *et al.* Ipilimumab plus sargramostim vs ipilimumab alone for treatment of metastatic melanoma: A randomized clinical trial. *JAMA - J. Am. Med. Assoc.* **312**, 1744–1753 (2014).

42. Neubert, N. J. *et al.* Broad and conserved immune regulation by genetically heterogeneous melanoma cells. *Cancer Res.* **77**, 1623–1636 (2017).
43. Deauvilleau, F. *et al.* Human natural killer cells promote cross-presentation of tumor cell-derived antigens by dendritic cells. *Int. J. Cancer* **136**, 1085–1094 (2015).
44. Nakasone, Y. *et al.* Host-derived MCP-1 and MIP-1 α regulate protective anti-tumor immunity to localized and metastatic B16 melanoma. *Am. J. Pathol.* **180**, 365–374 (2012).
45. Fu, B. *et al.* Natural killer cells promote immune tolerance by regulating inflammatory TH17 cells at the human maternal-fetal interface. *Proc. Natl. Acad. Sci.* **110**, E231–E240 (2013).
46. Ashkar, A. A., Di Santo, J. P. & Croy, B. A. Interferon gamma contributes to initiation of uterine vascular modification, decidual integrity, and uterine natural killer cell maturation during normal murine pregnancy. *J. Exp. Med.* **192**, 259–70 (2000).
47. Vacca, P. *et al.* Crosstalk between decidual NK and CD14⁺ myelomonocytic cells results in induction of Tregs and immunosuppression. *Proc. Natl. Acad. Sci. USA* **107**, 11918–23 (2010).
48. Buyounouski, M. K. *et al.* Melanoma Staging: Evidence-Based Changes in the American Joint Committee on Cancer Eighth Edition Cancer Staging Manual. *CA. Cancer J. Clin.* **67**, 245–253 (2017).
49. Knackstedt, T., Knackstedt, R. W., Couto, R. & Gastman, B. Malignant melanoma: Diagnostic and Management Update. *Plast. Reconstr. Surg.* **142**, 701–711 (2018).
50. Wang, E., Tian, Z. & Wei, H. Genomic expression profiling of NK cells in health and disease. *Eur. J. Immunol.* **45**, 661–678 (2015).
51. Michel, T. *et al.* Human CD56 bright NK Cells: An Update. *J. Immunol.* **196**, 2923–2931 (2016).
52. Themeau, T. A Package for Survival Analysis in S. *Version 2.38* (2015).

Acknowledgements

We are obliged to thank the patients and healthy blood donors for their dedicated collaboration. The authors gratefully acknowledge Nicole Montandon for sample processing, and Pascale Anderle and Julien Raclé for statistical advice. We also thank Karin de Visser, Werner Held and Paula Marcos Mondéjar for collaboration, support and expert advice, and Hanspeter Pircher for providing the KLRG1 antibody. This project was supported by SwissTransMed (KIP 18), Switzerland (to K.d.J.), the Cancer Research Institute, USA (to K.d.J., H.M.E.H.), the Swiss Cancer Research Foundation (to S.N.), Alfred and Annemarie von Sick, Switzerland (to H.M.E.H., H.O.S.) and the University of Lausanne, Switzerland (to A.E., P.B., D.E.S.).

Author Contributions

Conception and design: K.d.J., P.B. and D.E.S. Acquisition of data: K.d.J. and A.E. Analysis and interpretation of data: K.d.J., A.E., S.N., H.M.E.H., H.O.S., P.B. and D.E.S. Writing, review and revision of manuscript: K.d.J., A.E., S.N., H.M.E.H., H.O.S., P.B. and D.E.S. Technical and material support: S.N., H.M.E.H. and H.O.S. Study supervision: P.B. and D.E.S.

Additional Information

Supplementary information accompanies this paper at <https://doi.org/10.1038/s41598-019-40933-8>.

Competing Interests: The authors declare no competing interests.

Publisher's note: Springer Nature remains neutral with regard to jurisdictional claims in published maps and institutional affiliations.



Open Access This article is licensed under a Creative Commons Attribution 4.0 International License, which permits use, sharing, adaptation, distribution and reproduction in any medium or format, as long as you give appropriate credit to the original author(s) and the source, provide a link to the Creative Commons license, and indicate if changes were made. The images or other third party material in this article are included in the article's Creative Commons license, unless indicated otherwise in a credit line to the material. If material is not included in the article's Creative Commons license and your intended use is not permitted by statutory regulation or exceeds the permitted use, you will need to obtain permission directly from the copyright holder. To view a copy of this license, visit <http://creativecommons.org/licenses/by/4.0/>.

© The Author(s) 2019

8.4.1. Supplementary data of the manuscript

Circulating CD56^{bright} NK cells inversely correlate with survival of melanoma patients

Kaat de Jonge¹, Anna Ebering¹, Sina Nassiri^{1,3}, H  l  ne Maby-El Hajjami¹, Hajer Ouertatani-Sakouhi¹, Petra Baumgaertner¹ and Daniel E. Speiser^{1,2*}

¹ Dept. of Fundamental Oncology, University of Lausanne, Epalinges, Switzerland

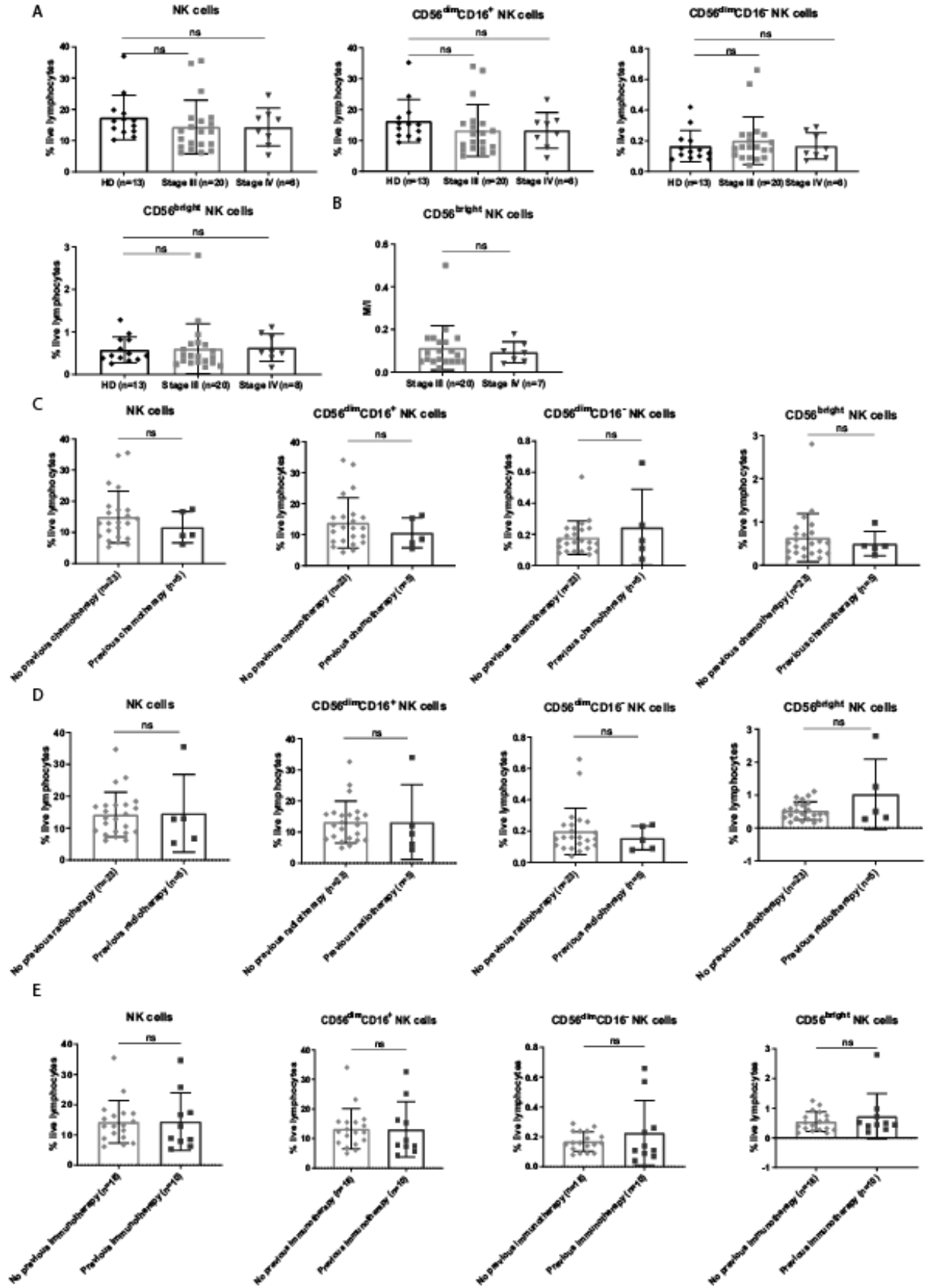
² Dept. of Oncology, University Hospital Center (CHUV), Lausanne, Switzerland

³ Swiss Institute of Bioinformatics (SIB), B  timent G  nopode, Lausanne, Switzerland

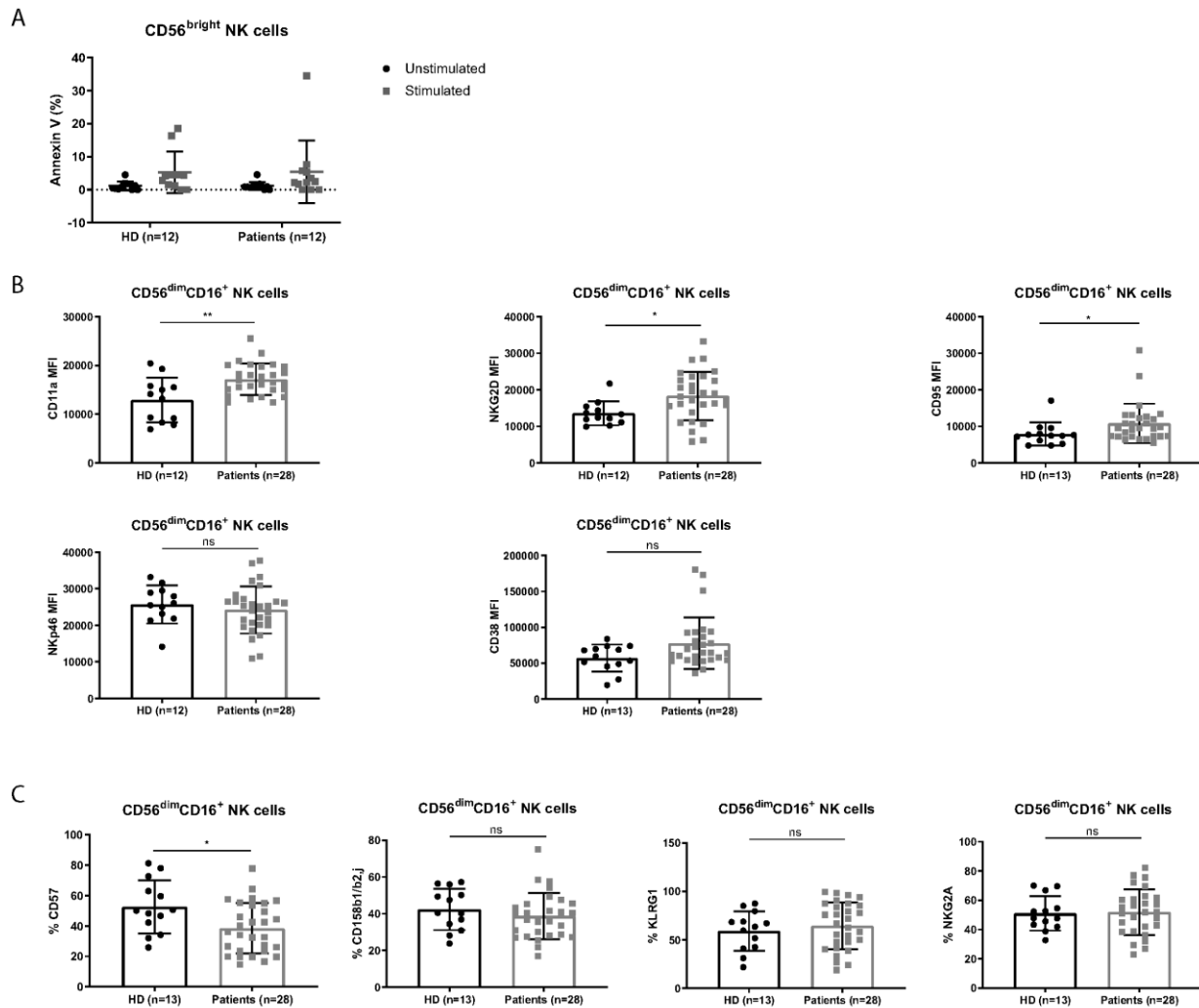
*** Corresponding author:** Daniel E. Speiser, Clinical Tumor Biology & Immunotherapy Group, Department of Oncology and Ludwig Cancer Research, University of Lausanne, Chemin des Boveresses 155, CH-1066 Epalinges, Switzerland, Phone: +41 21 314 01 82, Fax: +41 21 692 59 95, E-mail: doc@dspeiser.ch

Table of contents:

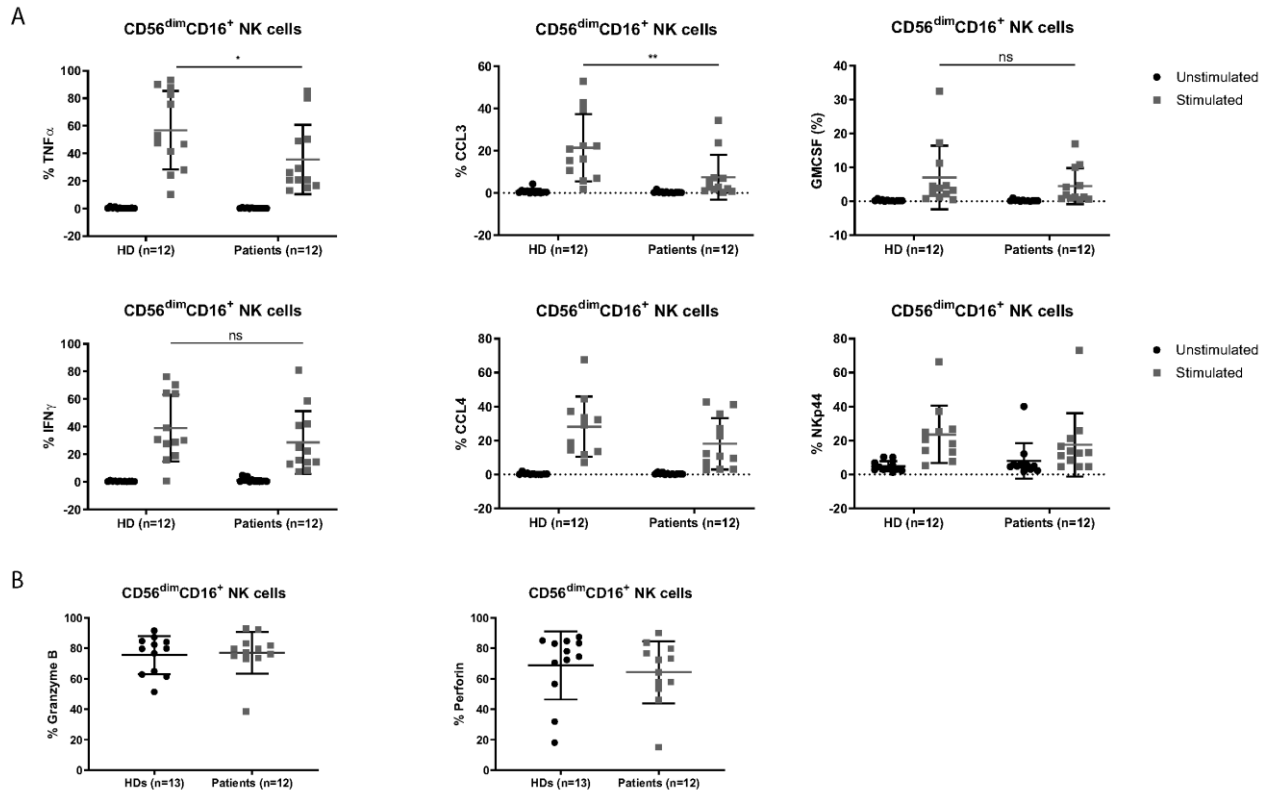
Supplementary Figure 1	2
Supplementary Figure 2	4
Supplementary Figure 3	5
Supplementary Figure 4	6
Supplementary Table 1	7



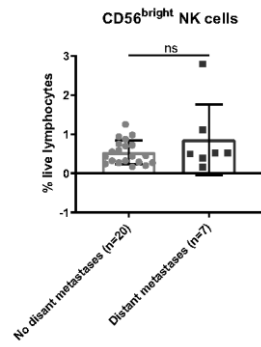
Supplementary Figure 1: Distribution of total NK cells, CD56^{bright}, CD56^{dim}CD16⁺ and CD56^{dim}CD16⁻ NK cells in different clinical conditions. A. Distribution of NK cell frequencies and their subsets (%) from patients with late stage (III/IV) melanoma and healthy donors. B. Distribution of the absolute numbers of CD56^{bright} NK cells in stage III and stage IV melanoma patients. C,D,E. Distribution of total NK cells, CD56^{bright}, CD56^{dim}CD16⁺ and CD56^{dim}CD16⁻ NK cells (%) in relation to previous chemotherapy (C), radiotherapy (D) or immunotherapy (E). ns not significant, * p<0.05, ** p<0.01, *** p<0.001, **** p<0.0001.



Supplementary Figure 2: Phenotypical characterization by flow cytometry of NK cells. A. Annexin V expression levels on CD56^{bright} NK cells in patients and healthy donors before and after activation (PMA/Ionomycin, 4 hours) B. Expression levels (MFI) of CD11a, NKG2D, CD95, NKp46 and CD38 on CD56^{dim}CD16⁺ NK cells. C: Summary histograms of the expression (%) of CD57, CD158b1,2,j, KLRG1 and NKG2A on CD56^{dim}CD16⁺ NK cells. ns not significant, * p<0.05, ** p<0.01, *** p<0.001, **** p<0.0001.



Supplementary Figure 3: Functional characterization of CD56^{dim}CD16⁺ NK cells by flow cytometry. A. Histograms of TNF α , GMCSF, CCL3, CCL4 and IFN γ production (%) (CD56^{dim}CD16⁺) as well as the expression level of NKp44 (%) in healthy donors and patients before and after stimulation (4h PMA/Ionomycin). B. Histograms of the expression levels of granzyme B and perforin by CD56^{dim}CD16⁺ NK cells. ns not significant, * $p < 0.05$, ** $p < 0.01$, *** $p < 0.001$, **** $p < 0.0001$.



Supplementary Figure 4: CD56^{bright} NK cells (%) from melanoma patients with or without distant metastases. ns not significant, * p<0.05, ** p<0.01, *** p<0.001, **** p<0.0001.

Supplementary Table 1: Clinical characteristics of the 29 late stage (III/IV) melanoma patients included in this study

Patient	Sex	Age	Diagnosis					Status at study entry					Study outcome				
			Melanoma type [‡]	TNM	Stage	Breslow	Clark	Age	TNM	Stage	Disease status [#]	Previous treatment [†]	Study entry date	Death (1=yes/0=no)	OS [†]	Relapse (1=yes/0=no)	PFS [†]
LAU 205	M	24	SSM	pT2aN1bM0	IIIB	1.40	IV	33	pT2aN2cM0	IIIB	NED	IFNa adjuvant, Immuno-therapy (a)	09.03.2005	1	50.6	1	25.2
LAU 321	M	60	SSM	pT3aN0M0	IIA	1.50	III	69	pT3aN3M1b	IV	ED	Immuno-therapy (b), Chemo-immuno-therapy (c)	30.06.2003	0	75.5	1	3.2
LAU 371	M	29	SSM	pT3aN1bM0	IIIB	2.38	IV	33	pT3aN1bM1b	IV	NED	Immuno-therapy (d)	28.07.2003	1	11.9	1	3.6
LAU 392	F	29	SSM	pT3aN0M0	IIA	2.50	IV	37	pT3aN3M0	IIIC	ED	Immuno-therapy (b)	16.09.2004	1	11.8	1	2.5
LAU 444	F	27	NM	pT3aN0M0	IIA	1.90	IV	33	pT3aN2cM1c	IV	ED	Radiotherapy, Immuno-therapy (e)	15.09.2003	1	30.8	1	15.2
LAU 618	F	69	NM	pT4aN0M0	IIB	8.00	V	74	pT4aN2cM0	IIIB	ED	IFNa adjuvant, Chemo-immuno-therapy (c)	26.05.2003	1	35.5	1	1.4
LAU 627	M	49	SSM	pT3bN1aM0	IIIB	2.23	IV	51	pT3bN2bM1b	IV	ED	NA	19.05.2003	1	15.2	1	3.4
LAU 648	M	64	UK	pT2aN0M0	IB	1.60	IV	70	pT2aN3M0	IIIC	NED	Radiotherapy, Immuno-therapy (e)	25.10.2004	0	153.7	0	153.7
LAU 660	F	22	NM	pT2bN0M0	IIA	1.72	IV	25	pT2bN0M1c	IV	NED	NA	16.08.2004	1	14.8	1	2.1
LAU 672	M	34	SSM	pT1aN0M0	IA	0.70	III	38	pT1aN3M0	IIIC	ED	IFNa adjuvant, Immuno-therapy (f), Chemo-immuno-therapy (c)	14.10.2003	1	45.5	1	1.9

LAU 701	F	70	UK	pT3bN0M0	IIB	2.50	IV	71	pT3bN3M0	IIIC	NED	Chemo-immunotherapy (c)	24.09.2003	0	140.6	1	2.9
LAU 706	F	64	UK	pTxN0M0	UK	UK	UK	67	pTxN3M0	IIIC	ED	Chemo-immunotherapy (c), Immuno-therapy (a)	08.11.2004	1	44.1	1	3.8
LAU 818	M	55	UK	pT3aN0M0	IIA	2.44	III	58	pT3aN2bM0	IIIB	NED	NA	09.05.2003	0	61.2	1	7.3
LAU 936	F	52	SSM	pT3aN0M0	IIA	2.70	IV	54	pT3aN1bM0	IIIB	NED	Radiotherapy	08.03.2006	1	15.1	1	1.5
LAU 944	F	20	OM	pT2aN0M0	IB	6.80	UK	28	pT2aN1bM0	IIIB	NED	Radiotherapy	26.01.2004	0	168.0	1	23.8
LAU 972	F	60	NM	pT2bN1aM0	IIIB	1.60	III	60	pT2bN1aM0	IIIB	NED	NA	02.09.2004	0	129.3	0	129.3
LAU 975	M	51	NM	pT4aN1bM0	IIIB	12.00	IV	52	pT4N1bM0	IIIB	NED	NA	11.04.2005	1	7.5	1	4.2
LAU 1013	M	55	SSM	pT3bN3M0	IIIC	3.00	IV	56	pT3bN3M0	IIIC	NED	NA	25.04.2005	1	25.1	1	8.8
LAU 1015	M	75	SSM	pT2aN0M1a	IV	1.20	III	75	pT2aN0M1a	IV	NED	NA	03.03.2005	1	50.7	1	8.9
LAU 1017	F	28	NM	pT3bN2bM0	IIIC	3.80	IV	28	pT3bN2bM0	IIIC	NED	NA	25.04.2005	1	22.0	1	1.4
LAU 1022	M	69	NM	pT2bN2bM0	IIIB	1.49	IV	69	pT2bN2bM0	IIIB	NED	NA	11.07.2005	1	19.8	1	8.8
LAU 1034	M	47	SSM	pT2aN2bM0	IIIB	1.35	III-IV	47	pT2aN2bM0	IIIB	NED	NA	15.08.2005	0	117.2	1	51.8
LAU 1090	M	68	NM	pT3aN2bM0	IIIB	3.10	IV	69	pT3aN2bM0	IIIB	ED	NA	20.02.2006	1	21.0	1	3.8
LAU 1106	M	36	SSM	pT2aN1aM0	IIIA	1.35	IV	36	pT2aN1aM0	IIIA	NED	NA	21.03.2006	0	106.8	0	106.8

LAU 1129	M	52	SSM	pT3N0M0	II	2.50	IV	66	pT3N3M0	IIIC	NED	Chemotherapy (g)	29.06.2006	1	17.0	1	9.4
LAU 1144	M	68	NeM	pT3aN0M0	IIA	0.60	IV	72	pT3aN0M1b	IV	NED	NA	19.09.2006	1	29.4	1	8.9
LAU 1164	M	51	UK	pTxNxM1a	IV	UK	UK	52	pTxNxM1a	IV	NED	NA	16.10.2006	0	56.6	0	56.6
LAU 1189	F	68	ALM	pT3bN2M0	IIIB	4.00	IV	68	pT3bN2M0	IIIB	NED	NA	05.06.2007	0	38.9	1	10.9
LAU 1264	M	46	SSM	pT3bN0M0	IIB	4.00	IV	48	pT3bN1bM0	IIIC	NED	Radiotherapy	11.10.2007	0	90.8	1	15.8

‡ The melanoma type is shown: ALM: acral lentiginous melanoma, NM: nodular melanoma, NeM: nevoid melanoma, OM: ocular melanoma, SSM: superficial spreading melanoma

UK: unknown.

The disease status before the start of the vaccination trial is presented: NED: no evidence of disease; ED: evidence of disease.

‡ Previous therapies are listed: All patients underwent surgery.

a: P40/ELA cancer vaccine study: Melan-A 26-35 (A27L) analogue peptide (ELA)+ P40 adjuvant

b: LUDWIG 96-010 cancer vaccine study: Melan-A 26-35 (A27L) analogue peptide (ELA)+ FluMa 58-66 peptide + low dose rhIL-2+ SB AS-2

c: Isolated limb perfusion with Melphalan+IFN γ +TNF α

d: LUDWIG 98-009 cancer vaccine study: Melan-A 26-35 (A27L) analogue peptide (ELA)+FluMa 58-66 peptide + SB AS-2

e: LUDWIG 96-010 cancer vaccine study: Melan-A 26-35 (A27L) analogue peptide (ELA)+ FluMa 58-66 peptide + low dose rhIL-2+ Montanide ISA-51

f: LUDWIG 96-010 cancer vaccine study: Melan-A 26-35 (A27L) analogue peptide (ELA)+ FluMa 58-66 peptide + Montanide ISA-51

g: Cisplatin+ Dacarbazine+ Methotrexate

NA (not applicable) means no systemic treatment was administered before the start of the vaccination trial.

The study outcome with overall survival (OS) and progression-free survival (PFS) is displayed. * Interval from the start of vaccination protocol to event (in months)

8.5. Discussion and perspectives

Our research identifies a possible biomarker for metastatic melanoma. We and others reported that CD56^{bright} NK cells inversely correlate with overall survival ²¹⁴. In the case of Tietze, *et al.* patients were included in a clinical trial receiving Ipilimumab (α -CTLA-4 antibody). However, patient numbers are very low in both case, 29 and 23 respectively. So these results need to be confirmed using larger cohorts.

It remains unclear if there is any link between the functionality of NK cells in the periphery and those present within the TME. However, serious questions have been raised about the relevance of NK cells within the TME as limited tissue infiltration has been reported in a number of cancer types like melanomas, hepatocellular carcinoma, breast cancer, renal cancer and colon cancers ^{215–217}. In two out of three of these studies NK cells were characterized as CD56⁺ by immunohistochemistry. However, CD56 is not exclusively expressed in NK cells. Moreover, these techniques haven't allowed for the differentiation between CD56^{bright} and CD56^{dim} NK cells. Other techniques like using RNA signatures to study TCGA data have not yielded any results yet, due to the difficulties of designing gene signatures of NK cell populations as well as their plasticity in tissues. Recent studies have shown a tissue signature in spleen compared to blood of humans ¹⁶². However, single cell RNA sequencing might provide a solution. Multiple single cell analysis in melanoma have shown clustering of cells identified as NK cells ^{218–220}. However, these have not been studied in detail.

We found that CD56^{bright} NK in the periphery of melanoma patients have an altered functionality. They produce lower levels of TNF α and GM-CSF. Further questions remain how or if these changes have any impact on tumour killing and/or interactions with other immune cells. We additionally found that NK cells from melanoma patients express higher levels of CD11a, CD95 and CD38. CD56^{bright} NK cells have been shown to inhibit CD4 T cell proliferation via the adenosine pathway ²²¹. CD73 another member of the adenosine pathway has already been shown to play an important tumour-promoting role in melanoma ^{222,223}. The role of CD38 on NK cells might be an interesting avenue to pursue as a possible therapy.

Overall, our data suggests that CD56^{bright} NK cells may have a negative effect on the anti-tumour response or could be used as a potential biomarker as our study provides evidence that the frequency and absolute numbers of CD56^{bright} NK cells inversely correlate with overall survival.

9. Characterisation of immune-modulating B cells in late stage melanoma patients

9.1. Introduction

Since the '80s multiple antibody types directed against tumour antigens have been discovered, indicating that B cells recognize and respond to tumour development^{224,225}. Since then new techniques have been developed to detect autoantibodies either in the serum via the SEREX method (serological analysis of tumour antigens by recombinant cDNA expression cloning) or the mini-array displaying distinct tumour-associated recombinant antigens^{226–228}. The presence or absence of tumour antigen-specific antibodies has been used as a diagnostic marker in a number of cancers. A panel of antigens (p53, c-myc, HER2, NY-ESO-1, BRCA1, BRCA2 and MUC1) were used to fish out antibodies from the sera of early breast cancer patients as well as patients with ductal carcinoma in situ. A response to one of the antigens was reported in 64 and 45% respectively²²⁹. A similar panel of antigens (p53, c- myc, HER2, NY-ESO-1, CAGE, MUC1 and GBU4-5) was used in patients with non-small cell lung cancer and small cell lung cancer. Antibody specific response could be measured in 76% of the patients²³⁰. Years before cancer induction antibodies directed against nuclear antigens, like p53 could be found in high risk patients, like people working/living in an asbestos environment or patients with liver cirrhosis or chronic hepatitis^{231,232}. However, autoantibodies do not only have value as diagnostic but also prognostic markers. The presence of antibodies against tumour antigens, has been associated in some cases with a poor prognosis. For examples α -NY-ESO-1 titers in hormone refractory prostate cancer²³³. Moreover, the titer seems to correlate with the size of the tumour mass in different tumour types²³⁴. Titers of anti-nuclear antibodies were associated with bad prognosis in breast cancer and gastric cancer^{235,236}. Other examples are the presence of α -laminin antibodies in breast cancer, α -p53 antibodies in breast, gastric, colon cancer, NSCLC, oral cancer^{237,238}. A positive correlation between antibody titers and prognosis has been found in prostate carcinoma (CTSP-1), hepatocellular carcinoma (p53), non-small cell lung cancer (antineural, MUC1, ANA), colon carcinoma (cardiolipin, tropomyosin, ds-DNA, MUC5AC), CLL (laminin receptor), CML (CML66), glioblastoma (GLEA3, PHF3), ovarian cancer (MUC1), gastric cancer (Thomsen-Friedenreich, MUC1), small cell lung cancer (SOX group B, ZIC2), Hodgkin lymphoma (carbo-anhydrase 1) and breast cancer (CEA, endostatin)^{239–253}.

In 1979 Wood *et al.* reported that the sera of some patients produced cytotoxicity *in vitro* against allogenic cells²⁵⁴. An antibody derived from peripheral B cells from a melanoma patients was able to induce ADCC *in vitro*²⁵⁵. ADCC is mediated by the binding of immunoglobulins to Fc Receptors. Four groups of FcR exists, classified based on their affinity for IgG, function and distribution. Fc γ RI and Fc γ RIII have a pro-inflammatory function mediated by intracellular tyrosine-based activating motives (ITAMs). Ligation

triggers ADCC by NK cells as well as cytokine release, oxidative burst and phagocytosis by macrophages on top of degranulation of mast cells. On the other hand, ligation of FcγRII inhibits these inflammatory response via tyrosine-based inhibitory motifs (ITIM) signalling. These receptors play thus a central role in determining the direction of the immune response ²⁵⁶. Terminal glycans on terminal Fc part of IgG determine a lot their binding capacity. For example, terminal galactose residues promote binding to C1q complement factor, whereas the absence of fructose increases ADCC by improved binding ^{257,258}. Sialylated immunoglobulins are able to bind to APCs and induce the upregulation of FcγRII. This glycosylation pattern was found on a part of the NY-ESO-1 specific antibodies in the circulation of melanoma patients ²⁵⁹. Immunoglobulins can also be carriers for latent TGFβ ²⁶⁰.

Class switched antibodies are not only present in the circulation but can also be found within the TME. Within the skin lesions of melanoma mRNA profiles indicate the presence of matured B cells and antibody response as indicated by class switching, shorter CDR3 regions, clonal expansion as well as distinct repertoire in healthy and malignant skin ²⁶¹. In breast cancer IgG and IgA antibodies have been found in the TME ²⁶². IgA isotypes were also observed in TLS in cutaneous melanoma, normally this isotype is only found in lymph nodes draining the mucosal tissues ²⁶³. Class-switching to IgA expressing cells is induced by TGFβ suggesting the presence of an immunosuppressive microenvironment ²⁶⁴. IgA⁺ B cells have been shown to produce IL-10 in liver cancer and thus directly suppress CTL responses ²⁶⁵. Another anti-inflammatory antibody is IgG4. Class switching to IgG4 is induced by a Th2 environment. It has poor FcR and complement binding. It has been reported in melanoma that B cells from melanoma lesions produced higher proportions of IgG4 than B cells from healthy counterparts. IgG4 antibodies not only lack effector functions but also compete with IgG1 for FcR binding ²⁶⁶. Some IgG4 expressing B cells have also been shown to produce IL-10 ⁸². Immunoglobulins can not only have a suppressive role but can also be important in the establishment of a chronically inflamed environment. Sustained inflammation is one of the emerging hall marks of cancer as described by Hanahan and Weinberg. Immune cells can provide in these settings growth, pro-angiogenic and survival factors as well as facilitate metastasis ²⁶⁷. Immune complexes, which are the association of immunoglobulins with complement, deposited within the tumour have been shown to be the result of leaky vasculature ²⁶⁸. Tumorigenesis is halted in a model of squamous cell carcinoma upon the absence of B and T cells. Transfer of B cells or serum from tumour-bearing mice restores tumour development ²⁶⁹. It was shown that accumulation of autoantibodies in the stroma interacts with resident and recruited myeloid cells via FcγR. This interaction leads to an array of responses from the innate immune compartment leading to tissue remodelling, angiogenesis, recruitment of leukocytes as a final results leading to squamous carcinogenesis ²⁷⁰.

B cells are able to infiltrate the tumour in multiple types of cancer^{271–275}. Their presence within the TME has been associated with a both favourable and poor prognosis in melanoma^{276–280}. Mostly, favourable prognosis are related to the presence of B cells in TLS²⁸¹. TLS are lymphoid like structures with distinct B and T cells zones that can be found outside the lymphoid tissues²⁸². The presence of TLS itself are associated with a favourable prognosis, these areas are important in generating effector and memory T cells within the tissues. In the B cells zones a germinal centre is present for memory generation of B cells and class switching^{283,284}. In patients with lung cancer or melanoma all stages of B cells were observed, naïve, memory B cells, class switching and plasma cells^{263,284}. B cells are in this capacity not only able to produce antigen but can also act as APCs²⁸⁵. Activated B cells were able *in vitro* to present antigens from melanoma lysates to T cells and efficiently activate them²⁸⁶. Higher clonality of CD4⁺ T cells was observed in lung cancer patients that had TLS present in the tumour with B cells continuously presenting antigens²⁸⁷. B cells are able to cross-present peptides on a class I MHC from a 30-mer peptides derived from the NY-ESO-1 antigen to CTL *in vitro*²⁸⁸. In high-grade ovarian cancer, B cells were found in close proximity to CD8 T cells, moreover they express MHC class I and II as well as co-stimulatory molecules CD40, CD80 and CD86. The combination of B and T cell presence correlates with survival²⁷³. It is thus important to consider the spatial repartition of B cells within the TME when considering their function.

In 1982 it became clear that B cells can also have a tumour promoting role. In a mice experiment, B cells were depleted using a chronic administration of an α -IgM antibody. This depletion led to a lower tumour incidence²⁸⁹. In a more recent study, Inoue *et al.* showed that splenic cells from wild type or B cell knock out mice co-cultured with irradiated tumour cell lines showed impaired production of IFN γ production by CD8 T and NK cells in the presence of B cells. *In vivo* experiments showed a similar results. The tumour promoting role of B cells was associated with their IL-10 production²⁹⁰. In a carcinogenesis mouse model it was shown that in the absence of the cytokine TNF α derived by B cells, CTLs produce more IFN γ and B cells produce less IL-10²⁹¹. In a 4T1 breast cancer model it was reported that metastasis was dependent on a subset of B cells, regulatory B cells (CD19⁺ CD25^{High} CD69^{High}) which were able to induce T_{regs} in a TGF β -dependent manner⁸⁷. The same group was also able to show that regulatory B cells have an important role in educating MDSCs. This educational process is also TGF β dependent⁹¹. It was shown that tumour cells are able to induce regulatory B cell formation, through the metabolite 5-lipoxygenase²⁹². Tumours can also have a long distance effect on B cells via exosomes. It has been shown by Pucci, *et al.* that tumour-derived extracellular vesicles interacts with B cells within the lymph nodes. As a consequence, B cells produced more immunoglobulins that induces in turn cancer growth. Transfer of sera to another mouse, accelerated tumour progression²⁹³.

In humans, a partial depletion of B cells using Rituximab in patients with colorectal cancer led to a reduction in tumour burden in 50% of patients at the end of the treatment ²⁹⁴. Different types of B_{regs} have been found in different types of cancer ²⁹⁵. In gastric cancer, IL-10 producing B cells expressing high levels of CD24 and CD38. Depletion of B_{regs} from the PBMCs increased the secretion of IFN γ by Th cells *in vitro*. Moreover, they were able to induce Tregs via TGF β ²⁹⁶. In patients with tongue squamous cell carcinoma double staining for IL-10 and CD19 showed double expression within the TME. Tongue squamous cell carcinoma cell lines were able to induce B_{regs}. This induction was blocked by an α -CD40L antibody. B_{regs} derived *in vitro* were able to induce T_{regs} independent of IL-10. The ratio of regulatory cells (B or T cells) compared to the whole population (B or T) correlated with overall survival of the patients ⁸⁴. Patients with hepatocellular carcinoma had more regulatory B cells in the circulation and in the evasive margins of the tumour. Regulatory B cells in the periphery correlated with clinical parameters like staging, venous infiltration and tumour multiplicity. When transferred into SCID mice, B_{regs} were able to promote tumour progression independent of T_{regs} ²⁹⁷. Additional mechanisms have been described apart from IL-10 and TGF β . It was reported that regulatory B cells from the PBMCs from patients with invasive carcinoma of the breast expressed a high level of PD-L1. A positive correlation was found between PD-L1⁺ B_{regs} and T_{regs}. An inverse correlation exists between PD-L1⁺ B_{regs} and CTL ²⁹⁸. Resistance to BRAF inhibitors is fairly common in melanoma. It was shown that melanoma cells produce the growth factor FGF-2. This in turn interacts with tumour-infiltrating B cells via FGR3. It activates them to produce IGF1, but also IL1, VEGF and PDGFA/B. Growth factor IGF1 has a feedback effect on melanoma cells, leading to an upregulation of FGR3 on melanoma cells, a positive feedback loop is thus instated where FGF2 produced by melanoma cells can act on themselves. This leads to a more heterogeneous population ²⁹⁹.

B cells have a dual role in tumour immunity. They can promote anti-tumour response via the presentation of antigens or by inducing ADCC. The tumour promoting roles of B cells can be either direct or indirect and are very complex (Figure 7). B cells can be a potential target to improve current treatment or find new avenues to treat patients that do not benefit from the current strategies ²⁸¹.

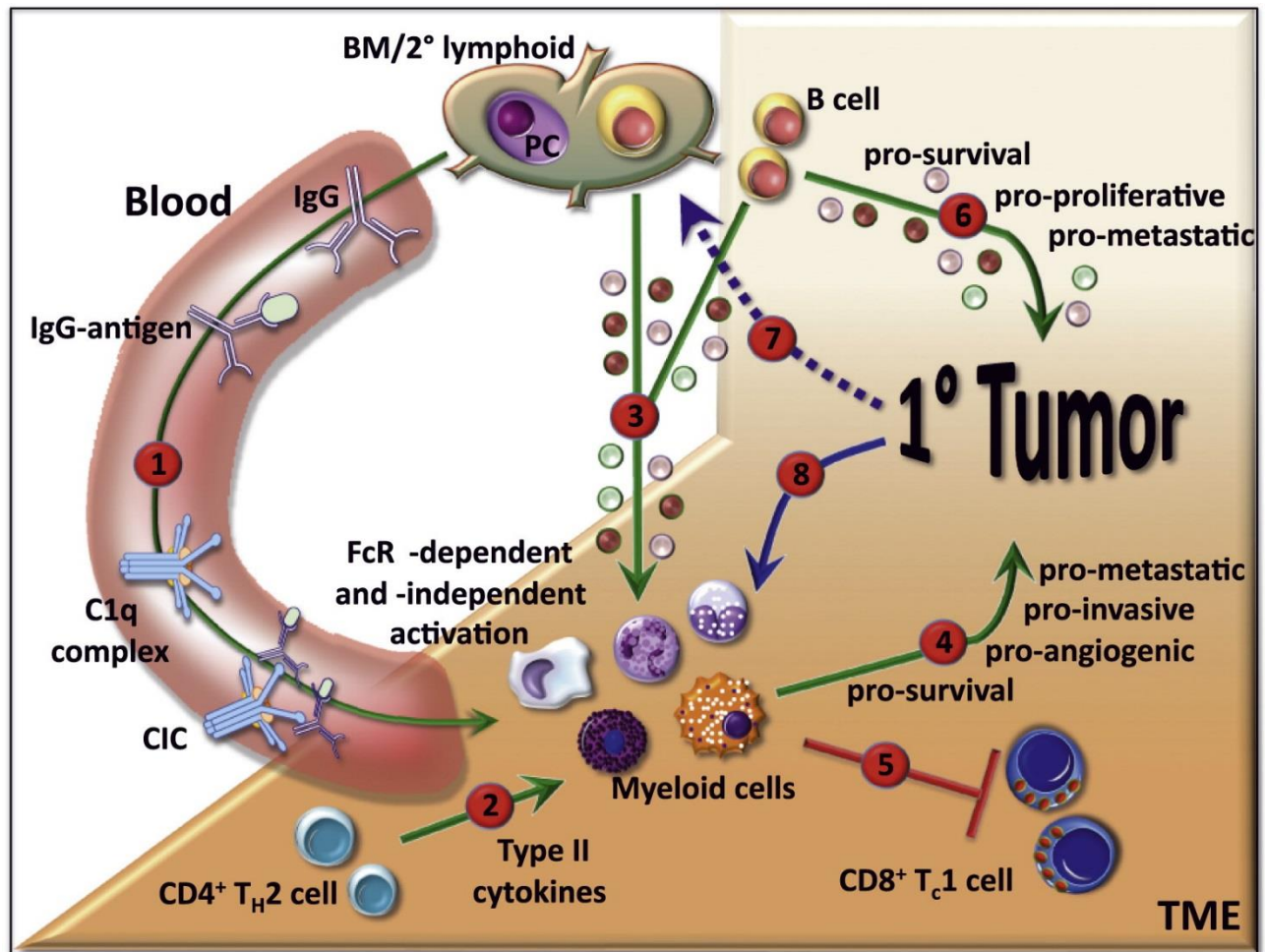


Figure 7|B cells can interact in multiple ways with the tumour and other immune cells within the TME. (1) Cancer-immune complexes (CIC) can act over a long distance and interact with FcR on cells from the myeloid compartment at the TME. (2) Type II cytokines produced by Th cells at the TME induce a type two polarization in those myeloid cells. (3) B cells can interact and activate myeloid cells in an FcR independent manner via cytokine production. (4) Myeloid cells are able to produce pro-tumoural factors that are pro-metastatic, pro-invasive, pro-angiogenic and pro-survival. (5) Myeloid cells limit CTL activation and tumour cell killing in the TME. (6) B cells produce pro-survival, pro-proliferative and pro-metastatic factors at the TME. (7) Tumour cells can induce regulatory B cells or pro-tumoural B cells via excreted factors. (8) Tumour cells recruit myeloid cells to the TME ³⁰⁰.

9.2. Aim

The role of B cells in the response to human melanoma is still unclear. Especially the role of B cells within the tumour micro-environment is poorly documented. Most studies have used CD19 or CD20 antibodies in immunohistochemistry, whereas phenotype and functionality of B cells remain mostly unknown. We decided to phenotypically and functionally characterize B cells within the periphery and the TME by using flow cytometry and RNA sequencing in melanoma patients before treatment. We screened patients enrolled in clinical studies including vaccination and immunotherapy trials and aimed at determining eventual correlations with clinical outcome.

Our goal is to advance the knowledge on the role of B cells in melanoma patients.

9.3. Material and Methods

9.3.1. Melanoma patients

Blood was obtained from melanoma patients included in three different clinical trials. Two of them were interventional and registered on ClinicalTrials.gov as follows: NCT00112229 and NCT00306566). One study was observational with EC number: 400/11. Patients were enrolled upon written informed consent. Eligibility criteria and study design has been previously described^{301–303}. The study was designed, approved and conducted according to relevant regulatory standards approved by the Ethics Commission for Clinical Research of the Faculty of Medicine and University of Lausanne (Lausanne, Switzerland), Swissmedic (Swiss Agency for Therapeutic Product) and the Protocol Review Committee of the Ludwig Institute for Cancer Research (New York). Only baseline samples from before the trial treatment were used in this study. Control PBMCs from healthy donors were isolated from blood donations obtained from the Blood Transfusion Centre.

Human melanoma tissue specimens used for RNA sequencing analysis were collected in the framework of the research protocol 87/06 approved by the Ethics Committee for Clinical Research of the Faculty of Biology and Medicine of the University of Lausanne.

9.3.2. Human cell preparation and flow cytometry

Patient or healthy donor PBMCs were isolated from whole blood cells by Lymphoprep (Axis-Shield) centrifugation gradient and cryopreserved in liquid nitrogen. Frozen PBMCs were thawed in a water bath at 37°C. Cells were kept, for resting, overnight at 37°C and 5% CO₂ in RPMI (Gibco), 10% FCS (Gibco) and 100U/ml IL-2 (Proleukin). Cells were then stimulated with 3 µg/ml CpG 7909 (PF-3512676) which was provided by Pfizer and Coley Pharmaceutical Group, Wellesley MA, for 14 hours after which 50ng/ml PMA (Sigma-Aldrich) and 500ng/ml Ionomycin (Thermo Fischer) was added. After another two hours 2nM Monensin (Sigma-Aldrich) and 10µg/ml Brefeldin A (Sigma-Aldrich) were added for another 4 hours. Control samples were kept in RPMI, 10% FCS Monensin and Brefeldin A were added at the same time point as their stimulated counterpart.

The first step in the staining for flow cytometry analysis is the blocking of the Fc-receptor to avoid unspecific staining using an Fc-blocking reagent (Miltenyi, 130-059-901). The following antibodies were used for the phenotyping and functional characterization of B cells from PBMCs: CD4 (BD Bioscience, 562970), CD8 (Biolegend, 344732), CD14 (Beckman Coulter, B01175), CD19 (Biolegend, 302208), CD27 (eBioscience, 61-0279-42), IgD (BD Bioscience, 555778), CD95 (Biolegend, 305606), CD126 (IL6-R) (BD Bioscience, 551850), PD-1 (Biolegend, 329920), T-bet (BD Bioscience, 562467), IL-2 (BD Bioscience,

554565), IL-4 (Biolegend, 500810), IL-5 (BD Pharmigen, 554396), IL-6 (Biolegend, 501106), IL-13 (BD Pharmigen, 561162), IL-17A (Biolegend, 512308), IFN γ (BD Pharmigen, 557844), TNF α (BD Pharmigen, 557996) and LT α (Invitrogen, BMS105FI).

After staining with extracellular antibodies a live/dead staining (LIVE/DEAD™ Fixable Near-IR Dead Cell Thermo Fisher Scientific Cat# L-34975) was performed. Cells were fixed at RT during 30 minutes (FoxP3 intracellular staining kit, eBioscience). Intracellular staining was performed at RT during 30 minutes in FoxP3 intracellular staining kit permeabilisation buffer (eBioscience). Cells were acquired using the Gallios flow cytometer (Beckman Coulter) and analysed using FlowJo 10.4.2 (FlowJo LCC).

9.3.3. Cell sorting and RNA sequencing

Tumour-specific T cells from tumour-infiltrated lymph nodes (TILN) were prepared after finely mincing surgery specimens to yield a single cell suspension, which was cryopreserved on the same day as the surgery was performed. Cell sorting by flow cytometry was performed in collaboration with Laure Tillé (Gregory Verdeil, UNIL, Lausanne). In short, cells were thawed and rested overnight in RPMI and FCS. B cells were sorted based on the expression of CD19 (Beckman Coulter, A96418) using the Astrios (BD Bioscience). Cells were sorted directly into RNA later (Invitrogen, AM720) to conserve RNA upon cryopreservation. RNA was extracted using the RNeasy Plus Micro kit (Qiagen, 74034) following the manufacturer's protocol. Quality of RNA was tested using a fragment analyser (Advanced Analytical). Total RNA from all samples used for sequencing had an RQN \geq 7. Libraries were obtained using the Clontech SMART-Seq v4 (Takara). Single read (100bp) was performed using an Illumina HiSeq 2500 sequencer (Illumina). These last two steps were performed at the Lausanne Genomics Technologies Facility (UNIL, Lausanne).

RNA-sequence quantification was performed using Kallisto³⁰⁴. In brief, target transcript sequences were obtained from ENSEMBLE (GRCh38.p12), and the abundance of transcripts was quantified using Kallisto 0.44.0 with sequence-based bias correction. All other parameters were set to default when running Kallisto. Kallisto's transcript-level estimates were further summarized at the gene-level using tximport 1.8.0 from Bioconductor³⁰⁵. For downstream analysis, lowly abundant genes were filtered out and differential expression analysis was performed using DESeq2 1.22.0 from Bioconductor³⁰⁶. Significant genes were identified using FDR $<$ 0.1. Gene Set Enrichment Analysis (GSEA) was performed using fgsea 1.8.0 package from Bioconductor with fold change estimates as gene-level statistic³⁰⁷. Prior to GSEA, ENSEMBL gene ids were converted to human gene symbols using biomaRt 2.38.0 from Bioconductor³⁰⁸. If a gene symbol was associated with more than one ENSEMBL id, the ENSEMBL id with maximum variation

was selected using the collapseRows functionality within the WGCNA R package ³⁰⁹. Signaling pathways analyzed by GSEA were obtained from the Hallmark gene sets of the MSigDB ³¹⁰. Heatmap was generated using the pheatmap R Package ³¹¹, with clustering distance and method set to Euclidean and ward.D2, respectively. RNA sequencing analysis was performed by Sina Nassiri (Prof. Daniel Speiser, UNIL, Lausanne).

9.3.4. Statistics and analysis

Significance of single comparisons was assessed using the Mann–Whitney test, multiple comparisons a Kruskal-Wallis test, using the GraphPad Prism 8 software. Overall survival (OS) was defined as the time between enrolment in the clinical trial and latest follow-up or death. The significance of Kaplan-Meier survival analysis was assessed by the Log-rank test (Prism 8).

9.4. Results

9.4.1. Patient B cells are potent cytokine producers

For the characterisation of B cell populations we used samples from patients from three different clinical trials. All samples were from the baseline time point, so none of the patients received any treatment at the time of sampling. One study included only early stage melanoma patients (stage I-II) who received virus-like particles for vaccination ³⁰². In a second study late stage melanoma patients (stage III-IV) were recruited into a vaccination trial using short Melan-A peptide and adjuvants to induce an immune response ³⁰¹. In the third and last trial patients received immunotherapy under the form of an α -CTLA-4 blocking antibody ³⁰³.

Carpenter, *et al.*, found a decrease in the memory compartment (CD27⁺ B cells) in metastatic melanoma patients in the blood ³¹². We however did not find a significant difference between memory cells either switched (IgD⁻) or unswitched (IgD⁺) memory B cells (Figure 8A). Moreover, we did not find any differences between the frequencies of circulating B cells or naïve B cells (Figure 8A).

Not much is known about the functionality of B cells in cancer patients apart from antibody production even though B cells are also known for their potent production of cytokines ³¹³. We found that B cells produce IL-2, GM-CSF, TNF α , LT α , IL-6 and IL-10 (Figure 8B,C). We did not find any significant differences between cytokine production in patients and healthy donor controls (Figure 8B,C). We did not observe any production of IL-4, IL-5, IL-13, IL-17A or IFN γ (data not shown).

9.4.2. Previous immunotherapy and stage of the patients correlate with B cell functionality

We observed a big range in the degree of cytokine production by B cells from melanoma patients. We decided to look into more detail into the clinical parameters that set these patients apart. Interestingly, B cells from stage III/IV melanoma patients produce less IL-2, TNF α and LT α than stage I/II patients (Figure 9A). These results show a partial impairment in B cell functionality from late stage patients (stage III/IV). Moreover, we found a deficiency in the functionality of patients having received previous immunotherapy. B cells from patients having received previous immunotherapy are less able to produce TNF α , LT α and IL-10 (Figure 9B). Immunotherapy includes mostly vaccinations with peptides as well as cytokines. An overview of the previous immunotherapy can be found in Table 1. Radiotherapy and chemotherapy had minor effects on the production of cytokines (Figure 9C,D).

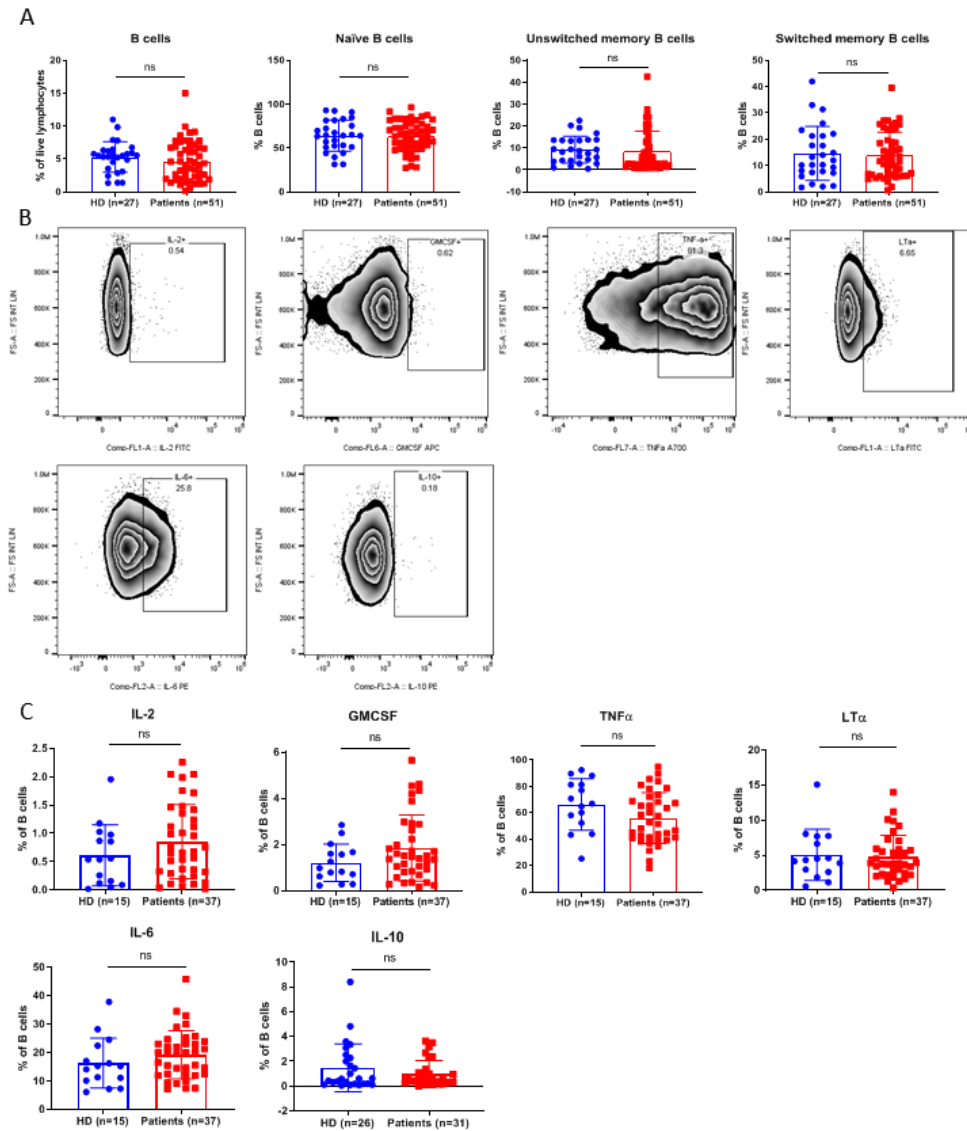


Figure 8 | Frequencies and functionalities of peripheral B cells. A. Frequencies of circulating B cells and its subsets including naïve, unswitched memory and switched memory B cells from healthy donors (n=27) and melanoma patients (n=51). B. Representative dot plots from a healthy donor of cytokine production by B cells. C. Summary of the cytokine production by B cells from healthy controls (n=15/26) and melanoma patients (n=37/31) after CpG and PMA/Ionomycin stimulation. ns not significant, * p<0.05, ** p<0.01, *** p<0.001, **** p<0.0001.

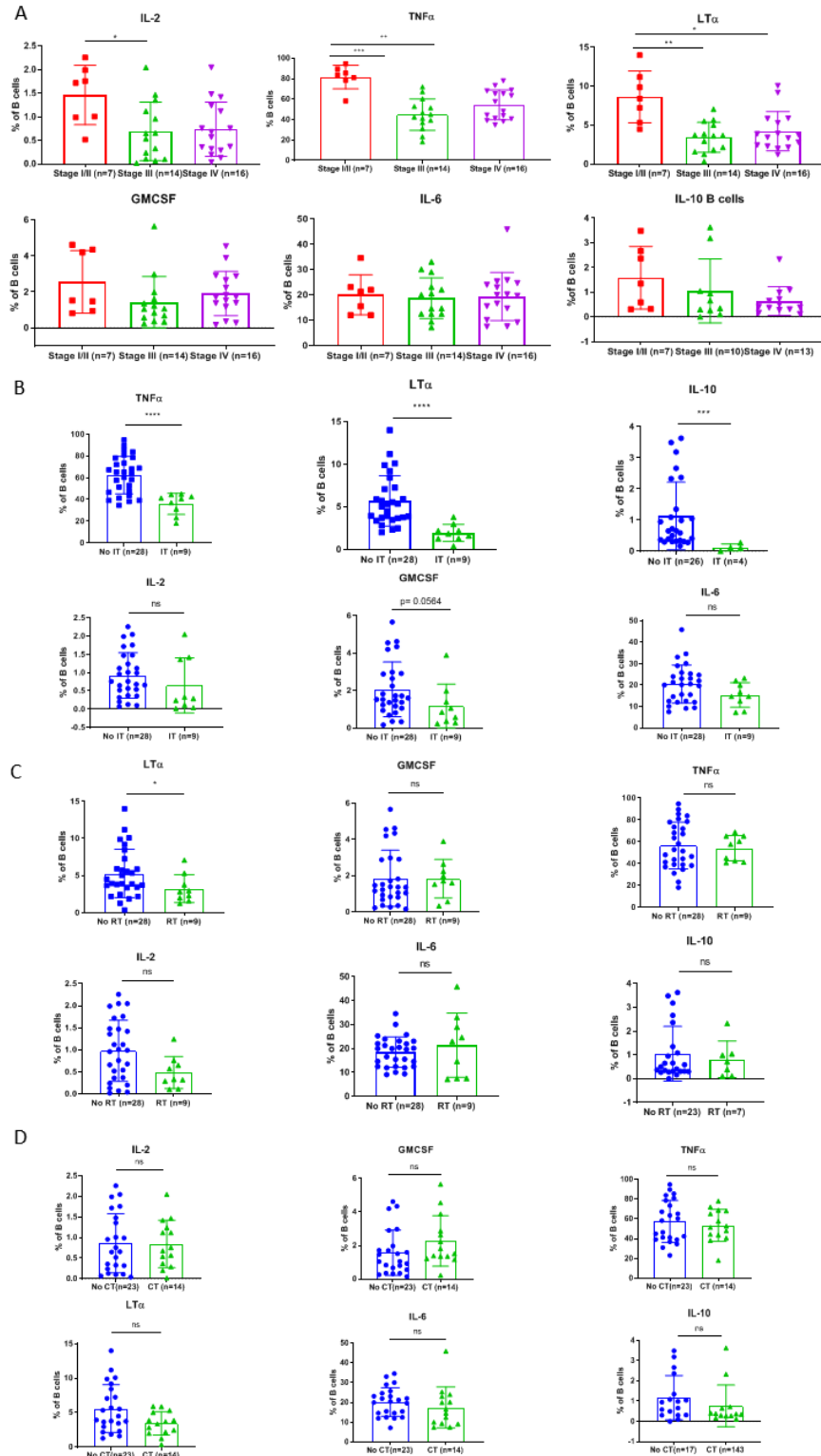


Figure 9 | Distribution of cytokine production by B cells (IL-2, GMCSF, TNF α , LT α , IL-6 and IL-10) in different clinical conditions. A. Distribution of cytokines produced by B cells from patients in stage I/II, III and IV. B,C,D. Distribution cytokine production by B cells in melanoma patients in relation to previous immunotherapy (IT) (B), radiotherapy (RT) (C), chemotherapy (CT) (D). ns not significant, * $p < 0.05$, ** $p < 0.01$, *** $p < 0.001$, **** $p < 0.0001$.

Table 1 | Detailed information about the patients that received previous immunotherapy as well as the type of immunotherapy received.

Patient	Immunotherapy
LAU 205	P40/ELA cancer vaccine study: Melan-A 26-35 (A27L) analogue peptide (ELA)+ P40 adjuvant
LAU 321	LUDWIG 96-010 cancer vaccine study: Melan-A 26-35 (A27L) analogue peptide (ELA)+ FluMa 58-66 peptide + low dose rhIL-2+ SB AS-2 Isolated limb perfusion with Melphalan+IFN γ +TNF α
LAU 371	LUDWIG 98-009 cancer vaccine study: Melan-A 26-35 (A27L) analogue peptide (ELA)+FluMa 58-66 peptide + SB AS-2
LAU 392	LUDWIG 96-010 cancer vaccine study: Melan-A 26-35 (A27L) analogue peptide (ELA)+ FluMa 58-66 peptide + low dose rhIL-2+ SB AS-2
LAU 444	LUDWIG 96-010 cancer vaccine study: Melan-A 26-35 (A27L) analogue peptide (ELA)+ FluMa 58-66 peptide + low dose rhIL-2+ Montanide ISA-51
LAU 618	Isolated limb perfusion with Melphalan+IFN γ +TNF α
LAU 648	LUDWIG 96-010 cancer vaccine study: Melan-A 26-35 (A27L) analogue peptide (ELA)+ FluMa 58-66 peptide + low dose rhIL-2+ Montanide ISA-51
LAU 672	LUDWIG 96-010 cancer vaccine study: Melan-A 26-35 (A27L) analogue peptide (ELA)+ FluMa 58-66 peptide + Montanide ISA-51 Isolated limb perfusion with Melphalan+IFN γ +TNF α
LAU 701	Isolated limb perfusion with Melphalan+IFN γ +TNF α
LAU 706	Isolated limb perfusion with Melphalan+IFN γ +TNF α P40/ELA cancer vaccine study: Melan-A 26-35 (A27L) analogue peptide (ELA)+ P40 adjuvant
LAU 518	Vaccinations with long NY-ESO-1 long-peptide and Montanide with CpG adjuvant
LAU 1131	VLP vaccination with Melan-A analogue peptide and Montanide
LAU 1394	Vaccinations with Melan-A ELA+ Melan-A EAA+ MAGE-A10+ NY-ESO-1 long-peptide and Montanide adjuvant
LAU 1397	Vaccinations with Melan-A ELA+ Melan-A EAA+ MAGE-A10+ NY-ESO-1 long-peptide and Montanide adjuvant Vaccinations with Melan-A ELA+ sLAG-3 long-peptide and Montanide adjuvant

9.4.3. Pro-inflammatory B cells correlate inversely with overall survival in Ipilimumab treated patients

Due to the heterogeneity in patients, we decided to focus on the patients treated with the checkpoint blocker Ipilimumab (α -CTLA-4). These are patients with the most advanced disease, mostly stage IV with substantial disease burden. B cells from patients produced more GMCSF than B cells from healthy donors. We did not see any differences between the production of IL-2, IL-6, IL-10, TNF α and LT α (Figure 10A). At a phenotypical level, we also observe higher expression of IL-6R and FasR and the transcription factor T-bet. We did not observe any differences between PD-1 expression on B cells from patients and healthy controls (Figure 10B). T-bet has been shown to be expressed in pathological B cells driving a lupus-like disease in mice³¹⁴.

Patients recruited in this clinical trial had an extensive follow-up, up to 7 years. The advantage of an Ipilimumab treatment is that significant numbers of patients had clear clinical responses, allowing the comparison of responders with non-responders. We found that B cells from non-responders produce more TNF α , IL-6 and IL-10, but less GMCSF (Figure 10C). This suggests that cytokine producing B cells are more potent in non-responders. None of the phenotypical markers was differentially expressed between responders and non-responders (data not shown). Interestingly, we found that IL-6, TNF α and IL-10 levels negatively correlate with overall survival (Figure 10D). This seems to indicate that both inflammatory and regulatory B cells have negative effects on patient prognosis. From our analysis it was impossible to determine if these are separate populations or a single multifunctional population of B cells.

9.4.4. B cells from the TME are significantly different from peripheral B cells from patients and healthy donor controls

The research presented above gives us an indication about the phenotype and the functionality of B cells within the periphery, but we do not know if this is reflected within the TME. To our knowledge, sorted B cells from the TME have not been sequenced to this date. We decided to sequence B cells from melanoma metastases (n=5), and corresponding B cells from the PBMCs (n=5). The data analysis was performed in collaboration with Sina Nassiri (Prof. Speiser lab, UNIL, Lausanne).

Visualization of significantly differentially expressed genes (FDR=0.1) of B cells from TILs compared to B cells from healthy donors in a heatmap shows that B cells cluster together based on their anatomical localization (Figure 11A). This indicates a stronger tissue signature than a patient signature. 131 genes are differentially expressed based on a false discovery rate of 0.1. The highest differentially expressed gene is the transcription factor SOX5. SOX5 is expressed during the later stages of B cell maturation when the proliferation capacity is reduced³¹⁵. Other genes in the top 30 include an interferon response gene (IFIT5),

immunoregulatory molecules (IDO1) and IgA heavy constant alpha 2 (Figure 11B). A top thirty genes based on the highest positive \log_2 of the fold change between TILs and PBMCs shows as well some of the same genes like SOX5, IDO1, IgA heavy constant alpha 2 and Immunoglobulin Lambda Variable 8-61, as well as some immune-related genes like CXCL11, CD86, Interferon Regulatory Factor 6 (IRF6) and Interleukin 4 Induced 1 (IL4I1) (Figure 11C). Gene enrichment analysis (GSEA) shows the presence of some important hallmarks, like Myc targets, interferon response as well as the inflammatory response and IL-6 signalling (Figure 11D).

There is evidence that B cells from the TILs are activated as can be seen from increased CD86 expression as well as the enrichment in inflammatory response genes and IL-6 signalling genes. The role of IL-6 produced by B cells may play an important role as well. We found that patients that do not respond to Ipilimumab treatment possess peripheral B cells that produce higher levels of IL-6. Moreover, high levels of IL-6 producing B cells inversely correlates with overall survival. Inflammatory genes are enriched in B cells from TILs, one of the hits within the GSEA enrichment is IL-6.

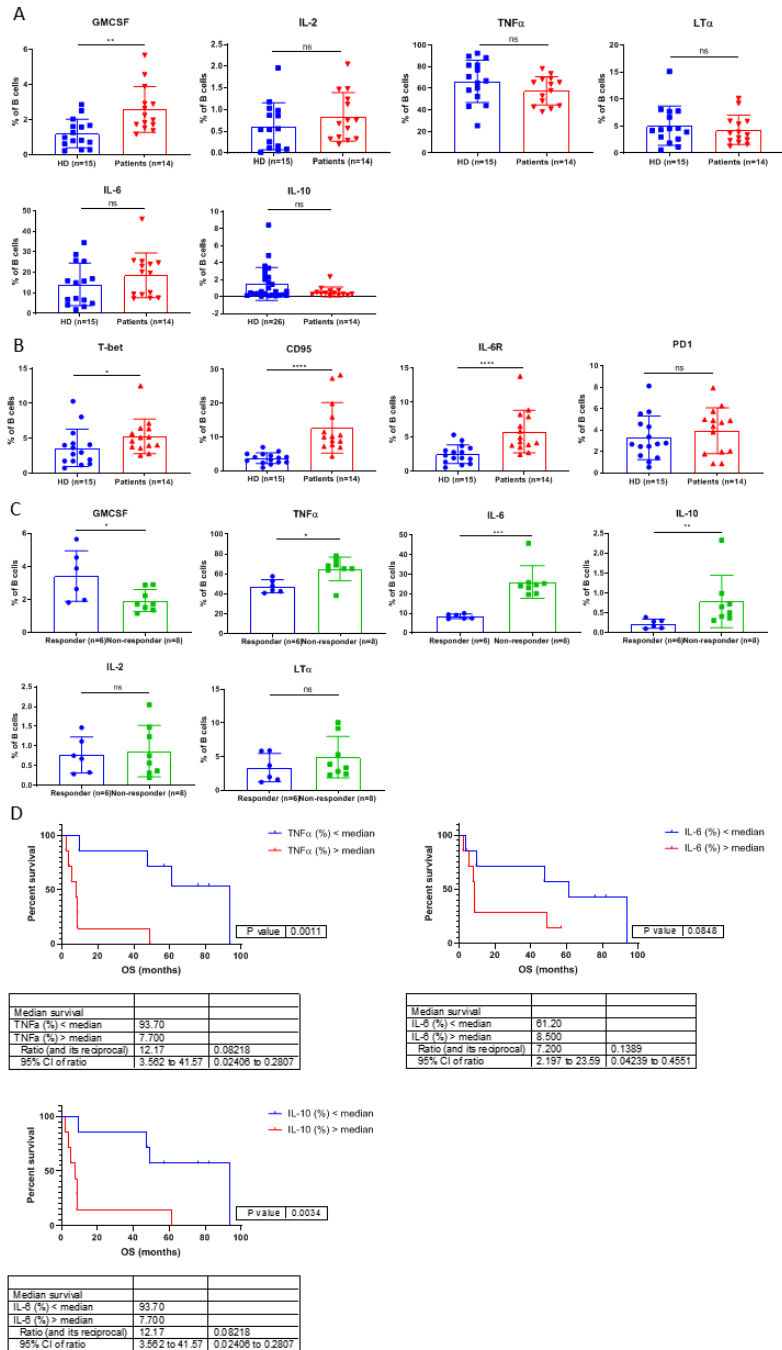
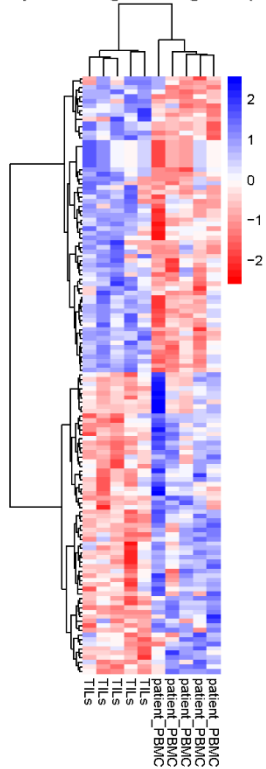


Figure 10 | Association of phenotypical and functional characteristics with clinical parameters of Ipilimumab. A. Cytokine production (%) in patients (n=14) and healthy donor controls (n=15/26). B. Phenotypical characteristics including T-bet (%) CD95 or FasR (%), IL-6R (%) and PD-1 (%) in patients (n=14) and healthy donor controls (n=15). C. Differentiation of patients into responders (n=6) and non-responders (n=8) to treatment and their associated cytokine production. D. Overall survival (log rank test) based on the median production of IL-6, TNFα and IL-10 in B cells from late stage melanoma patients. ns not significant, * p<0.05, ** p<0.01, *** p<0.001, **** p<0.0001.

A
Heatmap of 131 significant genes (TIL vs. PB)



Gene	Gene name	Log ₂ (Fold Change)	Adjusted p-value	
1	SOX5	SRY-box 5	3.31	0.000102
2	PCN2	Pecanex 2	-2.07	0.000102
3	GSTM3	Glutathione S-Transferase Mu 3	-2.82	0.000102
4	SPSB3	SplA/Ryanodine Receptor Domain And SOCS Box Containing 3	-1.02	0.00013
5	CD6	T-Cell Differentiation Antigen CD6	-2.09	0.00013
6	NTRK2	Neurotrophic Receptor Tyrosine Kinase 2	-3.26	0.00013
7	IFIT5	Interferon Induced Protein With Tetratricopeptide Repeats 5	1.66	0.00017
8	ITPR3	Inositol 1,4,5-Trisphosphate Receptor Type 3	-2.10	0.00075
9	EPHX2	Epoxide Hydrolase 2	-2.88	0.00075
10	PRKAB2	Protein Kinase AMP-Activated Non-Catalytic Subunit Beta 2	-1.51	0.00082
11	PPP1R3F	Protein Phosphatase 1 Regulatory Subunit 3F	-1.98	0.001135
12	AZIN2	Antizyme Inhibitor 2	-3.10	0.001135
13	RDX	Radiain	-1.23	0.001175
14	ARMCD4	Armadillo Repeat Containing X-Linked 4	-2.14	0.001548
15	NCOA1	Nuclear Receptor Coactivator 1	-1.09	0.002366
16	KLHL18	Kelch Like Family Member 18	1.37	0.002961
17	FCRL6	Fc Receptor Like 6	-2.89	0.003276
18	FRMD3	FERM Domain Containing 3	2.88	0.003661
19	TAPBP	TAP Binding Protein	2.43	0.004267
20	DAG1	Dystroglycan 1	2.10	0.004365
21	SLC38A5	Solute Carrier Family 38 Member 5	1.17	0.005653
22	IDO1	Indoleamine 2,3-Dioxygenase 1	2.72	0.006333
23	SLC9B1	Solute Carrier Family 9 Member B1	2.04	0.008537
24	ZWILCH	Zwisch Kinetochore Protein	1.41	0.008537
25	KBTBD8	Kelch Repeat And BTB Domain Containing 8	1.06	0.008537
26	GPR63	G Protein-Coupled Receptor 63	-2.11	0.01161
27	ZNF618	Zinc Finger Protein 618	2.61	0.012011
28	IGHA2	Immunoglobulin Heavy Constant Alpha 2	1.85	0.013255
29	NEIL2	Nei Like DNA Glycosylase 2	1.10	0.0142
30	PATL2	PAT1 Homolog 2	-1.50	0.0142

C

Gene	Gene name	Log ₂ (Fold Change)	Adjusted p-value	
1	SOX5	SRY-box 5	3.31	0.000102
2	FRMD3	FERM Domain Containing 3	2.88	0.003661
3	IDO1	Indoleamine 2,3-Dioxygenase 1	2.72	0.006333
4	ZNF618	Zinc Finger Protein 618	2.61	0.012011
5	HDX	Highly Divergent Homeobox	2.46	0.021018
6	TAPBP	TAP Binding Protein	2.43	0.004267
7	HSP5	Heat Shock Transcription Factor 5	2.37	0.05138
8	CXCL11	C-X-C Motif Chemokine Ligand 11	2.36	0.046178
9	IRF6	Interferon Regulatory Factor 6	2.280	0.051681
10	PODYL2	Podocalyxin Like 2	2.27	0.039288
11	KLHL15	Kelch Like Family Member 15	2.22	0.057662
12	NHLRC1	NHL Repeat Containing E3 Ubiquitin Protein Ligase 1	2.17	0.057662
13	DNASE1L3	Deoxyribonuclease 1 Like 3	2.11	0.039288
14	HSP90AASP	Heat Shock Protein 90 Alpha Family Class A Member 5, Pseudogene	2.10	0.099328
15	DAG1	Dystroglycan 1	2.10	0.004365
16	MVB12B	Multivesicular Body Subunit 12B	2.09	0.05138
17	SLCSB1	Solute Carrier Family 9 Member B1	2.04	0.008537
18	IGLV8-6L	Immunoglobulin Lambda Variable 8-6L	1.95	0.056681
19	TAPBP	TAP Binding Protein	1.87	0.056681
20	IGHA2	Immunoglobulin Heavy Constant Alpha 2	1.85	0.013255
21	IFIT5	Interferon Induced Protein With Tetratricopeptide Repeats 5	1.66	0.000179
22	PBLD	Phenazine Biosynthesis Like Protein Domain Containing	1.65	0.099706
23	CD86	CD86 molecule	1.58	0.093285
24	IL4I1	Interleukin 4 Induced 1	1.54	0.017357
25	CADML1	Cell Adhesion Molecule 1	1.52	0.029694
26	EEF2K3/MT	Eukaryotic Elongation Factor 2 Lysine Methyltransferase	1.49	0.076789
27	RPS9	Ribosomal Protein S9	1.42	0.049057
28	ZWILCH	Zwisch Kinetochore Protein	1.41	0.008537
29	KLHL18	Kelch Like Family Member 18	1.37	0.002961
30	PPA1	Pyrophosphatase (Inorganic) 1	1.33	0.036308

D

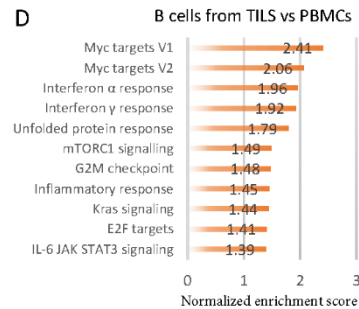


Figure 11| RNA sequencing of sorted B cells from melanoma metastatic lymph nodes and sorted B cells from the periphery from corresponding patients. A. A pairwise comparison represented in a heatmap of significantly differentially expressed genes comparing TILs and peripheral B cells with an FDR of 0.1. The heatmap is based on the z-score, red indicating negative and blue positive values. B. Top 30 differentially expressed genes, list based on adjusted p-values. C. Top 30 differentially expressed genes based on the biggest \log_2 of the fold change. C. Hallmarks enriched in B cells from TILs compared to PBMCs, enrichment was analysed using a pre-ranked list using GSEA with a nominal $p < 0.05$ and $FDR < 0.1$.

9.5. Discussion and perspectives

Different roles for B cells have been described especially in mouse tumour models, with pro-inflammatory as well as regulatory features³⁰⁰. However, the role of B cells in cancer patients is less described³¹⁶. We found that although B cell frequencies and subsets did not differ between patients and healthy donors, patients who received previous immunotherapy, mostly under the form of a peptide vaccination and adjuvants showed reduced production of TNF α , LT α and IL-10 as compared to patients not having received previous immunotherapy. Moreover, it seems that B cells become less functional with disease progression as indicated by stage.

These results made us focus on patients enrolled in a clinical trial receiving Ipilimumab (α -CTLA-4). Not much research has been performed trying to elucidate the role of B cells in clinical responses to checkpoint blockade. We focussed on the baseline time point in order to study characteristics of B cells driven by the disease.

We found that peripheral B cells from patients produce more GM-CSF and have a higher expression of T-bet, FasR and IL-6R. GM-CSF administration in melanoma in an adjuvant setting has shown limited success^{317,318}. On the other hand, it has also been shown to promote malignant cell growth in mouse models of head and neck squamous cell carcinomas³¹⁹. We also observed an upregulation of IL-6R on patient B cells, which is something we can also find on B cells from the TME. We observed an enrichment in genes involved in IL-6 signalling in B cells. This cytokine can have both pro and anti-inflammatory properties. Some of the hits within the inflammatory response hallmarks are IL-6, IL-10, IL-1B and LT α . Together with IDO1 found in the top hits, these results suggest that B cells from the TME are at the same time pro-inflammatory and regulatory, similarly as the circulating B cells. Both IL-10 and IL-6 produced by peripheral B cells negatively correlate with overall survival and can be found at higher levels produced by circulating B cells from non-responder patients. IL-6 plays an important role in B cell development and maturation of B cells and plasmablasts³²⁰. In combination with IL-1 β it has been able to induce regulatory B cells³²¹. This mechanism was described in gut-immunity, an environment where also IgA plays an important role and is the most prevalent isotype. We found that one of the genes overexpressed in B cells of the TME is part of the IgA molecule. IgA has been shown to be expressed by B cells in the TME of breast cancer as well²⁶². In liver cancer, IgA⁺ B cells were shown to express PD-1 and produce IL-10.²⁶⁵ IgA class-switching occurs in the presence of TGF β ³²². The presence of TGF β indicates an overall suppressive TME¹⁶¹.

Regulatory B cells have been quite elusive, since no transcription factor nor any surface markers have been found. Thus far the only way to identify them is with functionality^{81,323}. We found that circulating B cells

from non-responders produced more IL-10 than B cells from responders. In the TME we found that IL-10 was one of the hits within the inflammatory response hall marker significantly enriched in B cells from TILs compared to peripheral B cells. Regulatory B cells have been shown to limit T cell activation and proliferation as well as induce regulatory T cells⁸⁸. An additional pathway that could contribute to the suppressive character of intra-tumoural B cells is by the production of IDO1 which is one of the top hits we found by RNA sequencing. B cells have been shown to be able to regulate T cell response in an IDO-dependent manner³²⁴. It remains to be determined whether we can identify suppressive functions by the patients' B cells.

Suppression of T cell responses is not the only way in which B cells promote tumour progression. It has been shown that TNF α had a tumour promoting role in squamous cell carcinoma²⁹¹. We observed a negative correlation between TNF α and overall survival, moreover non-responsive patients to treatment produced more TNF α . However, we did not find any TNF α overexpression within the TME compared to peripheral B cells.

Overall, B cells have an immune-modulating phenotype by producing pro- as well as anti-inflammatory cytokines like IL-6, TNF α and IL-10. mRNA levels of IL-6, IL-10, LT α and IDO1 were also upregulated. Further research is needed to increase the number of patients. One of the possible avenues to follow is to use publicly available single cell RNA sequencing data from melanoma patients²¹⁸⁻²²⁰. During this previous research, as described in the literature, B cell profiles were not analysed in detail. Especially the recently published data from Sade-Feldman, *et al.*, is of particular interest to us since they used samples from before and after α -PD-1 and/or α -CTLA-4 treatment in melanoma patients²²⁰. They have described that a B cell cluster and not a plasma cluster was more frequent in responder patients, irrespective of the time point. However, the functional profile of these B cells has not been described in more detail²²⁰. It would be interesting to see if inflammatory genes are also enriched in these samples compared to corresponding blood samples. Moreover, we would like to see if the profile changes before and after treatment. We would like to complement this data, with flow cytometry analysis of B cells from tumour-infiltrated lymph nodes, including functionality after stimulation and phenotype. As controls we would also like to analyse lymph nodes from healthy donor controls. The discrepancies in the role of B cells could be explained by the favourable prognostic role of B cells when they are present in TLS compared to unaccompanied by T cells²⁸³. Our data is derived from TILNs where naturally a lot of B cells are present, it would be interesting to compare to non-lymphoid metastases.

Overall, our research suggests that B cells contribute to the pro-tumoural immune response by producing both inflammatory and regulatory cytokines. This opens up new avenues for therapy, since we find increased cytokine producing B cells in non-responding patients. B cells could thus be new targets, and/or exploited as biomarkers for therapy.

10.Characterization of a new lymphocytic population, termed Orphan lymphoid cells (OLC), in the blood of healthy humans

10.1. Introduction

Even though it was thought that all major lineages of immune cells had been discovered, 10 years ago a new type of immune cells was discovered, the ILCs ⁷. In mice, the ILC group cells, including ILCs and NKs, differentiate from the CLPs, which already expresses the IL7R α (CD127), the expression is conserved down to the ILC lineage but not the NK cell lineage ³²⁵. CLPs differentiate into integrin $\alpha_4\beta_7$ -expressing ILC progenitor α lymphoid precursors (α LP). This lineage differentiation is induced by transient expression of the transcription factor NFIL3 ³²⁶. NFIL3 induces the expression of transcription factors TOX and ID2 ^{327,328}. This stage is also called the early innate lymphoid progenitor (EILP). This EILP is able to give rise to the NK cell progenitor as well as the common helper ILC progenitor (CHILP) ³²⁹. CHILP1 express high levels of ID2 but no PD-1, they are able to give rise to lymphoid-tissue inducer cells. CHILP2 on the other hand, also express high levels of ID2 but also PD-1 as well as the transcription factor PLZF giving rise to the other ILC helper subsets (Figure 12) ³²⁶.

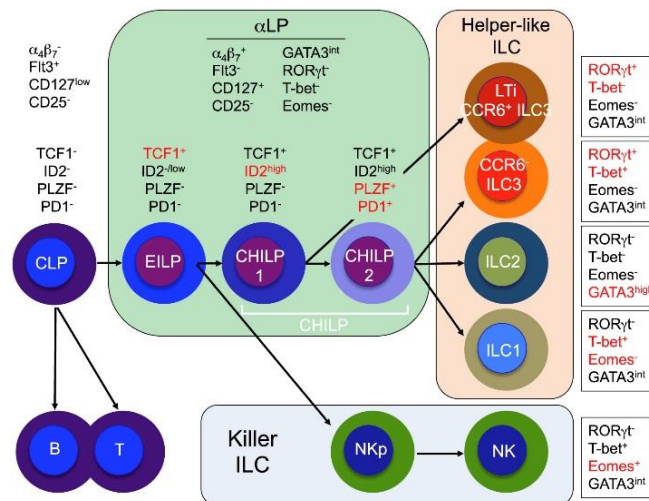


Figure 12| ILC and NK cell development originates in the bone marrow from CLP that in turn gives rise to α LP progenitors characterized by the expression of $\alpha_4\beta_7$ integrin. The first progenitor in this cascade is called the EILP and is able to give rise to all ILC subsets including NK cells. IL7R α is firmly expressed from this stage on. CHILP progenitors are no longer able to give rise to NK cells but only helper ILCs. CHILP1 characterised by high ID2 expression and absence of PD-1 and PLZF, CHILP1 is able to give rise to LTI cells. CHILP2 progenitors on the other hand express PD-1 and the transcription factor PLZF, they can give rise to helper ILC subsets: ILC1,2 and 3 ³³⁰.

The developmental path of ILCs and NK cells as well as at which step exactly their development differentiates is not entirely understood in humans. CLPs can be found in the human CD34⁺ compartment however, the exact phenotyping remains unclear ³³¹. NK cells, ILC1, ILC2s and ILC3s can be generated from

human CD34⁺ bone marrow cells *in vivo*, when transplanted in immune-deficient mice^{332,333}. *In vitro* differentiation from more CLP-like cells has been able to deliver NK, cells as well as ILC2s and ILC3s^{332,334}. More recently a subset of progenitor cells have been identified in the periphery of humans with the following phenotype: CD34⁻CD7⁺CD127⁺CD117⁺CD45RA⁺ that are able to give rise to all ILC subsets (helper and cytotoxic). Transcription factors found to be important in mice were also upregulated in human cells (TCF7, TOX, ID2, ZBTB16 and GATA3)³³⁵. Moreover, the phenotype of the CHILP is not clear either. CD34⁺CD45RA⁺α4β7⁺ precursor cells have been identified in human tonsils and lymph nodes, however they still have the potential to produce T cells and DCs, thus making further refinement necessary^{334,336}. In humans, the phenotypical differences between CILP and CHILP, indicating the difference between the potential of NK and/or ILC differentiation as it exists in mice is not clear³³⁷. Recently an NK cell precursor has been identified in cord blood, bone marrow and tonsils having the following phenotype: Lin⁻CD34⁺CD38⁺CD123⁻CD45RA⁺CD7⁺CD10⁺CD127⁻. It is unclear if they are able to give rise to ILC1 cells³³². ILC precursor 1 and 2 are still unknown in humans. However, ILC precursor 3 cells have been found in tonsils and the intestinal lamina propria expressing CD34, c-kit, α4β7⁺ as well as the transcription factor RORγT³³⁶. An overview can be found in Figure 13.

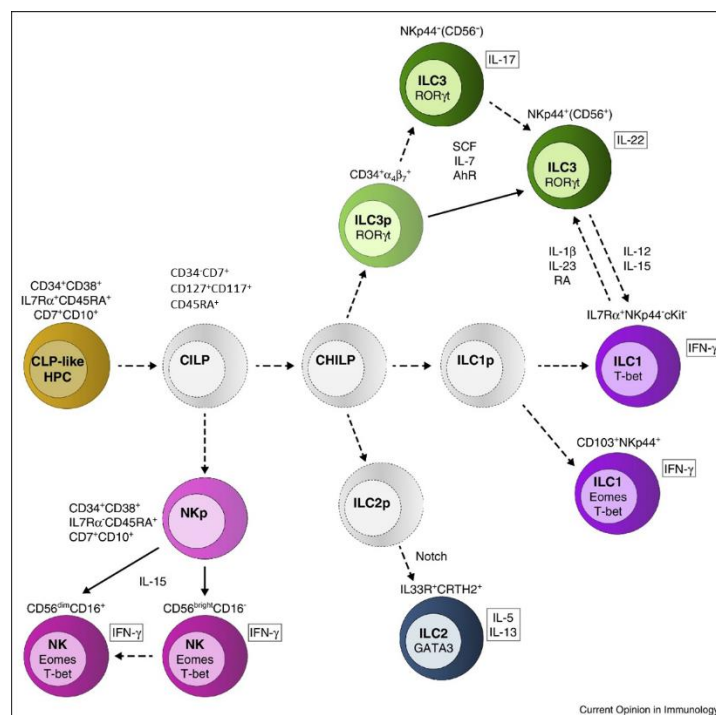


Figure 13| The lineage differentiation of human NK and ILCs starts in the bone marrow with a CLP like cell that differentiates further in CILP that can directly give rise to NKp as well as CHILP that in turn is able to produce ILC1p, ILC2p and ILC3p (adapted from³³⁷).

10.2. Aim

While characterizing NK cells, we identified a new type of human lymphoid cells in PBMC of healthy donors. Therefore we set the goal to confirm that these cells indeed represent a novel population, and to characterize them molecularly and functionally. We used flow cytometry and RNA sequencing to identify potential functions as well as to compare gene signatures to well-known immune cell types. In general, we aim at contributing to improved understanding of the human immune system by characterizing the lympho-hematopoietic system as comprehensively as possible.

10.3. Material and Methods

10.3.1. Human cell preparation and flow cytometry

Blood donations were obtained from the Blood Transfusion centre. PBMCs were isolated from whole blood cells by Lymphoprep (Axis-Shield) centrifugation gradient and used immediately.

The following antibodies were used for identification and phenotype of OLCs: CD3 (Biolegend, 300440), CD4 (Biolegend, 300538), CD8 (Immunotools, 21270083x2), CD14 (Biolegend, 325604), CD15 (Biolegend, 301904), CD16 (Biolegend, 302006), CD19 (Biolegend, 302206), CD20 (Biolegend, 302304), CD33 (Biolegend, 303304), CD34 (Biolegend, 343604), CD203 (Biolegend, 324614), FcεRIα (Biolegend, 334608). CD127 (eBioscience, 11-1278-73) and CD56 (Biolegend, 318304) make up the lineage markers. Additional antibodies used were: CD3 (Biolegend, 344806), CD62L (Biolegend, 322605), CD62L (Biolegend, 304824), CD132 (Biolegend, 338607), CD44 (BD Bioscience, 560532), CD45 (Biolegend, 304032), mouse IgG1 isotype control (Biolegend, 400150), mouse IgG2b isotype control (Biolegend, 400611) and mouse IgG2b isotype control (BD Bioscience, 560183). Afterwards, a live/dead staining (LIVE/DEAD™ Fixable Aqua Dead Cell Stain Thermo Fisher Scientific Cat# L34965) was performed.

Cells were acquired using the Gallios flow cytometer (Beckman Coulter) and the Amnis Imagestream (EMD Milipore). Data was analysed using FlowJo 10.4.2 (FlowJo LCC) and IDEAS 6.2 (EMD Milipore). Statistical significance was assessed using the Mann–Whitney test using the GraphPad Prism 8 software.

10.3.2. Cell sorting and RNA sequencing

PBMCs used for cells sorting were further processed for RNA sequencing. OLCs were selected based on the absence of markers stained by the following antibodies: CD3 (Biolegend, 344806), CD16 (Biolegend, 302008), CD19 (Biolegend, 302208), CD33 (Beckman Coulter, 6603042), CD56 (Biolegend, 318328), CD123 (Biolegend, 306010) and CD127 (BD Bioscience, 557938) were used for negative control. OLCs were positively selected using two antibodies: CD45 (Biolegend, 304012) and HLA-A,B,C (Biolegend, 311420). Cells were sorted immediately into RTL plus buffer (Qiagen) with DTT (Applichem).

RNA was extracted immediately after sorting using the RNeasy Plus Mini kit (Qiagen, 74136) following the manufacturer's protocol. Quality of RNA was tested using a fragment analyser (Advanced Analytical). Total RNA from all samples used for sequencing had an RQN \geq 6.4. Since RQN is not optimal, libraries were obtained using NuGen RNA-seq (TECAN). Single read (100bp) was performed using an Illumina HiSeq 2500 sequencer (Illumina). Library generation and sequencing were performed by the Lausanne Genomics Technology Facility (UNIL, Lausanne).

RNA sequencing analysis was performed by Julien Racle (Prof. David Gfeller, Ludwig Branch Lausanne). In short, gene expression from five RNA-seq datasets was integrated in the analysis. OLC dataset is the data that we generated including sorted OLCs, T cells and PBMC samples (obtained from 5 donors). ILC dataset was obtained from sorted ILCs, NK cells and T cells from 3 donors and ILC cell cultures. Hoek dataset (GEO accession GSE64655) contains samples from PBMC and sorted immune cells (B cell, monocytes, myeloid dendritic cells, neutrophils, NK cells and T cells) from 2 healthy donors, taken at different time points after an influenza vaccination, referred to hereafter as Imm_SRR174³³⁸. Linsley dataset (GEO accession GSE60424) includes samples from sorted immune cells (B cells, CD4+ T cells, CD8+ T cells, monocytes, neutrophils and NK cells) from 20 donors (healthy donors and other donors with amyotrophic lateral sclerosis, multiple sclerosis, type 1 diabetes or sepsis), referred to hereafter as Imm_SRR155³³⁹. Pabst dataset (GEO accession GSE51984) includes data from various sorted immune cells (B cells, granulocytes, monocytes, peripheral blood CD34+ cells and T cells) from 5 healthy donors. As neutrophils constitute more than 90% of granulocytes, we grouped together the neutrophils and granulocytes in our analyses, referred to hereafter as Imm_51984³⁴⁰.

The gene expression data from Pabst dataset was directly available as gene counts. For the other four datasets, the reads were aligned to the human genome, *hg19*, with *TopHat* version 2.0.13 using *Bowtie2* version 2.2.4 and *Samtools* version 1.2. *HTSeq* version 0.6.1 was then used to obtain the gene counts from these data^{341–344}. The gene counts were then normalized by the library size of each sample. Batch effects between the datasets were finally removed with help of *ComBat* found in the R-package *sva* version 3.28.0^{345,346}. Principal component analysis was performed on the top 1000 most variable genes, showing a clustering of the samples coming from a same cell type. The normalized expression of some selected immune-related genes is showed with boxplots indicating the median, first and third quartiles, grouping the samples by their cell type.

10.4. Results

10.4.1. Discovery of Orphan Lymphoid Cells (OLCs)

We have discovered a new subset of lymphocytes (OLCs) that make up around 0.2% of lymphocytes in the blood of healthy donors. We found OLCs in all studied healthy donors, at consistent frequencies (Figure 14A). These cells are negative for the major lineage markers (CD3, CD4, CD8, CD14, CD15, CD16, CD19, CD20, CD33, CD34, and CD56). They do also not express CD127/IL7R α , the major ILC marker in human PBMCs. Positive identification by flow cytometry is possible based on the OLC's expression of CD44 and CD45 (Figure 14B).

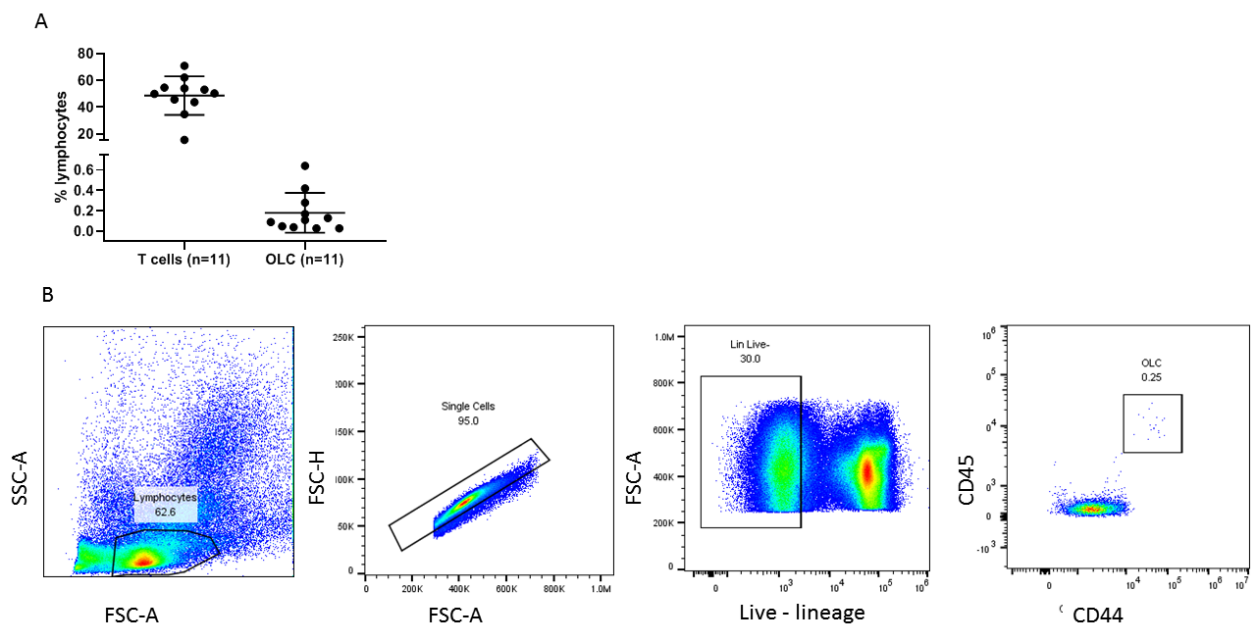


Figure 14| OLCs are found in the periphery of healthy donors. A. Frequencies of T cells and OLC in 11 healthy donors. B. OLCs are gating on lymphocytes, based on the forward and side scatter. Doublets are gated out and only live and lineage negative cells are selected. OLCs are CD45⁺ CD44⁺.

10.4.2. OLCs express the common γ – chain receptor

OLC express the common γ – chain receptor (CD132) at the same levels as T cells, clearly distinguishable from the background (isotype control; Figure 15A,B). Also CD44 expression was confirmed during the same experiment (Figure 15A,B). CD62L is partially expressed by OLCs and at a significant higher level than T cells (Figure 15A,B).

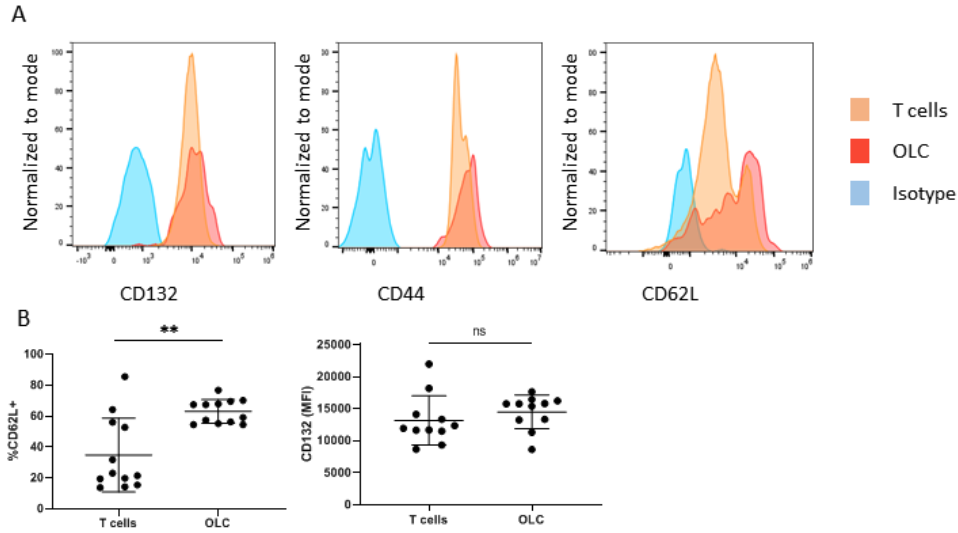


Figure 15 | Marker expression of OLCs. A. expression levels of CD123, CD44 and CD132 at the surface of T cells and OLCs. An appropriate isotype was used as a control. B. Histograms of the summary of the expression levels of CD132 and CD62L on OLCs and T cells. ns not significant, * $p < 0.05$, ** $p < 0.01$, *** $p < 0.001$, **** $p < 0.0001$.

10.4.3. OLCs are a morphologically homogeneous population

In order to characterize the morphology of OLCs, we performed a flow cytometry experiment by Amnis Image Stream (Merck). Bright field pictures were taken at 40X (Figure 16A) and 60X (Figure 16B) magnification. These pictures show a homogeneous population regarding the size of the cells and the morphology. Using the Amnis Image Stream allowed us to also investigate expression levels of CD62L as well as expression of CD45, CD44 and CD132 (Figure 16C). CD62L is expressed at variable intensities on the surface of OLCs. Even though CD44, CD45 and CD132 are expressed by all cells, the intensities vary.

10.4.4. RNA signatures represent a mixed T-NK cell signature

We aimed at a full molecular characterization of OLCs, as well as studying resemblance to other immune cells. Therefore we sorted OLCs from five different healthy donors. Simultaneously T cells were also sorted from the same donors. RNA sequencing was performed of OLCs, T cells and total PBMCs. PCA analysis shows that OLCs cluster together and far away from neutrophils, monocytes and myeloid DCs (Figure 17A). We see that OLCs cluster together with T cells as well as ILCs and NK cells. For these comparisons, our own data as well as publicly available data and data provided by Bérengère Salomé (Jandus Group, UNIL) was used. Analysis was performed in collaboration with Julien Racle (David Gfeller, Ludwig Branch Lausanne).

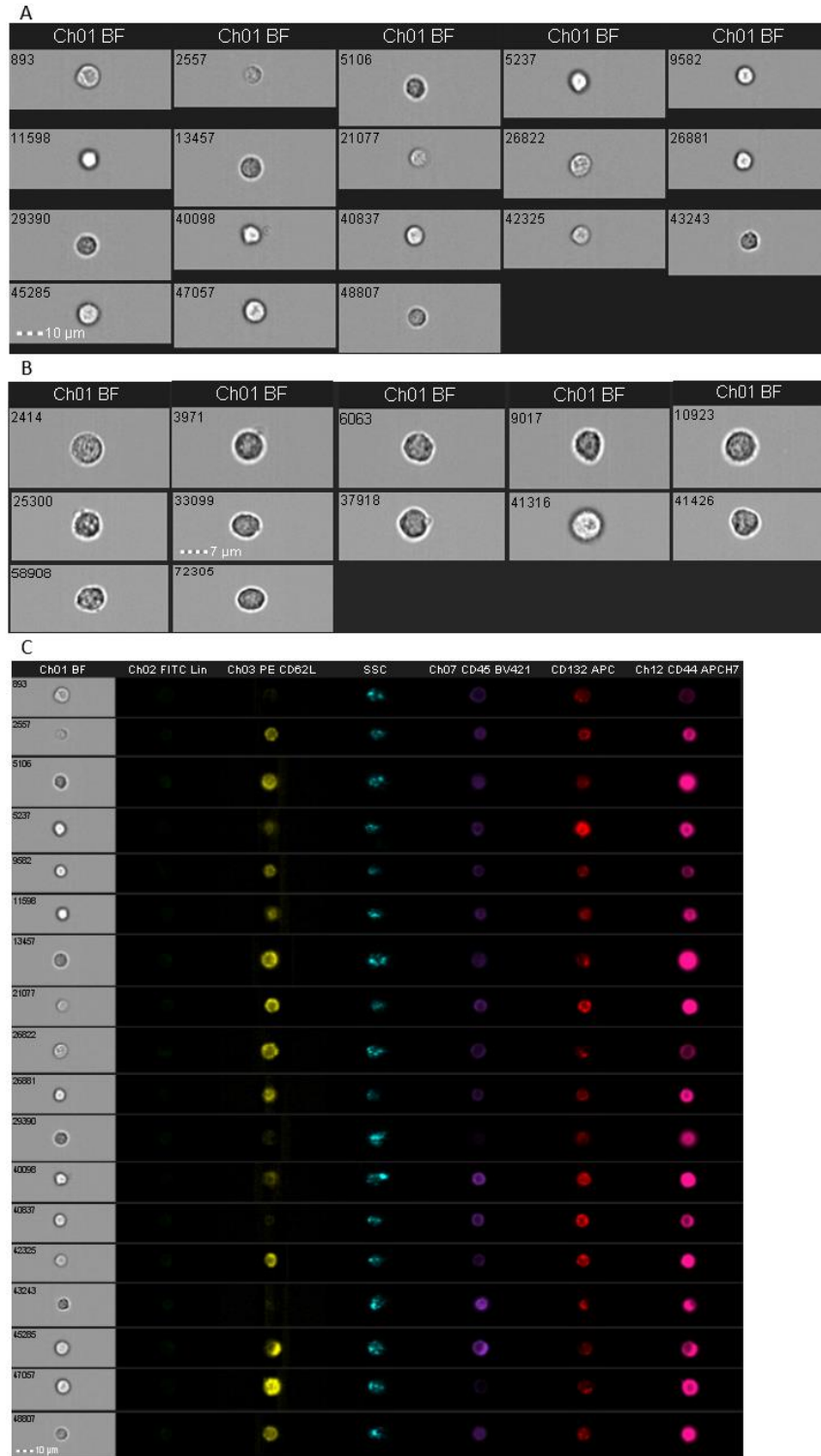


Figure 16| Amnis image stream analysis of OLCs. A. 40x magnification of OLCs seen as bright field images. B. 60x magnification of OLCs seen as bright field images. C. A 60x images of OLCs show the absence of lineage and dead marker staining, CD62L is expressed at mixed intensities on OLCs, CD44, CD132 and CD45.

Gene signature comparisons were used to compare between OLCs and various types of immune cells. Our own data was combined with publicly available data. We notice that OLCs do not express any CD14, CD19 or CD33 expression. Confirming that these cells are not myeloid or B cells. Even though we can observe a low expression of CD3ε, no CD8α or CD4 expression. We can observe some expression of FoxP3, granzyme A, LCK and CD45 (PTPRC), all at similar or lower levels than CD8 (Figure 17B).

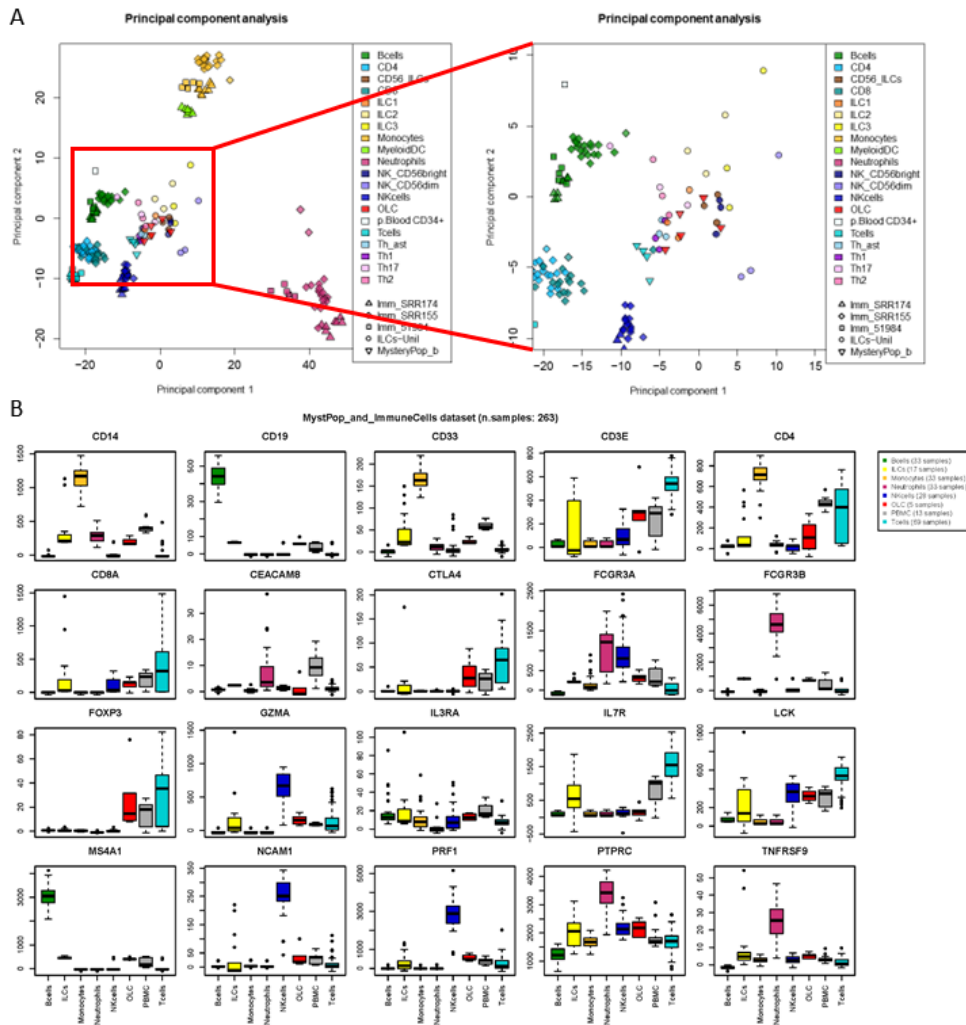


Figure 17| A. Principal component analysis of OLCs compared to data from 5 different sources, ours called MysteryPop_b, 3 publicly available data sources as well as data provided by the Jandus lab (ILC-UNIL). A zoom-in provides further detail. B. Gene signature comparisons with major lineage markers for the major immune populations.

Since we observed some expression of LCK as well as CD3ε we decided to take a closer look at T cell and TCR genes. We observe an overall lower expression of T cell (Figure 18A) and TCR signature genes (Figure 18B). This confirms that OLCs are different from T cells. However, we also observed the expression, albeit lower than in T cells, of some T cell related genes like Granzyme K, ICOS, CD28, SIRPG and SEPT1.

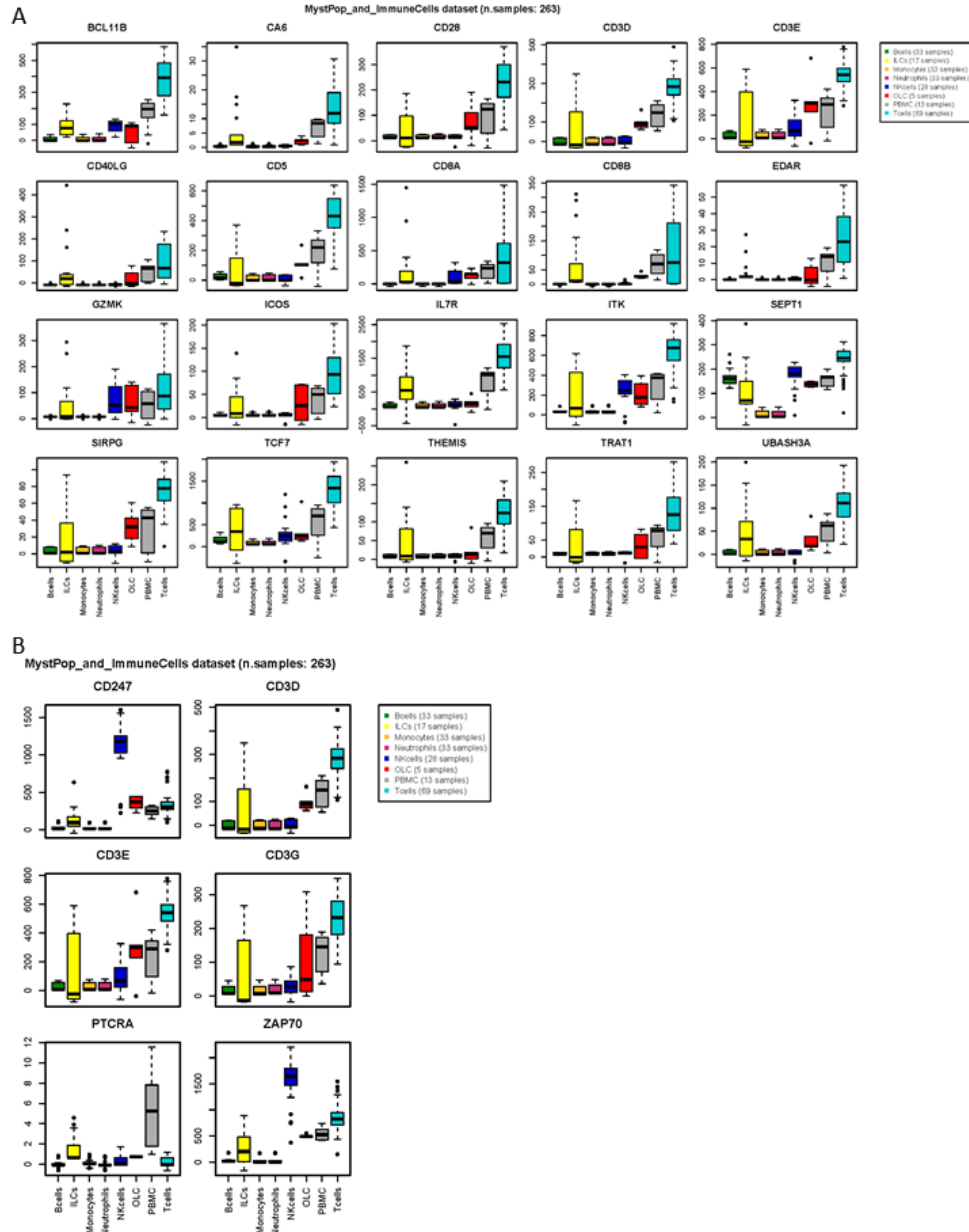


Figure 18| Gene signature comparison. A. T cell gene signature genes compared between OLCs, T cells and PBMCs from our own data as well as publicly available immune populations datasets. B. Gene signature comparison of TCR related genes.

Granzyme expression could also point us in the direction of NK cells. We thus performed a comparison between OLCs and NK cell gene signatures as well as ILC signatures. NK cell genes are expressed at lower levels than in publicly available NK cell gene expression data (Figure 19A). However, we can observe low expression of CD247 (TCR ζ), CTSW, IL2R β , NKG7 and SH2D1B. This profile confirms that OLCs are not NK cells, but nevertheless have low expression of some related genes. However, when looking at the gene signatures of ILCs we can observe lower expression of ILC-related genes (Figure 19B). We observe some expression of ID2 and IL12RB. Together with the absence of IL7R-expression (CD127) at the protein level

(selection of CD127-negative cells during sorting) as well as an absence on the RNA level (Figure 17B), makes us confident that OLCs are not a subset of ILCs. We conclude that OLCs have a mixed T-NK cell phenotype. Additional research is needed to further position OLCs within the immune network as well as elucidate their possible roles.

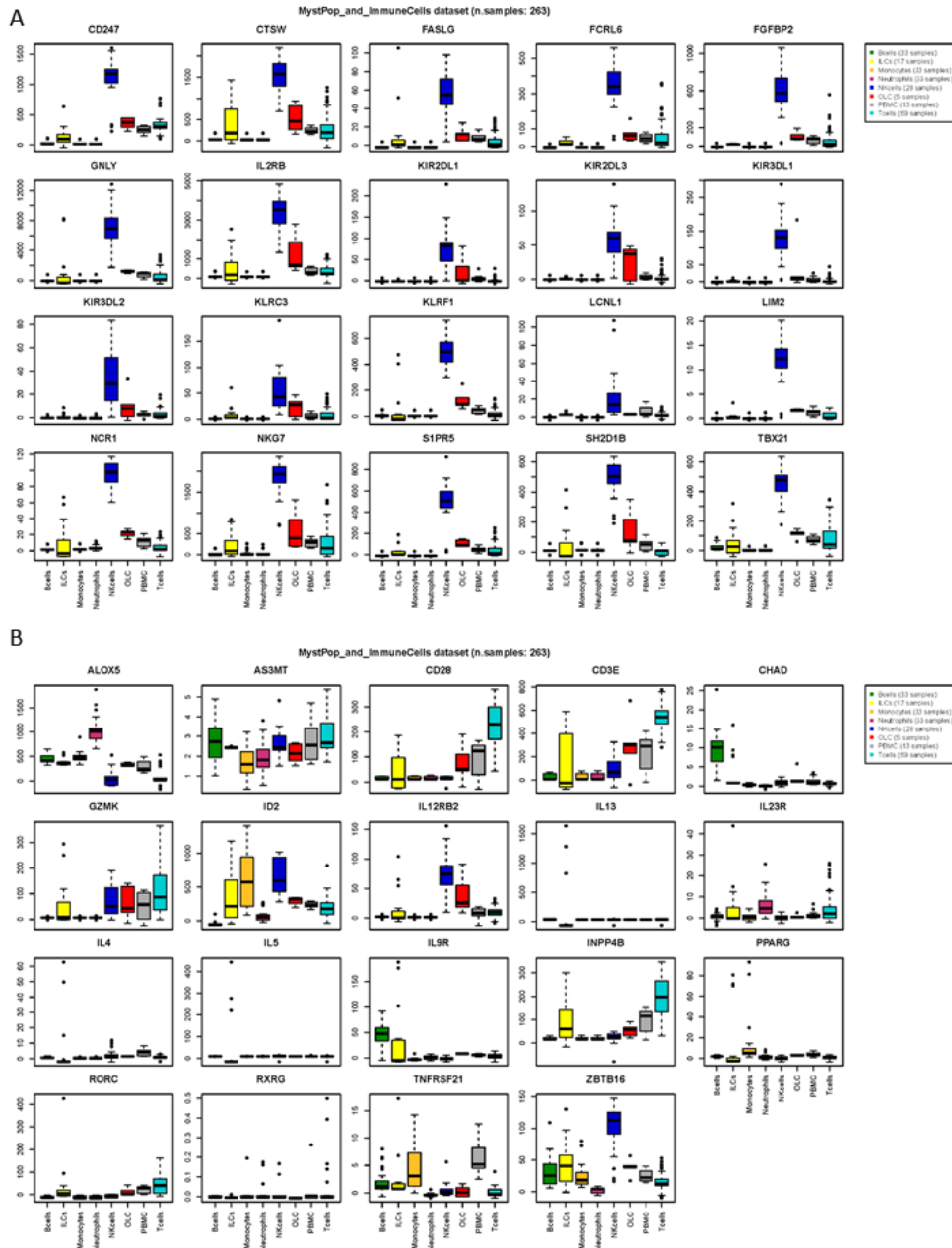


Figure 19| Gene signature comparison. A. NK cell gene signature genes compared between OLCs, T cells and PBMCs from our own data as well as publicly available immune populations datasets. B. Gene signature comparison of ILC related genes.

10.5. Discussion and Perspectives

Since the discovery of ILCs 10 years ago, the question was raised whether other immune cell populations are still escaping the attention of scientists³⁴⁷. We discovered a new population found within the lymphocyte gate (FSC/SSC) in peripheral blood of healthy donors. We called these cells Orphan Lymphoid Cells (OLCs), as they do not yet have specific functions.

OLCs are negative for all the major lymphocyte cell markers like CD3, CD4, CD8, CD14, CD15, CD16, CD19, CD20, CD33, CD56 as well as the ILC marker CD127. Positive markers expressed by OLCs are CD44 and CD45 that allow to identify OLCs as a homogenous population by flow cytometry. The common γ -chain receptor (CD132) is also expressed, as well as a partial expression of CD62L is observed. CD132 is expressed on T cells as well as NK cells and their precursors. The RNA sequencing data shows expression of CD122 or IL-2R β at low levels. This could indicate that OLCs might respond to IL-2 and IL-15 signalling like NK cells.

OLCs are a homogenous population based on PCA data where they cluster together. A homogenous population can also be found based on morphology. We documented this by using the Amnis Image Stream flow cytometer. Bright field pictures taken with a 60x magnification show a homogenous population in morphology and size. This gives us confidence that OLCs are a not a mixture of largely different cell types.

RNA sequencing of OLCs from different healthy donors reveals that they have a mixed T / NK cell signature, since they express some genes characteristic for T cells like CD3 ϵ , FOXP3, LCK, Granzyme K, ICOS, CD28, SIRPG and SEPT1, as well as some NK cell genes like: CD247 (TCR ζ), CTSW, IL2R β , NKG7 and SH2D1B. However, overall genes in these two signatures are either lower expressed or not expressed, showing us that they are distinctly different from NK and T cells. We did not find similarities with other immune cells like ILCs, B cells and myeloid derived cells.

We found expression of the two transcription factors FoxP3 and ID2. FoxP3 is the transcription factor expressed and highly specific for regulatory T cells³⁴⁸. ID2 has been shown to be important in the development of mouse NK cells and ILCs³³⁰. The role and function of ID2 in the development of human NK cells and ILCs is less clear³³⁵. Together with the expression of the common γ chain receptor, ID2 expression could indicate that OLCs are a precursor cell type. However, PCA analysis shows that they cluster away from CD34⁺ cells from the peripheral blood. It would be interesting to see if the gene signature of OLCs has any commonalities from the precursor cell types generated and sequenced by Renoux, *et al.*³³². For further exploration, *in vitro* experiments where OLCs are cultured with a cocktail of cytokines could elucidate if they differentiate into a different cell type. The cytokines would be a combination of all the

cytokines that can bind to a receptor including the common γ chain receptor, including but not limited to IL-2, IL-7 and IL-15. Based on the expression of common γ -receptor as well as IL2R β , we hypothesize that IL-2 and IL-15 could have the biggest chance of having specific effects. We also wonder if OLCs are able to upregulate cytokine receptors after stimulation e.g. via CD25. This would re-inforce the parallels between regulatory T cells and OLCs as we already found FoxP3 expression.

The function of OLCs remains elusive. The sequencing data shows us that they express some cytotoxicity genes like granzyme K and granzyme A. On the other hand we found expression of the regulatory transcription factor FoxP3. These possible functionalities seem quite contradictory. *In vitro* experiments, using isolated OLCs and different types of stimulants could allow to determine which cytokines are produced by OLCs upon stimulation. We propose to induce activation using multiple approaches including PMA/ionomycin stimulation, mitogen stimulation (PHA) or using a cytokine cocktail (high dose of IL-2 for example). Since OLCs are quite rare within PBMCs, we have only few cells available for analysis. It would thus be opportune to use a multiplex method as a read-out for cytokine production like MSD, Legendplex or Luminex.

It is possible that the presence of OLCs in the blood is rather transitory and that they are on route to the tissues. Analysis of multiple tissues including the bone marrow and lymphoid tissues could clarify their anatomical localizations and function within the immune system and within non-lymphoid tissues. Mouse models could also be used, however it is unclear for now if mice have OLCs.

Overall, we have discovered a new type of immune cells called Orphan Lymphoid Cells (OLCs). They have a mixed NK-T cell phenotype but do not express any of the lineage markers. They can be identified by their expression of CD45, CD44, CD132 and CD62L. Their place and overall function within the immune system remains unknown. More work is need to clarify their functionality, tissue distribution and link to other immune cells.

11. General discussion

Our first two aims for this PhD were to better understand the complexity of the immune response in patients with melanoma, in the hopes of advancing the knowledge leading to new therapeutic avenues as well as biomarker discovery.

In the first part we studied NK cell responses in late stage melanoma patients. We found that the frequencies and absolute number of CD56^{bright} NK cells inversely correlates with overall patient survival. It is possible that CD56^{bright} NK cells have negative effects on the anti-tumour response by inhibiting T cell responses, via CD38, perforin, CD11a and/or IFN γ . On the other hand, they produce less GM-CSF and TNF α , cytokines important in establishing an anti-tumour response. Thus, it remains open whether CD56^{bright} NK cells act through immune inhibition or are representative for an NK cell biology state with poor capability to kill tumours in vivo. Future studies are required to further clarify the roles of NK cell subsets and their interdependence.

In the second part of our study, we characterized B cell responses in PBMC of Ipilimumab treated melanoma patients. We found that pro-inflammatory as well as regulatory B cells from the periphery inversely correlate with overall survival as well as response to treatment. We also studied B cells from the TME of melanoma patients and found the same phenotype. Specifically, IDO1 is overexpressed and inflammatory genes and IL-6 signalling genes are also enriched.

These two projects create new avenues for biomarker development, for predicting overall survival as well as response to therapy. Additionally, we found that NK cells have partially impaired immune responses, creating a possible new target. On the other hand, B cells seem to be both inflammatory as well as regulatory. It is unclear if these are separate populations or if they are cells with a dual functionality. Additional research will further uncover which mechanisms drive these B cell responses in order to know where to interfere therapeutically.

In our third project, we discovered a new population of Orphan Lymphoid Cells (OLCs) that do not express any of the major hematopoietic lineage markers. They express however CD44, CD45, CD132 and partially CD62L. RNA sequencing shows a signature in between NK and T cells. The exact role of OLCs remains to be determined.

Overall during these projects, we contributed to the field of immunology, both to translational tumour immunology as well as to fundamental research.

12. References

1. Moens, E. & Veldhoen, M. Epithelial barrier biology: Good fences make good neighbours. *Immunology* **135**, 1–8 (2012).
2. Parkin, J. & Cohen, B. An overview of the immune system. *Lancet - Immunol.* **357**, 1777–1789 (2001).
3. MacLean, A. L., Cristina Lo Celso & P.H., M. S. Concise Review : Stem Cell Population Biology: Insights from Hematopoiesis. *Stem Cells Express* **35**, 80–88 (2017).
4. Luc, S., Buza-Vidas, N. & Jacobsen, S. E. W. Delineating the cellular pathways of hematopoietic lineage commitment. *Semin. Immunol.* **20**, 213–220 (2008).
5. Collin, M. & Bigley, V. Human dendritic cell subsets: an update. *Immunology* **154**, 3–20 (2018).
6. Kushwah, R. & Hu, J. Complexity of dendritic cell subsets and their function in the host immune system. *Immunology* **133**, 409–419 (2011).
7. Vivier, E. *et al.* Innate Lymphoid Cells: 10 Years On. *Cell* **174**, 1054–1066 (2018).
8. Hato, T. & Dagher, P. C. How the innate immune system senses trouble and causes trouble. *Clin. J. Am. Soc. Nephrol.* **10**, 1459–1469 (2015).
9. Afshar, M. & Gallo, R. L. Innate immune defense system of the skin. *Vet. Dermatol.* **24**, (2013).
10. Degn, S. E. & Thiel, S. Humoral Pattern Recognition and the Complement System. *Scand. J. Immunol.* **78**, 181–193 (2013).
11. Fukui, M., Imamura, R., Umemura, M., Kawabe, T. & Suda, T. Pathogen-associated molecular patterns sensitize macrophages to Fas ligand-induced apoptosis and IL-1 beta release. *J Immunol* **171**, 1868–1874 (2003).
12. Patel, S. Danger-Associated Molecular Patterns (DAMPs): the Derivatives and Triggers of Inflammation. *Curr. Allergy Asthma Rep.* **18**, (2018).
13. Medzhitov, R. Toll-like receptors and innate immunity. *Nat. Rev. Immunol.* **1**, 135–145 (2001).
14. Kumar, S., Ingle, H., Prasad, D. V. R. & Kumar, H. Recognition of bacterial infection by innate immune sensors. *Crit. Rev. Microbiol.* **39**, 229–246 (2013).
15. Kumar, H., Kawai, T. & Akira, S. Pathogen recognition by the innate immune system. *Int. Rev. Immunol.* **30**, 16–34 (2011).
16. Asehnoune, K., Villadangos, J. & Hotchkiss, R. S. Understanding host–pathogen interaction. *Intensive Care Med.* **42**, 2084–2086 (2016).
17. Vidya, M. K. *et al.* Toll-like receptors: Significance, ligands, signaling pathways, and functions in mammals. *Int. Rev. Immunol.* **37**, 20–36 (2018).
18. Jin, M. S. & Lee, J.-O. Structures of the toll-like receptor family and its ligand complexes. *Immunity* **29**, 182–91 (2008).

19. Lin, S. C., Lo, Y. C. & Wu, H. Helical assembly in the MyD88-IRAK4-IRAK2 complex in TLR/IL-1R signalling. *Nature* **465**, 885–890 (2010).
20. O’Neill, L. A. J. & Bowie, A. G. The family of five: TIR-domain-containing adaptors in Toll-like receptor signalling. *Nat. Rev. Immunol.* **7**, 353–364 (2007).
21. Frank, M. M. & Fries, L. F. The role of complement in inflammation and phagocytosis. *Immunol. Today* **12**, 322–326 (1991).
22. Gasque, P. Complement: A unique innate immune sensor for danger signals. *Mol. Immunol.* **41**, 1089–1098 (2004).
23. Geering, B., Stoeckle, C., Conus, S. & Simon, H. U. Living and dying for inflammation: Neutrophils, eosinophils, basophils. *Trends Immunol.* **34**, 398–409 (2013).
24. Wedemeyer, J. & Galli, S. J. Mast cells and basophils in acquired immunity. *Br. Med. Bull.* **56**, 936–55 (2000).
25. Borregaard, N., Sørensen, O. E. & Theilgaard-Mönch, K. Neutrophil granules: a library of innate immunity proteins. *Trends Immunol.* **28**, 340–345 (2007).
26. Kita, H. Eosinophils: multifaceted biologic properties and roles in health and disease. *Immunol. Rev.* **242**, 161–177 (2012).
27. Brinkmann, V. *et al.* Neutrophil extracellular traps kill bacteria. *Science* **303**, 1532–5 (2004).
28. Yousefi, S. *et al.* Catapult-like release of mitochondrial DNA by eosinophils contributes to antibacterial defense. *Nat. Med.* **14**, 949–953 (2008).
29. Miriam, M., Sathe, P., Helft, J., Miller, J. & Mortha, A. The Dendritic Cell Lineage: Ontogeny and Function of Dendritic Cells and Their Subsets in the Steady State and the Inflamed Setting. *Annu. Rev. Immunol.* **31**, 563–604 (2013).
30. Macri, C., Pang, E. S., Patton, T. & O’Keeffe, M. Dendritic cell subsets. *Semin. Cell Dev. Biol.* **84**, 11–21 (2018).
31. Joffre, O. P., Segura, E., Savina, A. & Amigorena, S. Cross-presentation by dendritic cells. *Nat. Rev. Immunol.* **12**, 557–569 (2012).
32. Swiecki, M. & Colonna, M. The multifaceted biology of plasmacytoid dendritic cells. *Nat. Rev. Immunol.* **15**, 471–485 (2015).
33. Murray, P. J. Macrophage Polarization. *Annu. Rev. Physiol.* **79**, 541–566 (2016).
34. Franken, L., Schiwon, M. & Kurts, C. Macrophages: Sentinels and regulators of the immune system. *Cell. Microbiol.* **18**, 475–487 (2016).
35. Martinez, F. O. & Gordon, S. The M1 and M2 paradigm of macrophage activation: time for reassessment. *F1000Prime Rep.* **6**, 1–13 (2014).
36. Jandus, P. *et al.* Human innate lymphoid cells (ILCs): Toward a uniform immune-phenotyping. *Cytom. Part B Clin. Cytom.* **94**, 392–399 (2017).

37. Ebbo, M., Crinier, A., Vély, F. & Vivier, E. Innate lymphoid cells: Major players in inflammatory diseases. *Nat. Rev. Immunol.* **17**, 665–678 (2017).
38. Chester, C., Fritsch, K. & Kohrt, H. E. Natural killer cell immunomodulation: Targeting activating, inhibitory, and co-stimulatory receptor signaling for cancer immunotherapy. *Front. Immunol.* **6**, 1–9 (2015).
39. Montaldo, E., Vacca, P., Moretta, L. & Mingari, M. C. Development of human natural killer cells and other innate lymphoid cells. *Semin. Immunol.* **26**, 107–113 (2014).
40. Campbell, K. S. & Hasegawa, J. Natural killer cell biology: An update and future directions. *J. Allergy Clin. Immunol.* **132**, 536–544 (2013).
41. Vivier, E. *et al.* Innate or Adaptive Immunity? The Example of Natural Killer Cells. *Science* **331**, 44–49 (2011).
42. Bonilla, F. A. & Oettgen, H. C. Adaptive immunity. *J. Allergy Clin. Immunol.* **125**, S33–S40 (2010).
43. Nikolich-Zugich, J., Slifka, M. K. & Messaoudi, I. The many important facets of T-cell repertoire diversity. *Nat. Rev. Immunol.* **4**, 123–132 (2004).
44. Elhanati, Y. *et al.* Inferring processes underlying B-cell repertoire diversity. *Philos. Trans. R. Soc. B Biol. Sci.* **370**, (2015).
45. Krueger, A., Ziętara, N. & Łyszkiwicz, M. T Cell Development by the Numbers. *Trends Immunol.* **38**, 128–139 (2017).
46. Sykulev, Y., Joo, M., Vturina, I., Tsomides, T. J. & Eisen, H. N. Evidence that a single peptide-MHC complex on a target cell can elicit a cytolytic T cell response. *Immunity* **4**, 565–571 (1996).
47. Chemali, M., Radtke, K., Desjardins, M. & English, L. Alternative pathways for MHC class I presentation: A new function for autophagy. *Cell. Mol. Life Sci.* **68**, 1533–1541 (2011).
48. Sercarz, E. E. & Maverakis, E. MHC-guided processing: Binding of large antigen fragments. *Nat. Rev. Immunol.* **3**, 621–629 (2003).
49. Hulpke, S. & Tampé, R. The MHC I loading complex: A multitasking machinery in adaptive immunity. *Trends Biochem. Sci.* **38**, 412–420 (2013).
50. Mantegazza, A. R., Magalhaes, J. G., Amigorena, S. & Marks, M. S. Presentation of phagocytosed antigens by MHC class I and II. *Traffic.* **14**, 135–152 (2014).
51. Fooksman, D. R. *et al.* Functional Anatomy of T Cell Activation and Synapse Formation. *Annu. Rev. Immunol.* **28**, 79–105 (2010).
52. Curtsinger, J. M. & Mescher, M. F. Inflammatory Cytokines as a Third Signal for T Cell Activation. *Curr. Opin. Immunol.* **22**, 333–340 (2010).
53. Pores-Fernando, A. T. & Zweifach, A. Calcium influx and signaling in cytotoxic T-lymphocyte lytic granule exocytosis. *Immunol. Rev.* **231**, 160–173 (2009).
54. Nakayamada, S., Takahashi, H., Kanno, Y. & O’Shea, J. J. Helper T cell diversity and plasticity. *Curr.*

Opin. Immunol. **24**, 297–302 (2012).

55. Walsh, K. P. & Mills, K. H. G. Dendritic cells and other innate determinants of T helper cell polarisation. *Trends Immunol.* **34**, 521–530 (2013).
56. Szabo, S. J. *et al.* A novel transcription factor, T-bet, directs Th1 lineage commitment. *Cell* **100**, 655–669 (2000).
57. Murphy, K. M. & Reiner, S. L. The lineage decisions of helper T cells. *Nat. Rev. Immunol.* **2**, 933–944 (2002).
58. Ko, L. J. & Engel, J. D. DNA-binding specificities of the GATA transcription factor family. *Mol. Cell. Biol.* **13**, 4011–22 (1993).
59. Korn, T., Bettelli, E., Oukka, M. & Kuchroo, V. K. IL-17 and Th17 Cells. *Annu. Rev. Immunol.* **27**, 485–517 (2009).
60. Hirota, K. *et al.* Fate mapping of IL-17-producing T cells in inflammatory responses. *Nat. Immunol.* **12**, 255–263 (2011).
61. Schmitt, N. & Ueno, H. Regulation of human helper T cell subset differentiation by cytokines. *Curr. Opin. Immunol.* **34**, 130–136 (2015).
62. Schmitt, E., Klein, M. & Bopp, T. Th9 cells, new players in adaptive immunity. *Trends Immunol.* **35**, 61–68 (2014).
63. Trifari, S., Kaplan, C. D., Tran, E. H., Crellin, N. K. & Spits, H. Identification of a human helper T cell population that has abundant production of interleukin 22 and is distinct from TH-17, TH1 and TH2 cells. *Nat. Immunol.* **10**, 864–871 (2009).
64. Crotty, S. Follicular Helper CD4 T Cells (T_{FH}). *Annu. Rev. Immunol.* **29**, 621–663 (2011).
65. Zhao, H., Liao, X. & Kang, Y. Tregs: Where we are and what comes next? *Front. Immunol.* **8**, (2017).
66. Pieper, K., Grimbacher, B. & Eibel, H. B-cell biology and development. *J. Allergy Clin. Immunol.* **131**, 959–71 (2013).
67. Cerutti, A., Puga, I. & Cols, M. Innate control of B cell responses. *Trends Immunol.* **32**, 202–211 (2011).
68. Schmidlin, H., Diehl, S. A. & Blom, B. New insights into the regulation of human B-cell differentiation. *Trends Immunol.* **30**, 277–285 (2009).
69. Klein, U., Rajewsky, K. & Küppers, R. Human Immunoglobulin (Ig)M⁺ IgD⁺ Peripheral Blood B Cells Expressing the CD27 Cell Surface Antigen Carry Somatic Mutated Variable Region Genes: CD27 as a General Marker for Somatic Mutated (Memory) B Cells. *J. Exp. Med.* **188**, 1679–1689 (1998).
70. Bagnara, D. *et al.* A Reassessment of IgM Memory Subsets in Humans. *J. Immunol.* **195**, 3716–3724 (2015).

71. Wei, C. *et al.* A New Population of Cells Lacking Expression of CD27 Represents a Notable Component of the B Cell Memory Compartment in Systemic Lupus Erythematosus. *J. Immunol.* **178**, 6624–6633 (2007).
72. Mahmood, Z. *et al.* CD27-IgD- memory B cells are modulated by in vivo interleukin-6 receptor (IL-6R) blockade in rheumatoid arthritis. *Arthritis Res. Ther.* **17**, 1–11 (2015).
73. Czajkowsky, D. M. & Shao, Z. The human IgM pentamer is a mushroom-shaped molecule with a flexural bias. *Proc. Natl. Acad. Sci.* **106**, 14960–14965 (2009).
74. Sun, Z. *et al.* Semi-extended solution structure of human myeloma immunoglobulin D determined by constrained X-ray scattering. *J. Mol. Biol.* **353**, 155–173 (2005).
75. Lu, L. L., Suscovich, T. J., Fortune, S. M. & Alter, G. Beyond binding: Antibody effector functions in infectious diseases. *Nat. Rev. Immunol.* **18**, 46–61 (2018).
76. Redpath, S., Michaelsen, T. E., Sandlie, I. & Clark, M. R. The influence of the hinge region length in binding of human IgG to human Fcγ receptors. *Hum. Immunol.* **59**, 720–727 (1998).
77. Kapur, R., Einarsdottir, H. K. & Vidarsson, G. IgG-effector functions: ‘The Good, The Bad and The Ugly’. *Immunol. Lett.* **160**, 139–144 (2014).
78. MacPherson, A. J., McCoy, K. D., Johansen, F. E. & Brandtzaeg, P. The immune geography of IgA induction and function. *Mucosal Immunol.* **1**, 11–22 (2008).
79. Marichal, T., Starkl, P., Mukai, K., Galli, S. J. & Tsai, M. IgE and mast cells in host defense against parasites and venoms. *Semin. Immunopathol.* **38**, 581–603 (2016).
80. Wan, T. *et al.* The crystal structure of IgE Fc reveals an asymmetrically bent conformation. *Nat. Immunol.* **3**, 681–686 (2002).
81. Rosser, E. C. & Mauri, C. Regulatory B Cells: Origin, Phenotype, and Function. *Immunity* **42**, 607–612 (2015).
82. Van De Veen, W. *et al.* IgG4 production is confined to human IL-10-producing regulatory B cells that suppress antigen-specific immune responses. *J. Allergy Clin. Immunol.* **131**, 1204–1212 (2013).
83. Schioppa, T. *et al.* B regulatory cells and the tumor-promoting actions of TNF- during squamous carcinogenesis. *Proc. Natl. Acad. Sci.* **108**, 10662–10667 (2011).
84. Zhou, X., Su, Y. X., Lao, X. M., Liang, Y. J. & Liao, G. Q. CD19+IL-10+regulatory B cells affect survival of tongue squamous cell carcinoma patients and induce resting CD4+T cells to CD4+Foxp3+regulatory T cells. *Oral Oncol.* **53**, 27–35 (2016).
85. Blair, P. A. *et al.* CD19+CD24^{hi}CD38^{hi} B Cells Exhibit Regulatory Capacity in Healthy Individuals but Are Functionally Impaired in Systemic Lupus Erythematosus Patients. *Immunity* **32**, 129–140 (2010).
86. Iwata, Y. *et al.* Characterization of a rare IL-10-competent B-cell subset in humans that parallels mouse regulatory B10 cells. *Blood* **117**, 530–541 (2011).

87. Olkhanud, P. B. *et al.* Tumor-evoked regulatory B cells promote breast cancer metastasis by converting resting CD4+T cells to T-regulatory cells. *Cancer Res.* **71**, 3505–3515 (2011).
88. Rosser, E. C., Blair, P. A. & Mauri, C. Cellular targets of regulatory B cell-mediated suppression. *Mol. Immunol.* **62**, 296–304 (2014).
89. Sattler, S. *et al.* IL-10-producing regulatory B cells induced by IL-33 (BregIL-33) effectively attenuate mucosal inflammatory responses in the gut. *J. Autoimmun.* **50**, 107–122 (2014).
90. Matsushita, T., Horikawa, M., Iwata, Y. & Tedder, T. F. Regulatory B cells (B10 cells) and regulatory T cells have independent roles in controlling experimental autoimmune encephalomyelitis initiation and late-phase immunopathogenesis. *J. Immunol.* **185**, 2240–52 (2010).
91. Bodogai, M. *et al.* Immunosuppressive and prometastatic functions of myeloid-derived suppressive cells rely upon education from tumor-associated B cells. *Cancer Res.* **75**, 3456–3465 (2015).
92. Clark, W. H. *et al.* A study of tumor progression: The precursor lesions of superficial spreading and nodular melanoma. *Hum. Pathol.* **15**, 1147–1165 (1984).
93. Colombet, M. *et al.* Cancer incidence and mortality patterns in Europe: Estimates for 40 countries and 25 major cancers in 2018. *Eur. J. Cancer* **103**, 356–387 (2018).
94. Heusser, R., Baumann, A. & Nosedà, G. Krebs in der Schweiz: wichtige Zahlen. *Krebsliga Schweiz* **23**, 588–596 (2017).
95. Cattaruzza, M. S. *et al.* Meta-analysis of risk factors for cutaneous melanoma: III. Family history, actinic damage and phenotypic factors. *Eur. J. Cancer* **41**, 2040–2059 (2005).
96. Gandini, S. *et al.* Meta-analysis of risk factors for cutaneous melanoma: I. Common and atypical naevi. *Eur. J. Cancer* **41**, 28–44 (2005).
97. Pasquini, P. *et al.* Meta-analysis of risk factors for cutaneous melanoma: II. Sun exposure. *Eur. J. Cancer* **41**, 45–60 (2004).
98. Green, A. *et al.* The association of use of sunbeds with cutaneous malignant melanoma and other skin cancers: A systematic review. *Int. J. Cancer* **120**, 1116–1122 (2007).
99. Hu, J. & Adar, S. The Cartography of UV-induced DNA Damage Formation and DNA Repair. *Photochem. Photobiol.* **93**, 199–206 (2017).
100. Mocellin, S., Verdi, D. & Nitti, D. DNA repair gene polymorphisms and risk of cutaneous melanoma: A systematic review and meta-analysis. *Carcinogenesis* **30**, 1735–1743 (2009).
101. Thomas, L. *et al.* Semiological Value of ABCDE Criteria in the Diagnosis of Cutaneous Pigmented Tumors. *Dermatology* **197**, 11–17 (1998).
102. Pentheroudakis, G., Dummer, R., Keilholz, U., Hauschild, A. & Guggenheim, M. Cutaneous melanoma: ESMO Clinical Practice Guidelines for diagnosis, treatment and follow-up. *Ann. Oncol.* **23**, (2012).
103. Buyyounouski, M. K. *et al.* Melanoma Staging: Evidence-Based Changes in the American Joint

- Committee on Cancer Eighth Edition Cancer Staging Manual. *CA. Cancer J. Clin.* **67**, 245–253 (2017).
104. Dummer, R. *et al.* Cutaneous melanoma: ESMO Clinical Practice Guidelines for diagnosis, treatment and follow-up. *Ann. Oncol.* (2015). doi:10.1093/annonc/mdy080
 105. Klemm, F. & Joyce, J. A. Microenvironmental regulation of therapeutic response in cancer. *Trends Cell Biol.* **25**, 198–213 (2015).
 106. Huang, S. K. S., Okamoto, T., Morton, D. L. & Hoon, D. S. B. Antibody responses to melanoma/melanocyte autoantigens in melanoma patients. *J. Invest. Dermatol.* **111**, 662–667 (1998).
 107. Ho, M. *et al.* Humoral immune response to mesothelin in mesothelioma and ovarian cancer patients. *Clin. Cancer Res.* **11**, 3814–3820 (2005).
 108. Lee, P. P. *et al.* Characterization of circulating T cells specific for tumor-associated antigens in melanoma patients. *Nat. Med.* **5**, 677–685 (1999).
 109. Romero, P. *et al.* Ex Vivo Staining of Metastatic Lymph Nodes by Class I Major Histocompatibility Complex Tetramers Reveals High Numbers of Antigen-experienced Tumor-specific Cytolytic T Lymphocytes. *J. Exp. Med.* **188**, 1641–1650 (1998).
 110. Knuth, A., Danowski, B., Oettgen, H. F. & Old, L. J. T-cell-mediated cytotoxicity against autologous malignant melanoma: analysis with interleukin 2-dependent T-cell cultures. *Proc. Natl. Acad. Sci.* **81**, 3511–3515 (1984).
 111. Coulie, P. G., Eynde, B. J. Van den, Bruggen, P. van der & Boon, T. Tumour antigens recognized by T lymphocytes: at the core of cancer immunotherapy. *Nat. Rev. Cancer* **14**, (2014).
 112. Verdegaal, E. M. E. *et al.* Neoantigen landscape dynamics during human melanoma-T cell interactions. *Nature* **536**, 91–95 (2016).
 113. Wallace H. Clark, J. *et al.* Model Predicting Survival in Stage I Melanoma Based on Tumor Progression. *J. Natl. Cancer Inst.* **81**, 1893–1904 (1989).
 114. Clemente, C. G. *et al.* Prognostic Value of TILs in vertical growth phase of primary cutaneous melanoma. *Cancer* **77**, 1303–1310 (1996).
 115. Mackensen, A. *et al.* Evidence for in situ amplification of tumor-specific cytotoxic T lymphocytes in a human regressive melanoma. *Cancer Res.* **53**, (1993).
 116. Tefany, F. J., Barnetson, R. S., Halliday, G. M., McCarthy, S. W. & McCarthy, W. H. Immunocytochemical analysis of the cellular infiltrate in primary regressing and non-regressing malignant melanoma. *Journal of Investigative Dermatology* **97**, 197–202 (1991).
 117. Galon, J. *et al.* Type, density, and location of immune cells within human colorectal tumors predict clinical outcome. *Science* **313**, 1960–1964 (2006).
 118. Whiteside, T. L. & Herberman, R. B. The role of natural killer cells in immune surveillance of cancer. *Curr. Opin. Immunol.* **7**, 704–710 (1995).

119. Iannello, A. & Raulet, D. H. Immune Surveillance of Unhealthy Cells by Natural Killer cells. *Cold Spring Harb Symp Quant Biol.* **78**, 2012 (2013).
120. Kim, S., Iizuka, K., Aguila, H. L., Weissman, I. L. & Yokoyama, W. M. In vivo natural killer cell activities revealed by natural killer cell-deficient mice. *Proc. Natl. Acad. Sci.* **97**, 2731–2736 (2000).
121. Robbins, P. F. *et al.* Mining exomic sequencing data to identify mutated antigens recognized by adoptively transferred tumor-reactive T cells. *Nat. Med.* **19**, 747–752 (2013).
122. Vogelstein, B. *et al.* Epitope Landscape in Breast and Colorectal Cancer. *Cancer Res.* **68**, 889–892 (2008).
123. Steinman, R. M., Turley, S., Mellman, I. & Inaba, K. The Induction of Tolerance by Dendritic Cells That Have Captured Apoptotic Cells. *J. Exp. Med.* **191**, 411–416 (2000).
124. Cavassani, K. A. *et al.* TLR3 is an endogenous sensor of tissue necrosis during acute inflammatory events. *J. Exp. Med.* **205**, 2609–2621 (2008).
125. Zitvogel, L. & Kroemer, G. Anticancer immunochemotherapy using adjuvants with direct cytotoxic effects. *J. Clin. Invest.* **119**, 2127–2130 (2009).
126. Kratky, W., Reis e Sousa, C., Oxenius, A. & Sporri, R. Direct activation of antigen-presenting cells is required for CD8+ T-cell priming and tumor vaccination. *Proc. Natl. Acad. Sci.* **108**, 17414–17419 (2011).
127. de Chaisemartin, L. *et al.* Characterization of Chemokines and Adhesion Molecules Associated with T cell Presence in Tertiary Lymphoid Structures in Human Lung Cancer. *Cancer Res.* **71**, 6391–6399 (2011).
128. Murray, T. *et al.* Very late antigen-1 marks functional tumor-resident CD8 T cells and correlates with survival of melanoma patients. *Front. Immunol.* **7**, 1–12 (2016).
129. Chen, D. S. & Mellman, I. Oncology meets immunology: The cancer-immunity cycle. *Immunity* **39**, 1–10 (2013).
130. Duan, S. & Thomas, P. G. Balancing immune protection and immune pathology by CD8+ T-cell responses to influenza infection. *Front. Immunol.* **7**, 1–16 (2016).
131. Schreiber, R. D., Old, L. J. & Smyth, M. J. Cancer immunoediting: Integrating the role of immunity in cancer suppression and promotion. *Science* **331**, 78 (2011).
132. Peggs, K. S., Quezada, S. A., Chambers, C. A., Korman, A. J. & Allison, J. P. Blockade of CTLA-4 on both effector and regulatory T cell compartments contributes to the antitumor activity of anti-CTLA-4 antibodies. *J. Exp. Med.* **206**, 1717–1725 (2009).
133. Curiel, T. J. *et al.* Specific recruitment of regulatory T cells in ovarian carcinoma fosters immune privilege and predicts reduced survival. *Nat. Med.* **10**, 942–949 (2004).
134. Strauss, L. *et al.* A Unique Subset of CD4+CD25highFoxp3+ T Cells Secreting Interleukin-10 and Transforming Growth Factor-1 Mediates Suppression in the Tumor Microenvironment. *Clin. Cancer Res.* **13**, 4345–4354 (2007).

135. Facciabene, A. *et al.* Tumour hypoxia promotes tolerance and angiogenesis via CCL28 and T reg cells. *Nature* **475**, 226–230 (2011).
136. Vargas, F. A. *et al.* Fc Effector Function Contributes to the Activity of Human Anti-CTLA-4 Antibodies. *Cancer Cell* **33**, 649-663.e4 (2018).
137. Almand, B. *et al.* Clinical significance of defective dendritic cell differentiation in cancer. *Clin. Cancer Res.* **6**, 1755–1766 (2000).
138. Mahnke, K., Schmitt, E., Bonifaz, L., Henk, A. & Jonuleit, H. Immature, but not inactive: the tolerogenic function of immature dendritic cells. *Immunol. Cell Biol.* **80**, 477–483 (2002).
139. Kumar, V., Patel, S., Tcyganov, E. & Gabrilovich, D. I. The nature of myeloid-derived suppressor cells in the tumor microenvironment. *Trends Immunol.* **37**, 208–220 (2016).
140. Jarosz-Biej, M. *et al.* M1-like macrophages change tumor blood vessels and microenvironment in murine melanoma. *PLoS One* **13**, e0191012 (2018).
141. Movahedi, K. *et al.* Different tumor microenvironments contain functionally distinct subsets of macrophages derived from Ly6C(high) monocytes. *Cancer Res.* **70**, 5728–5739 (2010).
142. Varney, M. L., Johansson, S. L. & Singh, R. K. Tumour-associated macrophage infiltration, neovascularization and aggressiveness in malignant melanoma: Role of monocyte chemoattractant protein-1 and vascular endothelial growth factor-A. *Melanoma Res.* **15**, 417–425 (2005).
143. Stockmann, C. *et al.* Deletion of vascular endothelial growth factor in myeloid cells accelerates tumorigenesis. *Nature* **456**, 814–819 (2008).
144. Ruffell, B., Affara, N. I. & Coussens, L. M. Differential macrophage programming in the tumor microenvironment. *Trends Immunol.* **33**, 119–126 (2012).
145. Neubert, N. J. *et al.* T cell-induced CSF1 promotes melanoma resistance to PD1 blockade. *Sci. Transl. Med.* **10**, (2018).
146. DeNardo, D. G. *et al.* Leukocyte Complexity Predicts Breast Cancer Survival and Functionally Regulates Response to Chemotherapy. *Cancer Discov.* **1**, 54–67 (2011).
147. Yan, D. *et al.* Inhibition of colony stimulating factor-1 receptor abrogates microenvironment-mediated therapeutic resistance in gliomas. *Oncogene* **36**, 6049–6058 (2017).
148. Olson, O. C., Kim, H., Quail, D. F., Foley, E. A. & Joyce, J. A. Tumor-Associated Macrophages Suppress the Cytotoxic Activity of Antimitotic Agents. *Cell Rep.* **19**, 101–113 (2017).
149. Dumont, N. *et al.* Breast Fibroblasts Modulate Early Dissemination, Tumorigenesis, and Metastasis through Alteration of Extracellular Matrix Characteristics. *Neoplasia* **15**, (2013).
150. Gok Yavuz, B. *et al.* Cancer associated fibroblasts sculpt tumour microenvironment by recruiting monocytes and inducing immunosuppressive PD-1+ TAMs. *Sci. Rep.* **9**, 3172 (2019).
151. Cohen, N. *et al.* Fibroblasts drive an immunosuppressive and growth-promoting microenvironment in breast cancer via secretion of Chitinase 3-like 1. *Oncogene* **36**, 4457–4468 (2017).

152. Neubert, N. J. *et al.* Broad and conserved immune regulation by genetically heterogeneous melanoma cells. *Cancer Res.* **77**, 1623–1636 (2017).
153. Hung T. Khong and Nicholas P. Restifo. Natural selection of tumor variants in the generation of ‘tumor escape’ phenotypes. *Nat. Immunol.* **3**, 999–1005 (2002).
154. Baitsch, L. *et al.* Extended co-expression of inhibitory receptors by human CD8 T-cells depending on differentiation, antigen-specificity and anatomical localization. *PLoS One* **7**, 1–10 (2012).
155. Blackburn, S. D. *et al.* Coregulation of CD8+T cell exhaustion by multiple inhibitory receptors during chronic viral infection. *Nat. Immunol.* **10**, 29–37 (2009).
156. Blattman, J. N. *et al.* Viral Immune Evasion Due to Persistence of Activated T Cells Without Effector Function. *J. Exp. Med.* **188**, 2205–2213 (2002).
157. Baitsch, L. *et al.* Exhaustion of tumor-specific CD8+ T cells in metastases from melanoma patients. *J. Clin. Invest.* **121**, 23–25 (2011).
158. Speiser, D. E., Ho, P. C. & Verdeil, G. Regulatory circuits of T cell function in cancer. *Nat. Rev. Immunol.* **16**, 599–611 (2016).
159. Mellman, I., Coukos, G. & Dranoff, G. Cancer immunotherapy comes of age. *Nature* **480**, (2011).
160. Khalil, D. N., Smith, E. L., Brentjens, R. J. & Wolchok, J. D. The future of cancer treatment: Immunomodulation, CARs and combination immunotherapy. *Nat. Rev. Clin. Oncol.* **13**, 273–290 (2016).
161. Quail, D. F. & Joyce, J. A. Microenvironmental regulation of tumor progression and metastasis. *Nat. Med.* **19**, 1423–1437 (2013).
162. Crinier, A. *et al.* High-Dimensional Single-Cell Analysis Identifies Organ-Specific Signatures and Conserved NK Cell Subsets in Humans and Mice. *Immunity* **49**, 971-986.e5 (2018).
163. Orange, J. S. Human natural killer cell deficiencies. *Curr. Opin. Allergy Clin. Immunol.* **6**, 399–409 (2006).
164. Walzer, T., Dalod, M., Robbins, S. H., Zitvogel, L. & Vivier, E. Review article Natural-killer cells and dendritic cells : “ l ’ union fait la force ”. *Blood* **106**, 2252–2258 (2005).
165. Martín-Fontecha, A. *et al.* Induced recruitment of NK cells to lymph nodes provides IFN- γ for TH1 priming. *Nat. Immunol.* **5**, 1260–1265 (2004).
166. Gerosa, F. *et al.* Reciprocal Activating Interaction between Natural Killer Cells and Dendritic Cells. *J. Exp. Med.* **195**, 327–333 (2002).
167. Krebs, P. *et al.* NK cell – mediated killing of target cells triggers robust antigen-specific T cell – mediated and humoral responses. **113**, 6593–6603 (2019).
168. Piccioli, D., Sbrana, S., Melandri, E. & Valiante, N. M. Contact-dependent Stimulation and Inhibition of Dendritic Cells by Natural Killer Cells. *J. Exp. Med.* **195**, 335–341 (2002).
169. Romagnani, C. *et al.* CD56brightCD16- Killer Ig-Like Receptor- NK Cells Display Longer Telomeres

- and Acquire Features of CD56dim NK Cells upon Activation. *J. Immunol.* **178**, 4947–4955 (2007).
170. Caligiuri, M. A. *et al.* Functional consequences of interleukin receptor expression on resting human lymphocytes: Identification of a Novel Natural Killer Cell Subset with High Affinity Receptors. *J. Exp. Med.* **171**, 1509–1526 (1990).
 171. Zotto, G. Del *et al.* Human NK cell receptors/markers: A tool to analyze NK cell development, subsets and function. *Cytom. Part A* **83A**, 702–713 (2013).
 172. Mandelboim, O. *et al.* Recognition of haemagglutinins on virus-infected cells by NKp46 activates lysis by human NK cells. *Nature* **409**, 1055–1060 (2001).
 173. Moretta, A. *et al.* Activating receptors and coreceptors involved in human natural killer cell-mediated cytotoxicity. *Annu. Rev. Immunol.* **19**, 197–223 (2001).
 174. Sung, A. P. *et al.* An improved method to quantify human NK cell-mediated antibody-dependent cell-mediated cytotoxicity (ADCC) per IgG FcR-positive NK cell without purification of NK cells. *J. Immunol. Methods* **452**, 63–72 (2018).
 175. Held, W. Tolerance and reactivity of NK cells: Two sides of the same coin? *Eur. J. Immunol.* **38**, 2930–2933 (2008).
 176. Lanier, L. L. Nk Cell Recognition. *Annu. Rev. Immunol.* **23**, 225–274 (2004).
 177. Cook, K. D. & Whitmire, J. K. The Depletion of NK Cells Prevents T Cell Exhaustion to Efficiently Control Disseminating Virus Infection. *J. Immunol.* **190**, 641–649 (2013).
 178. Andrews, D. M. *et al.* Innate immunity defines the capacity of antiviral T cells to limit persistent infection. *J. Exp. Med.* **207**, 1333–1343 (2010).
 179. Mandaric, S. *et al.* IL-10 Suppression of NK / DC Crosstalk Leads to Poor Priming of MCMV-Specific CD4 T Cells and Prolonged MCMV Persistence. *PLoS Pathog.* **8**, e1002846 (2012).
 180. Crome, S. Q., Lang, P. A., Lang, K. S. & Ohashi, P. S. Natural killer cells regulate diverse T cell responses. *Trends Immunol.* **34**, 342–349 (2013).
 181. Pallmer, K. & Oxenius, A. Recognition and regulation of T cells by NK cells. *Front. Immunol.* **7**, 1–13 (2016).
 182. Lee, S.-H., Kim, K.-S., Fodil-Cornu, N., Vidal, S. M. & Biron, C. A. Activating receptors promote NK cell expansion for maintenance, IL-10 production, and CD8 T cell regulation during viral infection. *J. Exp. Med.* **206**, 2235–2251 (2009).
 183. Crouse, J. *et al.* Type I Interferons Protect T Cells against NK Cell Attack Mediated by the Activating Receptor NCR1. *Immunity* **40**, 961–973 (2014).
 184. Waggoner, S. N., Daniels, K. A. & Welsh, R. M. Therapeutic Depletion of Natural Killer Cells Controls Persistent Infection. *J. Virol.* **88**, 1953–1960 (2014).
 185. Waggoner, S. N., Cornberg, M., Selin, L. K. & Welsh, R. M. Natural killer cells act as rheostats modulating antiviral T cells. *Nature* **481**, 394–398 (2012).

186. Imai, K., Matsuyama, S., Miyake, S., Suga, K. & Nakachi, K. Natural cytotoxic activity of peripheral-blood lymphocytes and cancer incidence: an 11-year follow-up study of a general population. *Lancet* **356**, 1795–1799 (2000).
187. Böttcher, J. P. *et al.* NK Cells Stimulate Recruitment of cDC1 into the Tumor Microenvironment Promoting Cancer Immune Control. *Cell* **172**, 1022–1028.e14 (2018).
188. Barry, K. C. *et al.* A natural killer–dendritic cell axis defines checkpoint therapy–responsive tumor microenvironments. *Nat. Med.* **24**, 1178–1191 (2018).
189. Vitale, M., Cantoni, C. & Pietra, G. Effect of tumor cells and tumor microenvironment on NK-cell function. *Eur. J. Immunol.* **44**, 1582–1592 (2014).
190. Freud, A. G., Mundy-Bosse, B. L., Yu, J. & Caligiuri, M. A. The Broad Spectrum of Human Natural Killer Cell Diversity. *Immunity* **47**, 820–833 (2017).
191. Hsia, J. *et al.* Prognostic Significance of Intratumoral Natural Killer Cells in Primary Resected Esophageal Squamous Cell Carcinoma. *Chang Gung Med. J.* **28**, 335–340 (2005).
192. Herpen, C. M. L. Van *et al.* Intratumoral Recombinant Human Interleukin-12 Administration in Head and Neck Squamous Cell Carcinoma Patients Modifies Locoregional Lymph Node Architecture and Induces Natural Killer Cell Infiltration in the Primary Tumor. *Clin. Cancer Res.* **11**, 1899–1909 (2005).
193. Ishigami, S. *et al.* Prognostic value of intratumoral natural killer cells in gastric carcinoma. *Cancer* **88**, 577–583 (2000).
194. Coca, S. *et al.* The prognostic significance of intratumoral natural killer cells in patients with colorectal carcinoma. *Cancer* **79**, 2320–2328 (1997).
195. Crouse, J., Xu, H. C., Lang, P. A. & Oxenius, A. NK cells regulating T cell responses: Mechanisms and outcome. *Trends Immunol.* **36**, 49–58 (2015).
196. Sun, C. *et al.* High NKG2A expression contributes to NK cell exhaustion and predicts a poor prognosis of patients with liver cancer. *Oncoimmunology* **6**, e1264562 (2017).
197. Platonova, S. *et al.* Profound coordinated alterations of intratumoral NK cell phenotype and function in lung carcinoma. *Cancer Res.* **71**, 5412–5422 (2011).
198. Mamessier, E. *et al.* Human breast cancer cells enhance self tolerance by promoting evasion from NK cell antitumor immunity. **121**, 2–6 (2011).
199. Bi, J. & Tian, Z. NK cell exhaustion. *Front. Immunol.* **8**, (2017).
200. Beldi-Ferchiou, A. *et al.* PD-1 mediates functional exhaustion of activated NK cells in patients with Kaposi sarcoma. *Oncotarget* (2016). doi:10.18632/oncotarget.12150
201. André, P. *et al.* Anti-NKG2A mAb Is a Checkpoint Inhibitor that Promotes Anti-tumor Immunity by Unleashing Both T and NK Cells. *Cell* 1731–1743 (2018). doi:10.1016/j.cell.2018.10.014
202. Bruno, A. *et al.* The Proangiogenic Phenotype of Natural Killer Cells in Patients with Non-Small Cell Lung Cancer. *Neoplasia* **15**, 133-IN7 (2013).

203. Carrega, P. *et al.* Natural killer cells infiltrating human nonsmall-cell lung cancer are enriched in CD56brightCD16⁻ cells and display an impaired capability to kill tumor cells. *Cancer* **112**, 863–875 (2008).
204. Keskin, D. B. *et al.* TGF β promotes conversion of CD16 NK cells with similarities to decidual NK cells. *Pnas* **104**, 3378–3383 (2006).
205. Bruno, A., Ferlazzo, G., Albini, A. & Noonan, D. M. A think tank of TINK/TANKs: Tumor-infiltrating/tumor-associated natural killer cells in tumor progression and angiogenesis. *J. Natl. Cancer Inst.* **106**, (2014).
206. Chiossone, L., Dumas, P. Y., Vienne, M. & Vivier, E. Natural killer cells and other innate lymphoid cells in cancer. *Nat. Rev. Immunol.* **18**, 671–688 (2018).
207. Carotta, S. Targeting NK Cells for Anticancer immunotherapy : Clinical and Preclinical Approaches. *Front. Immunol.* **7**, 1–10 (2016).
208. Rajagopalan, S., Bryceson, Y. T., Kuppusamy, S. P., Geraghty, D. E. & Meer, A. Van Der. Activation of NK Cells by an Endocytosed Receptor for Soluble HLA-G. *Plos Biol.* **4**, e9 (2006).
209. Morandi, F. *et al.* Soluble HLA-G dampens CD94 / NKG2A expression and function and differentially modulates chemotaxis and cytokine and chemokine secretion in CD56 bright and CD56 dim NK cells. *Blood* **118**, 5840–5851 (2011).
210. Mirjagic Martinovic, K. M. *et al.* Decreased expression of NKG2D, NKp46, DNAM-1 receptors, and intracellular perforin and STAT-1 effector molecules in NK cells and their dim and bright subsets in metastatic melanoma patients. *Melanoma Res.* **24**, 295–304 (2014).
211. Fregni, G. *et al.* Phenotypic and Functional Characteristics of Blood Natural Killer Cells from Melanoma Patients at Different Clinical Stages. *PLoS One* **8**, 1–9 (2013).
212. Ali, T. H. *et al.* Enrichment of CD56dimKIR+CD57+ highly cytotoxic NK cells in tumour-infiltrated lymph nodes of melanoma patients. *Nat. Commun.* **5**, 1–9 (2014).
213. Konjević, G., Mirajaić Martinovi, K., Jurišić, V., Babović, N. & Spužić, I. Biomarkers of suppressed natural killer (NK) cell function in metastatic melanoma: Decreased NKG2D and increased CD158a receptors on CD3-CD16+ NK cells. *Biomarkers* **14**, 258–270 (2009).
214. Tietze, J. K., Angelova, D., Heppt, M. V., Ruzicka, T. & Berking, C. Low baseline levels of NK cells may predict a positive response to ipilimumab in melanoma therapy. *Exp. Dermatol.* **26**, 622–629 (2017).
215. Halama, N. *et al.* Natural killer cells are scarce in colorectal carcinoma tissue despite high levels of chemokines and cytokines. *Clin. Cancer Res.* **17**, 678–689 (2011).
216. Balsamo, M. *et al.* Melanoma cells become resistant to NK-cell-mediated killing when exposed to NK-cell numbers compatible with NK-cell infiltration in the tumor. *Eur. J. Immunol.* **42**, 1833–1842 (2012).
217. Sconocchia, G. *et al.* Melanoma cells inhibit NK cell functions - Letter. *Cancer Res.* **72**, 5428–5429 (2012).

218. Jerby-Arnon, L. *et al.* A Cancer Cell Program Promotes T Cell Exclusion and Resistance to Checkpoint Blockade. *Cell* **175**, 984-997.e24 (2018).
219. Tirosh, I. *et al.* Dissecting the multicellular ecosystem of metastatic melanoma by single-cell RNA-seq. *Science* **352**, 189–196 (2016).
220. Sade-Feldman, M. *et al.* Defining T Cell States Associated with Response to Checkpoint Immunotherapy in Melanoma. *Cell* **175**, 998-1013.e20 (2018).
221. Morandi, F. *et al.* CD56^{bright} CD16⁻ NK Cells Produce Adenosine through a CD38-Mediated Pathway and Act as Regulatory Cells Inhibiting Autologous CD4⁺ T Cell Proliferation. *J. Immunol.* **195**, 965–972 (2015).
222. Monteiro, I. *et al.* CD73 expression and clinical significance in human metastatic melanoma. *Oncotarget* **9**, 26659–26669 (2018).
223. Bauché, D. *et al.* Autocrine Adenosine regulates tumor polyfunctional CD73+CD4+ effector T cells devoid of immune checkpoints. *Cancer Res.* **78**, canres.2405.2017 (2018).
224. Varda Rotter, Witte, O. N., Robert Coffman & Baltimore, D. Abelson Murine Leukemia Virus-Induced Tumors Elicit Antibodies Against a Host Cell Protein, P50. *J. Virol.* **36**, 547–555 (1980).
225. Carbone, D. P. *et al.* Development of Antibodies against p53 in Lung Cancer Patients Appears to Be Dependent on the Type of p53 Mutation. *Cancer Res.* **52**, 4168–4174 (1992).
226. Preuss, K. D., Zwick, C., Bormann, C., Neumann, F. & Pfreundschuh, M. Analysis of the B-cell repertoire against antigens expressed by human neoplasms. *Immunol. Rev.* **188**, 43–50 (2002).
227. Zhang, J. Y. *et al.* Enhancement of antibody detection in cancer using panel of recombinant tumor-associated antigens. *Cancer Epidemiol. Biomarkers Prev.* **12**, 136–143 (2003).
228. Beeton-Kempen, N. *et al.* Development of a novel, quantitative protein microarray platform for the multiplexed serological analysis of autoantibodies to cancer-testis antigens. *Int. J. Cancer* **135**, 1842–1851 (2014).
229. Chapman, C. *et al.* Autoantibodies in breast cancer: their use as an aid to early diagnosis. *Ann. Oncol.* **18**, 868–873 (2007).
230. Chapman, C. J. *et al.* Autoantibodies in lung cancer: Possibilities for early detection and subsequent cure. *Thorax* **63**, 228–233 (2008).
231. Imai, H., Nakano, Y., Kiyosawa, K. & Tan, E. Increasing titers and changing specificities of antinuclear antibodies in patients with chronic liver disease who develop hepatocellular carcinoma. *Cancer* **71**, 26–35 (1993).
232. Li, Y. *et al.* P53 Autoantibodies Predict Subsequent Development of Cancer. *Int. J. Cancer* **114**, 157–160 (2005).
233. Fosså, A. *et al.* NY-ESO-1 protein expression and humoral immune responses in prostate cancer. *Prostate* **59**, 440–447 (2004).
234. Jäger, E. *et al.* Humoral immune responses of cancer patients against ‘cancer-testis’ antigen NY-

- ESO-1: Correlation with clinical events. *Int. J. Cancer* **84**, 506–510 (1999).
235. Wasserman, J., Glas, U. & Blomgren, H. Autoantibodies in patients with carcinoma of the breast. *Clin. Exp. Immunol.* **19**, 417–422 (1975).
236. Al-Shukaili, A. K., Al-Jabri, A. A. & Al-Moundhari, M. S. Prognostic value of auto-antibodies in the serum of Omani patients with gastric cancer. *Saudi Med. J.* **27**, 1873–1877 (2006).
237. Barbouche, M. R., Romain, S., Avrameas, S., Piana, L. & Martin, P.-M. Prognostic Significance of Autoantibodies to Laminin in the Sera of Breast Cancer Patients: A Preliminary Report. *Eur. J. Clin. Chem. Clin. Biochem.* **32**, 511–514 (1994).
238. Soussi, T. p53 Antibodies in the sera of patients with various types of cancer: A review. *Cancer Res.* **60**, 1777–1788 (2000).
239. Parmigiani, R. B. *et al.* Antibodies against the cancer-testis antigen CTSP-1 are frequently found in prostate cancer patients and are an independent prognostic factor for biochemical-recurrence. *Int. J. Cancer* **122**, 2385–2390 (2008).
240. Saffroy, R. *et al.* Clinical significance of circulating anti-p53 antibodies in European patients with hepatocellular carcinoma. *Br. J. Cancer* **79**, 604–610 (1999).
241. Kurtenkov, O. *et al.* Humoral immune response to MUC1 and to the Thomsen-Friedenreich (TF) glycotope in patients with gastric cancer: Relation to survival. *Acta Oncol. (Madr).* **46**, 316–323 (2007).
242. Vural, B. *et al.* Frequency of SOX Group B (SOX1, 2, 3) and ZIC2 antibodies in Turkish patients with small cell lung carcinoma and their correlation with clinical parameters. *Cancer* **103**, 2575–2583 (2005).
243. Bachelot, T. *et al.* Autoantibodies to endostatin in patients with breast cancer: Correlation to endostatin levels and clinical outcome. *Br. J. Cancer* **94**, 1066–1070 (2006).
244. Haidopoulos, D. *et al.* Circulating anti-CEA antibodies in the sera of patients with breast cancer. *Eur. J. Surg. Oncol.* **26**, 742–746 (2000).
245. Lakota, J., Skultety, L., Dubrovcakova, M. & Altaner, C. Presence of serum carbonic anhydrase autoantibodies in patients relapsed after autologous stem cell transplantation indicates an improved prognosis. *Neoplasma* **55**, 488–492 (2008).
246. Blaes, F. *et al.* Antineural and antinuclear autoantibodies are of prognostic relevance in non-small cell lung cancer. *Ann. Thorac. Surg.* **69**, 254–258 (2002).
247. Hirasawa, Y. *et al.* Natural autoantibody to MUC1 is a prognostic indicator for non-small cell lung cancer. *Am. J. Respir. Crit. Care Med.* **161**, 589–594 (2000).
248. Kobold, S., Lütken, T., Cao, Y., Bokemeyer, C. & Atanackovic, D. Autoantibodies against tumor-related antigens: Incidence and biologic significance. *Hum. Immunol.* **71**, 643–651 (2010).
249. Kocer, B., McKolanis, J. & Soran, A. Humoral immune response to MUC5AC in patients with colorectal polyps and colorectal carcinoma. *BMC Gastroenterol.* **6**, 1–9 (2006).

250. Friedrichs, B. *et al.* Humoral Immune Responses against the Immature Laminin Receptor Protein Show Prognostic Significance in Patients with Chronic Lymphocytic Leukemia. *J. Immunol.* **180**, 6374–6384 (2008).
251. Yang, X.-F. *et al.* CML66, a broadly immunogenic tumor antigen, elicits a humoral immune response associated with remission of chronic myelogenous leukemia. *Proc. Natl. Acad. Sci.* **98**, 7492–7497 (2001).
252. Pallasch, C. P. *et al.* Autoantibodies against GLEA2 and PHF3 in glioblastoma: Tumor-associated autoantibodies correlated with prolonged survival. *Int. J. Cancer* **117**, 456–459 (2005).
253. Richards, E. R. *et al.* Antibodies reactive with the protein core of MUC1 mucin are present in ovarian cancer patients and healthy women. *Cancer Immunol. Immunother.* **46**, 245–252 (1998).
254. Wood, W. C., Kornblith, P. L., Quindlen, E. A. & Pollock, L. A. Detection of Humoral Immune Response to Human Brain Tumors. *Cancer* **1**, 86–90 (1979).
255. Gilbert, A. E. *et al.* Monitoring the Systemic Human Memory B Cell Compartment of Melanoma Patients for Anti-Tumor IgG Antibodies. *PLoS One* **6**, (2011).
256. Takai, T. Fc Receptors and Their Role in Immune Regulation and Autoimmunity - Unknown - 2005.pdf. *J. Clin. Immunol.* **25**, 1–18 (2005).
257. Satoh, M., Iida, S. & Shitara, K. Non-fucosylated therapeutic antibodies: The next generation of therapeutic antibodies. *Expert Opin Biol. Ther.* **6**, (2006).
258. Shields, R. L. *et al.* Lack of Fucose on Human IgG1 N-Linked Oligosaccharide Improves Binding to Human FcγRIII and Antibody-dependent Cellular Toxicity. *J. Biol. Chem.* **277**, 26733–26740 (2002).
259. Oaks, M., Taylor, S. & Shaffer, J. Autoantibodies targeting tumor-associated antigens in metastatic cancer Sialylated IggS as candidate anti-inflammatory antibodies. *Oncoimmunology* **2**, (2013).
260. Rowley, D. A. & Stach, R. M. B lymphocytes secreting IgG linked to latent transforming growth factor-β prevent primary cytolytic T lymphocyte responses. *Int. Immunol.* **10**, 355–363 (1998).
261. Saul, L. *et al.* IgG subclass switching and clonal expansion in cutaneous melanoma and normal skin. *Sci. Rep.* **6**, 1–12 (2016).
262. Garaud, S. *et al.* Antigen Specificity and Clinical Significance of IgG and IgA Autoantibodies Produced in situ by Tumor-Infiltrating B Cells in Breast Cancer. *Front. Immunol.* **9**, 1–12 (2018).
263. Cipponi, A. *et al.* Neogenesis of lymphoid structures and antibody responses occur in human melanoma metastases. *Cancer Res.* **72**, 3997–4007 (2012).
264. Mauri, C. & Blair, P. A. The incognito journey of a regulatory B cell. *Immunity* **41**, 878–880 (2014).
265. Shalapour, S. *et al.* Inflammation-induced IgA⁺ cells dismantle anti-liver cancer immunity. *Nature* **551**, 340–345 (2017).
266. Karagiannis, P. *et al.* IgG4 subclass antibodies impair antitumor immunity in melanoma. *J. Clin. Invest.* **123**, 1457–1474 (2013).

267. Hanahan, D. & Weinberg, R. A. Hallmarks of Cancer: The Next Generation. *Cell* **144**, 646–74 (2011).
268. Nakahara, T., Norberg, S. M., Shalinsky, D. R., Hu-Lowe, D. D. & McDonald, D. M. Effect of inhibition of vascular endothelial growth factor signaling on distribution of extravasated antibodies in tumors. *Cancer Res.* **66**, 1434–1445 (2006).
269. De Visser, K. E., Korets, L. V. & Coussens, L. M. De novo carcinogenesis promoted by chronic inflammation is B lymphocyte dependent. *Cancer Cell* **7**, 411–423 (2005).
270. Andreu, P. *et al.* FcR γ Activation Regulates Inflammation-Associated Squamous Carcinogenesis. *Cancer Cell* **17**, 121–134 (2010).
271. Yamaguchi, R. *et al.* Tumor-infiltrating lymphocytes are important pathologic predictors for neoadjuvant chemotherapy in patients with breast cancer. *Hum. Pathol.* **43**, 1688–1694 (2012).
272. Woo, J. R. *et al.* Tumor infiltrating B-cells are increased in prostate cancer tissue. *J. Transl. Med.* **12**, (2014).
273. Nielsen, J. S. *et al.* CD20+ tumor-infiltrating lymphocytes have an atypical CD27 - memory phenotype and together with CD8+ T cells promote favorable prognosis in ovarian cancer. *Clin. Cancer Res.* **18**, 3281–3292 (2012).
274. Martinet, L. *et al.* Human Solid Tumors Contain High Endothelial Venules: Association with T- and B-Lymphocyte Infiltration and Favorable Prognosis in Breast Cancer. *Cancer Res.* **71**, 5678–5687 (2011).
275. Hussein, M. R., Elasers, D. A. H., Fadel, S. A. & Omar, A. E. M. Immunohistological characterisation of tumour infiltrating lymphocytes in melanocytic skin lesions. *J. Clin. Pathol.* **59**, 316–324 (2006).
276. Martinez-Rodriguez, M., Thompson, A. K. & Monteagudo, C. A significant percentage of CD20-positive TILs correlates with poor prognosis in patients with primary cutaneous malignant melanoma. *Histopathology* **65**, 726–728 (2014).
277. Ladányi, A. Prognostic and predictive significance of immune cells infiltrating cutaneous melanoma. *Pigment Cell Melanoma Res.* **28**, 490–500 (2015).
278. Erdag, G. *et al.* Immunotype and immunohistologic characteristics of tumor-infiltrating immune cells are associated with clinical outcome in metastatic melanoma. *Cancer Res.* **72**, 1070–1080 (2012).
279. Garg, K. *et al.* Tumor-associated B cells in cutaneous primary melanoma and improved clinical outcome. *Hum. Pathol.* **54**, 157–164 (2016).
280. Nsengimana, J. *et al.* β -Catenin-mediated immune evasion pathway frequently operates in primary cutaneous melanomas. *J. Clin. Invest.* **128**, 2048–2063 (2018).
281. Tokunaga, R. *et al.* B cell and B cell-related pathways for novel cancer treatments. *Cancer Treat. Rev.* **73**, 10–19 (2019).
282. Sautès-Fridman, C. & Fridman, W. H. TLS in Tumors: What Lies Within. *Trends Immunol.* **37**, 1–2 (2016).

283. Dieu-Nosjean, M. C. *et al.* Tertiary lymphoid structures, drivers of the anti-tumor responses in human cancers. *Immunol. Rev.* **271**, 260–275 (2016).
284. Germain, C., Gnjatic, S. & Dieu-Nosjean, M. C. Tertiary lymphoid structure-associated B cells are key players in anti-tumor immunity. *Front. Immunol.* **6**, 1–14 (2015).
285. Coughlin, C. M., Vance, B. A., Grupp, S. A. & Vonderheide, R. H. RNA-transfected CD40-activated B cells induce functional T-cell responses against viral and tumor antigen targets: Implications for pediatric immunotherapy. *Blood* **103**, 2046–2054 (2004).
286. Schultze, J. L. *et al.* CD40-activated human B cells: an alternative source of highly efficient antigen presenting cells to generate autologous antigen-specific T cells for adoptive immunotherapy. *J. Clin. Invest.* **100**, 2757–2765 (1997).
287. Zhu, W. *et al.* A high density of tertiary lymphoid structure B cells in lung tumors is associated with increased CD4+T cell receptor repertoire clonality. *Oncoimmunology* **4**, (2015).
288. Gnjatic, S. *et al.* Cross-Presentation of HLA Class I Epitopes from Exogenous NY-ESO-1 Polypeptides by Nonprofessional APCs. *J. Immunol.* **170**, 1191–1196 (2003).
289. Brodt, P. & Gordon, J. Natural Resistance Mechanisms May Play a Role in Protection Against Chemical Carcinogenesis. *Cancer Immunol. Immunother.* **13**, 125–127 (1982).
290. Inoue, S., Leitner, W. W., Golding, B. & Scott, D. Inhibitory effects of B cells on antitumor immunity. *Cancer Res.* **66**, 7741–7747 (2006).
291. Schioppa, T. *et al.* B regulatory cells and the tumor-promoting actions of TNF- α during squamous carcinogenesis. *PNAS* **108**, 26–31 (2011).
292. Wejksza, K. *et al.* Cancer-Produced Metabolites of 5-Lipoxygenase Induce Tumor-Evoked Regulatory B Cells via Peroxisome Proliferator-Activated Receptor . *J. Immunol.* **190**, 2575–2584 (2013).
293. Pucci, F. *et al.* SCS macrophages suppress melanoma by restricting tumor-derived vesicle–B cell interactions. *Science* **352**, (2016).
294. Barbera-guillem, E. *et al.* B lymphocyte pathology in human colorectal cancer. Experimental and clinical therapeutic effects of partial B cell depletion. *Cancer Immunol. Immunother. Imm* **48**, 541–549 (2000).
295. He, Y. *et al.* The roles of regulatory B cells in cancer. *J. Immunol. Res.* **2014**, (2014).
296. Wang, W. *et al.* CD19+CD24hiCD38hiBregs involved in downregulate helper T cells and upregulate regulatory T cells in gastric cancer. *Oncotarget* **6**, 33486–33499 (2015).
297. Shao, Y. *et al.* Regulatory B cells accelerate hepatocellular carcinoma progression via CD40/CD154 signaling pathway. *Cancer Lett.* **355**, 264–272 (2014).
298. Guan, H. *et al.* PD-L1 is a critical mediator of regulatory B cells and T cells in invasive breast cancer. *Sci. Rep.* **6**, 1–10 (2016).
299. Somasundaram, R. *et al.* Tumor-associated B-cells induce tumor heterogeneity and therapy

- resistance. *Nat. Commun.* **8**, 1–16 (2017).
300. Gunderson, A. J. & Coussens, L. M. B cells and their mediators as targets for therapy in solid tumors. *Exp. Cell Res.* **319**, 1644–1649 (2013).
 301. Baumgaertner, P. *et al.* Vaccination-induced functional competence of circulating human tumor-specific CD8 T-cells. *Int. J. Cancer* **130**, 2607–2617 (2012).
 302. Braun, M. *et al.* Virus-like particles induce robust human T-helper cell responses. *Eur. J. Immunol.* **42**, 330–340 (2012).
 303. Romano, E. *et al.* Ipilimumab-dependent cell-mediated cytotoxicity of regulatory T cells ex vivo by nonclassical monocytes in melanoma patients. *Proc. Natl. Acad. Sci.* **112**, 6140–6145 (2015).
 304. Bray, N. L., Pimentel, H., Melsted, P. & Pachter, L. Near-optimal probabilistic RNA-seq quantification. *Nat. Biotechnol.* **34**, 525–7 (2016).
 305. Sonesson, C., Love, M. I. & Robinson, M. D. Differential analyses for RNA-seq : transcript-level estimates improve gene-level inferences [version 1 ; referees : awaiting peer review]. *F1000 Res.* 1–10 (2015). doi:10.12688/f1000research.7563.1
 306. Love, M. I., Huber, W. & Anders, S. Moderated estimation of fold change and dispersion for RNA-seq data with DESeq2. *Genome Biol.* **15**, 550 (2014).
 307. Sergushichev, A. A. An algorithm for fast preranked gene set enrichment analysis using cumulative statistic calculation. *bioRxiv* 060012 (2016). doi:10.1101/060012
 308. Durinck, S., Spellman, P. T., Birney, E. & Huber, W. Mapping identifiers for the integration of genomic datasets with the R/Bioconductor package biomaRt. *Nat. Protoc.* **4**, 1184 (2009).
 309. Salomon, D. R. *et al.* Strategies for aggregating gene expression data: The collapseRows R function. *BMC Bioinformatics* (2011). doi:10.1186/1471-2105-12-322
 310. Liberzon, A. *et al.* The Molecular Signatures Database Hallmark Gene Set Collection. *Cell Syst.* **1**, 417–425 (2015).
 311. Kolde, R. Package ‘ pheatmap ’. (2018).
 312. Carpenter, E. L. *et al.* Collapse of the CD27+ B-cell compartment associated with systemic plasmacytosis in patients with advanced melanoma and other cancers. *Clin. Cancer Res.* **15**, 4277–4287 (2009).
 313. Shen, P. & Fillatreau, S. Antibody-independent functions of B cells: A focus on cytokines. *Nat. Rev. Immunol.* **15**, 441–451 (2015).
 314. Rubtsova, K. *et al.* B cells expressing the transcription factor T-bet drive lupus-like autoimmunity. *J. Clin. Invest.* **127**, 1392–1404 (2017).
 315. Rakhmanov, M. *et al.* High levels of SOX5 decrease proliferative capacity of human B Cells, but permit plasmablast differentiation. *PLoS One* **9**, (2014).
 316. Fremd, C., Schuetz, F., Sohn, C., Beckhove, P. & Domschke, C. B cell-regulated immune responses

in tumor models and cancer patients. *Oncoimmunology* (2013).

317. Lawson, D. H. *et al.* Randomized, placebo-controlled, phase III trial of yeast-derived granulocyte-macrophage colony-stimulating factor (GM-CSF) versus peptide vaccination versus GM-CSF plus peptide vaccination versus placebo in patients with no evidence of disease after comp. *J. Clin. Oncol.* **33**, 4066–4076 (2015).
318. Grotz, T. E., Kottschade, L., Pavey, E. S., Markovic, S. N. & Jakub, J. W. Adjuvant GM-CSF improves survival in high-risk Stage IIIC melanoma: A single-center study. *Am. J. Clin. Oncol. Cancer Clin. Trials* **37**, 467–472 (2013).
319. Gutschalk, C. M., Herold-Mende, C. C., Fusenig, N. E. & Mueller, M. M. Granulocyte colony-stimulating factor and granulocyte-macrophage colony-stimulating factor promote malignant growth of cells from head and neck squamous cell carcinomas in vivo. *Cancer Res.* **66**, 8026–8036 (2006).
320. Hunter, C. A. & Jones, S. A. IL-6 as a keystone cytokine in health and disease. *Nat. Immunol.* **16**, 448–457 (2015).
321. Rosser, E. C. *et al.* Regulatory B cells are induced by gut microbiota-driven interleukin-1 β and interleukin-6 production. *Nat. Med.* **20**, 1334–1339 (2014).
322. Dedobbeleer, O., Stockis, J., van der Woning, B., Coulie, P. G. & Lucas, S. Cutting Edge: Active TGF- β 1 Released from GARP/TGF- β 1 Complexes on the Surface of Stimulated Human B Lymphocytes Increases Class-Switch Recombination and Production of IgA. *J. Immunol.* **199**, 391–396 (2017).
323. van de Veen, W. *et al.* Role of regulatory B cells in immune tolerance to allergens and beyond. *J. Allergy Clin. Immunol.* **138**, 654–665 (2016).
324. Johnson, B. A. *et al.* B-lymphoid cells with attributes of dendritic cells regulate T cells via indoleamine 2,3-dioxygenase. *PNAS* **107**, (2010).
325. Ghaedi, M. *et al.* Common-Lymphoid-Progenitor-Independent Pathways of Innate and T Lymphocyte Development. *Cell Rep.* **15**, 471–480 (2016).
326. Seillet, C. *et al.* Deciphering the Innate Lymphoid Cell Transcriptional Program. *Cell Rep.* **17**, 436–447 (2016).
327. Yu, X. *et al.* The basic leucine zipper transcription factor NFIL3 directs the development of a common innate lymphoid cell precursor. *Elife* **3**, 1–20 (2014).
328. Xu, W. *et al.* NFIL3 Orchestrates the Emergence of Common Helper Innate Lymphoid Cell Precursors. *Cell Rep.* **10**, 2043–2054 (2015).
329. Zook, E. C. & Kee, B. L. Development of innate lymphoid cells. *Nat. Immunol.* **17**, 775–782 (2016).
330. Diefenbach, A., Colonna, M. & Romagnani, C. The ILC World Revisited. *Immunity* **46**, 327–332 (2017).
331. Karamitros, D. *et al.* Single-cell analysis reveals the continuum of human lympho-myeloid progenitor cells. *Nat. Immunol.* **19**, 85–97 (2018).

332. Renoux, V. M. *et al.* Identification of a Human Natural Killer Cell Lineage-Restricted Progenitor in Fetal and Adult Tissues. *Immunity* **43**, 394–407 (2015).
333. Bernink, J. H. *et al.* Human type 1 innate lymphoid cells accumulate in inflamed mucosal tissues. *Nat. Immunol.* **14**, 221–229 (2013).
334. Freud, A. G. *et al.* A human CD34(+) subset resides in lymph nodes and differentiates into CD56bright natural killer cells. *Immunity* **22**, 295–304 (2005).
335. Lim, A. I. *et al.* Systemic Human ILC Precursors Provide a Substrate for Tissue ILC Differentiation. *Cell* **168**, 1086–1100.e10 (2017).
336. Montaldo, E. *et al.* Human ROR γ t+CD34+ Cells Are Lineage-Specified Progenitors of Group 3 ROR γ t+ Innate Lymphoid Cells. *Immunity* **41**, 988–1000 (2014).
337. Juelke, K. & Romagnani, C. Differentiation of human innate lymphoid cells (ILCs). *Curr. Opin. Immunol.* **38**, 75–85 (2016).
338. Hoek, K. L. *et al.* A cell-based systems biology assessment of human blood to monitor immune responses after influenza vaccination. *PLoS One* **10**, 1–24 (2015).
339. Linsley, P. S., Speake, C., Whalen, E. & Chaussabel, D. Copy number loss of the interferon gene cluster in melanomas is linked to reduced T cell infiltrate and poor patient prognosis. *PLoS One* **9**, (2014).
340. Pabst, C. *et al.* GPR56 identifies primary human acute myeloid leukemia cells with high repopulating potential in vivo. *Blood* **127**, 2018–2027 (2016).
341. Kim, D. *et al.* TopHat2: accurate alignment of transcriptomes in the presence of insertions, deletions and gene fusions. *Genome Biol.* **46**, 957–961 (2013).
342. Langmead, B. & Salzberg, S. L. Fast gapped-read alignment with Bowtie 2. *Nat. Methods* **9**, 357–9 (2012).
343. Li, H. *et al.* The Sequence Alignment/Map format and SAMtools. *Bioinformatics* **25**, 2078–2079 (2009).
344. Anders, S., Pyl, P. T. & Huber, W. HTSeq-A Python framework to work with high-throughput sequencing data. *Bioinformatics* **31**, 166–169 (2015).
345. Johnson, W. E., Li, C. & Rabinovic, A. Adjusting batch effects in microarray expression data using empirical Bayes methods. *Biostatistics* **8**, 118–127 (2007).
346. Leek, J. T., Johnson, W. E., Parker, H. S., Jaffe, A. E. & Storey, J. D. The SVA package for removing batch effects and other unwanted variation in high-throughput experiments. *Bioinformatics* **28**, 882–883 (2012).
347. Cupedo, T. *et al.* Human fetal lymphoid tissue-inducer cells are interleukin 17-producing precursors to RORC+ CD127+ natural killer-like cells. *Nat. Immunol.* **10**, 66–74 (2009).
348. Rudensky, A. Y. Regulatory T cells and Foxp3. *Immunol. Rev.* **241**, 260–268 (2011).

13. Annexes

During this PhD I have been blessed to be part of two fruitful collaborations. One within the lab led by former PhD student Natacha Bordry on unravelling the link between lymphatics and T cell infiltration within the tumour micro-environment in melanoma. I joined at the end of the project and was mostly involved with the analysis of multiplex stainings. The second successful collaboration was with Julien Racle with the group of Prof. Gfeller at the Ludwig Branch in Lausanne. We performed the validation for a deconvolution method based on bulk RNA sequencing.

Papers of the two projects have been published and are included below.

Lymphatic vessel density is associated with CD8⁺ T cell infiltration and immunosuppressive factors in human melanoma

Natacha Bordry ^{a,b,*}, Maria A. S. Broggi ^{b,h,*}, Kaat de Jonge ^a, Karin Schaeuble^a, Philippe O. Gannon^c, Periklis G. Foukas^{c,g}, Esther Danenberg^c, Emanuela Romano^{c,e}, Petra Baumgaertner^{a,c}, Manuel Fankhauser ^b, Noémie Wald^a, Laurène Cagnon^c, Samia Abed-Maillard ^{b,c}, Hélène Maby-El Hajjami ^a, Timothy Murray^a, Kalliopi Ioannidou ^a, Igor Letovanec ^d, Pu Yan^d, Olivier Michielin^c, Maurice Matter ^{c,g}, Melody A. Swartz^{b,f}, and Daniel E. Speiser ^{a,c}

^aClinical Tumor Biology and Immunotherapy Group, Department of Oncology and Ludwig Cancer Research, University of Lausanne (UNIL), Lausanne, Switzerland; ^bInstitute of Bioengineering and Swiss Institute for Experimental Cancer Research (ISREC), School of Life Sciences, Ecole Polytechnique Fédérale de Lausanne, Lausanne, Switzerland; ^cDepartment of Oncology, Lausanne University Hospital Center (CHUV) and University of Lausanne, Lausanne, Switzerland; ^dDepartment of Pathology, CHUV, Lausanne, Switzerland; ^eDepartment of Oncology, INSERM U932, Institut Curie, Paris, FRANCE; ^f2nd Department of Pathology, Attikon University Hospital, National and Kapodistrian University of Athens, Athens, Greece; ^gDepartment of Surgery, CHUV, Lausanne, Switzerland; ^hInstitute for Molecular Engineering, University of Chicago, Chicago, IL, USA

ABSTRACT

Increased density of tumor-associated lymphatic vessels correlates with poor patient survival in melanoma and other cancers, yet lymphatic drainage is essential for initiating an immune response. Here we asked whether and how lymphatic vessel density (LVD) correlates with immune cell infiltration in primary tumors and lymph nodes (LNs) from patients with cutaneous melanoma. Using immunohistochemistry and quantitative image analysis, we found significant positive correlations between LVD and CD8⁺ T cell infiltration as well as expression of the immunosuppressive molecules inducible nitric oxide synthase (iNOS) and 2,3-dioxygenase (IDO). Interestingly, similar associations were seen in tumor-free LNs adjacent to metastatic ones, indicating loco-regional effects of tumors. Our data suggest that lymphatic vessels play multiple roles at tumor sites and LNs, promoting both T cell infiltration and adaptive immunosuppressive mechanisms. Lymph vessel associated T cell infiltration may increase immunotherapy success rates provided that the treatment overcomes adaptive immune resistance.

ARTICLE HISTORY

Received 16 November 2017
Revised 25 February 2018
Accepted 13 March 2018

KEYWORDS

immunotherapy; lymphatics; tumor immunology; T cell inhibition; T cell promotion


Introduction

Over the last two decades, burgeoning research attention has been focused on understanding the complex interactions between evolving tumors and host immune responses, with consequences for the development of novel immunotherapies.¹⁻⁴ Despite the promotion of tumor antigen specific T cell responses by active immunization, checkpoint blockade or adoptive transfer, only a subset of patients experience clinical benefit.⁵ In melanoma, recent studies have sought predictive indicators (genetic or phenotypic) by comparing patients who respond to immunotherapies with those that do not.^{6,7} A variety of factors have been found to affect response to immunotherapy, including the preexisting immune cell infiltrate and the chemokine expression profile.^{8,9} Furthermore, cancers can develop adaptive immune resistance mechanisms that suppress anti-tumor T cell responses.^{10,11} In addition, further mechanisms may contribute to therapy failures, including mechanisms that impact on the recruitment of immune cells to tumors.¹² New and readily accessible/quantifiable biomarkers are

required to help identifying the underlying reasons in individual patients, and consequently adapt immune therapy strategies in order to increase patient survival.¹³

One feature of many cancers is the activation or expansion of lymphatic vessels. Local lymphatic vessel density (LVD) is known to be associated with metastasis in several human and experimental cancers. The lymphangiogenic factor Vascular Endothelial Growth Factor-C (VEGF-C), secreted by tumor-associated macrophages or tumor cells themselves, leads to increased LVD in the tumor microenvironment and in lymph nodes (LNs), correlating with increased metastasis and poor prognosis.¹⁴⁻²⁰ However, the mechanisms by which lymphangiogenesis promotes disease progression are not well understood. While increased LVD provide more surface area for tumor cells to enter the lymph and thereby migrate to distant sites, recent studies have highlighted additional important mechanisms. For example, VEGF-C activates lymphatic endothelial cells (LECs) to upregulate chemokine (C-C motif) ligand 21 (CCL21), a chemo-attractant for C-C chemokine receptor

CONTACT Daniel E. Speiser  doc@dspaiser.ch; Melody A. Swartz  melodyswartz@uchicago.edu

 Supplemental data for this article can be accessed on the publisher's website.

*These authors contributed equally to this article.

© 2018 The Author(s). Published with Taylor & Francis Group.

This is an Open Access article distributed under the terms of the Creative Commons Attribution-NonCommercial-NoDerivatives License (<http://creativecommons.org/licenses/by-nc-nd/4.0/>), which permits non-commercial re-use, distribution, and reproduction in any medium, provided the original work is properly cited, and is not altered, transformed, or built upon in any way.

7⁺ (CCR7) immune cells and tumor cells, leading to increased tumor invasion and entry into lymphatics in vitro and in mice.²¹⁻²³ More recently, it has been proposed that lymphangiogenesis could play important roles in modulating the immune microenvironment. In mouse models, increased CCL21 in the tumor microenvironment could promote fibroblast differentiation and matrix remodeling to resemble the stroma of lymph nodes, as well as promote T cell infiltration (including regulatory T cells) along with suppressive leukocyte subsets.²⁴ Furthermore, tumor-associated LECs may directly cross-present tumor antigens to CD8⁺ T cells and render them dysfunctional in the tumor microenvironment.^{25,26} LECs can also inhibit the maturation of dendritic cells,²⁷ secrete inhibitory molecules such as indoleamine 2,3-dioxygenase (IDO), inducible nitric oxide synthase (iNOS) and transforming growth factor beta (TGF- β), and impair T cell activation through expression of inhibitory receptor ligands (e.g. programmed cell death ligand 1 and 2 (PD-L1 and 2)).²⁸ Finally, a recent study demonstrated that in mice lacking dermal lymphatic vessels, melanomas failed to generate an inflammatory microenvironment and lacked T cell infiltration.²⁹ Taken together, these findings indicate a critical role for tumor-associated lymphatics in initiating and shaping the immune response.

Since these studies were performed in mice, in short-term studies with implanted tumors, we asked whether and how LVD correlates with the immune microenvironment in patients with cutaneous melanoma. Through immunohistochemistry (IHC) analysis of primary tumors and downstream LNs, using a dedicated method enabling quantitative assessment of unusually large tissue fields, we provide evidence that LVD indeed correlates with T cell infiltration and expression of immune suppressive molecules in human melanoma, not only locally but also in regional LNs, including in those that are not (yet) metastatic. Our findings suggest that while LVD and VEGF-C are prognostic factors for metastasis, they also are tightly correlated with the immune status of the tumor microenvironment and thus may have potential impact on the outcome of immunotherapy.

Results

Quantification of lymph vessels across entire tissue sections

To determine LVD we examined LECs by IHC staining in sections of tumors and draining LNs. We found high variability of LVD in different regions of the tumor, as well as high inter-patient heterogeneity. Thus, we first sought to establish a method of analyzing entire tumor sections for very wide and representative spatial assessment of LVD and related features of the immune microenvironment. We defined distinct tissue zones in the tumor and LN microenvironments to study 13 primary tumors, 23 metastatic LNs and 23 tumor-free LNs (i.e. neighboring distant lymph node without evidence of disease) and used whole-slide imaging software for quantifications in each zone (see Methods).

To define the localization of LECs in different human tissue sections we performed IHC using Prox-1 and podoplanin antibodies. Histological analysis confirmed that

podoplanin was specifically expressed on lymphatic vessels in different zones of the primary tumor (Fig. 1A), the tumor region of metastatic LNs (Fig. 1B) and the normal skin (Fig. S1A). In contrast, Prox-1 antibody was not well suited as LEC marker within these tissues, as certain tumor cells as well as skin epithelial cells may also be positive (Fig. 1A and B and Fig. S1A and B).

Up to now, histological quantification of human lymphatic vessels was mainly done by the so-called “hot spot” analysis³⁰ which usually considers only small tissue regions where density of lymphatic vessels was the highest. In contrast, our approach consisted of automated marker quantification in large but distinct tissue areas based on staining intensity. In order to validate the automated marker quantification method and characterize the best marker to identify LECs in the individual tissues, we performed automated quantification of Prox-1 and podoplanin, respectively, and correlated the results with our data from LEC counting by eye (see “LEC quantification” in Methods). We found that podoplanin quantified by automated whole tissue analysis correlated well with lymphatic vessels quantified per mm² by counting by eye in the different regions of the primary tumor (Fig. 1A) and in the tumor region of metastatic LNs (Fig. 1B). In agreement with our visual observation, automated quantification of Prox-1 did not correlate significantly with LEC counting by eye in primary tumor (Fig. 1A) and only minor in the tumor region of metastatic LNs (Fig. 1B) whereas the correlation for podoplanin was strong. In contrast to tumor bearing tissues, LEC quantification in tumor-free LNs was superior based on Prox-1 staining as compared to podoplanin staining, because podoplanin was also expressed by several other cell types in the lymph nodes, for example follicular dendritic cells (Fig. S1C). Indeed, automated quantification of Prox-1 showed a good correlation with the LEC counting by eye in tumor-free LNs (Fig. S1D). The combined use of both, Prox-1 and podoplanin by Immunofluorescence (IF) labeling confirmed the validity of our strategy to identify LECs in the different tissues analyzed (Fig. 1C). Therefore, based on these results, we chose for our broad quantification of LECs to use podoplanin expression in primary tumors and the tumor regions of metastatic LNs, and Prox-1 expression in tumor-free LNs.

Increased intratumoral lymph vessel density (LVD) and VEGF-C in earliest stages of primary melanoma

High LVD has been previously described in prominent “hot spots” both within and around primary cutaneous malignant melanoma.³¹ Moreover, melanoma lesions have been shown to have higher intratumoral and peritumoral LVD compared to benign melanocytic lesions, likely due to pro-lymphangiogenic factors, essentially VEGF-C, secreted by tumor cells.³²⁻³⁴ Detailed analysis of the distribution of LECs in primary tumors showed that LVD was already increased in the earliest stage of melanoma (melanoma *in situ*) in comparison to the adjacent normal skin. Furthermore our data confirmed that LVD is increased in primary melanoma, specifically in the invasive margin and the peritumoral regions (Fig. 2A). In order to

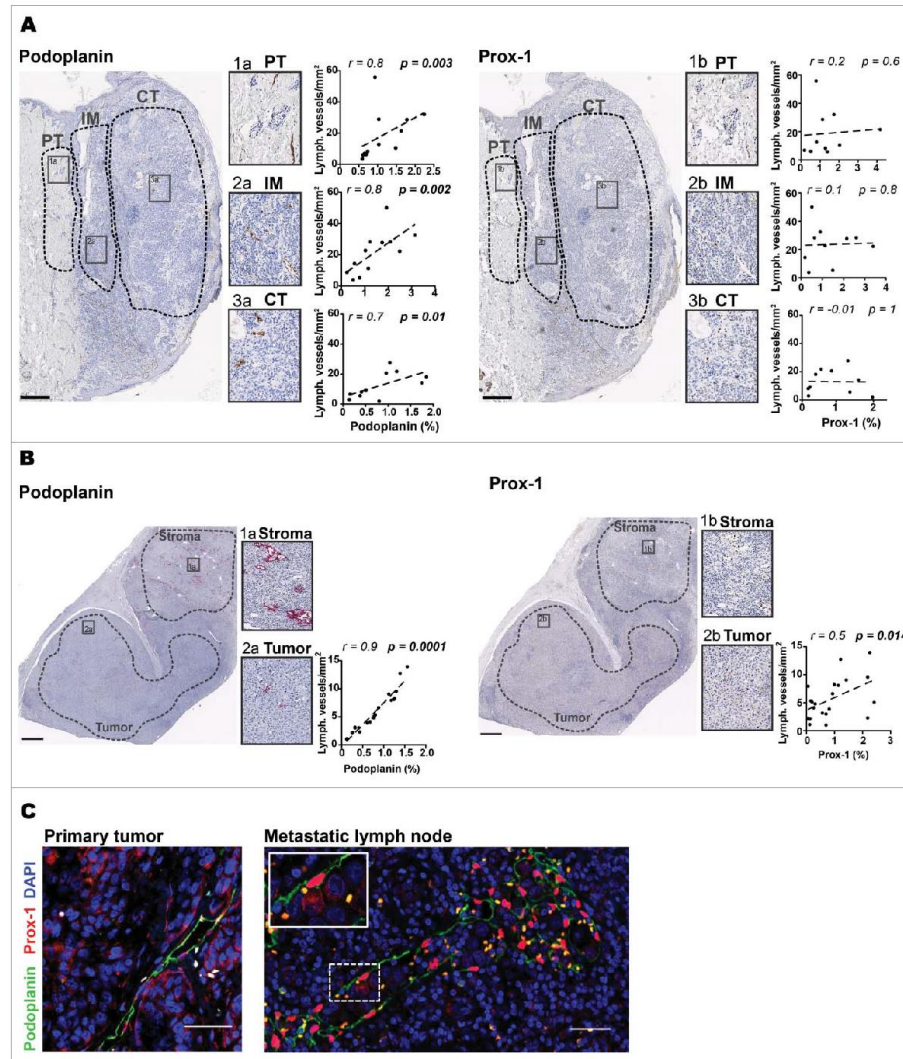


Figure 1. Comparison of lymph vessel density (LVD) assessment by automated pixel based large-scale quantification versus LEC counting by eye. Representative immunohistochemistry images showing podoplanin and Prox-1 staining of peritumoral area (PT), invasive margin (IM) and center of tumor (CT) of A) primary melanoma and B) stroma and tumor regions of metastatic lymph node sections (Scale bars in A) 500 μm ; in B) 1mm). Correlations of podoplanin or Prox-1 (% of pixel positive cells) counted by the ImageScope™ software (x-axis) versus counted by eye (y-axis) in IM (n = 12), CT (n = 11) and PT (n = 12) of primary tumors and in tumor regions of metastatic LNs (n = 22). C) Representative immunofluorescence images of podoplanin (green) and Prox-1 (red) co-localization in different tissues (20 \times , scale bar = 50 μm , DAPI, blue). All correlations were analyzed using non-parametric Spearman's test. (PT): peritumoral area, (IM): invasive margin, (CT): center of tumor.

determine the presence of VEGF-C and its association with LEC formation and distribution we performed immunostaining of VEGF-C in primary tumors and metastatic lymph nodes. Podoplanin positively correlated with VEGF-C only within melanoma *in situ* (Fig. 2B) while in primary melanoma and in the tumor regions of metastatic LNs these parameters did not correlate (Fig. S2A-F). These results are compatible with the notion that VEGF-C may play a role in lymphangiogenesis in early stage of melanoma formation.

LVD correlates with tumor infiltrating CD8⁺ T cells and expression of immune suppressive molecules

To investigate the potential associations of LVD with immune cell infiltrates, we next quantified the density of infiltrating lymphocytes expressing CD8, CD4, Foxp3 and CD19. Since LNs are important sites for tumor spread and immune responses, we not only analyzed the immune microenvironment of primary tumors, but also the one of the tumor regions within

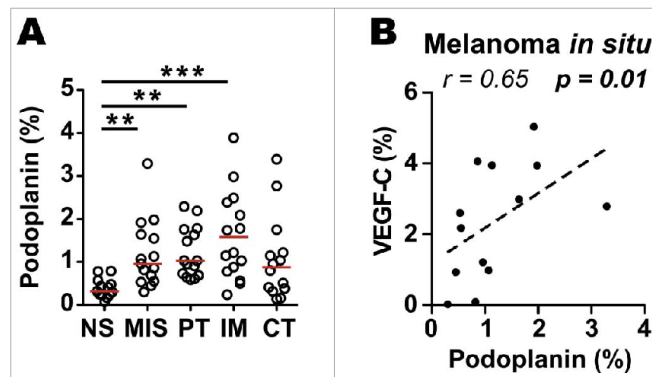


Figure 2. Increased lymphatic vessel density (LVD) in melanoma *in situ*, invasive margin and peritumoral area of primary melanomas. A) Quantification of podoplanin density (% of pixel positive cells) in normal skin (NS; n = 12), melanoma *in situ* (MIS; n = 14) and in the different histological zones of primary melanomas, i.e. peritumoral region (PT; n = 13), invasive margin (IM; n = 13) and center of tumor (CT; n = 12). Line indicates median. ***, $p \leq 0.001$; **, $p \leq 0.01$; one-way Kruskal-Wallis non-parametric test with post-hoc test Dunn correction. B) Correlation of podoplanin with VEGF-C density (% of pixel positive cells) in melanoma *in situ* (n = 13). Correlation was analyzed using non-parametric Spearman's test.

metastatic LNs. Interestingly, similar to the distribution of LECs we found the highest density of CD8⁺ T cells in peritumoral areas and the invasive margin of primary tumors (Fig. 3A). Quantitative analysis revealed that primary tumors showed strong positive correlations of CD8⁺ T cell infiltration with LVD (Fig. 3B). This correlation held true in all primary tumor regions analyzed (center of tumor, invasive margin and peritumoral regions). However, LVD showed only positive trends not reaching statistical significance for CD4⁺ cells, CD19⁺ cells and FoxP3⁺ regulatory T cells within primary tumors (Fig. S3A-C). A strong positive correlation between LVD and CD8⁺ T cells was also found in metastatic LNs (Fig. 3C). In contrast to primary tumors, in metastatic LNs we found positive associations between LVD and CD19⁺ cells and also with FoxP3⁺ cells (Fig. 3D), suggesting attraction of potentially immune suppressive cells by mechanisms involving lymphatic vessels. Together, these data propose that lymphangiogenic regions within the tumor may specifically chemoattract circulating T cells, consistent with studies in mouse melanoma, where VEGF-C was shown to upregulate CCL21 to attract CCR7⁺ immune cells.²⁴

Next, we investigated the correlation of LVD with the presence of immune suppressive factors by analyzing the expression of iNOS, IDO, and arginase-1 (Arg-1) in the same tissues. IF analysis revealed that both iNOS and IDO were mainly produced by cells surrounding lymphatic vessels rather than by the LECs in primary tumors (Fig. 4A, left panels). However, we found iNOS expression in the cytoplasm of LECs in metastatic LNs (Fig. 4A, right panels) suggesting that tumor-associated LECs can play direct roles in immune modulation. LVD positively correlated with iNOS expression in the invasive margin, and with IDO expression in the center of tumor (Fig. 4B, left panels). In the tumor region of metastatic LNs, iNOS and IDO expression were positively correlated with LVD (Fig. 4B, right panels). Arg-1 was neither expressed by LECs nor associated with LVD in any of the melanoma tissues analyzed (Fig. S4A and B).

VEGF-C correlates with T cell infiltration in primary melanoma and immune suppressive molecules in early stages of primary melanoma and metastatic LNs

Mouse melanomas have been reported to pre-condition future sites of LN metastasis by enhancing lymphangiogenesis, inducing an immune tolerant microenvironment and thus impairing the development of anti-tumor immunity.^{35,36} Furthermore, VEGF-C overexpression in mouse melanoma promoted an immune suppressive microenvironment in primary and downstream LNs.^{24,25} To address the potential role of VEGF-C in modulating host anti-tumor immunity in human melanoma, we quantified tumor sections immunostained for VEGF-C and immune markers. Interestingly, in the earliest stages of primary melanoma (melanoma *in situ*), we found strong positive correlations between VEGF-C expression and iNOS (Fig. 5A). Increased expression of VEGF-C correlated with elevated expression of iNOS and IDO in tumor regions of metastatic LNs (Fig. 5B-C). These results suggest that VEGF-C may have different roles in modulating the tumor microenvironment (TME) depending on tumor stage and tissue location.

LVD correlates with CD8⁺ T cells and immune suppressive molecules in tumor-free LNs adjacent to metastatic LNs

Mouse studies have suggested that melanomas can secrete factors that pre-condition potential future metastatic sites in LNs, and that this pre-conditioning is associated with increased LVD.^{35,36} Studies in humans have shown immunological differences in LNs close to the primary melanoma as compared to the more remote LNs, with regard to the capacity of paracortical dendritic cells and T cells to inhibit or enhance melanoma cell growth *in vitro*, as well as the density of high endothelial venules (HEVs).³⁷ To identify possible changes in distal LNs in our patients, we analyzed 23 tumor-free LNs, with the hypothesis that tumor-free LNs may differ depending on whether they were from LN dissections with one or more metastatic LNs

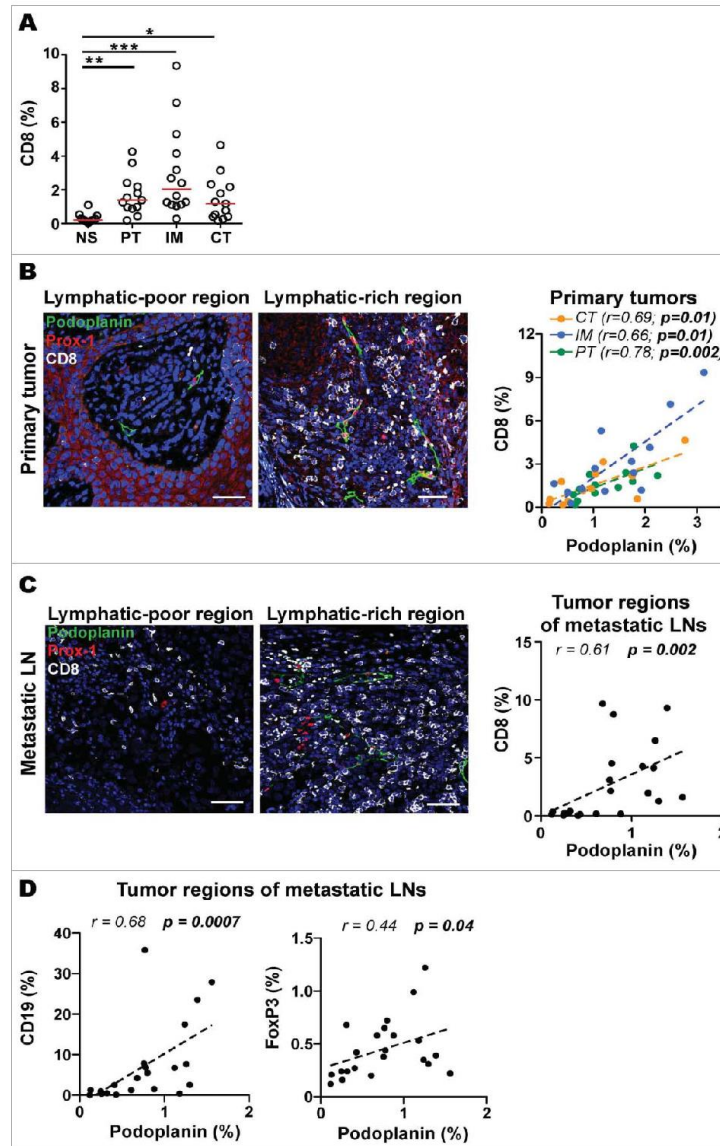


Figure 3. LVD correlates with infiltration of CD8⁺ T cells in primary tumors and tumor regions of metastatic lymph nodes (LNs). **A**) Quantification of CD8 density (% of pixel positive cells) in different zones of primary melanomas. Statistical significance was calculated using one-way Kruskal-Wallis non-parametric test with post-hoc test Dunn correction. Line indicates median. ***, $p \leq 0.001$; **, $p \leq 0.01$; *, $p \leq 0.05$. Representative immunofluorescence images showing lymphatic vessels (Prox-1, red; podoplanin, green) and CD8⁺ T cells (grey) in lymphatic-poor and -rich regions of a **B**) primary tumor and a **C**) metastatic LN (20X, Scale bar = 50 μ m, DAPI, blue). Correlations of podoplanin with CD8 density (% of pixel positive cells) in PT ($n = 13$), IM ($n = 13$) and CT ($n = 13$) of **B**) primary tumors and in **C**) metastatic LNs ($n = 23$). **D**) Correlations of podoplanin with CD19 ($n = 21$) and FoxP3 ($n = 22$) density (% of pixel positive cells) in tumor regions of metastatic LNs. All correlations were analyzed using non-parametric Spearman's test. (PT): peritumoral region, (IM): invasive margin, (CT): center of tumor.

(tumor-positive LN dissection; $n = 14$) versus dissections where all LNs were tumor-free (tumor-negative LN dissection; $n = 9$). Interestingly, tumor-free LNs from positive LN dissections had higher expression of Prox-1 as compared to LNs from negative LN dissections (Fig. 6A). Greater densities of CD8⁺ cells and CD4⁺ cells were seen in LNs from tumor-

positive LN dissections compared to negative LN dissections (Fig. 6B). In line with this, higher density for iNOS and Arg-1 were found in LNs from positive LN dissections (Fig. 6C). Interestingly, in tumor-free LNs from positive LN dissections, LECs were found to express iNOS (Fig. 6D), showing a positive correlation with iNOS expression (Fig. 6E) similar to that in

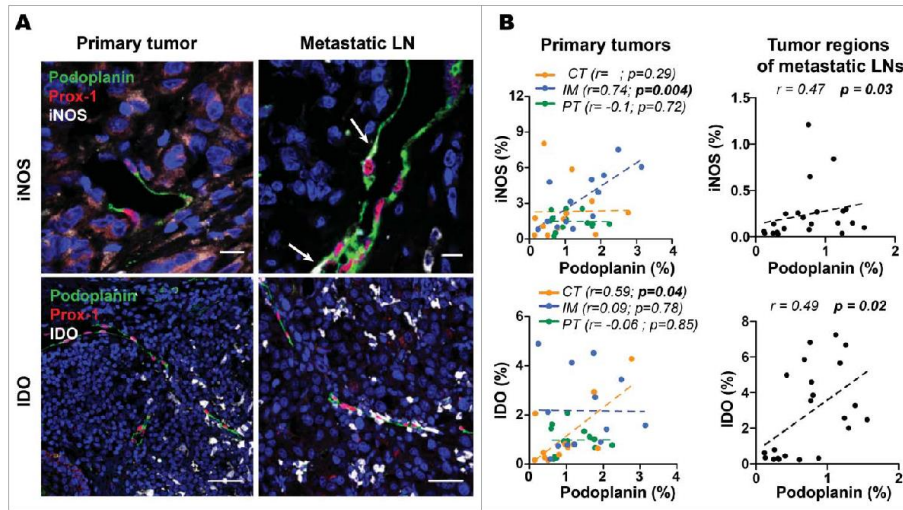


Figure 4. LVD correlates with expression of immune suppressive molecules in primary tumors and tumor regions of metastatic LNs. A) Representative immunofluorescence images in a section of a primary tumor and a metastatic LN showing that intratumoral lymphatic vessels (Prox-1, red; podoplanin, green) express iNOS (white, arrows) in metastatic LNs and do not express IDO (grey) in either location (63X upper panels Scale bar = 10 μm, and 40X lower panels, Scale bar = 50 μm, DAPI, blue). B) Correlations of podoplanin with iNOS and IDO density (% of pixel positive cells) in IM (n = 13), CT (n = 12) and PT (n = 13) of primary tumors and in metastatic LNs (n = 23). Correlations were analyzed using non-parametric Spearman's test. (IM): invasive margin, (CT): center of tumor, (PT): peritumoral region.

metastatic LNs (Fig. 4B). Together, these data indicate that tumor-free LNs adjacent to metastatic LNs have increased LVD, lymphocyte density and immunosuppressive features compared to LNs from tumor negative LN dissections.

Discussion

Multiple studies have demonstrated the clinical relevance of tumor-associated lymphatics and their involvement in malignant spread.³⁸⁻⁴⁰ In human melanoma, increased intra- and peritumoral LVD as well as the lymphatic growth

factor VEGF-C strongly correlate with metastatic dissemination.^{17,33,41-43} Lymphatic vessels may support migration of tumor cells, but may also modulate immune cells, as recently demonstrated in primary tumors and draining LNs in mice,^{24,25,44} raising the possibility that lymphatics mediate immune suppression and poor clinical outcome in cancer patients.^{19,31,42} Because corresponding human data are missing, we performed a very wide IHC analysis. Our findings reveal multiple correlations between lymphatic vessels and host immunity, suggesting immune mechanisms that act locally as well as loco-regionally in melanoma patients (Fig. 7).

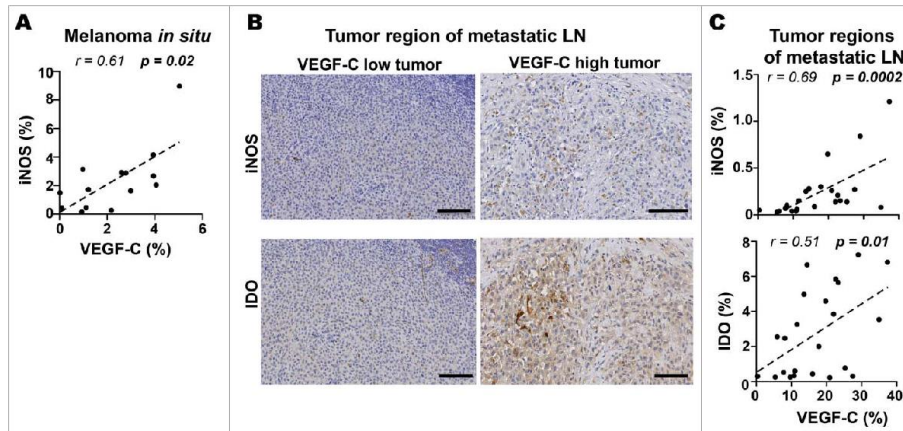


Figure 5. VEGF-C is associated with expression of immune suppressive molecules in melanoma *in situ* and tumor regions of metastatic LNs. A) Correlations of VEGF-C with iNOS density (% of pixel positive cells) in melanoma *in situ* (n = 14). B) Representative immunohistochemistry images showing iNOS and IDO expression in tumor region of VEGF-C-low and VEGF-C-high metastatic LN sections (Scale bar = 100 μm). C) Correlations of VEGF-C with iNOS (n = 23) and IDO (n = 23) density (% of pixel positive cells) in tumor regions of metastatic LNs. Correlations were analyzed using non-parametric Spearman's test. (IM): invasive margin, (CT): center of tumor, (PT): peritumoral region.

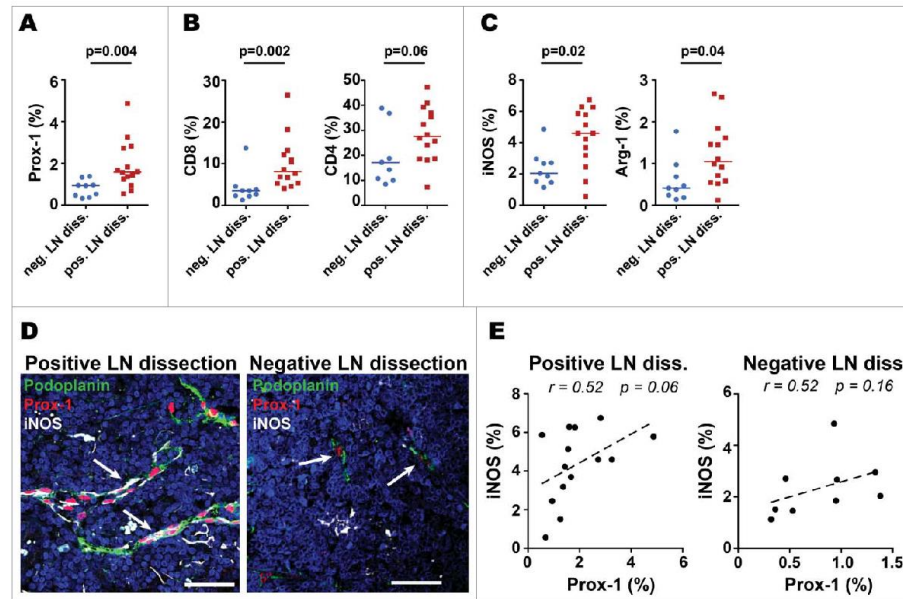


Figure 6. Tumor-free LNs that are adjacent to metastatic LNs have higher LVD, T cell infiltration and immune suppressive molecules than LNs from completely tumor-free LN-regions. Tumor-free LNs from negative LN dissections (neg. LN diss.; $n = 9$) were compared with tumor-free LNs from positive LN dissections (pos. LN diss.; $n = 14$). Density of A) lymphatic vessels, B) T cells and C) the immune suppressive molecules iNOS and Arg-1 (% of pixel positive cells). Line indicate median; data were analyzed with the unpaired t-test for normally distributed data sets and with a nonparametric unpaired Mann-Whitney U test for data sets that were not normally distributed. D) Representative immunofluorescence images showing that intratumoral lymphatic vessels (Prox-1, red and podoplanin, green) mainly expressed iNOS (white, arrow) in tumor-free LNs from positive LN dissections. Scale bars = $50\mu\text{m}$, Arrow bar highlighting lymphatic vessel structures. E) Correlations of Prox-1 with iNOS in tumor-free LNs from negative and positive LN dissections (% of pixel positive cells). Correlations were analyzed using non-parametric Spearman's test.

A standard methodology of lymphatic vessel quantification is based on the observation that lymphatics form areas of increased LVD density.⁴⁵ The majority of studies on LVD and clinical outcome of melanoma patients have used staining quantification methods based on visual inspection and selection

of “hot spots” (e.g. Weidner and Chalkley method).^{32,46,47} Despite the recent emergence of computer-assisted image analysis that reduces the variability and subjectivity in quantifying lymphatics, many studies are still based on either selected “hot spot” regions or randomly selected fields.^{16,43} We analyzed

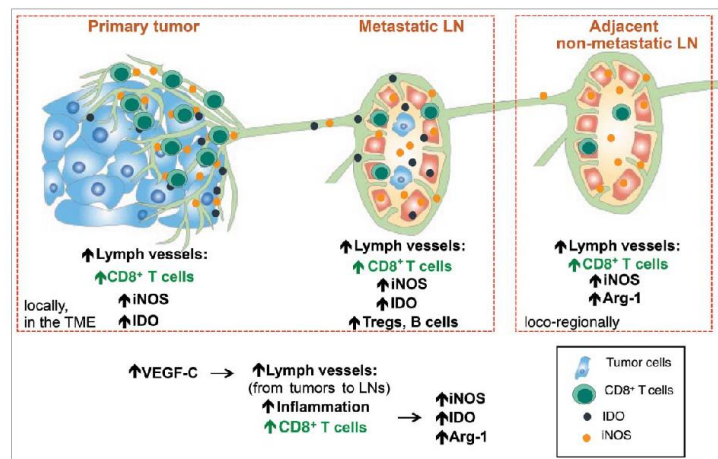


Figure 7. Increased lymphatic vessels density is associated with increased CD8⁺ T cell infiltration, together with increased expression of immunosuppressive molecules such as iNOS, IDO and Arg-1. This can be observed not only locally in primary tumors and metastatic lymph nodes (LNs) but also in adjacent non-metastatic LNs. Together, tumor derived VEGF-C induces lymphatic vessels that attract CD8⁺ T cells, with their known fundamental properties, namely the promotion of anti-tumor immune responses but also immune suppression (via adaptive immune resistance mechanisms).

specific regions as well as entire sections of different melanoma-associated tissues with a dedicated image analysis software, allowing quantitative assessment of unusually large tissue areas in a reproducible manner. Specifically, we used the pixel count algorithm (ImageScope™, Aperio) for large-scale quantification of lymphatics, lymphocytes and immune suppressive molecules. Pixel-based analysis has been validated as an accurate strategy for the assessment of cell density in tissue sections,⁴⁸ and may be more precise than cell-counting algorithms, especially in the setting of dense and relatively homogenous cell populations such as within the tumor mass.

In agreement with our findings, increased LVD has been described in and around primary melanomas compared to melanocytic nevi and normal dermis.³²⁻³⁴ We did not find statistically significant differences between intra- (either center of tumor or invasive margin) or peri-tumoral LVD as described by some^{46,49,50} but not other studies.^{43,51} Possible reasons for discrepancies could be the use of different image analysis and/or staining quantification strategies.

Many reports established the role of VEGF-C in promoting lymphangiogenesis and LN metastases in murine and human tumors.⁵² Nonetheless, VEGF-C expression did not always correlate with LVD in cutaneous melanoma.⁴⁶ Surprisingly, we found that VEGF-C correlated with LVD only in the earliest stage of primary melanoma. This suggests that VEGF-C mainly promotes lymphangiogenesis early in the development of the tumor.

Recently it was shown that tumor-associated lymphangiogenesis mediated intratumoral T cell infiltration in mice.²⁹ Our findings indicate that similar mechanisms are in place in humans, because LVD strongly correlated with CD8⁺ T cell infiltration in primary cutaneous melanoma as well as in metastases of draining LNs. Interestingly, these associations were found in the three different zones delimited in the primary tumor sections, implying that lymphatic activation may promote accumulation of CD8⁺ T cells not only around but also within the tumor mass.

Besides LECs, tertiary lymphoid structures (TLSs) are important components of tumor-associated immune functions. TLS are of increasing interest in tumor immunology because they are often associated with anti-tumor T cell responses and favorable prognosis of cancer patients.⁵³ Although high endothelial venules (HEVs) have been described in primary melanoma and have been linked to good clinical outcome,^{54,55} conflicting results exist in regard to the presence of TLSs in primary melanoma, in spite of the fact that the latter frequently contain HEVs.^{56,57} While we found a positive association between lymphatics and CD19⁺ cells in metastatic LNs, we did not detect many B cell clusters in the tumor samples examined here. The increased infiltration of B cells in association with lymphatic vessels in metastatic LNs may support the notion that lymphatics promote also the humoral immune response. Further investigations are required to elucidate the interactions between lymphatics and B cells, and their roles in cancer patients.

LECs can affect T cell fate as well as suppress dendritic cell-mediated T cell activation by secreting a variety of immune suppressive factors such as TGF- β , IDO and iNOS.⁵⁸ Kornek et al. reported that *in vitro*-expanded murine LECs mediated direct suppression of T cell proliferation, essentially depending on IFN- γ from activated T cells.⁵⁹ Nörder et al. demonstrated that human *in vitro* IFN- γ activated LECs produced IDO which

suppressed T cell activation.⁶⁰ Compatible with these *in vitro* studies, we observed significant associations between LVD and iNOS expression at the invasive margin and IDO expression in the center of tumor of primary melanomas, but also found significant correlations with CD8⁺ T cell infiltration.

In concert with primary tumors, our study identifies immune suppressive molecules in tumor-draining LNs, suggesting that immune mechanisms operating in metastatic LNs^{25,37,61,62} may at least in part be similar to those in primary tumors.⁶³ In contrast to primary tumors, we found a significant correlation between LECs and FoxP3⁺ lymphocytes. The question of whether regulatory T cells play an important role in melanoma progression and metastasis formation is still unanswered, and conflicting data have been reported with regard to clinical impact.⁶⁴

Several studies have identified alterations in both local and regional immune functions of metastatic LNs that may contribute to tumor expansion and metastasis formation.³⁷ However, only limited data exist showing possible effects of nearby metastases on immune functions of tumor-free LNs. Zuckerman et al. examined differences in immune cell signatures between tumor-free LNs of node negative breast cancer patients and tumor-invaded sentinel lymph nodes (SLNs), tumor-free SLNs or tumor-free non-sentinel lymph nodes (NSLNs) of node positive breast cancer patients.⁶⁵ This study provided the first evidence of altered immune regulation depending on whether neighboring LNs were metastatic or not. We investigated the immunological differences between tumor-free LNs from patients with positive versus negative LN dissections. Our data show that the tumor-free LNs from tumor-positive LN dissections had higher densities of LECs, T lymphocytes, iNOS and Arg-1, as compared to those from negative LN dissections, arguing that lymphatics may impact on immune regulation beyond the TME and prior to metastasis formation.

Together, we describe novel associations between LECs, lymphocytes and immune suppressive molecules within different tissues of melanoma patients. LECs were positively associated with locally enhanced CD8⁺ T cell infiltration as well as iNOS and IDO expression within primary melanoma tissues and in metastatic LNs. Tumor-free LNs showed similar associations, pointing to loco-regional effects. These results support the view that LECs are active modulators of anti-tumor immune responses within different human melanoma tissues. Our results should be validated in larger numbers of patients. Furthermore, as our study could only reveal correlations, further studies will be needed to refine the underlying mechanisms, e.g. by *ex-vivo* functional analysis combined with systems biology approaches and mechanistic mouse studies.

A major aim in the development of cancer immunotherapies is to overcome suppression of anti-tumor T cell responses. Our study suggests that LECs are implicated in the recruitment and attraction of CD8⁺ T cells as well as the expression of immune suppressive molecules. Therefore, LECs likely support both, promote and hinder anti-tumor T cell responses. Of note, the presence of a T cell-inflamed tumor microenvironment is indicative of an endogenous adaptive immune response against a given tumor, and is emerging as a useful predictive biomarker for response to immunotherapy.⁶⁶ Indeed, it was recently shown that highly infiltrated and lymphangiogenic murine tumors were more sensitive to immunotherapy, by recruiting T cells and antigen presenting cells through the

CCL21-CCR7 axis. Furthermore, serum VEGF-C was found to correlate with antitumor T cell responses and progression free survival of melanoma patients treated with immunotherapy.⁶⁷ Finally, therapeutic induction of lymphoid structures synergized with immunotherapy in mice.⁶⁸ Thus, novel combination immunotherapies may include the promotion of lymphatics despite that they are also implied in immune suppressive mechanisms and metastatic spread. Future therapy improvements may depend on the successful increase of the beneficial roles of lymphatics with simultaneous reduction of their negative effects.

Patients and methods

Patients

This study investigated 29 metastatic melanoma patients that had been included in a phase I vaccination trial (LUD 00-018 study, ClinicalTrials.gov Identifier NCT00112229) at the Ludwig Cancer Research Center (LICR, University Hospital, Lausanne, Switzerland) between 2003 and 2011 (Table S1), as described previously.^{69,70} Briefly, 29 HLA-A2⁺ patients with histologically proven metastatic melanoma of the skin expressing Melan-A/MART-1 received 1–4 cycles of monthly subcutaneous vaccinations with 100 μ g Melan-A/MART-1 A27L analog or native peptide (\pm a Tyrosinase peptide) and CpG-7909 (500 μ g PF-3512676/7909; provided by Pfizer/Coley Pharmaceutical Group) emulsified in incomplete Freund's adjuvant (300–600 μ l Montanide ISA-51; provided by Seppic). The patients were evaluated for treatment toxicity, immune response (CD8⁺ T cell response), tumor response and survival (Table S2). Of the 29 patients included in the study, 25 were selected for the present analysis and 4 were excluded (one patient had uveal melanoma and three patients did not have any FFPE tissues available). 19 primary melanoma samples from 15 patients, 33 metastatic LNs from 14 patients (23 metastatic LNs were taken before the vaccination and 10 metastatic LNs were taken long after the end of the vaccination trial) and 23 tumor-free LNs from 20 patients (17 tumor-free LNs were taken before the vaccination and 6 tumor-free LNs were taken long after the end of the vaccination trial) were obtained and were analyzed for their lymphocyte populations, lymphatic vessels and immunosuppressive molecules. 14 tumor-free LNs from 12 patients were from tumor-positive LN dissection and 9 tumor-free LNs from 8 patients were from tumor-negative LN dissection. The study was approved by the Ethics Committee of Canton of Vaud and the regulatory authorities, and conducted in compliance with all legal and regulatory requirements.

Immunohistochemistry (IHC)

Chromogenic IHC staining

4- μ m tick tissue sections of patient's formalin-fixed paraffin-embedded (FFPE) tissue specimen's were first deparaffinized in xylene and rehydrated by sequential incubation in EtOH/water solutions. Tissues were then treated with 3% H₂O₂ in distilled water for 5 minutes to quench endogenous peroxidase activity. Heat-induced antigen retrieval was performed in Tris-EDTA buffer (pH 9) for 1'30" in a steamer. Subsequently, sections were incubated at room temperature

with primary antibodies to CD8 (clone C8/144b, Dako, 1:30, 32 min), CD4 (clone 4B12, Novocastra, 1:10, 90 minutes), CD19 (clone BT51E, Novocastra, 1:50, 32 min), FoxP3 (clone 236a/E7, Abcam, 1:50, 60 min), podoplanin (clone D2-40, Covance, 1/400, 60 min), Prox-1 (R&D, 1:100, 32 min), VEGF-C (Invitrogen, 1:20, 40 min), IDO (from Brussels, 1:500, 40 min), iNOS (Thermoscientific, 1:75, 40 min), Arg-1 (Mybiosource, 1:300, 40 min), Melan-A (clone A103, Dako, 1:50, 32 min), melanosome (clone HMB45, Dako, 1:50, 32 min) and S100 (Novocastra, 1:800, 40 min) followed by a secondary anti-mouse (K4001, Dako), anti-rabbit (DK4003, Dako) or anti-goat antibody (Histofine RTU-Biosciences) RTU/HRP ENVISION for 30 minutes. 3-amino-9 ethylcarbazole (AEC) was used as a red chromogen (K3464, Dako) for CD4, S100, Melan-A and melanosome and Diaminobenzidine (DAB, K3468, Dako) as a brown chromogen (K3468, Dako) for the rest of the antibodies. After rinsing with water, sections were counterstained with Hematoxylin Gill II (Merck 1.05175) and coverslipped with xylol. CD8, CD4, CD19, FoxP3, podoplanin, Prox-1, Melan-A, S100 and Melanosome were done on Ventana BenchMark machine using Cell Conditioning 1 (CC1, 950-124, Ventana) as a buffer for heat-induced antigen retrieval with varied time for the different antibodies, other reagent and time was done as described above. iNOS, VEGF-C, Arg-1 and IDO stainings were done manually by the technician with the above-mentioned protocol. Positive controls included tonsil, lung, liver and colon. Immunostainings with appropriate isotype control antibodies were used as negative controls. For illustration purpose, representative images of the different stainings were taken from tumor-free LNs (Fig. S5).

Conventional immunofluorescence (IF) staining

As for chromogenic IHC staining, 4- μ m tick tissue sections were first deparaffinized in xylene and rehydrated by sequential incubation in EtOH/water solutions. Antigen retrieval was performed by 15 minute incubation in boiling Tris-EDTA buffer (pH 9), following 30 minutes incubation in blocking solution (TBS+0.01% Triton X-100+2%BSA+2%total serum from host secondary antibody). Sections were incubated overnight at 4°C with primary antibodies to CD8 (clone C8/144b, Dako, 1:30), podoplanin (clone D2-40, Covance, 1/200), Prox-1 (R&D, 1:100), iNOS (Thermoscientific, 1:75), Arg-1 (Mybiosource, 1:300), IDO (from Brussels, 1:500), CCL21 (Atlas antibodies, 1:200) and PD-L1 (Cell Signaling, 1:200). Alexa Fluor 488-labeled donkey anti-mouse IgG (Invitrogen, 1:400), 568-labeled donkey anti-goat IgG (Invitrogen, 1:600) and 647-labeled donkey anti-rabbit IgG (Invitrogen, 1:800) antibodies were used as secondary antibodies and incubated for 1 hour at room temperature. After stringent washes, sections were counterstained with DAPI (Vector Laboratories, Burlingame, CA) for 5 minutes and coverslipped with mounting medium (Vectashield mounting media). Positive controls were done on tonsils, LNs and skin tissues. Negative slides used TBS instead of primary antibody, with other conditions constant. Images were obtained with confocal microscope ZEISS LSM 700 UPRIGHT.

Image analysis

In primary melanoma, four relevant histological regions were defined: invasive margin (IM, defined as a tumor region of about 400- μm width between the tumor and the reticular dermis), center of tumor (CT), peritumoral region (PT, defined as a region of about 400- μm width in the dermis surrounding the invasive margin), and normal skin (NS, determined as a region of about 200- μm width separated by at least 1mm from tumor cells), as illustrated in Fig. S6A. IM, CT and PT were present in 13 sections of the 19 primary melanoma selected and analyzed (Table S3). The other 6 primary melanoma samples, the tumor mass were too small or confined in the epidermis such that these three zones could not be defined. Normal skin was identified in 12 primary tumor samples. We also selected 14 sections from 10 melanoma patients where tumor cells were still confined in the epidermis and have not grown deeper. Those are referred to as melanoma *in situ* (Table S3). Tumor cells were identified based on Melan-A, Melanosome (HMB45) and S100 positive staining or morphological criteria (large atypical and pleomorphic cells with abundant eosinophilic cytoplasm, visible nucleoli and mitosis) when all three markers were negative.

For the analysis of LN metastases, we pre-selected 33 metastatic LNs from 14 melanoma patients. 10 metastatic LNs were excluded from the analysis because of the presence of large regions of tumor necrosis (2/10), presence of excessive melanin pigments rendering analysis impossible (5/10), tumor metastasis size less than 1 mm² (1/10) or tumor metastasis size more than 98% of the entire LN (2/10). In the 23 remaining metastatic LNs, we defined 2 different zones corresponding to center of tumor and stroma (Fig. S6B). The center of tumor was determined as previously described for primary tumors. Stroma was defined as connective tissue surrounding the tumor cells (present in 14 (61%) metastatic LNs). Finally, we also studied tumor-free LNs that had been obtained through LN dissection surgery. We analyzed the total area without defining specific zones in these 23 tumor-free LNs (Table S4). Image analyses and determination of regions were approved by two blinded experienced pathologists.

Staining quantification

ImageScopeTM Aperio software

Whole slide digital images were obtained for each specimen stained with Chromogenic IHC staining using NanoZoomer 2-HT digital slide scanner (Hamamatsu). The resulting high-resolution digital images were analyzed with the ImageScopeTM software, version 12.1 (Aperio Technologies, Vista, CA, USA), using the pixel positive cell algorithm 9.1 as previously described and validated.⁴⁸ Briefly, this algorithm detects pixels that match input parameters set for the algorithm and generates four output values based on the pixel's color range: haematoxylin or negative signal (blue in mark-up image), weak positive (yellow in mark-up image), positive (orange in mark-up image) and strong positive

(brown in mark-up image) (Fig. S7). Using these parameters, the strong non-specific (brown) as well as the weak positive (yellow) signals were considered as debris background staining, whereas the positive value (orange) was considered as specific. Folds, debris, holes were also removed manually to be excluded from the staining quantification analysis. Quantification of the staining in the tissue selected was reported as a relative abundance ratio, which was based on the number of positive pixels (orange) divided by the total number of pixels (blue + yellow + orange + brown). The relative abundance ratio was reported in % and represented the percentage of density per tissue area for the quantified staining. Results obtained were controlled to match with visual inspection. The pixel positive cell algorithm was applied on primary tumors, tumor-free LNs and metastatic LNs.

Quantification of LECs

LECs are typically identified by expression of the nuclear transcription factor Prox-1 and the surface markers podoplanin and Lyve-1. However, depending on their tissue location and state of development, LEC expression of these markers can be variable, and furthermore, other cell types within the tumor microenvironment can also express these markers.^{45,71} Some tumor-associated macrophages express Lyve-1, and cancer-associated fibroblasts found in the stroma can express podoplanin. As expected, in our tissue sections, LECs expressed podoplanin and nuclear Prox-1 in all tissues analyzed, but these markers were also found in other types of cells depending on the region evaluated (see result section and Fig. S1). Consequently, when comparing expression in the same tissue sections, Prox-1 and podoplanin did not necessarily correlate in the tumor regions (i.e. center of tumor and invasive margin) (Fig. S8). Indeed, we noticed a positive trend in peritumoral area and a positive correlation in normal skin, underlining that the expression of Prox-1 was not a reliable marker of intratumoral LECs. For validation of our quantification strategy and the identification of lymphatic vessels, we counted the lymphatic vessels by eye in the different regions of primary tumors, in the tumor area of metastatic LNs and in the entire section of non-metastatic LNs by combining IHC markers (i.e. podoplanin or Prox-1) with vessel morphology. The counting by eye was done in the same regions as the automated image analysis, covering the whole areas. The number of lymphatic vessels per area was then divided by the total surface area, resulting in lymphatic vessels per mm² for each region.

Identification of LECs may be improved by simultaneously using multiple markers which can be achieved with multiplex IF techniques. However, good quality stainings and analysis of wide areas and whole tissue sections is difficult (staining must be homogenous) and was not possible at the time when this work was done. Therefore, we used single marker LEC identification using IHC, allowing large-scale assessment and quantification. In addition, we used IF images for illustration purpose and for in-depth analysis of correlations found in IHC.

Statistics

To compare only two data sets, unpaired t- tests (normal distribution of data points) or Mann–Whitney U tests (data points not normally distributed) were used to assess statistical significance. To visualize correlations of two different markers, raw data received from the pixel positive cell algorithm (ImageScope™, see Image Analysis) were plotted and a line with linear regression was fitted into the plot. Correlation coefficients were calculated using Spearman's non-parametric test. To compare multiple groups, One-Way Kruskal-Wallis non-parametric tests were applied with post-hoc test Dunn correction. A two-tailed *p* value of ≤ 0.05 was considered to be significant. Analyses were performed with Prism (version 6.0b, GraphPad Software, La Jolla, CA, USA). Statistics were approved by a certified statistician.

Grant support

This research was supported by the ISREC Foundation (Switzerland), the Cancer Research Institute (USA), Ludwig Cancer Research (USA), the Swiss Cancer League (3507-08-2014 and 3312-08-2013), the Swiss National Science Foundation (CRSII3_160708 and 320030-152856), SwissTransMed (KIP 18) and the Rector's Conference of the Swiss Universities (crus.ch), Alfred and Annemarie von Sick, the Wilhelm Sander Foundation, the European Research Council (AdG-323053), the Gabriela and Theodor Kummer Foundation (Switzerland), the Erna Hamburger Foundation (Switzerland) and the Société Académique Vaudoise (Switzerland).

Disclosure of potential conflicts of interest

No potential conflicts of interest were disclosed.






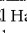
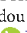



Acknowledgments

We are obliged to the patients for their dedicated collaboration. The authors gratefully acknowledge Susana Leubat, Véronique Noguét, Solange Gros and Isabelle Surchet for tissue processing and staining, Pascale Anderle for statistical advice, Alain Michel for slide scanning and the Pathology Departments of the Universities of Geneva, Neuchâtel, Sion, and Basel as well as Meditest, Promed and Synlabs for providing tissues. We also thank Bianca Martins-Moura, Angela Orcurto, Christine Geldhof, Paula Marcos Mondéjar, Loredana Leyvraz, Lana Kandalaf, Kim Ellefsen, Lionel Trueb, Pierre Combe, Sylvie Rusakiewicz, Amanda Lund, Daniel Hohl, Olivier Gaide, Laurence Feldmeyer, Krisztian Homicsko, Doug Hanahan and George Coukos for collaboration, support and expert advice, and thank Benoit Van den Eynde and Luc Pilotte for providing the IDO antibody.

Authors' contributions

Conception and design: N.B., M.A.B., M.M., M.A.S., D.E.S.
 Development of methodology: N.B., M.A.B., P.O.G., M.A.S., D.E.S.
 Acquisition of data: N.B., M.A.B., K.D.J., E.D., P.B., L.C., S.A.M., H.M.E.H., E.R.
 Analysis and interpretation of data: N.B., M.A.B., K.D.J., K.S., P.O.G., E.D., P.G.F., P.B., L.C., S.A.M., H.M.E.H., E.R., M.A.S., D.E.S.
 Writing, review and revision of manuscript: N.B., M.A.B., K.S., P.O.G., M.F., N.W., T.M., K.I., M.M., M.A.S., D.E.S.
 Technical and material support: L.L., P.Y., E.D., P.G.F., P.B., O.M., E.R.
 Study supervision: M.A.S., D.E.S.

ORCID

Natacha Bordry  <http://orcid.org/0000-0002-3523-438X>
 Maria A. S. Broggi  <http://orcid.org/0000-0001-7909-5097>
 Kaat de Jonge  <http://orcid.org/0000-0003-2306-5555>
 Manuel Fankhauser  <http://orcid.org/0000-0001-7714-6524>
 Samia Abed-Maillard  <http://orcid.org/0000-0003-4773-8072>
 Hélène Maby-El Hajjami  <http://orcid.org/0000-0002-5786-5991>
 Kalliopi Ioannidou  <http://orcid.org/0000-0001-9097-4199>
 Igor Letovanec  <http://orcid.org/0000-0002-0410-3491>
 Maurice Matter  <http://orcid.org/0000-0003-1816-3003>
 Daniel E. Speiser  <http://orcid.org/0000-0003-2031-3250>

References

1. Farkona S, Diamandis EP, Blasutig IM. Cancer immunotherapy: the beginning of the end of cancer? *BMC Med.* 2016;14:73. doi:10.1186/s12916-016-0623-5. PMID:27151159.
2. Sharma P, Allison JP. Immune checkpoint targeting in cancer therapy: toward combination strategies with curative potential. *Cell.* 2015;161:205–14. doi:10.1016/j.cell.2015.03.030. PMID:25860605.
3. Maus MV, Fraietta JA, Levine BL, Kalos M, Zhao Y, June CH. Adoptive immunotherapy for cancer or viruses. *Annu Rev Immunol.* 2014;32:189–225. doi:10.1146/annurev-immunol-032713-120136. PMID:24423116.
4. Peggs KS, Quezada SA, Allison JP. Cancer immunotherapy: Costimulatory agonists and co-inhibitory antagonists. *Clin Exp Immunol.* 2009;157:9–19. doi:10.1111/j.1365-2249.2009.03912.x. PMID:19659765.
5. Hamid O, Robert C, Daud A, Hodi FS, Hwu W-J, Kefford R, Wolchok JD, Hersey P, Joseph RW, Weber JS, et al. Safety and Tumor Responses with LAMBROLIZUMAB (Anti-PD-1) in Melanoma. *N Engl J Med.* 2013;369:134–44. doi:10.1056/NEJMoa1305133. PMID:23724846.
6. Inoue H, Park J-H, Kiyotani K, Zewde M, Miyashita A, Jinnin M, Kuniwa Y, Okuyama R, Tanaka R, Fujisawa Y, et al. Intratumoral expression levels of PD-L1, GZMA, and HLA-A along with oligoclonal T cell expansion associate with response to nivolumab in metastatic melanoma. *oncoimmunology.* 2016;5:1–7. doi:10.1080/2162402X.2016.1204507.
7. Ulloa-Montoya F, Louahed J, Dizier B, Bruselle O, Spiessens B, Lehmann FF, Suci S, Kruit WHJ, Eggermont AMM, Vansteenkiste J, et al. Predictive Gene Signature in MAGE-A3 Antigen-Specific Cancer Immunotherapy. *J Clin Oncol.* 2013;31:2388–95. doi:10.1200/JCO.2012.44.3762. PMID:23715562.
8. Spranger S, Spaepen RM, Zha Y, Williams J, Meng Y, Ha TT, Gajewski TF. Up-Regulation of PD-L1, IDO, and Tregs in the Melanoma Tumor Microenvironment Is Driven by CD8+ T Cells. *Sci Transl Med.* 2013;5:200ra116–6. doi:10.1126/scitranslmed.3006504. PMID:23986400.
9. Liu C, Peng W, Xu C, Lou Y, Zhang M, Wargo JA, Chen J, Li HS, Watowich S, Yang Y, et al. BRAF Inhibition Increases Tumor Infiltration by T cells and Enhances the Anti-tumor Activity of Adoptive Immunotherapy in Mice. *Clin Cancer Res.* 2013 Jan 15;19(2):393–403. doi:10.1158/1078-0432.CCR-12-1626.
10. Taube JM, Anders RA, Young GD, Xu H, Sharma R, McMiller TL, Chen S, Klein AP, Pardoll DM, Topalian SL, et al. Colocalization of Inflammatory Response with B7-H1 Expression in Human Melanocytic Lesions Supports an Adaptive Resistance Mechanism of Immune Escape. *Sci Transl Med.* 2012;4:127ra37–7. doi:10.1126/scitranslmed.3003689. PMID:22461641.
11. Ribas A. Adaptive Immune Resistance: How Cancer Protects from Immune Attack. *Cancer Discov.* 2015;5:915–9. doi:10.1158/2159-8290.CD-15-0563. PMID:26272491.
12. Spranger S, Gajewski TF. Impact of oncogenic pathways on evasion of antitumor immune responses. *Nat Rev Cancer.* 2018;1–9. PMID:29217839.
13. Netzer R, Fleishman SJ. Inspired by nature. *Science* 2016;352:657–8. doi:10.1126/science.aaf7599. PMID:27151851.
14. Skobe M, Hawighorst T, Jackson DG, Prevo R, Janes L, Velasco P, Ricciardi L, Alitalo K, Claffey K, Detmar M. Induction of tumor

- lymphangiogenesis by VEGF-C promotes breast cancer metastasis. *Nat Med.* 2001;7:192–8. doi:10.1038/84643. PMID:11175850.
15. Stacker SA, Caesar C, Baldwin ME, Thornton GE, Williams RA, Prevo R, Jackson DG, Nishikawa S, Kubo H, Achen MG. VEGF-D promotes the metastatic spread of tumor cells via the lymphatics. *Nat Med.* 2001;7:186–91. doi:10.1038/84635. PMID:11175849.
 16. Dadras SS, Paul T, Bertocini J, Brown LF, Muzikansky A, Jackson DG, Ellwanger U, Garbe C, Mihm MC, Detmar M. Tumor lymphangiogenesis: A novel prognostic indicator for cutaneous melanoma metastasis and survival. *Am J Pathol.* 2003;162:1951–60. doi:10.1016/S0002-9440(10)64328-3. PMID:12759251.
 17. Schietroma C, Cianfarani F, Lacal PM, Odorasio T, Orecchia A, Kani-takis J, D'Atri S, Failla CM, Zambruno G. Vascular endothelial growth factor-C expression correlates with lymph node localization of human melanoma metastases. *Cancer.* 2003 Aug 15;98(4):789–97. doi:10.1002/cncr.11583.
 18. Mandriota SJ. Vascular endothelial growth factor-C-mediated lymphangiogenesis promotes tumour metastasis. *EMBO J.* 2001;20:672–82. doi:10.1093/emboj/20.4.672. PMID:11179212.
 19. Rinderknecht M, Detmar M. Tumor lymphangiogenesis and melanoma metastasis. *J Cell Physiol.* 2008;216:347–54. doi:10.1002/jcp.21494. PMID:18481261.
 20. Christiansen A, Detmar M. Lymphangiogenesis and Cancer. *Genes Cancer.* 2011 Dec;2(12):1146–58. doi:10.1177/1947601911423028.
 21. Issa A, Le TX, Shoushtari AN, Shields JD, Swartz MA. Vascular endothelial growth factor-C and C-C chemokine receptor 7 in tumor cell-lymphatic cross-talk promote invasive phenotype. *Cancer Res.* 2009;69:349–57. doi:10.1158/0008-5472.CAN-08-1875. PMID:19118020.
 22. Shields JD, Fleury ME, Yong C, Tomei AA, Randolph GJ, Swartz MA. Autologous chemotaxis as a mechanism of tumor cell homing to lymphatics via interstitial flow and autocrine CCR7 signaling. *Cancer Cell.* 2007;11:526–38. doi:10.1016/j.ccr.2007.04.020. PMID:17560334.
 23. Shields JD, Emmett MS, Dunn DBA, Joory KD, Sage LM, Rigby H, Mortimer PS, Orlando A, Levick JR, Bates DO. Chemokine-mediated migration of melanoma cells towards lymphatics—a mechanism contributing to metastasis. *Oncogene.* 2007;26:2997–3005. doi:10.1038/sj.onc.1210114. PMID:17130836.
 24. Shields JD, Kourtis IC, Tomei AA, Roberts JM, Swartz MA. Induction of lymphoidlike stroma and immune escape by tumors that express the chemokine CCL21. *Science.* 2010;328:749–52. doi:10.1126/science.1185837. PMID:20339029.
 25. Lund AW, Durues FV, Hirose S, Raghavan VR, Nembrini C, Thomas SN, Issa A, Hugues S, Swartz MA. VEGF-C promotes immune tolerance in B16 melanomas and cross-presentation of tumor antigen by lymph node lymphatics. *Cell Rep.* 2012;1:191–9. doi:10.1016/j.celrep.2012.01.005. PMID:22832193.
 26. Hirose S, Vokali E, Raghavan VR, Rincon-Restrepo M, Lund AW, Corthésy-Henrioud P, Capotosti F, Halin Winter C, Hugues S, Swartz MA. Steady-state antigen scavenging, cross-presentation, and CD8+ T cell priming: A new role for lymphatic endothelial cells. *J Immunol.* 2014;192:5002–11. doi:10.4049/jimmunol.1302492. PMID:24795456.
 27. Podgrabinska S, Kamalu O, Mayer L, Shimaoka M, Snoeck H, Randolph GJ, Skobe M. Inflamed lymphatic endothelium suppresses dendritic cell maturation and function via Mac-1/ICAM-1-dependent mechanism. *J Immunol.* 2009;183:1767–79. doi:10.4049/jimmunol.0802167. PMID:19587009.
 28. Swartz MA, Lund AW. Lymphatic and interstitial flow in the tumour microenvironment: linking mechanobiology with immunity. *Nat Rev Cancer.* 2012 Feb 24;12(3):210–9. doi:10.1038/nrc3186.
 29. Lund AW, Wagner M, Fankhauser M, Steinskog ES, Broggi MA, Spranger S, Gajewski TF, Alitalo K, Eikesdal HP, Wiig H, et al. Lymphatic vessels regulate immune microenvironments in human and murine melanoma. *J Clin Invest.* 2016;126:3389–402. doi:10.1172/JCI79434. PMID:27525437.
 30. Pastushenko I, Conejero C, Carapeto FJ. Lymphangiogenesis: Implications for Diagnosis, Treatment, and Prognosis in Patients With Melanoma. *Actas Dermo-Sifiligráficas (English Edition).* 2015;106:7–16. doi:10.1016/j.adengl.2014.11.001.
 31. Dadras SS, Lange-Asschenfeldt B, Velasco P, Nguyen L, Vora A, Muzikansky A, Jahnke K, Hauschild A, Hirakawa S, Mihm MC, et al. Tumor lymphangiogenesis predicts melanoma metastasis to sentinel lymph nodes. *Mod Pathol.* 2005;18:1232–42. doi:10.1038/modpathol.3800410. PMID:15803182.
 32. Giordagze TA, Zhang PJ, Pasha T, Coogan PS, Acs G, Elder DE, Xu X. Lymphatic vessel density is significantly increased in melanoma. *J Cutan Pathol.* 2004;31:672–7. doi:10.1111/j.0303-6987.2004.00249.x. PMID:15491327.
 33. Shields JD, Borsetti M, Rigby H, Harper SJ, Mortimer PS, Levick JR, Orlando A, Bates DO. Lymphatic density and metastatic spread in human malignant melanoma. *Br J Cancer.* 2004;90:693–700. doi:10.1038/sj.bjc.6601571. PMID:14760386.
 34. Massi D, De Nisi MC, Franchi A, Mourmouras V, Baroni G, Panoles J, Santucci M, Miracco C. Inducible nitric oxide synthase expression in melanoma: implications in lymphangiogenesis. *Mod Pathol.* 2009;22:21–30. doi:10.1038/modpathol.2008.128. PMID:18660796.
 35. Hirakawa S, Brown LF, Kodama S, Paavonen K, Alitalo K, Detmar M. VEGF-C-induced lymphangiogenesis in sentinel lymph nodes promotes tumor metastasis to distant sites. *Blood.* 2007;109:1010–7. doi:10.1182/blood-2006-05-021758. PMID:17032920.
 36. Harrell MI, Iritani BM, Ruddell A. Tumor-induced sentinel lymph node lymphangiogenesis and increased lymph flow precede melanoma metastasis. *Am J Pathol.* 2007;170:774–86. doi:10.2353/ajpath.2007.060761. PMID:17255343.
 37. Cochran AJ, Huang R-R, Lee J, Itakura E, Leong SPL, Essner R. Tumour-induced immune modulation of sentinel lymph nodes. *Nat Rev Immunol.* 2006;6:659–70. doi:10.1038/nri1919. PMID:16932751.
 38. Pasquali S, van der Ploeg APT, Mocellin S, Stretch JR, Thompson JF, Scolyer RA. Lymphatic biomarkers in primary melanomas as predictors of regional lymph node metastasis and patient outcomes. *Pigment Cell Melanoma Res.* 2013;26:326–37. doi:10.1111/pcmr.12064. PMID:23298266.
 39. Lund AW, Medler TR, Leachman SA, Coussens LM. Lymphatic Vessels, Inflammation, and Immunity in Skin Cancer. *Cancer Discov.* 2016;6:22–35. doi:10.1158/2159-8290.CD-15-0023. PMID:26552413.
 40. Stacker SA, Williams SP, Karnezis T, Shayan R, Fox SB, Achen MG. Lymphangiogenesis and lymphatic vessel remodelling in cancer. *Nat Rev Cancer.* 2014;14:159–72. doi:10.1038/nrc3677. PMID:24561443.
 41. Boone B, Blokh W, De Bacquer D, Lambert J, Ruiter D, Brochez L. The role of VEGF-C staining in predicting regional metastasis in melanoma. *Virchows Arch.* 2008;453:257–65. doi:10.1007/s00428-008-0641-6. PMID:18679715.
 42. Pastushenko I, Vermeulen PB, Carapeto FJ, Van den Eynden G, Rutten A, Ara M, Dirix LY, Van Laere S. Blood microvessel density, lymphatic microvessel density and lymphatic invasion in predicting melanoma metastases: systematic review and meta-analysis. *Br J Dermatol.* 2014;170:66–77. doi:10.1111/bjd.12688. PMID:24134623.
 43. Massi D. Tumour lymphangiogenesis is a possible predictor of sentinel lymph node status in cutaneous melanoma: a case-control study. *Journal of Clinical Pathology.* 2006;59:166–73. doi:10.1136/jcp.2005.028431. PMID:16443733.
 44. Tewalt EF, Cohen JN, Rouhani SJ, Guidi CJ, Qiao H, Fahl SP, Conaway MR, Bender TP, Tung KS, Vella AT, et al. Lymphatic endothelial cells induce tolerance via PD-L1 and lack of costimulation leading to high-level PD-1 expression on CD8 T cells. *Blood.* 2012 Dec 6;120(24):4772–82. doi:10.1182/blood-2012-04-427013.
 45. Van der Auwera I, Cao Y, Tille JC, Pepper MS, Jackson DG, Fox SB, Harris AL, Dirix LY, Vermeulen PB. First international consensus on the methodology of lymphangiogenesis quantification in solid human tumours. *Br J Cancer.* 2006 Dec 18;95(12):1611–25. doi:10.1038/sj.bjc.6603445.
 46. Straume O, Jackson DG, Akslen LA. Independent prognostic impact of lymphatic vessel density and presence of low-grade lymphangiogenesis in cutaneous melanoma. *Clin Cancer Res.* 2003;9:250–6. PMID:12538477.
 47. Valencak J, Heere-Ress E, Kopp T, Schoppmann SF, Kittler H, Pehamberger H. Selective immunohistochemical staining shows significant prognostic influence of lymphatic and blood vessels in patients with



Simultaneous enumeration of cancer and immune cell types from bulk tumor gene expression data

Julien Racle^{1,2}, Kaat de Jonge³, Petra Baumgaertner³, Daniel E Speiser³, David Gfeller^{1,2*}

¹Ludwig Centre for Cancer Research, Department of Fundamental Oncology, University of Lausanne, Epalinges, Switzerland; ²Swiss Institute of Bioinformatics, Lausanne, Switzerland; ³Department of Fundamental Oncology, Lausanne University Hospital (CHUV), Epalinges, Switzerland

Abstract Immune cells infiltrating tumors can have important impact on tumor progression and response to therapy. We present an efficient algorithm to simultaneously estimate the fraction of cancer and immune cell types from bulk tumor gene expression data. Our method integrates novel gene expression profiles from each major non-malignant cell type found in tumors, renormalization based on cell-type-specific mRNA content, and the ability to consider uncharacterized and possibly highly variable cell types. Feasibility is demonstrated by validation with flow cytometry, immunohistochemistry and single-cell RNA-Seq analyses of human melanoma and colorectal tumor specimens. Altogether, our work not only improves accuracy but also broadens the scope of absolute cell fraction predictions from tumor gene expression data, and provides a unique novel experimental benchmark for immunogenomics analyses in cancer research (<http://epic.gfellerlab.org>).

DOI: <https://doi.org/10.7554/eLife.26476.001>

*For correspondence: david.gfeller@unil.ch

Competing interests: The authors declare that no competing interests exist.

Funding: See page 18

Received: 02 March 2017

Accepted: 10 November 2017

Published: 13 November 2017

Reviewing editor: Alfonso Valencia, Barcelona Supercomputing Center - BSC, Spain

© Copyright Racle et al. This article is distributed under the terms of the [Creative Commons Attribution License](https://creativecommons.org/licenses/by/4.0/), which permits unrestricted use and redistribution provided that the original author and source are credited.

Introduction

Tumors form complex microenvironments composed of various cell types such as cancer, immune, stromal and endothelial cells (Hanahan and Weinberg, 2011; Joyce and Fearon, 2015). Immune cells infiltrating the tumor microenvironment play a major role in shaping tumor progression, response to (immuno-)therapy and patient survival (Fridman et al., 2012). Today, gene expression analysis is widely used to characterize tumors at the molecular level. As a consequence, tumor gene expression profiles from tens of thousands of patients are available across all major tumor types in databases such as Gene Expression Omnibus (GEO [Edgar et al., 2002]) or The Cancer Genome Atlas (TCGA [Hoadley et al., 2014]). Unfortunately, flow cytometry or immunohistochemistry (IHC) measurements to quantify the number of both malignant and tumor-infiltrating immune cells are rarely performed for samples analyzed at the gene expression level. Therefore, to correctly interpret these data in particular from an immuno-oncology point of view (Angelova et al., 2015; Gentles et al., 2015; Hackl et al., 2016; Li et al., 2016; Linsley et al., 2015; Rooney et al., 2015; Şenbabaoğlu et al., 2016; Zheng et al., 2017), reliable and carefully validated bioinformatics tools are required to infer the fraction of cancer and immune cell types from bulk tumor gene expression data.

To this end, diverse bioinformatics methods have been developed. Some aim at estimating tumor purity based on copy number variation (Carter et al., 2012; Li and Li, 2014), or expression data (Ahn et al., 2013; Clarke et al., 2010; Quon et al., 2013; Yoshihara et al., 2013), but do not provide information about the different immune cell types. Others focus on predicting the relative

eLife digest Malignant tumors do not only contain cancer cells. Normal cells from the body also infiltrate tumors. These often include a variety of immune cells that can help detect and kill cancer cells. Many evidences suggest that the proportion of different immune cell types in a tumor can affect tumor growth and which treatments are effective.

Researchers often study tumors by measuring the expression of genes, i.e., which genes are active in tumors. However, the proportion of different cell types in the tumor is often not measured for tumors studied at the gene expression level.

Racle et al. have now demonstrated that a new computer-based tool can accurately detect all the main cell types in a tumor directly from the expression of genes in this tumor. The tool is called “Estimating the Proportion of Immune and Cancer cells” – or EPIC for short. It compares the level of expression of genes in a tumor with a library of the gene expression profiles from specific cell types that can be found in tumors and uses this information to predict how many of each type of cell are present. Experimental measurements of several human tumors confirmed that EPIC’s predictions are accurate.

EPIC is freely available online. Since the active genes in tumors from many patients have already been documented together with clinical data, researchers could use EPIC to investigate whether the cell types in a tumor affect how harmful it is or how well a particular treatment works on it. In the future, this information could help to identify the best treatment for a particular patient and may reveal new genes that cause malignant tumors to develop and grow.

DOI: <https://doi.org/10.7554/eLife.26476.002>

proportions of cell types by fitting reference gene expression profiles from sorted cells (Gong and Szustakowski, 2013; Li et al., 2016; Newman et al., 2015; Qiao et al., 2012) or with the help of gene signatures (Becht et al., 2016; Zhong et al., 2013). These approaches have been recently applied to cancer genomics data to investigate the influence of immune infiltrates on survival or response to therapy (Charoentong et al., 2017; Gentles et al., 2015; Şenbabaoğlu et al., 2016) or predict potential targets for cancer immunotherapy (Angelova et al., 2015; Li et al., 2016). However, none of these methods provides quantitative information about both cancer and non-malignant cell type proportions directly from tumor gene expression profiles. In addition, reference gene expression profiles used in previous studies have been mainly obtained from circulating immune cells sorted from peripheral blood and were generally based on microarrays technology. Finally, several of these approaches have not been experimentally validated in solid tumors from human patients.

Here, we developed a robust approach to simultaneously Estimate the Proportion of Immune and Cancer cells (EPIC) from bulk tumor gene expression data. EPIC is based on a unique collection of RNA-Seq reference gene expression profiles from either circulating immune cells or tumor-infiltrating non-malignant cell types (i.e., immune, stromal and endothelial cells). To account for the high variability of cancer cells across patients and tissue of origin, we implemented in our algorithm the ability to consider uncharacterized, possibly highly variable, cell types. To validate our predictions in human solid tumors, we first analyzed melanoma samples with both flow cytometry and RNA-Seq. We then collected publicly available IHC and single-cell RNA-Seq data of colorectal and melanoma tumors. All three validation datasets showed that very accurate predictions of both cancer and non-malignant cell type proportions could be obtained even in the absence of *a priori* information about cancer cells.

Results

Reference gene expression profiles from circulating and tumor-infiltrating cells

EPIC incorporates reference gene expression profiles from each major immune and other non-malignant cell type to model bulk RNA-Seq data as a superposition of these reference profiles (Figure 1A,B). To tailor our predictions to recent gene expression studies, we first collected and curated RNA-Seq profiles of various human innate and adaptive circulating immune cell types

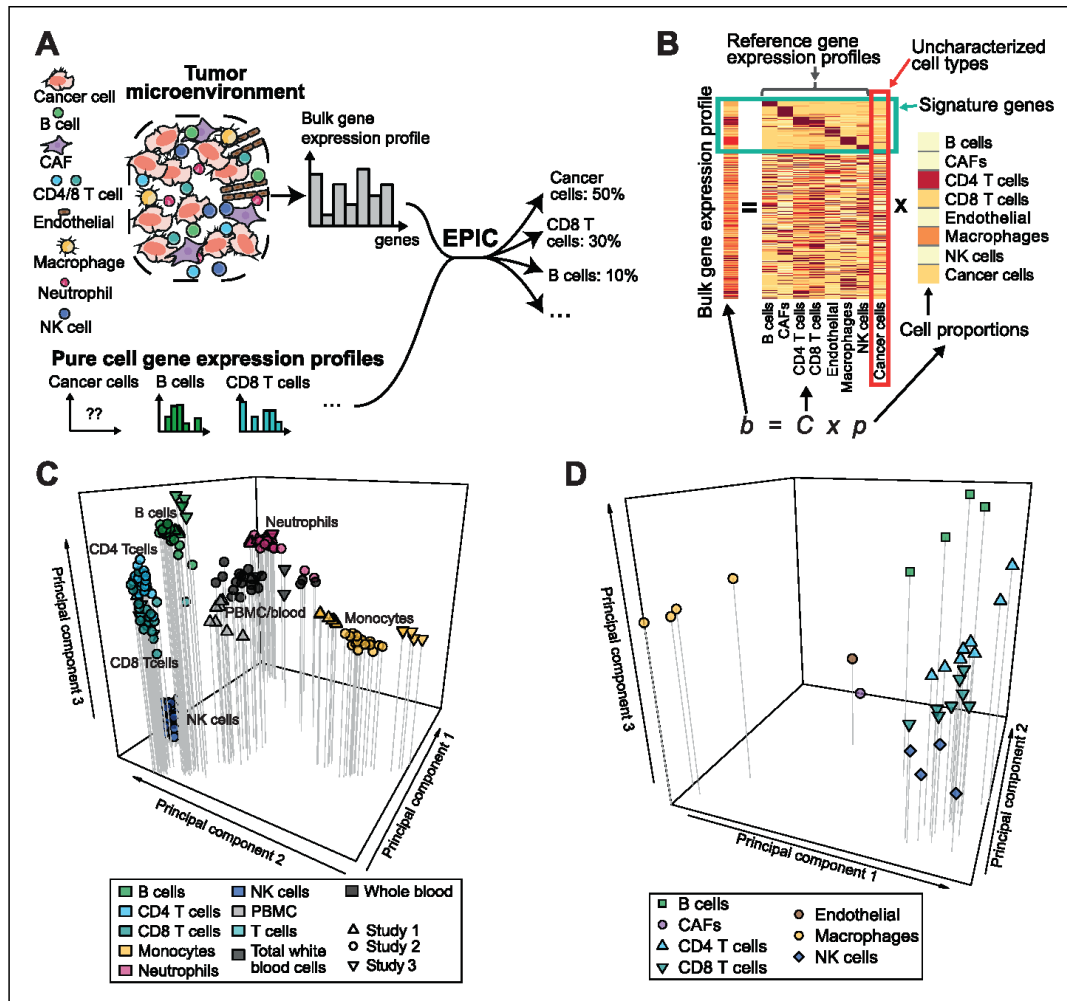


Figure 1. Estimating the proportion of immune and cancer cells. (A) Schematic description of our method. (B) Matrix formulation of our algorithm, including the uncharacterized cell types (red box) with no or very low expression of signature genes (green box). (C) Low dimensionality representation (PCA based on the 1000 most variable genes) of the samples used to build the reference gene expression profiles from circulating immune cells (study 1 [Hoek et al., 2015], study 2 [Linsley et al., 2014], study 3 [Pabst et al., 2016]). (D) Low dimensionality representation (PCA based on the 1000 most variable genes) of the tumor-infiltrating cell gene expression profiles from different patients. Each point corresponds to cell-type average per patient of the single-cell RNA-Seq data of *Tirosh et al. (2016)* (requiring at least 3 cells of a given cell type per patient). Only samples from primary tumors and non-lymphoid tissue metastases were considered. Projection of the original single-cell RNA-Seq data can be found in **Figure 1—figure supplement 1**. DOI: <https://doi.org/10.7554/eLife.26476.003>

The following figure supplements are available for figure 1:

Figure supplement 1. Low dimensionality representation of the tumor-infiltrating cell samples.

DOI: <https://doi.org/10.7554/eLife.26476.004>

Figure supplement 2. Cell type mRNA content.

DOI: <https://doi.org/10.7554/eLife.26476.005>

(Hoek et al., 2015; Linsley et al., 2014; Pabst et al., 2016) (CD4 T cells, CD8 T cells, B cells, NK cells, Monocytes and Neutrophils) from a diverse set of patients analyzed in different centers (see Materials and methods). Principal component analysis (PCA) of these data (Figure 1C) showed that samples clustered first according to cell type and not according to experiment of origin, patient age, disease status or other factors, suggesting that they could be used as *bona fide* reference expression profiles across different patients. Reference gene expression profiles for each major immune cell type were built from these RNA-Seq samples based on the median normalized counts per gene and cell type. The variability in expression for each gene was also considered when predicting the various cell proportions based on these reference profiles (see Materials and methods and Supplementary file 1).

Immune cells differ in their gene expression profiles depending on their state and site of origin (e.g., blood or tumors) (Ganesan et al., 2017; Speiser et al., 2016; Zheng et al., 2017). To study the potential effect of these differences on our predictions, we established reference gene expression profiles of each major tumor-infiltrating immune cell type (i.e., CD4 T, CD8 T, B, NK, macrophages). We further derived reference profiles for stromal cells (i.e. cancer-associated fibroblasts (CAFs)) and endothelial cells. These reference gene expression profiles were obtained as cell type averages from the single-cell RNA-Seq data of melanoma patients from Tirosh and colleagues (Tirosh et al., 2016), considering only samples from primary tumor and non-lymphoid tissue metastasis (see Materials and methods and Supplementary file 2). As for circulating immune cell data, principal component analysis of the tumor-infiltrating cells' gene expression profiles showed that samples clustered first according to cell type (Figure 1D and Figure 1—figure supplement 1, see also results in [Tirosh et al., 2016]).

Cancer and non-malignant cell fraction predictions

Reference gene expression profiles from each of the immune and other non-malignant (i.e., stromal and endothelial) cell types were then used to model bulk gene expression data as a linear combination of m different cell types (Figure 1B). To include cell types like cancer cells that show high variability across patients and tissues of origin, we further implemented in our algorithm the ability to consider an uncharacterized cell population. Mathematically this was done by taking advantage of the presence of gene markers of non-malignant cells that are not expressed in cancer cells. Importantly, we do not require our signature genes to be expressed in exactly one cell type, but only to show very low expression in cancer cells. The mRNA proportion of each immune and other non-malignant cell type was inferred using least-square regression, solving first our system of equations for the marker genes (green box in Figure 1B, see Materials and methods). The fraction of cancer cells was then determined as one minus the fraction of all non-malignant cell types. Cell markers used in this work were determined by differential expression analysis based on our reference cell gene expression profiles as well as gene expression data from non-hematopoietic tissues (see Materials and methods and Appendix 1—table 1). Finally, to account for different amounts of mRNA in different cell types and enable meaningful comparison with flow cytometry and IHC data, we measured the mRNA content of all major immune cell types as well as of cancer cells (Figure 1—figure supplement 2) and used these values to renormalize our predicted mRNA proportions (see Materials and methods).

Validation in blood

We first tested our algorithm using three datasets comprising bulk RNA-Seq data from PBMC (Hoek et al., 2015; Zimmermann et al., 2016) or whole blood (Linsley et al., 2014), as well as the corresponding proportions of immune cell types determined by flow cytometry (Figure 2A). These data were collected from various cancer-free human donors (see Materials and methods). Overall, very accurate predictions were obtained by fitting reference profiles from circulating immune cells, considering either all cell types together (Figure 2A) or each cell type separately (Figure 2—figure supplement 1). When comparing with other widely used cell fraction prediction methods (Becht et al., 2016; Gong and Szustakowski, 2013; Li et al., 2016; Newman et al., 2015; Quon et al., 2013; Zhong et al., 2013), we observed a clear improvement (Figure 2B and Figure 2—figure supplement 1). Of note, the very high correlation values can partly result from the broad range of different cell fractions in our data (Figure 2A) and we emphasize that these

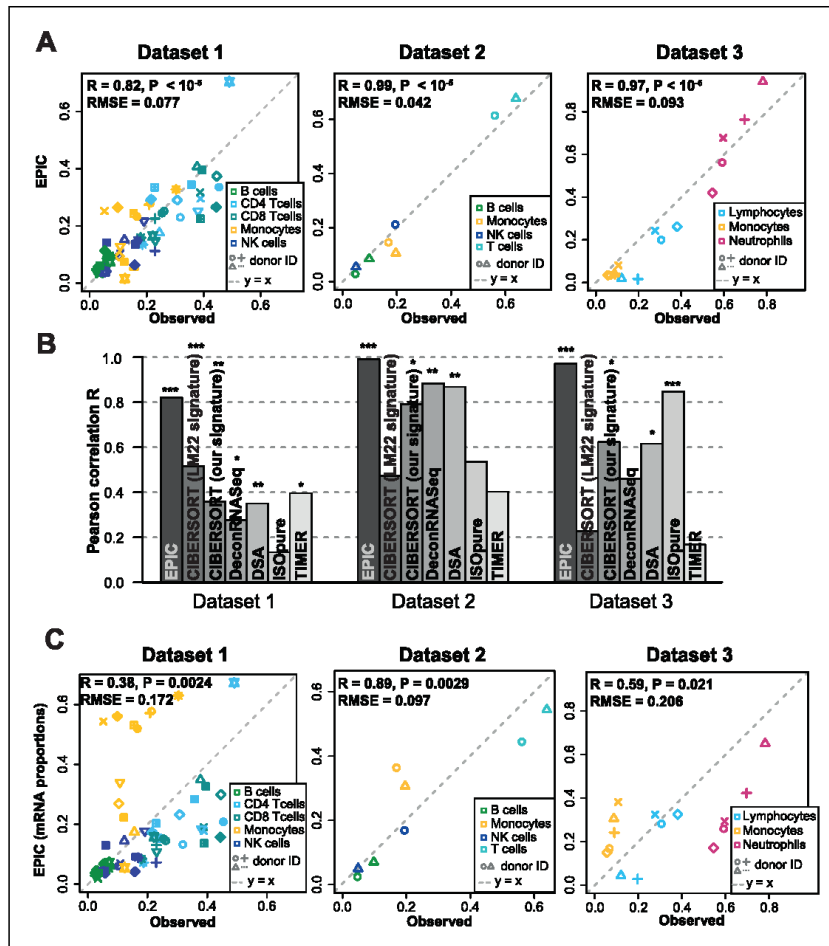


Figure 2. Predicting cell fractions in blood samples. (A) Predicted vs. measured immune cell proportions in PBMC (dataset 1 (Zimmermann et al., 2016), dataset 2 (Hoek et al., 2015)) and whole blood (dataset 3 (Linsley et al., 2014)); predictions are based on the reference profiles from circulating immune cells. (B) Performance comparison with other methods. Significant correlations are indicated above each bar (* $p < 0.05$; ** $p < 0.01$; *** $p < 0.001$). (C) Predicted immune cells' mRNA proportions (i.e., without mRNA renormalization step) vs. measured values in the same datasets. Correlations are based on Pearson correlation; RMSE: root mean squared error. Proportions of cells observed experimentally are given in *Supplementary file 3B-D*. DOI: <https://doi.org/10.7554/eLife.26476.006>

The following figure supplements are available for figure 2:

Figure supplement 1. Comparison of multiple cell fraction prediction methods in blood datasets.

DOI: <https://doi.org/10.7554/eLife.26476.007>

Figure supplement 2. Effect of including an mRNA renormalization step for multiple cell fraction prediction methods.

DOI: <https://doi.org/10.7554/eLife.26476.008>

Figure supplement 3. Effect of the various steps in EPIC on the prediction accuracy.

DOI: <https://doi.org/10.7554/eLife.26476.009>

Figure supplement 4. Results with or without known reference profiles for T cells for the cell fraction predictions from various methods.

DOI: <https://doi.org/10.7554/eLife.26476.010>

correlation values should only be used to compare methods tested on the same datasets (Figure 2B). The root mean squared error (RMSE), which is less dependent on such 'outlier data points', shows also improved accuracy for EPIC compared to other methods (Figure 2—figure supplement 1B).

The renormalization by mRNA content, which had not been considered in previous approaches, appeared to be important for predicting actual cell fractions (Figure 2C). Moreover, we observed that most other methods could also benefit from such a renormalization step, be it for the global prediction of all cell types together or for the predictions of each cell type (Figure 2—figure supplement 2). A conceptually related approach was developed by Baron et al. (2016), but the rescaling was done on the gene expression reference profiles (in their case of pancreatic cells) based on the total number of transcripts per cell type and the prediction of the proportion of pancreatic cells from a bulk sample was carried out with CIBERSORT (Newman et al., 2015). For comparison purpose, we implemented such an *a priori* renormalization step in EPIC as well, and observed similar results than with the *a posteriori* renormalization (Figure 2—figure supplement 3).

With respect to the other methods, EPIC has two other main distinctive features: (i) it allows for a cell type without a known reference gene expression profile (such a feature is also part of ISOpure [Quon et al., 2013]) and (ii) it integrates information about the variability in each signature gene from the reference gene expression profiles. The latter point slightly improves the prediction accuracy but to a lesser extent than the renormalization by mRNA (Figure 2—figure supplement 3). The former point cannot be tested directly in the blood samples as only cell types with known reference gene expression profiles are composing these samples. Therefore, to test the effect of including a cell type without a known reference profile, we removed all the T cell subsets from the reference gene expression profiles and predicted the proportion of the other cell types in the bulk samples, allowing for one uncharacterized cell type in EPIC. As expected, the results from EPIC including or not the T cell reference profiles remained nearly unchanged, while the other methods suffered from this, except for DSA (Zhong et al., 2013) which is based only on signature genes and not reference profiles (Figure 2—figure supplement 4). Such an advantage of EPIC is especially useful in the context of tumor samples where in general no reference gene expression profile is available for the cancer cells.

Validation in solid tumors

To validate our predictions in tumors, we collected single cell suspensions from lymph nodes of four metastatic melanoma patients (see Materials and methods). A fraction of the cell suspension was used to measure the different cell type proportions with flow cytometry (CD4 T, CD8 T, B, NK, melanoma and other cells comprising mostly stromal and endothelial cells; Supplementary file 3A), and the other fraction was used for bulk RNA sequencing (Figure 3—figure supplement 1). EPIC was first run with reference profiles from circulating immune cells. We observed a remarkable agreement between our predictions and experimentally determined cell fractions (Figure 3A). The high correlation value is possibly driven by the two samples containing about 80% of melanoma cells, but we stress that all predicted cell proportions fall nearly on the 'y = x' line. This clearly indicates that the absolute cell fractions were correctly predicted for all cell types, as confirmed by a low RMSE. Of note, the proportion of melanoma cells could be very accurately predicted even in the absence of a *priori* information about their gene expression.

As a second validation, we compared EPIC predictions with IHC data from colon cancer (Becht et al., 2016) (see Materials and methods). Although a limited number of immune cell types had been assayed in this study, we observed a significant correlation between cell proportions measured by IHC and our predictions, except for the CD8 T cells (Figure 3B).

As a third validation, we used recent single-cell RNA-Seq data from 19 melanoma samples (Tirosh et al., 2016). We applied EPIC on the average expression profile over all single cells for each patient and compared the results with the actual cell fractions (see Materials and methods). Here again, our predictions were consistent with the observed cell fractions, even for melanoma cells for which we did not assume any reference gene expression profile (Figure 3C). Notably, the predicted cell fractions from melanoma cells as well as from all other immune cell types fall nearly on the y = x line, showing that not only the relative cell type proportions could be predicted but also the absolute proportions for all cell types.

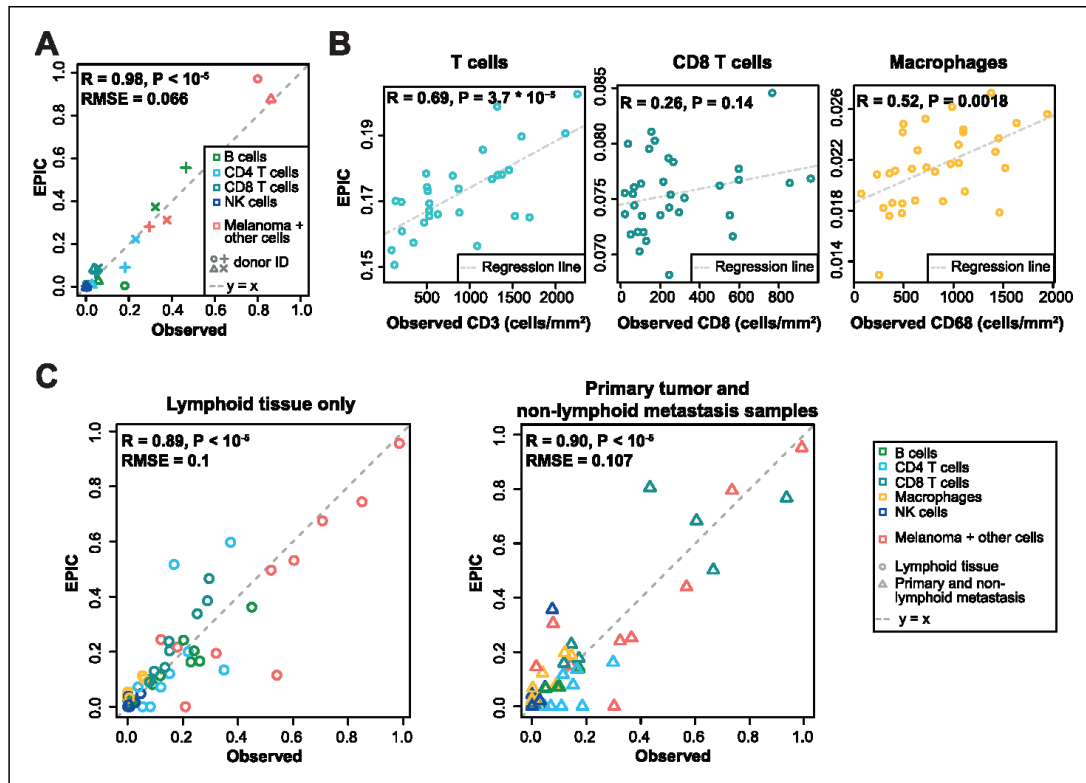


Figure 3. Predicting cell fractions in solid tumors with reference profiles from circulating cells. (A) Comparison of EPIC predictions with our flow cytometry data of lymph nodes from metastatic melanoma patients. (B) Comparison with immunohistochemistry data from colon cancer primary tumors (Becht et al., 2016). (C) Comparison with single-cell RNA-Seq data (Tirosch et al., 2016) from melanoma samples either from lymphoid tissues or primary and non-lymphoid metastatic tumors. Correlations are based on Pearson correlation. Proportions of cells observed experimentally are given in Supplementary file 3A,E.

DOI: <https://doi.org/10.7554/eLife.26476.011>

The following figure supplement is available for figure 3:

Figure supplement 1. Sketch of the experiment designed to validate EPIC predictions starting from in vivo tumor samples.

DOI: <https://doi.org/10.7554/eLife.26476.012>

We next compared these predictions to those obtained with reference profiles from tumor-infiltrating cells, including also CAFs and endothelial cells (Figure 4). For the single-cell RNA-Seq data (Figure 4C), we applied a leave-one-out procedure, to avoid using the same samples both to build the reference profiles and the bulk RNA-Seq data used as input for the predictions (see Materials and methods). Overall, predictions did not change much compared to those based on circulating immune cell reference gene expression profiles (Figure 4), except for the IHC data where the predictions for CD8 T cells and macrophages clearly improved (Figure 4B). Moreover, we could observe some differences between the results obtained from circulating immune cell reference gene expression profiles and those from tumor-infiltrating cell reference gene expression profiles, when considering the proportions from each cell type independently (Figures 3–4 and Figure 4—figure supplement 1): (i) predictions for CD8 T cells and macrophages improved in the datasets of primary tumors and non-lymph node metastases but not in the datasets from lymph node metastases; (ii)

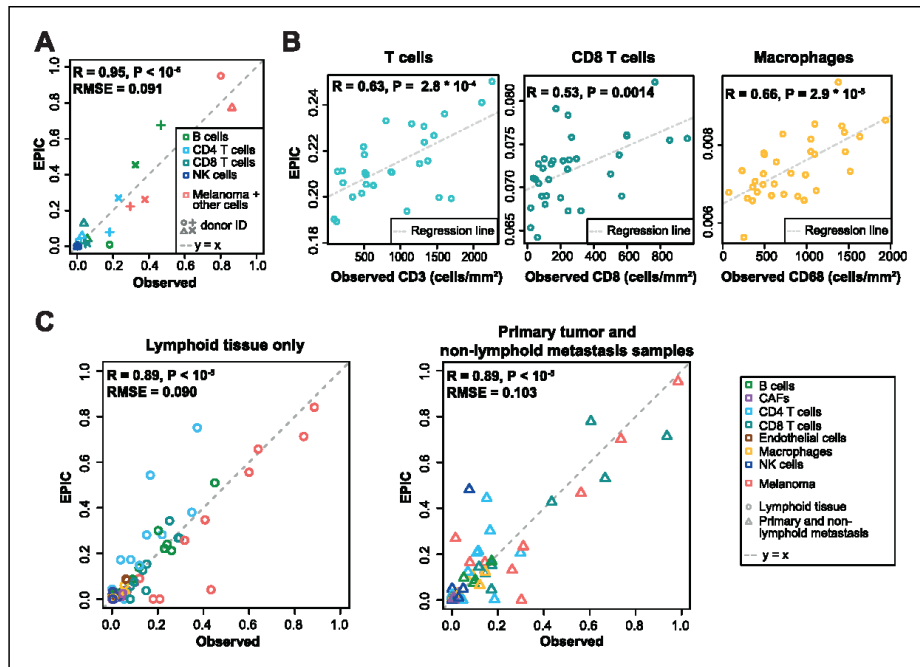


Figure 4. Predictions with reference profiles from tumor-infiltrating cells. Same as *Figure 3* but based on reference profiles built from the single-cell RNA-Seq data of primary tumor and non-lymphoid metastatic melanoma samples from *Tirosh et al. (2016)*. (A) Comparison with flow cytometry data of lymph nodes from metastatic melanoma patients. (B) Comparison with IHC from colon cancer primary tumors (*Becht et al., 2016*). (C) Comparison with single-cell RNA-Seq data (*Tirosh et al., 2016*). For primary tumor and non-lymphoid metastasis samples, a leave-one-out procedure was used (see Materials and methods). Proportions of cells observed experimentally are given in *Supplementary file 3A,E*.

DOI: <https://doi.org/10.7554/eLife.26476.013>

The following figure supplement is available for figure 4:

Figure supplement 1. Comparison of EPIC results per cell type for gene expression reference profiles from circulating or tumor-infiltrating immune cells.

DOI: <https://doi.org/10.7554/eLife.26476.014>

predictions for B and NK cells displayed similar accuracy based on the circulating cells or tumor-infiltrating cells profiles for all datasets; and (iii) CAFs and endothelial cells were not available for the blood-based reference profiles but the proportion of these cells could be well predicted based on the reference profiles constructed from tumor-infiltrating cells (*Figure 4* and *Figure 4—figure supplement 1*).

Benchmarking of other methods

We took advantage of our unique collection of independent validation datasets to benchmark other methods for predictions of immune cell type fractions in human tumors. We first compared the results of EPIC and ISOpure (*Quon et al., 2013*), which is the only other method that can consider uncharacterized cell types and therefore predict the fraction of cancer and immune cell types based only on RNA-seq data. EPIC displayed improved accuracy in all three datasets (*Figure 5A*, and *Figure 5—figure supplements 1–4*). To benchmark other methods, we then restricted our analysis to the predictions of the different immune cell types (*Figure 5B* and *Figure 5—figure supplements 1–4*). Predictions from EPIC were in general more accurate, especially when considering all cell types

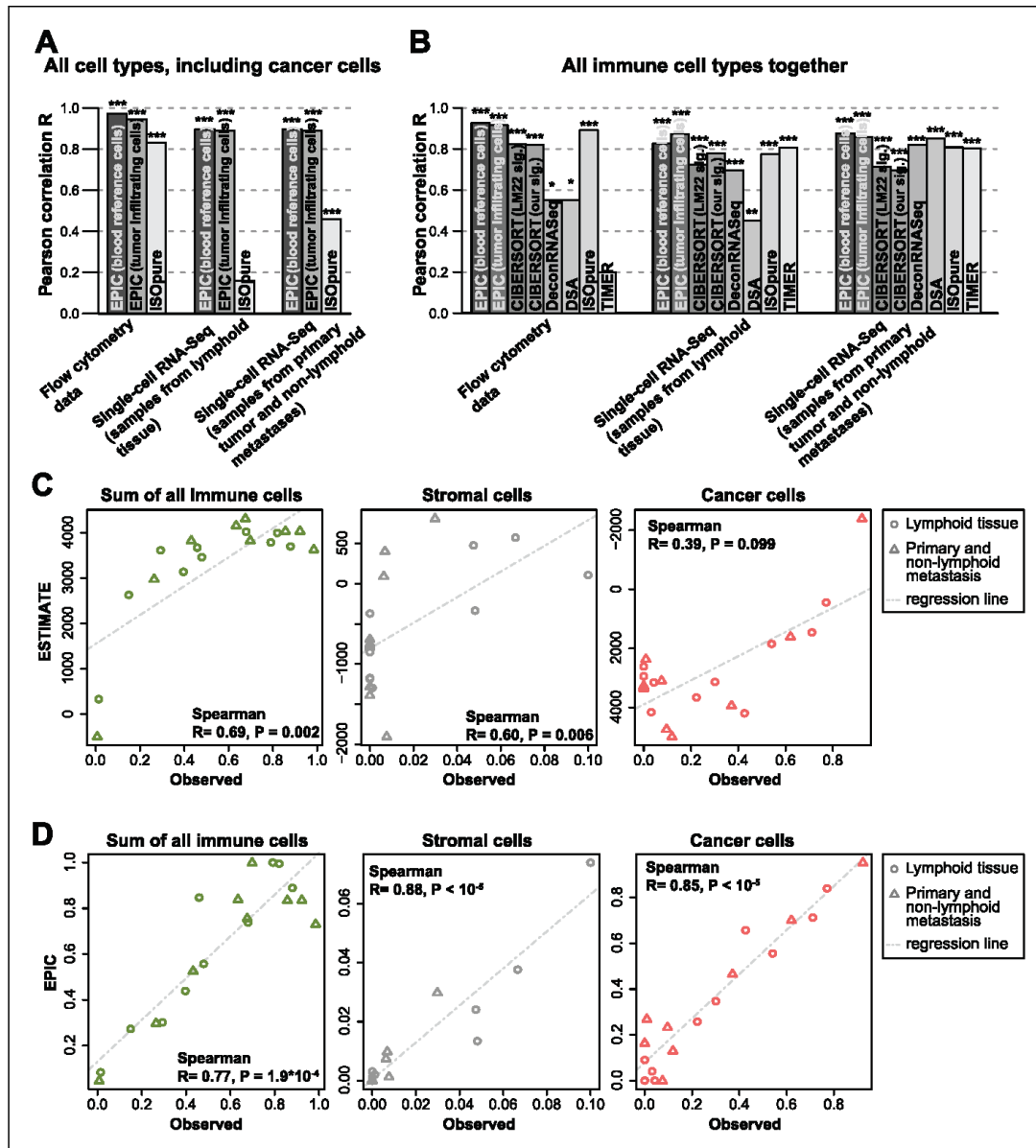


Figure 5. Performance comparison with other methods in tumor samples. (A) Pearson correlation R-values between the cell proportions predicted by EPIC and ISOpure and the observed proportions measured by flow cytometry or single-cell RNA-Seq (Tirosh et al., 2016), considering all cell types together (i.e., B, CAFs, CD4 T, CD8 T, endothelial, NK, macrophages and cancer cells). (B) Same analysis as in Figure 5A but considering only immune cell types (i.e., B, CD4 T, CD8 T, NK and macrophages) in order to include more methods in the comparison. (C) Analysis of ESTIMATE predictions in the single-cell RNA-Seq dataset for the sum of all immune cells, the proportion of stromal cells (cancer-associated fibroblasts) and the proportion of

Figure 5 continued on next page

Figure 5 continued

cancer cells (cells identified as melanoma cells in Tirosh et al.). (D) Same as **Figure 5C** but for EPIC predictions of immune, stromal and cancer cells. Significant correlations in (A–B) are indicated above each bar (* $p < 0.05$; ** $p < 0.01$; *** $p < 0.001$).

DOI: <https://doi.org/10.7554/eLife.26476.015>

The following figure supplements are available for figure 5:

Figure supplement 1. Comparison of multiple cell fraction prediction methods in tumor datasets.

DOI: <https://doi.org/10.7554/eLife.26476.016>

Figure supplement 2. Comparison of cell fraction prediction methods with flow cytometry data of melanoma tumors.

DOI: <https://doi.org/10.7554/eLife.26476.017>

Figure supplement 3. Comparison of cell fraction prediction methods with immunohistochemistry data in colon cancer data (Becht et al., 2016) for T cell, CD8 T cell and macrophage infiltration values.

DOI: <https://doi.org/10.7554/eLife.26476.018>

Figure supplement 4. Comparison of cell fraction prediction methods with single-cell RNA-Seq data from melanoma tumors (Tirosh et al., 2016).

DOI: <https://doi.org/10.7554/eLife.26476.019>

Figure supplement 5. Comparison between ESTIMATE scores (A) and EPIC predictions (B) in our new flow cytometry dataset.

DOI: <https://doi.org/10.7554/eLife.26476.020>

Figure supplement 6. Predicting Thelper and Treg cell fractions in tumors.

DOI: <https://doi.org/10.7554/eLife.26476.021>

together. Nevertheless, when restricting the comparisons to relative cell type proportions, some methods like MCPcounter (Becht et al., 2016) and TIMER (Li et al., 2016) were quite consistent in their predictions across the various datasets and showed similar accuracy as EPIC for the cell types considered in these methods (Figure 5—figure supplements 1–4). Of note, MCPcounter could not be included in the global prediction comparison as this method returns scores that are not comparable between different cell types. Predictions from DSA (Zhong et al., 2013) were also quite accurate when available, but in multiple cases some cell type proportions returned by the method were simply equal to 0 in all samples (Figure 5—figure supplements 1–4 – correlation values were replaced by NA in these cases).

Immune, stromal and tumor purity scores (Yoshihara et al., 2013) based on gene set enrichment analysis were also correlated with the total fraction of immune cells, stromal cells and the fraction of cancer cells (correlation was not significant for the tumor purity score – Figure 5C and Figure 5—figure supplement 5). However, these correlations were considerably lower than those obtained with our approach (Figure 5D and Figure 5—figure supplement 5). Moreover, such scores are less quantitative and are thus more difficult to interpret with respect to actual cell type proportions.

Next, we performed some explorative analysis to test if such cell fraction prediction methods could go further into the details of the T cell subsets. Based on the single-cell RNA-seq data from Tirosh and colleagues (Tirosh et al., 2016), we identified CD4+ Treg and Thelper cells (see Materials and methods), and built reference gene expression profiles for these cell types as we had done for the other cell types. As before, a leave-1-out procedure at the patient level was used to predict the proportions for these cell types based on the bulk samples constructed from this single-cell RNA-seq data. We observed significant correlations, but the R-values are lower than before (Figure 5—figure supplement 6), suggesting that we may be reaching the limits of cell fraction prediction methods for cell types that show lower abundance and substantial transcriptional similarity. Of note, CIBERSORT using either the LM22 signature or our newly derived signature did not perform better than EPIC.

Discussion

By combining RNA-Seq profiles of all major immune and other non-malignant cell types established from both circulating and tumor-infiltrating cells together with information about cell morphology (i.e., mRNA content) and algorithmic developments to consider uncharacterized and possibly highly variable cell types, EPIC overcomes several limitations of previous approaches to predict the fraction of both cancer and immune or other non-malignant cell types from bulk tumor gene expression data. From an algorithmic point of view, EPIC takes advantage of the fact that cancer cells, in general, express no or only low levels of immune and stromal markers. Therefore the method can be

broadly applied to most solid tumors, as confirmed by our validation in melanoma and colorectal samples, but it will not be suitable for hematological malignancies like leukemia or lymphoma.

The accuracy of the predictions for some cell types might be sensitive to the origin or condition of the immune cells used for establishing reference profiles. For instance, we observed that CD8 T cells and macrophages from primary tumors and non-lymph node metastases samples were best predicted using the reference profiles from tumor-infiltrating cells. This may be explained by the fact that the reference profiles from circulating cells corresponded to resting CD8 T cells and monocytes as only few activated C8 T cells and no macrophages are circulating in blood.

Overall, our results suggest that for primary tumors or non-lymphoid tissue metastases reference gene expression profiles from tumor-infiltrating immune cells are more appropriate, while for lymph node metastases, profiles from either circulating or tumor-infiltrating immune cells could be used.

One known limitation of cell fraction predictions arises when some cell types are present at very low frequency (*Shen-Orr and Gaujoux, 2013*). Our results suggest that predictions of cell proportions are reliable within an absolute error of about 8%, as estimated by the root mean squared error (*Figure 3* and *Figure 4—figure supplement 1B*). These estimates are consistent with the lower detection limit proposed by other groups (*Becht et al., 2016; Zhong et al., 2013*) and may explain why the relative proportions of NK cells, which are present at lower frequency in melanoma tumors (*Balch et al., 1990; Sconocchia et al., 2012*), could not be predicted with accuracy comparable to other cell types (*Figure 4—figure supplement 1*). While this may prevent applications of cell fraction predictions in some tumor types that are poorly infiltrated, many other tumors, like melanoma or colorectal cancer, display high level of infiltrating immune cells and the role of immune infiltrations on tumor progression and survival appears to be especially important in these tumors (*Clemente et al., 1996; Fridman et al., 2012; Galon et al., 2006*).

Another limitation of cell fraction predictions arises when considering cell types that show high transcriptional similarity. For instance, Treg in *Figure 5—figure supplement 6* could not be well predicted neither by EPIC nor CIBERSORT. This can be understood because the gene expression profiles of Thelper and Treg are highly similar with only a few genes expressed differently between the two, making it harder for cell fraction prediction methods to work accurately. In addition, Treg were present at a proportion lower than 10% in all samples (*Supplementary file 3E*). For such cases, gene set enrichment approaches, although less quantitative, may be more convenient, possibly combining them with the predictions obtained by EPIC for the main immune cell types.

Our predictions for the fraction of uncharacterized cells may include non-malignant cells, such as epithelial cells from neighboring tissues in addition to cancer cells. Compared to recent algorithms that first predict tumor purity based on exome sequencing data, and later infer the relative fraction of immune cell types (*Li et al., 2016*), the predictions of EPIC for immune and stromal cells are likely more quantitative because they can implicitly consider the presence of not only cancer cells but also other non-malignant cells for which reference profiles are not available. Moreover, EPIC does not require both exome and RNA-Seq data from the same tumor samples, thereby reducing the cost and amount of experimental work for prospective studies, and broadening the scope of retrospective analyses of cancer genomics data to studies that only include gene expression data.

Recent technical developments in single-cell RNA-Seq technology enable researchers to directly access information about both the proportion of all cell types together with their gene expression characteristics (*Carmona et al., 2017; Efroni et al., 2015; Jaitin et al., 2014; Singer et al., 2016; Stegle et al., 2015; Tirosch et al., 2016*). Such data are much richer than anything that can be obtained with computational deconvolution of bulk gene expression profiles and this technology may eventually replace standard gene expression analysis of bulk tumors. Nevertheless, it is important to realize that, even when disregarding the financial aspects, single-cell RNA-Seq of human tumors is still logistically and technically very challenging due to high level of cell death upon sample manipulation (especially freezing and thawing) and high transcript dropout rates (*Finak et al., 2015; Saliba et al., 2014; Stegle et al., 2015*). Moreover, one cannot exclude that some cells may better survive the processing with microfluidics devices used in some single-cell RNA-Seq platforms, thereby biasing the estimates of cell type proportions. It is therefore likely that bulk tumor gene expression analysis will remain widely used for several years. Our work shows how we can exploit recent single-cell RNA-Seq data of tumors obtained from a few patients to refine cell fraction predictions in other patients that could not be analyzed with this technology, thereby overcoming some

limitations of previous computational approaches that relied only on reference gene expression profiles from circulating immune cells.

In this work, we provide a detailed and biologically relevant validation of our predictions using actual tumor samples from human patients analyzed with flow cytometry, IHC and single-cell RNA-Seq. We note that the slightly lower agreement between our predictions and IHC data may be partly explained by the fact that the exact same samples could not be used for both gene expression and IHC analyses because of the incompatibility between the two techniques. Nevertheless, the overall high accuracy of our predictions indicates that infiltrations of major immune cell types can be quantitatively studied directly from bulk tumor gene expression data using computational approaches such as EPIC.

EPIC can be downloaded as a standalone R package (<https://github.com/GfellerLab/EPIC/releases/tag/v1.1>) (Racle, 2017) and can be used with reference gene expression profiles pre-compiled from circulating or tumor-infiltrating cells, or provided by the user. EPIC is also available as a web application (<http://epic.gfellerlab.org>) where users can upload bulk samples gene expression data and perform the full analysis.

Materials and methods

Code availability

EPIC has been written as an R package. It is freely available on GitHub (<https://github.com/GfellerLab/EPIC>; copy archived on <https://github.com/elifesciences-publications/EPIC>) for academic non-commercial research purposes. Version v1.1 of the package was used for our analyses.

In addition to the R package, EPIC is available as a web application at the address: <http://epic.gfellerlab.org>.

Prediction of cancer and immune cell type proportions

In EPIC, the gene expression of a bulk sample is modeled as the sum of the gene expression profiles from the pure cell types composing this sample (Figure 1A,B). This can be written as (Venet *et al.*, 2001):

$$b = C \times p \quad (1)$$

Where b is the vector of all n genes expressed from the bulk sample to deconvolve; C is a matrix ($n \times m$) of the m gene expression profiles from the different cell types; and p is a vector of the proportions from the m cell types in the given sample (Figure 1B).

Matrix C consists of $m-1$ columns corresponding to various reference non-malignant cell types whose gene expression profiles are known, and a last column corresponding to uncharacterized cells (i.e. mostly cancer cells, but possibly also other non-malignant cell types not included in the reference profiles). EPIC assumes the reference gene expression profiles from the non-malignant cell types are well conserved between patients. Such a hypothesis is supported by the analysis in Figure 1C,D. The uncharacterized cells can be more heterogeneous between patients and EPIC makes no assumption on them.

EPIC works with RNA-seq data, which is implicitly normalized. We use data normalized into transcripts per million (TPM) because it has some properties needed for the full cell proportion prediction to work, as will be shown in the next paragraphs. Therefore, instead of the raw data from Equation (1), we are working with TPM-normalized data, which correspond to the following:

$$\begin{aligned} \bar{b}_i &= \frac{10^6}{\sum_{k=1}^n b_k} \cdot \frac{b_i}{l_i} \\ \bar{C}_{ij} &= \frac{10^6}{\sum_{k=1}^m c_{ik}} \cdot \frac{c_{ij}}{l_i} \end{aligned} \quad (2)$$

Where \bar{b} and \bar{C} are the TPM-normalized bulk sample and reference cell gene expression profiles respectively and l_i is the length of gene i .

Using these, Equation (1) is rewritten to:

$$\bar{b} = \bar{C} \times \bar{p} \tag{3}$$

where

$$\bar{p}_j = \frac{\sum_{k=1}^n \frac{C_{kj}}{l_k}}{\sum_{i=1}^n \frac{b_i}{l_i}} \cdot p_j \tag{4}$$

This normalization guarantees the sum of the new proportions, \bar{p} , is equal to 1:

$$\sum_{i=1}^n \bar{b}_i \stackrel{\text{from eq. 2}}{=} \sum_i \left(\frac{10^6}{\sum_k \frac{b_k}{l_k}} \cdot \frac{b_i}{l_i} \right) = 10^6$$

and

$$\begin{aligned} \sum_{i=1}^n \bar{b}_i \stackrel{\text{from eq. 3}}{=} \sum_i (\bar{C} \times \bar{p})_i &= \sum_{i=1}^n \sum_{j=1}^m \bar{C}_{ij} \cdot \bar{p}_j \stackrel{\text{from eq. 2}}{=} \sum_j \left[\left(\frac{10^6}{\sum_k \frac{C_{kj}}{l_k}} \cdot \sum_i \frac{C_{ij}}{l_i} \right) \cdot \bar{p}_j \right] = 10^6 \cdot \sum_j \bar{p}_j \\ &\Rightarrow \sum_{j=1}^m \bar{p}_j = 1 \end{aligned} \tag{5}$$

In addition to \bar{p} and \bar{C} we also define \bar{p}^* and \bar{C}^* , which are the same except that they include the normalized proportions and profiles from the reference cell types only (i.e. they have one less element and one less column than \bar{p} and \bar{C} respectively).

Using these normalized quantities, EPIC then solves **Equation (3)** for a subset of n_s equations corresponding to the n_s signature genes (S) that are expressed by one or more of the reference cell types but only expressed at a negligible level in the uncharacterized cells (**Figure 1B**). Previous computational work (*Clarke et al., 2010; Gosink et al., 2007*) showed that the proportion from uncharacterized cells in bulk samples could indeed be inferred with help of genes not expressed by the uncharacterized cells. Importantly, cell-specific signature genes are well established and widely used in flow cytometry to sort immune cells. Thus, EPIC solves the following system of equations:

$$\bar{b}_{i|_{i \in S}} = ((\bar{C}^* \times \bar{p}^*)_i + \bar{C}_{im} \cdot \bar{p}_m)_{i \in S} = (\bar{C}^* \times \bar{p}^*)_{i \in S} \tag{6}$$

where the term corresponding to the uncharacterized cells (m) vanished thanks to the definition of the signature genes ($\bar{C}_{im|_{i \in S}} \cong 0$).

The solution to **Equation (6)** can be estimated by a constrained least square optimization. EPIC takes advantage of the known variability for each gene in the reference profile, to give weights in the function to minimize:

$$f(\bar{p}^*) = \sum_{i \in S} w_i [\bar{b}_i - (\bar{C}^* \times \bar{p}^*)_i]^2 \tag{7}$$

with constraints

$$\begin{cases} \bar{p}_j^* \geq 0 \\ \sum_{j=1}^{m-1} \bar{p}_j^* \leq 1 \end{cases}$$

Here, the weights, w_i , give more importance to the signature genes with low variability in the reference gene expression profiles. In EPIC, these weights are given by:

$$w_i = \min(u_i, 100 \cdot \text{median}(u_i))$$

where

$$u_i = \sum_{j=1}^{m-1} \frac{\bar{C}_{ij}^*}{V_{ij} + \varepsilon}$$

\bar{V} is the matrix of the TPM-based variability of each gene for each of the reference cells (**Supplementary files 1–2**), ϵ is a small number to avoid division by 0, and the term ' $100 \cdot \text{median}(u_i)$ ' is used to avoid giving too much weight to few of the genes.

Finally, thanks to **Equation (5)**, the proportion for the uncharacterized cells can be obtained by:

$$\bar{p}_m = 1 - \sum_{j=1}^{m-1} \bar{p}_j \quad (8)$$

Since we used normalized gene expression data, values of \bar{p} correspond actually to the fraction of mRNA coming from each cell type, rather than the cell proportions. As the mRNA content per cell type can vary significantly (**Figure 1—figure supplement 2**), the actual proportions of each cell type can be estimated as:

$$p_j = \alpha \cdot \frac{\bar{p}_j}{r_j} \quad (9)$$

where r_j is the amount of RNA nucleotides in cell type j (or equivalently the total weight of RNA in each cell type) and α is a normalization constant to have $\sum p_j = 1$.

Another method, DeMix (**Ahn et al., 2013**), starts from **Equation (1)** to estimate the proportion and gene expression profile from cancer cells in mixed samples. In this method the mixed sample is assumed to be composed only by two cell types: cancer cells (without any *a priori* known gene expression profile) and normal cells (with known gene expression data, which can either come from tumor-matched or unmatched samples). This method was developed for microarray data and shows that it was important to use the raw data as input assuming it follows a log-normal distribution as is the case for microarray, instead of working with log-transformed data like most other methods did. DeMix estimates the variance of the gene expression in the normal samples and uses this in the maximum likelihood estimation to predict the cancer cell gene expression and proportions, using thus implicitly a gene-specific weight for each gene. EPIC was derived for RNA-seq data and is directly using linear (non-log) data. Notably, when solving the linear regression from **Equation (7)** in EPIC, we are not assuming any specific distribution for the gene expression and the weights we give to each gene are simply based on their interquartile range in the reference samples. Other measures of gene variability could however be given as input into EPIC's *R*-package. Contrary to DeMix, another important assumption performed in EPIC is that our signature genes are not expressed by the cancer cells, so that we can easily estimate the proportion of multiple non-malignant cell types composing the bulk samples.

Flow cytometry and gene expression analysis of melanoma samples

Patients agreed to donate metastatic tissues upon informed consent, based on dedicated clinical investigation protocols established according to the relevant regulatory standards. The protocols were approved by the local IRB, that is, the 'Commission cantonale d'éthique de la recherche sur l'être humain du Canton de Vaud'. Lymph nodes (LN) were obtained from stage III melanoma patients, by lymph node dissection that took place before systemic treatment. The LN from one patient was from the right axilla and the LNs from the other three patients were from the iliac and ilio-obturator regions (**Appendix 2—table 1**). Single cell suspensions were obtained by mechanical disruption and immediately cryopreserved in RPMI 1640 supplemented with 40% FCS and 10% DMSO. Single cell suspensions from four lymph nodes were thawed and used in parallel experiments of flow cytometry and RNA extraction. In order to limit the number of dead cells after thawing, we removed those cells using a dead cell removal kit (Miltenyi Biotec). Proportions of CD4 T (CD45⁺/CD3⁺/CD4⁺/Melan-A⁻), CD8 T (CD45⁺/CD3⁺/CD8⁺/Melan-A⁻), NK (CD45⁺/CD56⁺/CD3⁻/CD33⁻/Melan-A⁻), B (CD45⁺/CD19⁺/CD3⁻/CD33⁻/Melan-A⁻) and Melan-A expressing tumor cells (**Supplementary file 3A**) were acquired via flow cytometry using the following antibodies: anti-CD3 BV711 (RRID:AB_2566035), anti-CD4 BUV737 (RRID:AB_2713927), anti-CD8 PE-Cy5 (RRID:AB_2713928), anti-CD56 BV421 (RRID:AB_11218798), anti-CD19 APCH7 (RRID:AB_1645728), anti-CD33 PE-Cy7 (RRID:AB_2713932), anti-CD45 APC (RRID:AB_314400), anti-Melan-A FITC (RRID:AB_2713930) and Fixable Viability Dye eFluor 455UV (eBioscience). Data was acquired on a BD LSR II SORP flow cytometry machine (BD Bioscience). Analysis was performed using FlowJo (Tree Star).

Cell proportions were based on viable cells only. In parallel total RNA was extracted using the RNAeasy Plus mini kit (Qiagen) following the manufactures' protocol. Starting material always contained minimum 0.2×10^6 cells. RNA was quantified and integrity was analyzed using a Fragment Analyser (Advanced Analytical). Total RNA from all samples used for sequencing had an RQN ≥ 7 . Libraries were obtained using the Truseq stranded RNA kit (Illumina). Single read (100 bp) was performed using an Illumina HiSeq 2500 sequencer (Illumina).

Post processing of the sequencing was done using Illumina pipeline Casava 1.82. FastQC (version 0.10.1) was used for quality control. RNA-seq reads alignment to the human genome, *hg19*, and TPM quantification were performed with RSEM (Li and Dewey, 2011) version 1.2.19, using Bowtie2 (Langmead and Salzberg, 2012) version 2.2.4 and Samtools (Li et al., 2009) version 1.2.

RNA-Seq data from this experiment have been deposited in NCBI's Gene Expression Omnibus (Edgar et al., 2002) and are accessible through GEO Series accession number GSE93722 (<https://www.ncbi.nlm.nih.gov/geo/query/acc.cgi?acc=GSE93722>).

Amount of mRNA per cell type

Healthy donor peripheral blood was obtained through the blood transfusion center in Lausanne. PBMCs were purified by density gradient using Lymphoprep (Axis-Shield). Mononuclear cells were stained in order to sort monocytes, B, T and NK cells using the following antibodies: CD14 FITC (RRID:AB_130992), CD19 PE (RRID:AB_2716572), CD3 APC (RRID:AB_130788), CD56 BV421 (RRID:AB_11218798) and fixable live/dead near IR stain (ThermoFisher Scientific). 1×10^6 live cells from each cell type were sorted using the BD FACS ARIA III (BD Biosciences). Total RNA was extracted using the RNAeasy Plus mini kit (Qiagen) following the manufactures' protocol and quantified using a Fragment Analyser (Advanced Analytical). Values obtained are given in **Figure 1—figure supplement 2A**.

The mRNA content for the cancer cells was estimated from the flow cytometry data described in the previous section from the four patients with melanoma. For this we used the forward scatter width, which is a good proxy of cell size and mRNA content (Padovan-Merhar et al., 2015; Tzur et al., 2011), and observed that cancer cells had similar amount of mRNA than B, NK and T cells (**Figure 1—figure supplement 2B**). We thus used a value of 0.4 pg of mRNA per cancer cell.

Public external datasets used in this study

- Dataset 1 was obtained from Zimmermann and colleagues (Zimmermann et al., 2016), through ImmPort (<http://www.immport.org>), accession SDY67. It includes RNA-Seq samples from PBMC of healthy donors before and after influenza vaccination. In addition, the original flow cytometry results files were available, containing multiple immune cell markers. As an independent validation of EPIC, we used the data from 12 pre-vaccination samples of healthy donors and we computed the corresponding immune cell proportions from the flow cytometry files merging the results from their *innate* and *Treg panels* (obtaining B, CD4 T, CD8 T, NK cells and monocytes, **Supplementary file 3B; Figure 2A**).
- Dataset 2 was obtained from Hoek and colleagues (Hoek et al., 2015), GEO accession GSE64655. This corresponds to RNA-Seq samples from two different donors. Samples have been taken before an influenza vaccination and also 1, 3 and 7 days after the vaccination (56 samples in total). In their experiment, the authors measured RNA-Seq from bulk PBMC samples and also from sorted immune cells (B, NK, T cells, myeloid dendritic cells, monocytes and neutrophils). In addition, flow cytometry was performed to measure the proportion of these cell types in PBMC before the influenza vaccination (personally communicated by the authors; **Supplementary file 3C**).
- Dataset 3 was obtained from Linsley and colleagues (Linsley et al., 2014), GEO accession GSE60424. This dataset includes 20 donors (healthy donors and other donors with amyotrophic lateral sclerosis, multiple sclerosis, type one diabetes or sepsis), for a total of 134 samples. RNA-Seq from these donors has been extracted from whole blood and sorted immune cells (B, NK cells, monocytes, neutrophils, CD4 T and CD8 T cells). In addition to RNA-Seq data, complete blood counts data were available for 5 of these donors (personally communicated by the authors; **Supplementary file 3D**).
- Dataset 4 was obtained from Pabst and colleagues (Pabst et al., 2016), GEO accession GSE51984. This includes RNA-Seq from five healthy donors. Samples are from total white blood cells and sorted immune cells (B cells, granulocytes, monocytes and T cells).

- Colon cancer dataset was obtained from Becht and colleagues (*Becht et al., 2016*), GEO accession GSE39582. This corresponds to microarrays of primary colon cancer tumors. In addition to gene expression data, immunohistochemistry data of CD3, CD8 and CD68 was available for 33 patients (personally communicated by the authors).
- Single-cell RNA-Seq data from tumor-infiltrating cells were obtained from Tirosh and colleagues (*Tirosh et al., 2016*), GEO accession GSE72056. This corresponds to 19 donors and comprises primary tumors, lymph node metastasis or other lesions. It includes 4645 cells. Cell type identity was taken from *Tirosh et al. (2016)* (B, NK, T cell, macrophage, CAFs, endothelial cell, cancer cell as well as cells not assigned a specific cell type). Among the T cells, we then defined subsets based on their gene expression: CD4 T cells (expressing CD4 but not CD8A nor CD8B) and CD8 T cells (expressing CD8A or CD8B but not CD4). The other T cells not corresponding to one of these two groups were removed from further analyses. We further defined among the CD4 T cells: Treg (expressing either FOXP3 or CD25 above the median among CD4 T cells) and Thelper (those CD4 T cells not belonging to Treg group). In silico reconstructed bulk samples from each donor were obtained as the average per gene from all samples of the given donor. The corresponding cell fractions from these bulk samples were obtained as the number of cells from each cell type divided by the total number of cells (*Supplementary file 3E*). In the results, we split this dataset in two depending on the origin of the biopsies: lymphoid tissues for samples obtained from lymph node and spleen metastases, vs. the rest of samples, which were obtained from primary tumor and other metastases.

For the above datasets 2 and 3, we obtained raw *fastq* files. RNA-seq reads alignment to the human genome, *hg19*, and TPM quantification were performed with *RSEM* (*Li and Dewey, 2011*) version 1.2.19, using *Bowtie2* (*Langmead and Salzberg, 2012*) version 2.2.4 and *Samtools* (*Li et al., 2009*) version 1.2.

For the other datasets, we directly obtained the summary counts data from the respective studies without mapping the reads by ourselves, and we transformed these counts to TPM wherever necessary.

Reference gene expression profiles from circulating cells

Reference gene expression profiles of sorted immune cells from peripheral blood were built from the datasets 2, 3 and 4 described in previous section. We verified no experimental biases were present in these data through unsupervised clustering of the samples, with help of a principal component analysis based on the normalized expression from the 1000 most variable genes (*Figure 1C*).

The median value of TPM counts was computed per cell type and per gene. Similarly, the interquartile range of the TPM counts was computed per cell type and gene, as a measure of the variability of each gene expression in each cell type. Values of these reference profiles are given in *Supplementary file 1*. Granulocytes from dataset 4 and neutrophils from datasets 2 and 3 were combined to build the reference profile for neutrophils (neutrophils constitute more than 90% of granulocytes). No reference profile was built for the myeloid dendritic cells as only few samples of these sorted cells existed and they were all from the same experiment. Monocytes are not found in tumors but instead there are macrophages, mostly from monocytic lineage, that are infiltrating tumors and that are not found in blood. For this reason, we also used the monocyte reference gene expression profile as a proxy for macrophages when applying EPIC to tumor samples. Such an assumption gave coherent results as observed in the results.

Reference profiles from tumor-infiltrating cells

We also built gene expression reference profiles from tumor-infiltrating cells. These are based on the single-cell RNA-Seq data from Tirosh and colleagues (*Tirosh et al., 2016*) described above. We only used the non-lymphoid tissue samples to build these tumor-infiltrating cell's profiles, avoiding in this way potential 'normal immune cells' present in the lymph nodes and spleen. These reference profiles (*Supplementary file 2*) were built in the same way as described above for the reference profiles of circulating immune cells, but based on the mean and standard deviation instead of median and interquartile range respectively, due to the nature of single-cell RNA-Seq data and gene dropout present with such technique.

When testing EPIC with these profiles for the single-cell RNA-Seq datasets, for the samples of primary tumor and other non-lymph node metastases, a leave-one-out procedure was applied: for each donor we built reference cell profiles based only on the data coming from the other donors.

Cell marker gene identification

EPIC relies on signature genes that are expressed by the reference cells but not by the uncharacterized cells (e.g., cancer cells). For each reference cell type, we thus built a list of signature genes through the following steps:

1. The samples (from the peripheral blood datasets) from each immune cell type were tested for overexpression against:
 - a. the samples from each other immune cell of peripheral blood datasets (1 cell type vs. 1 other cell type at a time);
 - b. the samples of the Illumina Human Body Map 2.0 Project (ArrayExpress ID: E-MTAB-513) considering all non-immune related tissues;
 - c. the samples from GTEx (*GTEx Consortium, 2015*) from each of the following tissues (one tissue at a time): adipose subcutaneous; bladder; colon-transverse; ovary; pancreas; testis (data version V6p).
2. Only genes overexpressed in the given cell type with an adjusted p -value < 0.01 for all these tests were kept. Conditions 1b) and 1c) are there to ensure signature genes are expressed in the immune cells and no other tissues.
3. The genes that passed 2) were then ranked by the fold change from the overexpression tests to preselect the genes showing the biggest difference between the various cell types.
4. The list of genes was then manually curated, comparing the expression of the genes per cell type in the peripheral blood datasets and the tumor-infiltrating cells dataset: only genes expressed at similar levels between the blood and tumor-infiltrating cells were kept (to avoid differences due to exhaustion phenotype for example). Genes expressed at much higher levels than the other genes were also removed from the signature as these could have biased the least-square optimization towards good predictions for these genes only.
5. In addition to CD4 and CD8 T cells signatures, we built a signature list of general T cell genes in the same way as described above, and it contains genes expressed at similar levels in the two T cell subtypes. This general T cell signature is also part of EPIC, even when predicting the proportions of the T cell subsets.
6. For the tumor-infiltrating cell reference profiles, signature genes from CAFs, endothelial cells and macrophages were also needed. These were built in a similar way than above, considering the overexpression from each of these cell types against each other cell type from the tumor-infiltrating cells data.

All the differential expression tests were performed with *DESeq2* (*Love et al., 2014*).

Appendix 1—table 1 summarizes the full list of signature genes per cell type.

Prediction of cell proportions in bulk samples with other tools

We compared EPIC's predictions with those from various cell fraction prediction methods. These other methods were run with the following packages (using the default options when possible):

- CIBERSORT (*Newman et al., 2015*) (R package version 1.03) was run based on two different gene expression reference profiles:
 - based on the LM22 reference profiles derived in (*Newman et al., 2015*). For comparison with the experimentally measured cell proportions, we summed together the sub-types predictions of CIBERSORT within each major immune cell type.
 - based on the reference profiles and signature genes we derived here for EPIC.
- DeconRNASeq (v1.16) (*Gong and Szustakowski, 2013*) does not contain immune cell reference profiles and we used the reference profiles we derived here as well as the corresponding signature genes. We present the results with 'use.scale' parameter set to FALSE, which usually gave better results.
- DSA (*Zhong et al., 2013*) only needs a gene signature per cell type to estimate the proportion of cells in multiple bulk samples together. We used the implementation of DSA found in Cell-Mix (*Gaujoux and Seoighe, 2013*) R package (version 1.6.2). As DSA needs many samples to estimate simultaneously the proportions of cells in these samples, we considered all the PBMC samples from Hoek et al. data when fitting this dataset (eight samples) and all whole blood samples from Linsley et al. data when fitting this other dataset (20 samples), even though the cell proportions have been measured experimentally only for 2 and 5 samples respectively. For the gene signature, we used the same genes as those used for EPIC (*Appendix 1—table 1*; markers of B cells, CD4 T cells, CD8 T cells, monocytes, neutrophils and NK cells for the

predictions in the blood datasets; markers of B cells, CAFs, CD4 T cells, CD8 T cells, endothelial cells, macrophages, and NK cells for the predictions in solid tumors).

- ISOpure (Quon *et al.*, 2013) estimates the profile and proportion of cancer cells by comparing many bulk samples containing cancer cells and many healthy bulk samples of the same tissue. Although the primary goal is not to compute the proportions of the different cell types composing a sample, cell fractions can still be obtained with this method. In particular, one output of ISOpure is how much each of the healthy reference samples is contributing to a given bulk sample. Instead of using bulk healthy samples, we used our cell reference profiles, so that each 'reference sample' corresponded to a different cell type. These reference samples and the bulk samples were then subsetted by the same signature genes that we derived for EPIC. ISOpure was then run based on these data. The contribution of each cell type was taken as the relative contribution outputted by ISOpure from each of the reference cell sample. The R implementation ISOpureR (Anghel *et al.*, 2015) version 1.0.21 was used.
- MCP-counter (Becht *et al.*, 2016) (R package version 1.1.0) was run with the 'HUGO_symbols' chosen as features or with 'affy133P2_probesets' for the microarray-based IHC dataset.
- TIMER (Li *et al.*, 2016) predictions were obtained by slightly adapting the available source code. The reference profiles available in TIMER were used directly. In addition to bulk gene expression, tumor purity estimates based on DNA copy number variation are needed in TIMER to refine the gene signature. As this information is not available in our benchmarking datasets, we kept all the original immune gene signatures for the predictions in blood. For the tumor datasets, we used the gene signatures obtained from the TCGA data for melanoma or colorectal cancer depending on the origin of cancer.
- ESTIMATE (Yoshihara *et al.*, 2013) was run with their R package version 1.0.11.

For CIBERSORT, DeconRNASeq and ISOpure, when run based on our gene expression reference profiles, we used the reference profiles from peripheral blood immune cells for the predictions in blood and the reference profiles from tumor-infiltrating cells for the predictions in solid tumors.

List of abbreviations

CAFs: cancer-associated fibroblasts; EPIC: acronym for our method to 'Estimate the Proportion of Immune and Cancer cells'; GEO: Gene Expression Omnibus; IHC: immunohistochemistry; PCA: principal component analysis; RMSE: root mean squared error; TCGA: The Cancer Genome Atlas; TPM: transcripts per million.

Acknowledgements

We are grateful to H el ene Maby-El Hajjami for compiling the clinical data. We thank Kristen L. Hoek, Andrew Link and their colleagues (Hoek *et al.*, 2015), Cate Speak, Scott Presnell and their colleagues (Linsley *et al.*, 2014), Aur elien De Reynies, Etienne Becht and their colleagues (Becht *et al.*, 2016), for providing us with additional data relating to their published studies. Computations were performed at the Vital-IT (<http://www.vital-it.ch>) Center for high-performance computing of the Swiss Institute of Bioinformatics.

Additional information

Funding

Funder	Grant reference number	Author
Center for Advanced Modeling Science		Julien Racle David Gfeller
Schweizerischer Nationalfonds zur F�orderung der Wissenschaftlichen Forschung	Project grant 31003A_173156	Julien Racle David Gfeller

The funders had no role in study design, data collection and interpretation, or the decision to submit the work for publication.

Author contributions

Julien Racle, Conceptualization, Data curation, Software, Formal analysis, Validation, Investigation, Visualization, Methodology, Writing—original draft, Writing—review and editing; Kaat de Jonge, Investigation, Methodology, Writing—review and editing; Petra Baumgaertner, Resources, Supervision, Investigation, Methodology; Daniel E Speiser, Resources, Supervision, Methodology, Writing—review and editing; David Gfeller, Conceptualization, Resources, Supervision, Funding acquisition, Validation, Methodology, Writing—original draft, Project administration, Writing—review and editing

Author ORCIDs

Julien Racle,  <http://orcid.org/0000-0002-0100-0323>

David Gfeller,  <http://orcid.org/0000-0002-3952-0930>

Ethics

Human subjects: Patients involved in this study agreed to donate metastatic tissues upon informed consent, based on dedicated clinical investigation protocols established according to the relevant regulatory standards. The protocols were approved by the local IRB, i.e. the Commission cantonale d'éthique de la recherche sur l'être humain du Canton de Vaud.

Decision letter and Author response

Decision letter <https://doi.org/10.7554/eLife.26476.047>

Author response <https://doi.org/10.7554/eLife.26476.048>

Additional files**Supplementary files**

- Supplementary file 1. Gene expression reference profiles, built from TPM (transcripts per million) normalized RNA-Seq data of immune cells sorted from blood as described in the Materials and methods: 'Reference gene expression profiles from circulating cells'. The file includes two sheets: (A) the reference gene expression values; (B) the gene variability relating to the reference profile. Columns indicate the reference cell types; rows indicate the gene names.
DOI: <https://doi.org/10.7554/eLife.26476.022>

- Supplementary file 2. Gene expression reference profiles built from tumor-infiltrating cells obtained from TPM normalized single-cell RNA-Seq data as described in the Materials and methods: 'Reference profiles from tumor-infiltrating cells'. The file includes two sheets: (A) the reference gene expression values; (B) the gene variability relating to the reference profile. Columns indicate the reference cell types; rows indicate the gene names.
DOI: <https://doi.org/10.7554/eLife.26476.023>

- Supplementary file 3. Proportion of cells measured in the different datasets: (A) this study; (B) dataset 1 (Zimmermann et al., 2016); (C) dataset 2 (Hoek et al., 2015); (D) dataset 3 (Linsley et al., 2014); and (E) single-cell RNA-Seq dataset (Tirosh et al., 2016). The 'Other cells' type corresponds always to the rest of the cells that were not assigned to one of the given cell types from the tables.
DOI: <https://doi.org/10.7554/eLife.26476.024>

- Transparent reporting form

DOI: <https://doi.org/10.7554/eLife.26476.025>

Major datasets

The following dataset was generated:

Author(s)	Year	Dataset title	Dataset URL	Database, license, and accessibility information
Racle J, de Jonge K, Baumgaertner P, Speiser DE, Gfeller D	2017	Simultaneous enumeration of cancer and immune cell types from tumor gene expression data	https://www.ncbi.nlm.nih.gov/geo/query/acc.cgi?acc=GSE93722	Publicly available at the NCBI Gene Expression Omnibus (accession no: GSE93722)

The following previously published datasets were used:

Author(s)	Year	Dataset title	Dataset URL	Database, license, and accessibility information
Poland G	2015	Bioinformatics Approach to 2010-2011 TIV Influenza A/H1N1 Vaccine Immune Profiling	http://www.immport.org/immport-open/public/study/study/displayStudyDetail/SDY67	Available at ImmPort (accession no: SDY67)
Hoek KL, Link AJ	2015	A Cell-based Systems Biology Assessment of Human Blood to Monitor Immune Responses After Influenza Vaccination	https://www.ncbi.nlm.nih.gov/geo/query/acc.cgi?acc=GSE64655	Publicly available at the NCBI Gene Expression Omnibus (accession no: GSE64655)
Speake C, Linsley PS, Whalen E, Chaussabel D, Prensnel SR, Mason MJ, Gersuk VH, O'Brien KK, Nguyen Q, Greenbaum CJ, Buckner JH, Malhotra U	2015	Next generation sequencing of human immune cell subsets across diseases	https://www.ncbi.nlm.nih.gov/geo/query/acc.cgi?acc=GSE60424	Publicly available at the NCBI Gene Expression Omnibus (accession no: GSE60424)
Sauvageau G, Pabst C, Yeh J	2016	RNA-Seq analysis of human adult peripheral blood populations	https://www.ncbi.nlm.nih.gov/geo/query/acc.cgi?acc=GSE51984	Publicly available at the NCBI Gene Expression Omnibus (accession no: GSE51984)
Marisa L, de Reyniès A, Duval A, Selves J, Gaub M, Vescovo L, Etienne-Grimaldi M, Schiappa R, Guenet D, Ayadi M, Kirzin S, Chazal M, Fléjou J, Benchimol D, Pencreach E, Lagarde A, Piard F, Elias D, Olschwang S, Milano G, Laurent-Puig P, Boige V	2013	Gene expression Classification of Colon Cancer defines six molecular subtypes with distinct clinical, molecular and survival characteristics [Expression]	https://www.ncbi.nlm.nih.gov/geo/query/acc.cgi?acc=GSE39582	Publicly available at the NCBI Gene Expression Omnibus (accession no: GSE39582)
Tirosh I, Izar B	2016	Single cell RNA-seq analysis of melanoma	https://www.ncbi.nlm.nih.gov/geo/query/acc.cgi?acc=GSE72056	Publicly available at the NCBI Gene Expression Omnibus (accession no: GSE72056)

References

- Ahn J, Yuan Y, Parmigiani G, Suraokar MB, Diao L, Wistuba II, Wang W. 2013. DeMix: deconvolution for mixed cancer transcriptomes using raw measured data. *Bioinformatics* **29**:1865–1871. DOI: <https://doi.org/10.1093/bioinformatics/btt301>, PMID: 23712657
- Angelova M, Charoentong P, Hackl H, Fischer ML, Snajder R, Krogsdam AM, Waldner MJ, Bindea G, Mlecnik B, Galon J, Trajanoski Z. 2015. Characterization of the immunophenotypes and antigenomes of colorectal cancers reveals distinct tumor escape mechanisms and novel targets for immunotherapy. *Genome Biology* **16**:64. DOI: <https://doi.org/10.1186/s13059-015-0620-6>, PMID: 25853550
- Anghel CV, Quon G, Haider S, Nguyen F, Deshwar AG, Morris QD, Boutros PC. 2015. ISOpureR: an R implementation of a computational purification algorithm of mixed tumour profiles. *BMC Bioinformatics* **16**:156. DOI: <https://doi.org/10.1186/s12859-015-0597-x>, PMID: 25972088
- Balch CM, Riley LB, Bae YJ, Salmeron MA, Platsoucas CD, von Eschenbach A, Itoh K. 1990. Patterns of human tumor-infiltrating lymphocytes in 120 human cancers. *Archives of Surgery* **125**:200–205. DOI: <https://doi.org/10.1001/archsurg.1990.01410140078012>, PMID: 1689143
- Baron M, Veres A, Wolock SL, Faust AL, Gaujoux R, Vetere A, Ryu JH, Wagner BK, Shen-Orr SS, Klein AM, Melton DA, Yanai. 2016. A single-cell transcriptomic map of the human and mouse pancreas reveals inter- and intra-cell population structure. *Cell Systems* **3**:346–360. DOI: <https://doi.org/10.1016/j.cels.2016.08.011>, PMID: 27667365

- Becht E, Giraldo NA, Lacroix L, Buttard B, Elarouci N, Petitprez F, Selves J, Laurent-Puig P, Sautès-Fridman C, Fridman WH, de Reyniès A. 2016. Estimating the population abundance of tissue-infiltrating immune and stromal cell populations using gene expression. *Genome Biology* **17**:218. DOI: <https://doi.org/10.1186/s13059-016-1070-5>, PMID: 27765066
- Carmona SJ, Teichmann SA, Ferreira L, Macaulay IC, Stubbington MJ, Cvejic A, Gfeller D. 2017. Single-cell transcriptome analysis of fish immune cells provides insight into the evolution of vertebrate immune cell types. *Genome Research* **27**:451–461. DOI: <https://doi.org/10.1101/gr.207704.116>, PMID: 28087841
- Carter SL, Cibulskis K, Helman E, McKenna A, Shen H, Zack T, Laird PW, Onofrio RC, Winckler W, Weir BA, Beroukhi R, Pellman D, Levine DA, Lander ES, Meyerson M, Getz G. 2012. Absolute quantification of somatic DNA alterations in human cancer. *Nature Biotechnology* **30**:413–421. DOI: <https://doi.org/10.1038/nbt.2203>, PMID: 22544022
- Charoentong P, Finotello F, Angelova M, Mayer C, Efremova M, Rieder D, Hackl H, Trajanoski Z. 2017. Pan-cancer immunogenomic analyses reveal genotype-immunophenotype relationships and predictors of response to checkpoint blockade. *Cell Reports* **18**:248–262. DOI: <https://doi.org/10.1016/j.celrep.2016.12.019>, PMID: 28052254
- Clarke J, Seo P, Clarke B. 2010. Statistical expression deconvolution from mixed tissue samples. *Bioinformatics* **26**:1043–1049. DOI: <https://doi.org/10.1093/bioinformatics/btq097>, PMID: 20202973
- Clemente CG, Mihm MC, Bufalino R, Zurrida S, Collini P, Cascinelli N. 1996. Prognostic value of tumor infiltrating lymphocytes in the vertical growth phase of primary cutaneous melanoma. *Cancer* **77**:1303–1310. DOI: [https://doi.org/10.1002/\(SICI\)1097-0142\(19960401\)77:7<1303::AID-CNCR12>3.0.CO;2-5](https://doi.org/10.1002/(SICI)1097-0142(19960401)77:7<1303::AID-CNCR12>3.0.CO;2-5), PMID: 8608507
- Edgar R, Domrachev M, Lash AE. 2002. Gene Expression Omnibus: NCBI gene expression and hybridization array data repository. *Nucleic Acids Research* **30**:207–210. DOI: <https://doi.org/10.1093/nar/30.1.207>, PMID: 11752295
- Efroni I, Ip PL, Navy T, Mello A, Birnbaum KD. 2015. Quantification of cell identity from single-cell gene expression profiles. *Genome Biology* **16**:9. DOI: <https://doi.org/10.1186/s13059-015-0580-x>, PMID: 25608970
- Finak G, McDavid A, Yajima M, Deng J, Gersuk V, Shalek AK, Slichter CK, Miller HW, McElrath MJ, Prlic M, Linsley PS, Gottardo R. 2015. MAST: a flexible statistical framework for assessing transcriptional changes and characterizing heterogeneity in single-cell RNA sequencing data. *Genome Biology* **16**:278. DOI: <https://doi.org/10.1186/s13059-015-0844-5>, PMID: 26653891
- Fridman WH, Pagès F, Sautès-Fridman C, Galon J. 2012. The immune contexture in human tumours: impact on clinical outcome. *Nature Reviews Cancer* **12**:298–306. DOI: <https://doi.org/10.1038/nrc3245>, PMID: 22419253
- GTEX Consortium. 2015. Human genomics. The Genotype-Tissue Expression (GTEx) pilot analysis: multitissue gene regulation in humans. *Science* **348**:648–660. DOI: <https://doi.org/10.1126/science.1262110>, PMID: 25954001
- Galon J, Costes A, Sanchez-Cabo F, Kirilovsky A, Mlecnik B, Lagorce-Pagès C, Tosolini M, Camus M, Berger A, Wind P, Zinzindohoué F, Bruneval P, Cugnenc PH, Trajanoski Z, Fridman WH, Pagès F. 2006. Type, density, and location of immune cells within human colorectal tumors predict clinical outcome. *Science* **313**:1960–1964. DOI: <https://doi.org/10.1126/science.1129139>, PMID: 17008531
- Ganesan AP, Clarke J, Wood O, Garrido-Martin EM, Chee SJ, Mellows T, Samaniego-Castruita D, Singh D, Seumois G, Alzetani A, Woo E, Friedmann PS, King EV, Thomas GJ, Sanchez-Elsner T, Vijayanand P, Ottensmeier CH. 2017. Tissue-resident memory features are linked to the magnitude of cytotoxic T cell responses in human lung cancer. *Nature Immunology* **18**:940–950. DOI: <https://doi.org/10.1038/ni.3775>, PMID: 28628092
- Gaujoux R, Seoighe C. 2013. CellMix: a comprehensive toolbox for gene expression deconvolution. *Bioinformatics* **29**:2211–2212. DOI: <https://doi.org/10.1093/bioinformatics/btt351>, PMID: 23825367
- Gentles AJ, Newman AM, Liu CL, Bratman SV, Feng W, Kim D, Nair VS, Xu Y, Khuong A, Hoang CD, Diehn M, West RB, Plevritis SK, Alizadeh AA. 2015. The prognostic landscape of genes and infiltrating immune cells across human cancers. *Nature Medicine* **21**:938–945. DOI: <https://doi.org/10.1038/nm.3909>, PMID: 26193342
- Gong T, Szustakowski JD. 2013. DeconRNASeq: a statistical framework for deconvolution of heterogeneous tissue samples based on mRNA-Seq data. *Bioinformatics* **29**:1083–1085. DOI: <https://doi.org/10.1093/bioinformatics/btt090>, PMID: 23428642
- Gosink MM, Petrie HT, Tsinoremas NF. 2007. Electronically subtracting expression patterns from a mixed cell population. *Bioinformatics* **23**:3328–3334. DOI: <https://doi.org/10.1093/bioinformatics/btm508>, PMID: 17956877
- Hackl H, Charoentong P, Finotello F, Trajanoski Z. 2016. Computational genomics tools for dissecting tumour-immune cell interactions. *Nature Reviews Genetics* **17**:441–458. DOI: <https://doi.org/10.1038/nrg.2016.67>, PMID: 27376489
- Hanahan D, Weinberg RA. 2011. Hallmarks of cancer: the next generation. *Cell* **144**:646–674. DOI: <https://doi.org/10.1016/j.cell.2011.02.013>, PMID: 21376230
- Hoadley KA, Yau C, Wolf DM, Cherniack AD, Tamborero D, Ng S, Leiserson MDM, Niu B, McLellan MD, Uzunangelov V, Zhang J, Kandoth C, Akbani R, Shen H, Omberg L, Chu A, Margolin AA, Van't Veer LJ, Lopez-Bigas N, Laird PW, et al. 2014. Multiplatform analysis of 12 cancer types reveals molecular classification within and across tissues of origin. *Cell* **158**:929–944. DOI: <https://doi.org/10.1016/j.cell.2014.06.049>, PMID: 25109877
- Hoek KL, Samir P, Howard LM, Niu X, Prasad N, Galassie A, Liu Q, Allos TM, Floyd KA, Guo Y, Shyr Y, Levy SE, Joyce S, Edwards KM, Link AJ. 2015. A cell-based systems biology assessment of human blood to monitor

- immune responses after influenza vaccination. *PLoS One* **10**:e0118528. DOI: <https://doi.org/10.1371/journal.pone.0118528>, PMID: 25706537
- Jaitin DA, Kenigsberg E, Keren-Shaul H, Elefant N, Paul F, Zaretsky I, Mildner A, Cohen N, Jung S, Tanay A, Amit I. 2014. Massively parallel single-cell RNA-seq for marker-free decomposition of tissues into cell types. *Science* **343**:776–779. DOI: <https://doi.org/10.1126/science.1247651>, PMID: 24531970
- Joyce JA, Fearon DT. 2015. T cell exclusion, immune privilege, and the tumor microenvironment. *Science* **348**: 74–80. DOI: <https://doi.org/10.1126/science.aaa6204>, PMID: 25838376
- Langmead B, Salzberg SL. 2012. Fast gapped-read alignment with Bowtie 2. *Nature Methods* **9**:357–359. DOI: <https://doi.org/10.1038/nmeth.1923>, PMID: 22388286
- Li H, Handsaker B, Wysoker A, Fennell T, Ruan J, Homer N, Marth G, Abecasis G, Durbin R, 1000 Genome Project Data Processing Subgroup. 2009. The Sequence Alignment/Map format and SAMtools. *Bioinformatics* **25**:2078–2079. DOI: <https://doi.org/10.1093/bioinformatics/btp352>, PMID: 19505943
- Li B, Dewey CN. 2011. RSEM: accurate transcript quantification from RNA-Seq data with or without a reference genome. *BMC Bioinformatics* **12**:323. DOI: <https://doi.org/10.1186/1471-2105-12-323>, PMID: 21816040
- Li B, Li JZ. 2014. A general framework for analyzing tumor subclonality using SNP array and DNA sequencing data. *Genome Biology* **15**:473. DOI: <https://doi.org/10.1186/s13059-014-0473-4>, PMID: 25253082
- Li B, Severson E, Pignon JC, Zhao H, Li T, Novak J, Jiang P, Shen H, Aster JC, Rodig S, Signoretti S, Liu JS, Liu XS. 2016. Comprehensive analyses of tumor immunity: implications for cancer immunotherapy. *Genome Biology* **17**:174. DOI: <https://doi.org/10.1186/s13059-016-1028-7>, PMID: 27549193
- Linsley PS, Speake C, Whalen E, Chaussabel D. 2014. Copy number loss of the interferon gene cluster in melanomas is linked to reduced T cell infiltrate and poor patient prognosis. *PLoS One* **9**:e109760. DOI: <https://doi.org/10.1371/journal.pone.0109760>, PMID: 25314013
- Linsley PS, Chaussabel D, Speake C. 2015. The relationship of immune cell signatures to patient survival varies within and between tumor types. *PLoS One* **10**:e0138726. DOI: <https://doi.org/10.1371/journal.pone.0138726>, PMID: 26398410
- Love MI, Huber W, Anders S. 2014. Moderated estimation of fold change and dispersion for RNA-seq data with DESeq2. *Genome Biology* **15**:550. DOI: <https://doi.org/10.1186/s13059-014-0550-8>, PMID: 25516281
- Newman AM, Liu CL, Green MR, Gentles AJ, Feng W, Xu Y, Hoang CD, Diehn M, Alizadeh AA. 2015. Robust enumeration of cell subsets from tissue expression profiles. *Nature Methods* **12**:453–457. DOI: <https://doi.org/10.1038/nmeth.3337>, PMID: 25822800
- Pabst C, Bergeron A, Lavallée VP, Yeh J, Gendron P, Norddahl GL, Kros J, Boivin I, Deneault E, Simard J, Imren S, Boucher G, Eppert K, Herold T, Bohlander SK, Humphries K, Lemieux S, Hébert J, Sauvageau G, Barabé F. 2016. GPR56 identifies primary human acute myeloid leukemia cells with high repopulating potential in vivo. *Blood* **127**:2018–2027. DOI: <https://doi.org/10.1182/blood-2015-11-683649>, PMID: 26834243
- Padovan-Merhar O, Nair GP, Bialesch AG, Mayer A, Scarfone S, Foley SW, Wu AR, Churchman LS, Singh A, Raj A. 2015. Single mammalian cells compensate for differences in cellular volume and DNA copy number through independent global transcriptional mechanisms. *Molecular Cell* **58**:339–352. DOI: <https://doi.org/10.1016/j.molcel.2015.03.005>, PMID: 25866248
- Qiao W, Quon G, Cszasz E, Yu M, Morris Q, Zandstra PW. 2012. PERT: a method for expression deconvolution of human blood samples from varied microenvironmental and developmental conditions. *PLoS Computational Biology* **8**:e1002838. DOI: <https://doi.org/10.1371/journal.pcbi.1002838>, PMID: 23284283
- Quon G, Haider S, Deshwar AG, Cui A, Boutros PC, Morris Q. 2013. Computational purification of individual tumor gene expression profiles leads to significant improvements in prognostic prediction. *Genome Medicine* **5**:29. DOI: <https://doi.org/10.1186/gm433>, PMID: 23537167
- Racle J. 2017. EPIC. *GitHub*. 66c8ba00. <https://github.com/GfellerLab/EPIC>
- Rooney MS, Shukla SA, Wu CJ, Getz G, Hacohen N. 2015. Molecular and genetic properties of tumors associated with local immune cytolytic activity. *Cell* **160**:48–61. DOI: <https://doi.org/10.1016/j.cell.2014.12.033>, PMID: 25594174
- Saliba AE, Westermann AJ, Gorski SA, Vogel J. 2014. Single-cell RNA-seq: advances and future challenges. *Nucleic Acids Research* **42**:8845–8860. DOI: <https://doi.org/10.1093/nar/gku555>, PMID: 25053837
- Sconocchia G, Arriga R, Tornillo L, Terracciano L, Ferrone S, Spagnoli GC. 2012. Melanoma cells inhibit NK cell functions. *Cancer Research* **72**:5428–5429. DOI: <https://doi.org/10.1158/0008-5472.CAN-12-1181>, PMID: 23047870
- Shen-Orr SS, Gaujoux R. 2013. Computational deconvolution: extracting cell type-specific information from heterogeneous samples. *Current Opinion in Immunology* **25**:571–578. DOI: <https://doi.org/10.1016/j.coi.2013.09.015>, PMID: 24148234
- Singer M, Wang C, Cong L, Marjanovic ND, Kowalczyk MS, Zhang H, Nyman J, Sakuishi K, Kurtulus S, Gennert D, Xia J, Kwon JYH, Nevin J, Herbst RH, Yanai I, Rozenblatt-Rosen O, Kuchroo VK, Regev A, Anderson AC. 2016. A distinct gene module for dysfunction uncoupled from activation in tumor-infiltrating T cells. *Cell* **166**: 1500–1511. DOI: <https://doi.org/10.1016/j.cell.2016.08.052>, PMID: 27610572
- Speiser DE, Ho PC, Verdeil G. 2016. Regulatory circuits of T cell function in cancer. *Nature Reviews Immunology* **16**:599–611. DOI: <https://doi.org/10.1038/nri.2016.80>, PMID: 27526640
- Stegle O, Teichmann SA, Marioni JC. 2015. Computational and analytical challenges in single-cell transcriptomics. *Nature Reviews Genetics* **16**:133–145. DOI: <https://doi.org/10.1038/nrg3833>, PMID: 25628217
- Subrahmanyam YV, Yamaga S, Prashar Y, Lee HH, Hoe NP, Kluger Y, Gerstein M, Goguen JD, Newburger PE, Weissman SM. 2001. RNA expression patterns change dramatically in human neutrophils exposed to bacteria. *Blood* **97**:2457–2468. DOI: <https://doi.org/10.1182/blood.V97.8.2457>, PMID: 11290611

- Tirosh I, Izar B, Prakadan SM, Wadsworth MH, Treacy D, Trombetta JJ, Rotem A, Rodman C, Lian C, Murphy G, Fallahi-Sichani M, Dutton-Regester K, Lin JR, Cohen O, Shah P, Lu D, Genshaft AS, Hughes TK, Ziegler CG, Kazer SW, et al. 2016. Dissecting the multicellular ecosystem of metastatic melanoma by single-cell RNA-seq. *Science* **352**:189–196. DOI: <https://doi.org/10.1126/science.aad0501>, PMID: 27124452
- Tzur A, Moore JK, Jorgensen P, Shapiro HM, Kirschner MW. 2011. Optimizing optical flow cytometry for cell volume-based sorting and analysis. *PLoS One* **6**:e16053. DOI: <https://doi.org/10.1371/journal.pone.0016053>, PMID: 21283800
- Venet D, Pécasse F, Maenhaut C, Bersini H. 2001. Separation of samples into their constituents using gene expression data. *Bioinformatics* **17 Suppl 1**:S279–S287. DOI: https://doi.org/10.1093/bioinformatics/17.suppl_1.S279, PMID: 11473019
- Yoshihara K, Shahmoradgoli M, Martínez E, Vegesna R, Kim H, Torres-García W, Treviño V, Shen H, Laird PW, Levine DA, Carter SL, Getz G, Stenke-Hale K, Mills GB, Verhaak RG. 2013. Inferring tumour purity and stromal and immune cell admixture from expression data. *Nature Communications* **4**:2612. DOI: <https://doi.org/10.1038/ncomms3612>, PMID: 24113773
- Zheng X, Zhang N, Wu HJ, Wu H. 2017. Estimating and accounting for tumor purity in the analysis of DNA methylation data from cancer studies. *Genome Biology* **18**:17. DOI: <https://doi.org/10.1186/s13059-016-1143-5>, PMID: 28122605
- Zhong Y, Wan YW, Pang K, Chow LM, Liu Z. 2013. Digital sorting of complex tissues for cell type-specific gene expression profiles. *BMC Bioinformatics* **14**:89. DOI: <https://doi.org/10.1186/1471-2105-14-89>, PMID: 23497278
- Zimmermann MT, Oberg AL, Grill DE, Ovsyannikova IG, Haralambieva IH, Kennedy RB, Poland GA. 2016. System-wide associations between DNA-methylation, gene expression, and humoral immune response to influenza vaccination. *PLoS One* **11**:e0152034. DOI: <https://doi.org/10.1371/journal.pone.0152034>, PMID: 27031986
- Şenbabaoğlu Y, Gejman RS, Winer AG, Liu M, Van Allen EM, de Velasco G, Miao D, Ostrovskaya I, Drill E, Luna A, Weinhold N, Lee W, Manley BJ, Khalil DN, Kaffenberger SD, Chen Y, Danilova L, Voss MH, Coleman JA, Russo P, et al. 2016. Tumor immune microenvironment characterization in clear cell renal cell carcinoma identifies prognostic and immunotherapeutically relevant messenger RNA signatures. *Genome Biology* **17**:231. DOI: <https://doi.org/10.1186/s13059-016-1092-z>, PMID: 27855702

Appendix 1

DOI: <https://doi.org/10.7554/eLife.26476.026>

Appendix 1—table 1. Gene markers used per cell type. Only markers of cell types present in the respective reference gene expression profiles are used.

Cell type	Genes markers
B cells	BANK1, CD79A, CD79B, FCER2, FCRL2, FCRL5, MS4A1, PAX5, POU2AF1, STAP1, TCL1A
CAFs	ADAM33, CLDN11, COL1A1, COL3A1, COL14A1, CRISPLD2, CXCL14, DPT, F3, FBLN1, ISLR, LUM, MEG3, MFAP5, PRELP, PTGIS, SFRP2, SFRP4, SYNPO2, TMEM119
CD4 T cells	ANKRD55, DGKA, FOXP3, GCNT4, IL2RA, MDS2, RCAN3, TBC1D4, TRAT1
CD8 T cells	CD8B, HAUS3, JAKMIP1, NAA16, TSPYL1
Endothelial cells	CDH5, CLDN5, CLEC14A, CXorf36, ECSCR, F2RL3, FLT1, FLT4, GPR4, GPR182, KDR, MMRN1, MMRN2, MYCT1, PTPRB, RHOJ, SLCO2A1, SOX18, STAB2, VWF
Macrophages	APOC1, C1QC, CD14, CD163, CD300C, CD300E, CSF1R, F13A1, FPR3, HAMP, IL1B, LILRB4, MS4A6A, MSR1, SIGLEC1, VSIG4
Monocytes	CD33, CD300C, CD300E, CECR1, CLEC6A, CPVL, EGR2, EREG, MS4A6A, NAGA, SLC37A2
Neutrophils	CEACAM3, CNTNAP3, CXCR1, CYP4F3, FFAR2, HIST1H2BC, HIST1H3D, KY, MMP25, PGLYRP1, SLC12A1, TAS2R40
NK cells	CD160, CLIC3, FGFBP2, GNLY, GNPTAB, KLRF1, NCR1, NMUR1, S1PR5, SH2D1B
T cells	BCL11B, CD5, CD28, IL7R, ITK, THEMIS, UBASH3A

DOI: <https://doi.org/10.7554/eLife.26476.027>

Appendix 2

DOI: <https://doi.org/10.7554/eLife.26476.028>

Appendix 2—table 1. Characteristics of the patients with metastatic melanoma and corresponding lymph node samples.

Patient	Age (years)	Gender	Tissue
LAU125	59	male	iliac lymph node
LAU355	70	female	iliac-obturator lymph node
LAU1255	87	male	axillary lymph node
LAU1314	81	male	iliac-obturator lymph node

DOI: <https://doi.org/10.7554/eLife.26476.029>

14. Curriculum Vitae

Kaat de Jonge

Born of July 23rd 1991, Belgium

Address: Avenue de La Harpe 49, 1006 Lausanne

Email: kaatdejonge@gmail.com

Phone: +41768166237

Skype: kaatdj

Education

2014- current

PhD fellow, Clinical tumor biology & immunotherapy group, Department of fundamental oncology and Ludwig Cancer Center, University of Lausanne

2009 – 2014

Bio-engineering, cell and gene biotechnology, Vrije Universiteit Brussel

Master project within the immunoparasitology group at the cellular and molecular immunology unit at the VUB using *Leishmania major* as a model in mouse to unravel Th differentiation

Publications

Jonge, K. De *et al.* Circulating CD56 bright NK cells inversely correlate with survival of melanoma patients. 1–10 (2019).

Kauffmann, F. *et al.* STAT6 mediates footpad immunopathology in the absence of IL-12p40 following infection of susceptible BALB/c mice with *Leishmania major*. *Front. Immunol.* **9**, 1–11 (2018).

Bordry, N. *et al.* Lymphatic vessel density is associated with CD8+T cell infiltration and immunosuppressive factors in human melanoma. *Oncoimmunology* **7**, (2018).

Racle, J., de Jonge, K., Baumgaertner, P., Speiser, D. E. & Gfeller, D. Simultaneous enumeration of cancer and immune cell types from bulk tumor gene expression data. *Elife* **6**, 1–25 (2017).

Teaching

2014 – current

Teaching of practical work 2nd year medical students and 3rd year biology students at the University of Lausanne, Switzerland

Supervision master student thesis at the University of Lausanne

Supervision of student's pre-master project at the University of Lausanne

Professional experience

2013

Internship at Complix NV, Ghent

Determining the stability of different Alphabody constructs

2007 – 2011

Volunteering as an animator during inclusion summer camps, Leuven region

Organizing summer camps for 50+ children including 1/4 with special needs

Organizing activities for children ranging between 4-15 years old

Languages

Dutch - Mother tongue, fluent in speaking and writing

French - Fluent in speaking and proficient in writing

English - Fluent in speaking and writing

Technical skill

IT - Microsoft (Word, PowerPoint, Excel), Illustrator (basic), R programming (basic), FlowJo, Prism

Cell Biology - Isolation of PBMCs, negative and positive selection of primary cells from PBMCs, lymphocyte proliferation, killing assay, tumour cell line culture, cell activation

Flow cytometry - Frequent user of BD and Beckmann coulter machines (up to 16 colors)

Proteomics - ELISA, MSD; Bead array technology, solubility assays, CD spectrometry

Genomics - total RNA extraction (sequencing grade), real time PCR (SYBR green), DNA cloning

Conference participation

Oral presentation

2017 – Annual congress Swiss Society for allergology and immunology, Sankt Gallen, Switzerland

Talk title: Characterization of immune modulatory B cells in melanoma patients

2017 - Joint EPFL-UNIL PhD Retreat, Les Diablerets, Switzerland

Talk title: Identifying immunosuppressive cell subsets in melanoma

2016 – Wolfsberg immunology meeting, conference for PhD students in immunology in Switzerland

Talk title: Identifying novel immunosuppressive lymphocyte subsets in melanoma

2016 - Joint EPFL-UNIL PhD Retreat, Les Diablerets, Switzerland

Talk title: Identifying immunosuppressive cell subsets in melanoma

Poster presentation

2018 – European congress of immunology, Amsterdam, the Netherlands

Poster title: Circulating CD56^{bright} NK cells inversely correlate with the survival of melanoma patients

2018 - Annual congress Swiss Society for allergology and immunology, Interlaken, Switzerland

Poster title: Circulating CD56^{bright} NK cells inversely correlate with the survival of melanoma patients

2017 - Faculty & Staff Retreat of the Swiss Cancer Center Lausanne, Switzerland

Poster title: Characterization of immune modulatory B cells in melanoma patients

2017 – World immune regulation meeting, Davos, Switzerland

Poster title: Characterization of immune modulatory B cells in melanoma patients

2016 - Faculty & Staff Retreat of the Swiss Cancer Center Lausanne, Switzerland

Poster title: Characterization of peripheral B cells in melanoma patients

2016 - Annual congress Swiss Society for allergology and immunology, Montreux, Switzerland

Poster title: CD56^{bright} NK cells in PBMC correlate with unfavorable clinical outcome in melanoma patients

2015 - Faculty & Staff Retreat of the Swiss Cancer Center Lausanne, Switzerland

Poster title: Marker negative cells residing in the lymphocyte gate

2015 - European congress of immunology, Vienna, Austria

Poster title: Marker negative cells residing in the lymphocyte gate

2015 - Wolfsberg immunology meeting, conference for PhD students in immunology in Switzerland

Poster title: Possible involvement of B and NK cells in T cell inhibition and clinical outcome of melanoma patients

2015 - Joint EPFL-UNIL PhD Retreat, Les Diablerets, Switzerland

Poster title: Possible involvement of B and NK cells in T cell inhibition and clinical outcome of melanoma patients

Extracurricular activities

2013 – 2014

Treasurer BEST (Board of European Students of Technology), Brussels

Being part of a 5 person team that organises inter-European events (+50 people) as well as balancing spending an income of the local affiliate

2012 – 2013

Secretary BEST (Board of European Students of Technology), Brussels

Being part of a 5 person team that organises inter-European events (+50 people) and running day to day operations

Hobbies and interests

Sports: horse riding, skiing, running, hiking

Traveling

Reading, music (violin, 9 years)

Membership

Swiss Society for Allergology and Immunology (SSAI)

The European Association for Cancer Research (EACR)